Aspects of Applied Holography

by

Daniel Kevin O'Keeffe

A thesis submitted in conformity with the requirements
for the degree of Doctor of Philosophy
Graduate Department of Physics
University of Toronto

Abstract

Aspects of Applied Holography

Daniel Kevin O'Keeffe

Doctor of Philosophy

Graduate Department of Physics

University of Toronto

2015

In this thesis we investigate applications of holography in the context of condensed matter physics. We study crossover solutions related to understanding the singular behaviour of hyperscaling violating (HSV) geometries within an Einstein-Maxwell-dilaton theory with curvature squared corrections. This theory has three couplings η_i for the three R^2 invariants and two theory functions: a dilaton potential $V(\phi)$ and a dilaton-dependent gauge coupling $f(\phi)$. We find solutions of this theory, parametrized by a dynamical critical exponent z and HSV parameter θ. We obtain restrictions on the form of the theory functions required to support HSV-type solutions using three physical inputs: the null energy condition (NEC), causality $z \geq 1$, and $d_{\text{eff}} \equiv d - \theta$ lying in the range $0 < d_{\text{eff}} \leq d$. The NEC constraints are linear in the η_i and polynomial in d, z, θ. The allowed ranges of z, θ change depending on the signs of η_i. For the case of Einstein-Weyl gravity, we further narrow down the theory functions and solution parameters required for crossover solutions interpolating between HSV, AdS_{d+2} near the boundary, and $AdS_2 \times \mathbb{R}^d$ in the interior.

We study aspects of holographic disorder by considering a model of perturbatively charged disorder in $D = 4$ dimensions. Starting from initially uncharged AdS_4, a randomly fluctuating boundary chemical potential is introduced by turning on a bulk gauge field parameterized by a disorder strength $\overline{V}$ and a characteristic scale k_0. Accounting for gravitational backreaction, we construct an asymptotically AdS solution perturbatively

in the disorder strength. The disorder averaged geometry displays unphysical divergences in the deep interior. We explain how to remove these divergences and arrive at a well behaved solution. The disorder averaged DC conductivity is calculated and is found to contain a correction to the AdS result. The correction appears at second order in the disorder strength and scales inversely with k_0. We discuss the extension to a system with a finite initial charge density. The disorder averaged DC conductivity may be calculated by adopting a technique developed for holographic lattices.

Dedication

To my parents Diana and Patrick and my grandparents Shirley and Frederick

Acknowledgements

It is a pleasure to acknowledge my gratitude to the following people.

First and foremost, my advisor, Prof. Amanda Peet for guidance and encouragement.

The members of my supervisory committee, Prof. Peter Krieger and Prof. Erich Poppitz for guidance and valuable comments.

Prof. Amanda Peet and Prof. Ben Burrington for encouragement, insightful discussions and valuable courses.

Dr. Ida Zadeh for helpful discussions, comments and support.

Fellow student Ian Jardine for enlightening discussions and fellowship.

My friend Daisy for constant encouragement and support.

Staff members of the Department of Physics at the University of Toronto: Teresa Baptista, Krystyna Biel, Steven Butterworth, Julian Comanean, Elizabeth Glover, Helen Iyer, Joane Magnaye, and April Seeley for brilliant support and encouragement.

Cathy Santos for endless encouragement, support, love and for putting up with me throughout the writing of this thesis.

My brothers Seamus and Brendan, and extended family. Especially my grandmother Shirley d'Allmen and grandfather Frederick d'Allmen for teaching me countless valuable lessons. Special thanks to my mother Diana and father Patrick for constant encouragement, support and advice throughout the years.

Contents

List of Figures

Chapter 1

Introduction

1.1 Overview and Synthesis

This thesis is concerned with applications of gauge/gravity duality, which is one of the most remarkable advances in theoretical physics of the last quarter century. Broadly speaking, the idea is that some quantum field theories (QFT) without gravity are equivalent to a different theory with gravity in one higher dimension. This assertion has wide reaching implications for various branches of physics, including condensed matter physics, particle physics, cosmology, gravitational physics and even fluid dynamics. Many of these topics will be explored in more detail throughout this thesis. Firstly though, it is important to place the contents of this thesis within the broader context of physics.

As will be explained in detail in section 1.2.1, many of the celebrated results of gauge/gravity duality (a.k.a holography) are born out of string theory. The original example of a holographic duality, called the AdS/CFT correspondence, is a conjectured equivalence between a type IIB superstring theory on a certain gravitational background called anti de Sitter space (AdS) and a field theory with a specific type of symmetry (conformal field theory or CFT) [1]. At first glance, such an assertion may seem absurd- how can a theory with gravity be equivalent to a theory without gravity? While there is

as of yet no general formal proof of this particular equivalence, the conjecture has passed such an astounding number of non-trivial checks that the current general attitude is that it is correct. We will review this duality and its checks in greater detail below as well as discuss other examples of holographic dualities which have also passed equally (or in some cases more) impressive non-trivial checks.

The fact that string theory makes an appearance in holographic duality is not surprising. While string theory started out as a proposed model for the strong nuclear force [2], it was eventually realized that it contains gravity, making it a potential theory of quantum gravity. There are actually five perturbative string theories which live in ten dimensions, which are all related by string duality and to an eleven dimensional theory called M-theory.

Generically, string theory contains a massless spin two graviton (which describes gravity) as well as other states corresponding to gauge bosons, fermions, etc. On top of fundamental open and closed strings, string theory also contains non-perturbative objects called Dp-branes which arise as loci where open strings end. These objects are extended along p spatial dimensions. At low energies, string theory recovers general relativity [2]. This observation suggests that string theory may be useful for understanding one of the deepest problems of modern theoretical physics, namely, how does gravity behave at extremely small scales.

General relativity breaks down at extremely small distance (Planck scale: $l_p \approx 1.6 \times 10^{-33}$cm). Near a curvature singularity, general relativity ceases to provide a valid description of physics and some new theory must take over, requiring new physics. For this reason, black holes make prototypical playgrounds for exploring the consequences of new physics at small distance scales. The expectation is that quantum effects somehow come in and "cure" the singular behaviour; this can happen quite broadly in string theory. Some geometries which appear singular in general relativity are regular in string theory due to the extended nature of strings.

It is natural to wonder how much more string theory can teach us about quantum gravity. Gravitational string theory aims at understanding exactly this question. This programme has led to a number of successes over the years, prime among which is the derivation of the entropy of a black hole from a microscopic perspective [3]. This original construction has been generalized to other kinds of black holes, see [4] for a review. The origin of the entropy of a black hole is a longstanding problem in general relativity and strikes at the heart of quantum gravity, where a theory which accounts for the microscopic degrees of freedom is needed. Taking this a step further, the fuzzball programme takes the perspective that conventional black hole geometries emerge as a coarse-graining over string theoretic microstates [5], [6]. The picture which emerges is that black holes should be thought of as being made up of string theory ingredients. One message to take away from this picture is that string theory tools unlock the entropy for black holes; these very same tools led to the discovery of the AdS/CFT correspondence.

The original AdS/CFT correspondence was discovered by studying the dynamics of a stack of coincident $D3$-branes. In this system, there are open strings with endpoints on the branes as well as closed strings living in the full ten dimensions. In a certain low energy limit, the open and closed strings decouple and the brane system is equally well described by the closed strings or the open strings. The closed string side is described by a gravitational theory whereas the open string side is described by a field theory. Both models are describing the same system, hence they should be equivalent. In other words, both theories offer a "dual" description of the same physics. This picture repeats itself in other systems, giving other examples of holographic dualities.

Gauge/gravity dualities contain another surprisingly useful feature; they are weak/strong dualities. In other words, when the string theory is weakly coupled, the QFT is strongly coupled and vice versa. Strongly coupled quantum field theories are not well understood. The standard textbook approach to understanding QFTs is to work at weak coupling where we can understand the behaviour of the theory perturbatively. This approach does

not work at strong coupling and it can be difficult to say much about a field theory in this limit. The string dual is described by general relativity at weak coupling, which we understand quite well. In this way, we can use the duality to understand strongly coupled field theories by studying related quantities in Einstein gravity.

This approach has been applied to many systems by now. Holography has been used to describe aspects of QCD, in particular the exotic state of matter called the quark-gluon plasma, which is a state of matter made up of asymptotically free quarks and gluons at high temperatures. Holographic techniques provide a calculation for the shear viscosity of such a plasma [7], model a confinement-deconfinement transition [8], as well as model the effects of drag as quarks move through the plasma [9], [10], [11]. Such a state of matter is the focus of experimental efforts at the Relativistic Heavy Ion Collider (RHIC) as well as at the Large Hadron Collider (LHC).

Strongly coupled field theories arise frequently in condensed matter physic contexts, often making theoretical calculations difficult. Holography has been applied to several contemporary condensed matter systems such as high temperature superconductors and strange metals. Holographic superconductors are a class of asymptotically AdS black holes which, in conjunction with gauge/gravity duality, describe a superconducting state in the dual theory [12]. Such constructions may be useful in understanding the physics of strongly coupled high temperature superconductors. Furthermore, strange metals comprise a class of materials which deviate from the standard Fermi liquid theory description. Their physics is largely controlled by a strongly coupled fixed point, described by a finite temperature conformal field theory. Holographic models have been used to approach these systems with the aim of capturing broad features of their behaviour [13], [14]. Both holographic superconductors and strange metals will be discussed in more detail in sections 1.4.4 and 1.5.5 respectively.

String theory also contains de Sitter (dS) vacua [15]. dS describes an expanding spacetime and is described by a solution to general relativity with a positive cosmolog-

ical constant, like our own expanding universe, motivating applications of string theory to cosmology. In the context of holography, cosmological applications have led to the formulation of a dS/CFT correspondence which aims at relating quantum gravity on dS to a conformal field theory [16]. This particular duality is currently not as well understood as the AdS/CFT correspondence.

A particularly surprising application of holography is to fluid mechanics. It turns out that the Einstein equations in five dimensions (with a negative cosmological constant) contain the four dimensional Navier-Stokes equations, leading to a fluid/gravity correspondence. For every fluid solution there is a corresponding black hole solution with a temperature and a velocity field which matches the fluid [17]. Using this formalism, a new pseudovector contribution to the charge current of a charged fluid was discovered [18], [19] which corrects old classic textbook results [20]. The fluid/gravity correspondence is an active area of investigation with one aim being shedding light on longstanding problems of turbulence in fluid mechanics. More details about the fluid/gravity correspondence will be given in section 1.4.3.

Increasingly realistic holographic models necessitates new, less symmetric, gravitational solutions. As such, the advent of holography has also sparked renewed interest in finding and classify solutions of general relativity and more complex theories, e.g. supergravity and theories with more interesting matter content. Prominent examples include asymptotically AdS hairy black holes discovered in the context of holographic superconductors [12] as well as numerically constructed black hole solutions which display turbulent horizons [21].

Principles of quantum information theory make an important apperance in holographic constructions. In [22], a proposal for computing the entanglement entropy between regions in a CFT from the gravitational dual is given. Entanglement entropy is a measure of the degree to which quantum states are correlated, i.e. entangled. The conjecture states that entanglement entropy in a conformal field theory is encoded in the

area of the minimal surfaces in the dual spacetime geometry. This conjecture was subsequently proved in [23]. By now, other entanglement probes have been considered and found to have geometric interpretations in a gravity dual. Examples include differential entropy [24], and entanglement negativity [25]. These observations suggest that many of the details about the structure of spacetime in the dual gravity theory are encoded in the entanglement properties of the field theory.

It is a tempting question to ask how much the duality can tell us about the black hole information paradox. Hawking discovered that black holes radiate [26], [27] and that the quanta emitted by black holes do not carry carry information about anything behind the horizon; only information associated with conserved charges can be measured at infinity like mass and charge. In this sense, black holes eat information; any information about a state which falls into a black hole appears to be lost. This is in sharp contrast to quantum mechanics where time evolution is unitary and information is not lost.

Gauge/gravity duality tell us that the entire description of a collapsing black hole can be formulating in terms of a unitary gauge theory, meaning that the entire collapse process itself should be unitary and information cannot be lost. This argument does not resolve the information paradox [28], however, as it does not provide a mechanism by which information can be returned. It turns out that the situation is richer than previously imagined. By appealing to the monogamy of entanglement, [29] showed that the following three statements are incompatible: information is not lost (i.e. unitary evolution), effective field theory works near the black hole horizon, and nothing bad happens to an observer falling through the horizon. The second statement about effective field theory is tantamount to trusting general relativity near the horizon. If we do, the third point is where things go wrong: the infalling observer encounters something dramatic at the horizon called a "firewall". Whether or not a firewall does occur is a question aimed at understanding just how good of an effective theory general relativity is near a horizon; this question remains unsettled. An interesting potential resolution to

the problem is centred on arguments from quantum information theory. In [30], it was argued that quantum information theory places constraints on getting information out of a black hole and that limits on quantum computing may prevent an observer from being able to detect a firewall. However this eventually turns out, the picture which has developed in recent years is that quantum information theory constraints are crucial for understanding quantum gravity.

The nexus for all of these interesting themes in physics is holography. At the most basic level, it provides us with a set of tools to address questions related to all of the topics discussed above and as such makes up one of the corner stones of modern theoretical physics. In the next section 1.2 we will begin by motivating the existence of a holographic principle from the perspective of gravitational physics before launching into details about the original string theory construction of the AdS/CFT correspondence. Our ultimate goal in the first chapter will be to map out the lay of the land for modern holography, to introduce the set of tools which make gauge/gravity duality powerful for applications, and to orient ourselves in the vast literature on applied holography. Our aim will be to set up the necessary context to introduce our novel results presented in chapters 2 and 3. Finally, chapter 4 will strive to point out some fruitful directions for future explorations in applied holography.

1.2 Gauge/Gravity duality

Gauge/gravity duality has its roots in the holographic principle [31], [32] which asserts that the physics of a gravitational theory may be encoded in a lower dimensional field theory. A simple way to motivative this picture is through black hole thermodynamics. The entropy of a black hole is given by the Bekenstein-Hawking formula

$$S_{BH} = \frac{A_H}{4G_N}\,, \tag{1.2.1}$$

where A_H is the area of the black hole horizon and G_N is the Newton constant. In other words, the entropy of a black hole is proportional to an area rather than a volume as might be naïvely expected [1]. The maximum amount of entropy in a region V is equal to the entropy, S_{BH}, of the biggest black hole that can fit inside the region. To see why this is true, consider a setup in which there is some mass, less than the mass required to form a black hole, and an entropy greater than that of a black hole. Start adding mass to the system; this causes both the total mass and the entropy to increase. Continuing in this way, a black hole will eventually form, at which point the entropy of the system will need to decrease down to S_{BH}, violating the second law of thermodynamics. This behaviour is in stark contrast with a regular field theory where the maximum entropy in a region scales like the volume of the region. This observation hints at the notion that the dual field theory will need to live in one lower dimension than the gravitational theory in order to get the entropy on both sides to scale correctly.

A model of exactly this kind of duality is described by the now famous AdS_5/CFT_4 correspondence between type IIB superstring theory on the product space $AdS_5 \times S^5$ and $3+1$ dimensional $\mathcal{N}=4$ supersymmetric Yang-Mills (SYM) [1]. Here, AdS_5 refers to $4+1$ dimensional anti de Sitter space. This specific duality will be discussed in some detail in section 1.2.1. Other examples were also conjectured in [1] including a duality between a $1+1$ dimensional $\mathcal{N}=(4,4)$ CFT and type IIB superstring theory on $AdS_3 \times S^3 \times \mathcal{M}_4$, where the four dimensional manifold $\mathcal{M}_4$ is either a four torus T^4 or $K3$. Also conjectured was a duality between M-theory on $AdS_4 \times S^7/\mathbb{Z}_k$ and $AdS_7 \times S^4$ being dual to a $2+1$ dimensional $\mathcal{N}=6$ Chern-Simons theory and a $5+1$ dimensional $\mathcal{N}=(2,0)$ CFT, respectively. Recently, holographic dualities have also been conjectured between Vasiliev higher spin theories and vector model CFTs in $2+1$ dimensions [34] and a minimal coset CFT in $1+1$ dimensions [35].

[1] Our units follow the conventions of [33]. This will be the case throughout the rest of this thesis unless explicitly stated.

Notably, gauge/gravity correspondence defines a weak/strong duality; when the field theory is strongly coupled the gravity theory reduces to classical type IIB supergravity. The weak/strong nature of the duality sits at the heart of its applicability as it provides an avenue for investigating strongly coupled phenomena. This thesis will be interested in applications of gauge/gravity duality where an exact understanding of the theories used in the duality may be lacking, so it is important to understand how such a duality can be taken seriously on general grounds. A useful review in this context is [36]. Broadly, the gauge/gravity duality conjecture states that under the right circumstances, a quantum field theory may be described by an equivalent gravitational theory in one higher dimension. More specifically, a gravitational theory on some background geometry is physically equivalent to a quantum field theory (QFT) without gravity living on the boundary of the spacetime. Consider a bulk geometry which is asymptotically AdS_{d+1}

$$ds^2 = \frac{z^2}{L^2}\left(-dt^2 + dx_i^2\right) + \frac{L^2}{z^2}dz^2\,, \tag{1.2.2}$$

where L is the radius of curvature of AdS and z is the radial coordinate. In these coordinates the boundary is at $z \to \infty$. Asymptotically AdS spaces have a number of features which make a holographic duality likely. In particular, partial waves do not fall off asymptotically as $z \to \infty$ as they do in flat space, suggesting that the boundary can know what is happening in the rest of the spacetime and vice versa. Also, this geometry is conformally flat as can be seen by switching coordinates to $r = L^2/z$. The boundary is conformal to Minkowski space and this is where the dual field theory will be thought to live. Furthermore, in $2+1$ dimensions, the symmetry algebra of asymptotically AdS_3 spacetimes reduces to the Virasoro algebra at the boundary. In fact, this result was known for some time before the advent of the AdS/CFT correspondence [37].

The AdS metric (1.2.2) is scale invariant under the transformation $x^\mu \to \lambda x^\mu$ and $z \to z/\lambda$, where x^μ denotes all of the coordinates other than the radial coordinate z, and λ is a constant. In fact, the isometries of AdS_{d+1} encode full conformal invariance, so the dual field theory must be a conformal field theory (CFT) [36]. A CFT is scale

invariant, so under the transformation $x^\mu \to \lambda x^\mu$ of the boundary coordinates any energy scale E must transform as $E \to E/\lambda$ by dimensional analysis. Comparing this with the transformation required of the bulk radial coordinate suggests that $E \sim z$, meaning that the radial direction in the bulk encodes the energy scale of the dual field theory. This statement will be made more precise in section 1.2.1 when we discuss the UV/IR relations. At this point, it suffices to see that $z \to \infty$ corresponds to the UV in the dual field theory, while $z \to 0$ corresponds to the IR, suggesting a renormalization group (RG) flow interpretation of the radial direction in the bulk. This correspondence can be seen within a radial Hamilton-Jacobi framework [38].

Anti de Sitter space is a solution to Einstein gravity with a negative cosmological constant. At the very minimum then, the bulk gravitational theory should be described by the Einstein-Hilbert action with a negative cosmological constant plus some possible matter sector. Examples of possible matter sectors will be discussed in section 1.2.1 as well as in sections 1.4 and 1.5 in the context of applied holography. Nothing has been assumed about the geometry in the interior towards decreasing z. The duality may be understood by fixing the asymptotic condition that the spacetime geometry approaches AdS (1.2.2) at large z. The existence of a large class of possible interior solutions is central to the applicability of holography to modelling the phenomenology associated with the boundary theory. Relaxing the requirement of having a negative cosmological constant has also been studied leading to a dS/CFT correspondence for positive cosmological constant [16]. As of yet, there is no microscopic derivation of this duality and it seems to require a non-unitary dual field theory. There is also a proposed dual between the extreme Kerr black hole and a chiral two-dimensional CFT with central charge proportional to the angular momentum of the Kerr black hole [39]. The black hole geometry in this duality is extreme in the sense that its angular momentum J is maximally large. For reviews, see [40] and [41].

The next feature to understand is how the number of degrees of freedom in the bulk

match up with that of the boundary theory. In line with the holographic principle, the maximum entropy described by the bulk theory is the entropy of the largest black hole that can fit inside. This corresponds to a black hole whose event horizon is right at the boundary of the geometry. In this case

$$A_H = \int d^{d-1}x \left(\frac{z^{d-1}}{L^{d-1}}\right)_{z\to\infty,\, t=\text{const}} \to \infty\,. \tag{1.2.3}$$

The fact that the integral diverges is not surprising; it indicates that a regularization protocol is necessary. This is in line with the expectation from the field theory which may suffer from divergences. In section 1.3.2 a detailed prescription for holographic renormalization will be discussed.

The field theory may be regularized by putting it in a box of side length L and introducing a lattice with a spacing ϵ. Suppose that at each lattice site there are N^b degrees of freedom, where b is a positive constant. The precise value of b is, at the moment, not important. For the AdS_5/CFT_4 it will turn out that $b = 2$. For $M2$-brane holography, $b = 3/2$, while for $M5$-branes $b = 3$. In the more exotic higher spin/vector model dualities discussed in section 1.2.3 it will turn out that $b = 1$ in $3 + 1$ bulk dimensions. It follows that the total number of degrees of freedom in the boundary theory is then $(L/\epsilon)^{d-1}N^b$.

In order to regulate the horizon area, a radial cutoff near the boundary is introduced. It is convenient to change coordinates to $r = L^2/z$, as this will make comparison with the field theory result easier. To this end, the boundary cutoff is placed at $r = \epsilon$ and the Bekenstein-Hawking entropy is

$$S_{BH} = \frac{A_H}{4G_N} = \frac{L^{d-1}}{4G_N}\left(\frac{L}{\epsilon}\right)^{d-1}\,. \tag{1.2.4}$$

Comparing this result to the number of degrees of freedom from the regulated boundary theory we find that $L^{d-1}/G_N \sim N^b$ [36].

Throughout this discussion, the bulk theory has been assumed to be, at a minimum, Einstein gravity. To stay within this classical regime, the radius of curvature of AdS

should be very large compared to the Planck length. Recall that in $D = d+1$ dimensions, $16\pi G_N = (2\pi)^{d-2} l_D^{d-1}$, where l_D is the D-dimensional Planck length [42]. Hence, we insist that $L^{d-1}/G_N \gg 1$, meaning that $N \gg 1$ in the dual field theory.

As we will see, this large N condition will fit in naturally with the 't Hooft limit in the dual theory and will serve as the basis for understanding the weak/strong nature of gauge/gravity duality. In other words, when the bulk theory is classical gravity, the dual field theory is strongly coupled. This property is central to the applicability of holography; it provides us with a powerful tool for studying strongly coupled field theories.

With the general idea of holography in mind, we now describe some explicit examples.

1.2.1 String origins: AdS_5/CFT_4

The AdS_5/CFT_4 duality states that type IIB superstring theory with N units of five form flux on $AdS_5 \times S^5$ is dual to $\mathcal{N} = 4$ super Yang-Mills (SYM) in four spacetime dimensions with gauge group $SU(N)$ [1]. While there is as of yet no full path integral proof of this conjecture, it can nevertheless be motivated by studying the dynamics of $D3$-branes and may be studied in particular regions of parameter space as we will describe below. By now, there are many reviews on this subject including [43], [44], [45], [46].

In order to motivate the duality, it is useful to study the dynamics of $D3$-branes and see that their dynamics may be described equivalently from a gravity perspective or from the perspective of the gauge theory living on their worldvolume.

The gravity theory in this duality is type IIB superstring theory. In the low energy limit, an effective description of the gravitational physics (i.e. closed strings) is provided by type IIB supergravity. The theory lives in $D = 10$ and has $\mathcal{N} = 2$ chiral supersymmetries. The field content includes the graviton G_{MN}, a two-form B_2 and the dilaton Φ, an axion C_0, a two-form C_2, a four-form C_4 (which has a self-dual field strength), two Majorana-Weyl gravitinos ψ_{Ma} and two Majorana-Weyl dilatinos λ_a [2]. Recall that the

dilaton controls the string coupling $g_s = e^{\phi}$ with $\phi = \langle \Phi \rangle$.

In what follows, capital letters $M, N, \ldots$ will denote ten dimensional spacetime indices and small letters $a, b, \ldots$ label the supersymmetries, $a = 1, \ldots, \mathcal{N}$. Starting from the equations of motion, it is possible to construct an action for this theory provided that the self-duality of the field strength associated with C_4 is imposed separately

$$\begin{aligned} S_{IIB} = \frac{1}{2\kappa_{10}^2} \int \sqrt{-G}\, e^{-2\Phi} \left(R_G + 4\partial_M \Phi \partial^M \Phi - \frac{1}{2} |H_3|^2 \right) \\ - \frac{1}{4\kappa_{10}^2} \int \left[\sqrt{-G} \left(|F_1|^2 + |\tilde{F}_3|^2 + \frac{1}{2} |\tilde{F}_5|^2 \right) + C_4 \wedge H_3 \wedge F_3 \right] + \text{fermions}\,, \end{aligned} \tag{1.2.5}$$

where

$$|F_p|^2 = \frac{1}{p!} G^{M_1 N_1} \cdots G^{M_p N_p} F_{M_1 \ldots M_p} F_{N_1 \ldots N_p}\,, \tag{1.2.6}$$

The new quantities in (1.2.5) are defined as: $F_{n+1} = dC_n$, $H_3 = dB_2$, $\tilde{F}_3 = F_3 - C_0 H_3$ and $\tilde{F}_5 = F_5 - (1/2) C_2 \wedge H_3 + (1/2) B_2 \wedge F_3$ and R_G is the Ricci scalar associated to the ten dimensional metric G_{MN} [2].

In order to see how the correspondence is manifested, we will focus on a stack of N $D3$-branes. In this case, the spacetime metric (the bulk) sourced by the stack is [46]

$$ds_{10}^2 = H(r)^{-1/2} \left(-dt^2 + dx_1^2 + dx_2^2 + dx_3^2 \right) + H(r)^{1/2} \left(dr^2 + r^2 d\Omega_5^2 \right)\,, \tag{1.2.7}$$

where the x_i are the directions along the branes, while the radial coordinate r denotes the transverse directions. $d\Omega_5^2$ is the metric on the unit five sphere. The harmonic functions $H(r)$ are given by

$$H(r) = 1 + \frac{L^4}{r^4}\,, \tag{1.2.8}$$

with

$$L^4 = 4\pi g_s N l_s^4\,. \tag{1.2.9}$$

The solutions for the bosonic fields are $g_s = e^{\phi} = \text{constant}$, $C = \text{constant}$, $B = A_2 = 0$, $F_{5 \mu\nu\rho\alpha\beta} = \epsilon_{\mu\nu\rho\alpha\beta\eta} \partial^{\eta} H(r)$, where the indices here run over the directions transverse to the stack [44]. Notice that the dilaton is constant here.

There are two interesting limits to study, $r \gg L$ and $r \ll L$. In the former limit $H(r) \approx 1$ and this corresponds to a flat $\mathbb{R}^{1,9}$ region of the geometry. Conversely, taking the limit $r \ll L$ leads to a bulk $AdS_5 \times S^5$ geometry which can be seen by changing the radial coordinate to $z = L^2/r$ with the resulting metric

$$ds_{10}^2 = \frac{L^2}{z^2}\left(-dt^2 + dz^2 + dx_1^2 + dx_2^2 + dx_3^2\right) + L^2 d\Omega_5^5\,, \tag{1.2.10}$$

where the radius of the AdS geometry and of five sphere is L in (1.2.9). This limit will be of primary interest to the duality. Notice that the AdS_5 part of the geometry is conformally flat. The boundary of the AdS_5 is at $z \to \infty$ ($r = 0$ in the original coordinates) the conformally related Minkowski space at this radial position is where the dual field theory will be thought to live. This limit corresponds to zooming in very close to the stack of branes. The stack of N $D3$-branes may also be studied from the point of view of open string physics, which leads to the identification of a worldvolume gauge theory.

Dp-branes contain a gauge theory living on their worldvolume. Recall that open strings may end on Dp-branes and that the endpoints of strings are charged. This immediately suggests that the worldvolume theory living on the Dp-brane should contain a gauge field. For a single brane, this is a $U(1)$ gauge field. There are a variety of other process that may occur as well, for example a closed string may interact with a brane and become an open string with its endpoints attached to the brane. Similarly, an open string may form closed strings and break off from a brane. There are also other degrees of freedom associated to the brane; they correspond to deformations and rigid motions of the brane [46]. These are parameterized in terms of the coordinates transverse to the $(p+1)$ dimensions of the Dp-brane. For each of the $9-p$ spatial directions, there is a scalar X^r which lives on the Dp-brane world volume. We will be primarily interested in a stack of N $D3$-branes. It is possible for open strings to start on one brane in the stack and end on another. In this case, the gauge field described by the string endpoints is not just a $U(1)$ field but is promoted to $U(N)$. The gauge field and scalars X^r transform under

the adjoint representation of the $U(N)$ gauge field. In this case, the low energy effective action which accounts for these excitations is the non-Abelian DBI (Dirac-Born-Infeld) action. For a single brane, the Abelian DBI action is [2]

$$S = S_{\rm DBI} + S_{\rm WZ}\,, \tag{1.2.11}$$

where

$$S_{\rm DBI} = -\frac{1}{g_s(2\pi)^p l_s^{p+1}} \int d^{p+1}\sigma e^{-\Phi} \sqrt{-{\rm det}\mathbb{P}\left[G_{MN} + (2\pi\alpha' F_{MN} + B_{MN})\right]}\,, \tag{1.2.12}$$

where $\mathbb{P}$ denotes the pullback to the worldvolume and σ are the worldvolume coordinates. Also

$$S_{\rm WZ} = -\frac{1}{(2\pi)^p l_s^{p+1}} \int \mathbb{P}\exp(2\pi\alpha' F_2 + B_2) \wedge \oplus_n C_n\,. \tag{1.2.13}$$

Note that the DBI action is not the full effective action for the theory. The DBI action only concerns powers of the field strength. In particular, for the non-Abelian case, it neglects terms involving covariant derivatives of the field strength. The DBI action should be thought of as a valid low energy approximation to the dynamics of a D-brane when the background fields and worldvolume gauge fields are slowly varying with respect to the string scale. The non-Abelian case also displays some peculiar behaviour compared to the Abelian action such as the Myers effect [47]. In the Abelian case, the scalar fields X^r are interpreted as the transverse coordinates on the brane. In the $U(N)$ case, these fields are described by $N \times N$ matrices, making this interpretation unclear. Myers considered an example of N $D0$-branes in the background of a constant four-form flux and showed that this inherent uncertainty results in a fuzzy description of the brane positions. The mean-square value of the coordinates defines a fuzzy sphere; a non-commutative sphere.

There is a $U(1)$ subgroup that describes an overall translation of the entire stack. This is not a particularly interesting feature and may be decoupled from the rest leaving a $SU(N)$ gauge theory living on the worldvolume of the brane.

In the $D3$-brane case, there are six scalar fields X^r as the worldvolume has $3+1$ dimensions. The DBI action in this case may be expanded in powers of $F_{\mu\nu}$ and $\partial_\mu X^q$

and the resulting action is identified as $\mathcal{N} = 4$ SYM with an $SU(N)$ gauge group plus $\alpha' = l_s^2$ and g_s corrections. The Yang-Mills coupling in terms of g_s is [46]

$$g_{\rm YM}^2 = 4\pi g_s \,. \tag{1.2.14}$$

The Lagrangian for $\mathcal{N} = 4$ SYM is [44]

$$\mathcal{L} = \frac{1}{g_{\rm YM^2}} \mathrm{tr} \left\{ -\frac{1}{2}F^2 + \frac{\theta_I}{8\pi^2} F_{ij}\tilde{F}^{ij} - \sum_a i\bar{\lambda}^a \bar{\sigma}^i D_i \lambda_a - \sum_r D_i X^r D^i X^r \right.$$
$$\left. + \sum_{a,b,r} C_r^{ab} \lambda_a [X^r, \lambda_b] + \sum_{a,b,r} \bar{C}_{rab} \bar{\lambda}^a [X^r, \bar{\lambda}^b] + \frac{1}{2} \sum_{r,s} [X^r, X^s]^2 \right\} , \tag{1.2.15}$$

where the parameter $\theta_I \in [0, 2\pi]$ is the instanton angle. The constants C_r^{ab} are the Clifford matrices for $SO(6)_R \cong SU(4)_R$ associated to the R-symmetry of the theory. The index conventions used here are that $i\,, j$ are $3+1$ dimensional spacetime indices, $r\,, s$ label the scalar fields (there are six), $a = 1, \ldots, 4$ label the supercharges (i.e. $\mathcal{N} = 4$). Also, D_i is the usual covariant derivative and $\tilde{F}$ is the Hodge dual of F. The σ^i are the Pauli matrices.

The theory contains a gauge field, A_i, six scalar fields X^r and four two-component, complex Weyl spinors λ^a. The fields transform under the adjoint representation of $SU(N)$. This can be understood by noting that the theory describes the dynamics associated to the endpoints of open strings which connect the $D3$-branes. The Lagrangian (1.2.15) may be obtained from $D = 10$, $\mathcal{N} = 1$ SYM by dimensional reduction on a six-torus T^6.

By construction, the theory described by (1.2.15) is invariant under $\mathcal{N} = 4$ Poincaré supersymmetry in the superconformal phase [44]. This phase is characterized by minimizing the potential $\sum_{r,s}[X^r, X^s]^2$ in (1.2.15). The easiest way to do this is to set the vacuum expectation value (vev) of each scalar field X^r to vanish. This vacuum preserves the full conformal invariance of the Lagrangian (1.2.15). Invariance under translations, Lorentz transformations, dilations and special conformal transformations combine into full conformal symmetry. Furthermore, the theory contains Poincaré supersymmetries

generated by supercharges and their complex conjugates, R-symmetry, and conformal supersymmetries. The latter are generated since special conformal transformations and the Poincaré supersymmetries do not commute. Putting all the pieces together, the overall symmetry group is the supergroup $SU(2,2|4)$ [44].

By combining the Yang-Mills coupling with N, the 't Hooft coupling here is $\lambda = g_{\rm YM}^2 N$. By taking the simultaneous limit $g_{\rm YM} \to 0$ and $N \to \infty$, non-planar diagrams become suppressed by powers of $1/N$. This limit will be interesting in what follows.

Thus far, the dynamics of the $D3$-brane stack is described by an open string part in the form of the worldvolume theory, a bulk closed string part given by the gravity action, and potential interactions between the brane and bulk parts which arise from couplings between the bulk R-R fields and the $SU(N)$ field strength on the brane worldvolumes.

Comparing the gravity and gauge theory descriptions of the stack of $D3$-branes leads to the identification of (1.2.9) and (1.2.14). This is a crucial step as we still need to determine over what range it is valid to compare SYM theory to the supergravity solution. Supergravity is a good approximation to string theory when dilaton and string tension corrections are small. Solving for g_s and rearranging gives

$$\left(\frac{L}{l_s}\right)^4 = \lambda \,. \tag{1.2.16}$$

Using (1.2.14) and the definition of λ gives

$$g_s = \frac{\lambda}{4\pi N} \,. \tag{1.2.17}$$

The next step is to take the limit that $N \gg 1$ while holding λ fixed. From (1.2.17), this means that dilaton corrections, which correspond to string loop corrections, are small. Furthermore, taking $\lambda \gg 1$, it follows from (1.2.16) that L is much larger than the string scale and string tension corrections are suppressed. This is called the decoupling limit. As a consequence, using (1.2.16) and the definition of the ten dimensional Planck constant, the AdS radius is much larger than the Planck scale $L \gg l_p$.

In the decoupling limit, the interactions between the open strings ending on the $D3$-branes and the closed strings in the bulk are turned off. After taking this limit, $\mathcal{N} = 4$ SYM remains on the $D3$-branes and the bulk is described by the supergravity solution in the near horizon limit. Since the stack of $D3$-branes may be described in either language, the two are declared to be same, leading to the statement of the AdS/CFT conjecture.

In summary, what we have seen is that there exists an equivalent description of the stack of N $D3$-branes, from the point of view of gravitational (closed string) physics and the worldvolume $\mathcal{N} = 4$ SYM theory (open string). This relation looks valid so long as $N \gg 1$, $\lambda \gg 1$, meaning that strongly coupled $\mathcal{N} = 4$ SYM in the planar limit is described by type IIB supergravity on $AdS_5 \times S^5$. The field theory side is characterized by an expansion in $\lambda^{-1/2}$, whereas the gravity side has an expansion in α'. It is conjectured that the duality is true for all N and g_{YM} on the field theory side, being dual to full type IIB string theory on $AdS_5 \times S^5$ on the gravity side which is called the strong form of the duality. [44].

In section 1.2, it was hinted that the radial direction in the bulk geometry corresponds to the energy scale of the dual field theory. Importantly, this means that in order to understand the dual field theory at all energy scales, it is necessary to utilize the entire bulk geometry. Moving away from the boundary region, the geometry may deviate away from AdS. This radial evolution reflects how the dual field theory behaves at different energy scales. This observation emphasizes the importance of AdS asymptotics in setting up the duality. It is through this boundary condition that the correspondence between bulk and boundary observables is established.

Within the AdS_5/CFT_4 duality, the relationship between the radial direction and the energy scale of the dual field theory may be established by considering a string stretched between two $D3$-branes. By slowly pulling one of the branes off of the stack, the string is stretched out. The tension of a string is just $T = 1/2\pi\alpha'$. For a relativistic string, the tension is a linear mass (energy) density, so $T \sim E/r$. Hence, $E \sim r$. While this

argument gets the point across, the result may be established more rigourously. In fact, an important point is that not every bulk supergravity probe will respect exactly the same energy-radius relation. For the case here of $D3$ branes it turns out that conformal invariance fixes the scaling $E \sim r$. The coefficients may be fixed by studying how supergravity probes propagate in the background sourced by the stack of branes, leading to the UV/IR relations [1], [48], [49].

It is also easy to establish that the symmetries on both sides of the duality match. In the superconformal phase of $\mathcal{N} = 4$ SYM that we have discussed above, the full symmetry group is $SU(2,2|4)$ which has a maximal bosonic subgroup $SU(2,2) \times SU(4)_R \cong SO(2,4) \times SO(6)_R$ [44], where the subscript R identifies the group associated to the R-symmetry of the theory. The bosonic symmetry group matches the symmetries of $AdS_5 \times S^5$ since the group of isometries of AdS_5 is $SO(2,4)$ and the S^5 encodes the usual group of rotations $SO(6)$, hence the bulk geometry has a full isometry group $SO(2,4) \times SO(6)$, matching the bosonic symmetries on the field theory side. The gravity solution also contains the right number of fermionic symmetries. $AdS_5 \times S^5$ is a maximally supersymmetric solution of type IIB theory with 32 preserved supersymmetries, matching the 32 supercharges of $\mathcal{N} = 4$ SYM which is also maximally supersymmetric [46]. When combined with the bosonic symmetries encoded in the spacetime geometry, the full symmetry group on the bulk side is $SU(2,2|4)$, precisely matching the field theory side.

The correspondence may be generalized by adding finite temperature of the field theory [50], [51]. This corresponds to including a black hole in the bulk geometry. The field theory temperature is dual to the Hawking temperature of the black hole. Note that by adding a black hole to the geometry, a special radial position is introduced, namely the position of the horizon. This is sensible, as adding temperature to the field theory breaks the conformal invariance as there is now a scale. This scale is encoded by the appearance of the horizon position on the gravity side.

The role of the S^5 part of the bulk geometry may be understood by noting that any field on $AdS_5 \times S^5$ can be expressed as a tower of fields purely in AdS_5. This can be seen by performing a dimensional reduction on the S^5. The resulting bulk action for a ten dimensional matter field with gravity is schematically [46]

$$S = \frac{1}{16\pi G_5} \int d^5x \left[\sqrt{-g} \left(R_5 + \frac{12}{L^2} \right) + \mathcal{L}_{\text{matter}} \right], \tag{1.2.18}$$

where G_5 and R_5 are the five dimensional Newton constant and Ricci scalar, respectively. The second term in the action is the cosmological constant for an asymptotically AdS spacetime. $\mathcal{L}_{\text{matter}}$ is the matter Lagrangian in five dimensions. An instructive example is a massless scalar in ten dimensions. Note that by taking the $\alpha' \to 0$ limit, we are essentially left with only massless modes on the supergravity side. Massive modes result from dimensional reduction on the S^5 following the Kaluza-Klein procedure [46]. For a massless scalar, the resulting five dimensional equations of motion are $\Box\phi - m^2\phi = 0$, where $m^2 = l(l+4)/L^4$ with $l = 0, 1, 2, \ldots$ are the eigenvalues of the Laplacian on S^5.

The final step is to construct an actual one-to-one mapping between operators and states on both sides of the duality. A procedure for how to accomplish this is outlined in [50] and [51]. A large list of some of the various correspondences may be found in [44]. A few examples include the axion $C \sim \text{tr}(F\tilde{F})$ and the gravitino $\psi \sim \text{tr}\,(\lambda X^r)$ with $r \geq 1$.

Note that in the correspondence described above, the gravity side metric is the Poincaré patch of AdS. The duality may also be formulated in global AdS where the dual theory lives on the boundary $\mathbb{R} \times S^3$, which is the Einstein static universe [51]. Global time translations in the Einstein static universe are generated by a Hamiltonian H which is linear combination of the generators of translations and special conformal transformations on $\mathbb{R}^{1,3}$. By redefining the Hamiltonian, the CFT can be thought of as living on $\mathbb{R} \times S^3$. The isometries of the bulk spacetime are dual to the conformal group of the field theory. Changing to this new Hamiltonian means identifying the generator of global time translations in the bulk. In other words, the bulk should be global AdS [43].

The particular example of the AdS_5/CFT_4 duality provides a powerful realization of

the holographic principle. Other proposals include $D1D5$ [43], [52], $M2$ [53] and $M5$ [43] dualities, as well as higher spin/vector model dualities in four [54] and three [35] bulk dimensions . Further important developments include the breaking of supersymmetry [55] as well as the connection to integrability [56].

1.2.2 ABJM theory

The degrees of freedom of D-branes may be understood in terms of the strings that stretch between them. Such an intuitive picture is not available in M-theory and understanding the degrees of freedom associated with membranes is difficult. Early progress for multiple $M2$-branes was made in [57] and later in [58] which lead to an important example of a holographic duality between M-theory on $AdS_4 \times \mathbb{C}^4/\mathbb{Z}_k$ and an $\mathcal{N} = 6$, $U(N) \times U(N)$ Chern-Simons gauge theory with integer levels $(k, -k)$, called ABJM theory (Aharony, Bergman, Jafferis, Maldacena). It contains a matter sector with four matter supermultiplets in the bifundamental representation of the $U(N) \times U(N)$ gauge group. For reviews see [53], [59] and [60]. For $N = 1$, the moduli space of ABJM is $\mathbb{C}^4/\mathbb{Z}_k$. This is the same moduli space as a single $M2$-brane probing the singular point of a $\mathbb{C}^4/\mathbb{Z}_k$ orbifold [59]. This result carries through for general N, hinting at the possibility of the duality. For ABJM theory, $\lambda = N/k$ plays the role of the 't Hooft coupling, so that the theory becomes weakly coupled for $N \ll k$. Conversely, for $N \gg k$, the field theory is strongly coupled and the gravity side reduces to 11-dimensional supergravity.

Consider a stack of N $M2$-branes. The extremal geometry sourced by the stack is [53]

$$ds_{11}^2 = H(r)^{-2/3}\left(-dt^2 + dx_1^2 + dx_2^2\right) + H(r)^{1/3}\left(dr^2 + r^2 d\Omega_7^2\right) , \tag{1.2.19}$$

where $d\Omega_7^2$ is the metric on a unit seven sphere. Here, r denotes the direction transverse to the stack while the directions along the branes are x_1 and x_2. The harmonic function $H(r)$ is given by

$$H(r) = 1 + \frac{R^6}{r^6} , \tag{1.2.20}$$

with $R^6 = 32\pi^2 N l_p^2$. Here, l_p is the eleven dimensional Planck length. The solution for the four-form (field strength) is [53]

$$F_4 = d^3x \wedge dH(r)^{-1} \,. \tag{1.2.21}$$

The duality conjectures that placing the stack of $M2$-branes at the singularity of a $\mathbb{C}^4/\mathbb{Z}_k$ orbifold in the near horizon limit, provides a gravity dual for ABJM theory. Note that in this case, the $d\Omega_7^2 \to ds_7^2$ in the gravity solution (1.2.19), where ds_7^2 is the metric on a unit $S^7/\mathbb{Z}_k$. The near horizon geometry is $AdS_4 \times S^7/\mathbb{Z}_k$ [59].

There is an interesting and puzzling feature about the proposed duality between M-theory and ABJM theory. The duality predicts that, at strong coupling, the number of degrees of freedom scales like $N^{3/2}$. This is markedly different from the behaviour seen in the original AdS_5/CFT_4 duality where the number of degrees of freedom scales like N^2. The latter result is easy to understand by labelling the endpoints of strings stretched between the stack of N $D3$-branes. One way to see how the gravity dual makes this prediction about strongly ABJM theory is to work at finite temperature. The gravity solution in this case is [53]

$$ds_{11}^2 = H(r)^{-2/3}\left(-f(r)dt^2 + dx_1^2 + dx_2^2\right) + H(r)^{1/3}\left(\frac{dr^2}{f(r)} + r^2 ds_7^2\right) , \tag{1.2.22}$$

where $f(r) = 1 - r_0^6/r^6$, with r_0 being the horizon position. $H(r)$ and F_4 are still given by (1.2.20) and (1.2.21) respectively. A simple way to see that the number of degrees of freedom scales like $N^{3/2}$ is to compute the Bekenstein-Hawking entropy at large λ, the leading order result is [53]

$$S_{BH} = \frac{2^{7/3}\pi^2 V_2 T^2 k^{1/2} N^{3/2}}{3^3} + \cdots \,, \tag{1.2.23}$$

where V_2 is the spatial volume of the stack of $M2$-branes. Another way to establish this result is to compute the free energy, which can be obtained from the gravity dual by evaluating the on-shell Euclidean action (note that it is important to take care to

renormalize the action first). The result is [60]

$$F(\mathbb{S}^3) \approx -\sqrt{\frac{2\pi^6}{27\,\mathrm{Vol}(\mathbb{S}^7/\mathbb{Z}_k)}}N^{3/2}\,, \tag{1.2.24}$$

where $\mathrm{Vol}(\mathbb{S}^7/\mathbb{Z}_k)$ is the volume of the unit $\mathbb{S}^7/\mathbb{Z}_k$. This result should be matched to the free energy of (Euclidean) ABJM theory on $\mathbb{S}^3$, since the partition function of a CFT on $\mathbb{S}^3$ encodes the number of degrees of freedom in the theory [51].

This exotic looking duality actually provides a powerful check on holography. Generally speaking, calculating anything on the field theory side of the duality at strong coupling is difficult. Nevertheless, for some supersymmetric QFTs a technique called path integral localization provides a tool for accessing strongly coupled results. The idea is as follows [60]. Suppose $S[\psi]$ is the action for some theory where the set of fields described by this theory is collectively labeled as ψ. Suppose further that this theory admits a Grassmann-odd symmetry, δ. Also, denote $\delta^2 = B_s$, which is a Grassmann-even symmetry of the theory. The partition function of the theory is augmented by adding a localizing term, that is

$$Z(\epsilon) = \int \mathcal{D}\psi e^{-S[\psi]-\epsilon\delta G}\,, \tag{1.2.25}$$

where G is a Grassman-odd operator which is invariant under B_s. Assuming that the path integral measure is invariant under δ, it follows that Z is independent of ϵ

$$\frac{dZ}{d\epsilon} = -\int \mathcal{D}\psi\delta\left(G\,e^{-S[\psi]-\epsilon\delta G}\right) = 0\,, \tag{1.2.26}$$

where the last equality follows from the assumption that δ is a symmetry of the integrand. Therefore, Z may be evaluated at any value of ϵ. In particular, taking the large ϵ limit is useful. If the δG has a positive definite bosonic part $(\delta G)_B$, then the integral localizes to configurations with $(\delta G)_B = 0$, which allows the path integral to be expressed in terms of a finite dimensional integral on this part of field space which can often be evaluated [60].

In [61], the technique of path integral localization was used to compute the free

energy of ABJM theory on $\mathbb{S}^3$ at strong coupling and found remarkable agreement with the holographic calculation, providing an honest path integral level check of the duality.

1.2.3 Higher spin: vector holography

A surprising class of holographic theories is the duality between a boundary CFT and Vasiliev higher spin gauge theory in AdS. Vasiliev theory is an interacting model of massless higher fields. For an up to date review see [62]. According to conventional wisdom, such a theory does not a priori make sense, since the Weinberg-Witten theorem and the Weinberg low-energy theorem tell us that there is no non-trivial S-matrix for interacting fields of spin greater than two. Vasiliev theory gets around this by working in a constant curvature background, namely AdS.

Working in a constant curvature background allows the theory to evade the standard arguments against the existence of non-trivial higher spin interactions. The reason is that the non-zero cosmological constant effectively imposes an IR cutoff on the theory and the higher spin interactions, thereby circumventing the Weinberg low-energy theorem. Furthermore, there are no asymptotic states in AdS, meaning that there is no well-defined S-matrix to begin with. For a review geared towards addressing these concerns see [63].

The result of this observation about curved spacetime leads to the Vasiliev equations. These are a fully consistent set of non-linear equations of motion for higher spin fields that describe interactions between particles of all spins. In AdS, the notion of massless is set by the curvature of background spacetime. The addition of a non-zero cosmological constant Λ defines a mass scale which scales like $\mathcal{O}(\sqrt{\Lambda})$. In this sense, there should be no difference between a massless particle and a particle with a Compton wavelength greater than the AdS radius $L \sim 1/\sqrt{\Lambda}$. In the Vasiliev theory, the gauge theory algebra is extended to a higher spin algebra which does not close unless all spins are included. In particular, the theory contains spin two, so gravity is always present. The theory

also contains a scalar field which is massive in four dimensions and massless in three dimensions. Actually, the Vasiliev equations are nominally background independent with AdS and dS being vacuum solutions. It should be pointed out that it is not known if the Vasiliev equations can be obtained from an action principle. Therefore, a precise procedure for how to quantize such a theory is unknown meaning that the existence of a higher spin gauge theory is only known at the classical level. It is an open question as to whether or not such a quantum theory can be defined by using holography.

Seeing as an AdS solution exists, it is natural to wonder if a higher spin theory can be dual to a CFT in the spirit of the AdS/CFT correspondence. This conjecture was actually raised some time ago [34] and later verified in [64]. For a review see [54]. By painstakingly evaluating correlation functions, it has been shown that an AdS_4 higher spin theory reproduces the results of both the bosonic and fermionic free and critical $\mathcal{O}(N)$ vector models. The bosonic case is described by the so-called A-type minimal Vasiliev model which describes a consistent truncation to fields of spin $s = 0, 2, 4, \ldots$ and the additional massive scalar field is assigned even parity. The fermionic duality arises from the B-type minimal Vasiliev model which also described fields of spin $s = 0, 2, 4, \ldots$ and the additional massive scalar is assigned odd parity (i.e. it is a pseudoscalar). The dualities have been extended to included all non-negative integer spins. The boundary theories in this case are either the bosonic or fermionic $U(N)$ vector models. There is a less understood dS/CFT version as well, first proposed in [65], which suggests that Vasiliev theory on dS_4 is dual to a theory of anti-commuting scalars.

The fact that the dual field theories are free was actually previously predicted. It has been shown in [66] that the existence of a conserved higher spin current places restrictions on the structure of the correlation functions of the theory, so much so that they match the results of a free theory.

The AdS_4/CFT_3 higher spin duality also encodes interesting gravitational physics. The holographic dictionary in this case relates $G_N \sim 1/N$, which is in contrast the usual

AdS/CFT setup where $G_N \sim 1/N^2$. This scaling may be understood by the fact that the bulk theory is a Vasiliev higher spin theory and not just Einstein gravity.

In [35], a duality between AdS_3 Vasiliev higher spin theory and a minimal model coset CFT with a $\mathcal{W}_N$ symmetry was discovered for large N. While technically complicated, the duality turns out to be extremely interesting as it was recently shown that the AdS_3 version of Vasiliev higher spin gauge theory may be understood as a subsector of string theory in the tensionless limit [67]. This is an important observation, suggesting the Vasiliev higher spin theory may provide a new avenue for exploring quantum gravity without appealing to full string theory. In other words, Vasiliev theory may provide an in-between theory with more structure than the low-energy limit of Einstein gravity, but less complex than the full string theory. It should be noted that this is believed to be only possible within the AdS_3 version of the Vasiliev higher spin theory. String theory already contains a tower of higher spin fields, the Hagedorn tower, for which the density of states grows exponentially with spin. For the Vasiliev theory in dimensions greater than three, the density of states of the higher spin fields grows linearly with spin. It is only in AdS_3 that the density of states grows exponentially with spin, and so has a possibility of describing a limit of string theory.

Considerably more is also understood about the gravitational physics encoded by three dimensional higher spin theories. In particular, the existence of black holes has been considered. For a review see [68]. Since the gauge group now contains spin two and higher, black hole horizons are no longer gauge invariant objects. That is, the existence of the horizon is not an invariant quantity under a higher spin gauge transformation. Three dimensional gravity is special in that the graviton does not have any propagating degrees of freedom. Nevertheless, in an asymptotically AdS space, there can still be nontrivial dynamics and this is captured by the dual two-dimensional CFT living on the boundary. It is possible to reformulate gravity in $2+1$ dimensions in terms of a Chern-Simons theory. By extending this construction to include higher spin fields, a

holonomy condition is proposed which diagnoses the existence of a black hole horizon. More specifically, it is shown that if this holonomy condition is satisfied, there exists a higher spin gauge transformation which makes the solution a black hole, meaning that there is a horizon and the higher spin fields are smooth there. This formulation has been used to explore the thermodynamics of three dimensional black hole solutions with higher spins as well as construct a generalization to the Cardy formula to include higher spin fields in the boundary theory [68], [69].

Explicit examples of holographic dualities are interesting from a formal perspective, shedding light on previously unknown relationships between seemingly unrelated theories. The further development of full fledged examples will be central towards aiding our understanding of what exactly quantum gravity is. For the kinds of applications we have in mind throughout the rest of this thesis, it will be crucial to be able to calculate quantities from one side of a gauge/gravity duality pair and translate them into concepts on the other side. In the next section we will review the construction of the holographic dictionary, given the minimal ingredients necessary for the existence of a duality.

1.3 Applications: how to compute quantities with holography

In order to make holography useful for real world application, it is necessary to have a well formed dictionary which allows us to translate concepts and quantities from one side of the duality to the other. Aspects of the boundary theory are encoded in surprising and not entirely obvious ways on the bulk gravity side. Often times, field theoretic concepts become "geometrized" on the gravity side, meaning they are expressed by some aspect of the bulk geometry. In this section we will review the construction of the holographic dictionary, including aspects of renormalization, as well as explore a few pertinent examples.

1.3.1 The dictionary

The holographic principle asserts that some quantum field theories in d dimensions are completely equivalent to a gravity theory in $d+1$ dimensions. Exactly what the theories on either side of the correspondence are is not fixed at this stage. We have seen examples of how formal gauge/gravity dualities arise in section 1.2. For the purposes of application, we will be less interested in complete examples of holographic dualities, and more interested in extracting features of strongly coupled field theories. The holographic dictionary is well established for spacetimes that are asymptotically AdS and we will be interested in these kinds of geometries in this section. Note however that extensions of the holographic dictionary to non-asymptotically AdS geometries do exist, as will be discussed in section 1.5.3.

AdS is a maximally symmetric solution to pure Einstein gravity with a negative cosmological constant and it is conformally flat. AdS is special in the sense that it has a timelike boundary at spatial infinity. In fact partial waves don't fall off in AdS as they do in flat spacetime. In this way, the boundary of spacetime can "know" about what's happening the interior and vice versa. As in the AdS_5/CFT_4 case, the holographic radial coordinate r encodes the energy scale of the dual field theory. Any asymptotically AdS spacetime can be written in Fefferman-Graham coordinates [70]

$$ds^2 = \frac{L^2}{r^2}\left(dr^2 + g_{ab}(r,\vec{x})dx^a dx^b\right) , \tag{1.3.1}$$

where L is a constant which sets the curvature scale of AdS, r is the radial coordinate which spans from $r=0$ at the boundary and $r=\infty$ in the interior. $g_{ab}(r,\vec{x})$ is the boundary metric which can be a function of the boundary coordinates and the radial coordinate (note, this is not the metric the dual field theory will live on) as $r \to 0$ it obeys an expansion

$$g_{ab}(r,\vec{x}) = g_{(0)ab}(\vec{x}) + \left(\frac{r}{L}\right) g_{(1)ab}(\vec{x}) + \left(\frac{r}{L}\right)^2 g_{(2)ab}(\vec{x}) + \cdots . \tag{1.3.2}$$

For pure gravity, plugging this expansion in the Einstein equations shows that the

$g_{(k)ab} = 0$ for k odd. The metric on the boundary is then the pullback of $g_{(0)ab}$. Selecting $g_{(0)ab} = \eta_{ab}$ returns the Poincaré patch of AdS. $g_{(0)ab}$ is only fixed up to conformal transformation, meaning that an asymptotically AdS geometry defines a conformal class of boundary metrics, not a unique metric. This result is also true for Einstein gravity coupled to matter, provided the matter contribution does not dominate over the cosmological constant so as not to destroy the asymptotic structure of the geometry. In terms of holography, this means that the dual operators are either marginal or relevant, so as not to disrupt the conformal UV fixed point.

A near boundary expansion, similar to (1.3.2), is true for other bulk field as well. In general, the expansion takes the form [70]

$$F(r,\vec{x}) = \left(\frac{r}{L}\right)^m \Bigg[F_{(0)}(\vec{x}) + \left(\frac{r}{L}\right) F_{(1)}(\vec{x}) + \left(\frac{r}{L}\right)^2 F_{(2)}(\vec{x}) + \cdots + \left(\frac{r}{L}\right)^n \left(F_{(n)}(\vec{x}) + \tilde{F}_{(n)}(\vec{x}) \ln\left(\frac{r}{L}\right) + \cdots\right)\Bigg] . \tag{1.3.3}$$

The field equations are second order differential equations, so there will be two independent solutions. These solutions scale differently asymptotically which is reflected in the expansion (1.3.3) by the power r^m and r^n. The coefficient $F_{(n)}$ is the Dirichlet boundary condition for the second solution which is independent of the one which starts at order r^m. Taking the expansion (1.3.3) and plugging in into the corresponding field equation results in a series of equations for each power of r. The idea is to solve each equation iteratively and constrain the coefficients in terms of lower order ones as much as possible. The general result is that $F_{(1)}, \cdots F_{(n-1)}$ and $\tilde{F}_{(n)}$ all turn out to be uniquely determined as functions of $F_{(0)}$ which itself is interpreted as a source term for a dual operator in the boundary field theory via the holographic prescription. $F_{(n)}$ is not determined by the near boundary expansion of the bulk field equations. Again, this is to be expected as this coefficient is related to the second linearly independent solution. Finally, $\tilde{F}_n$ is related to conformal anomalies of the dual theory [70]. For the metric, this will turn out to be the corresponding Weyl anomaly of the dual CFT. As a example, a scalar of mass

m behaves as

$$\phi(r,\vec{x}) = \left(\frac{r}{L}\right)^{d-\Delta}\left[\phi_{(0)}(\vec{x}) + \left(\frac{r}{L}\right)\phi_{(1)}(\vec{x}) + \cdots + \left(\frac{r}{L}\right)^{2\Delta-d}\left(\phi_{(2\Delta-d)}(\vec{x}) + \cdots\right)\right], \tag{1.3.4}$$

where Δ is a solution to $m^2L^2 - \Delta(\Delta - d) = 0$, or

$$\Delta = \frac{d}{2} \pm \sqrt{\frac{d^2}{4} + m^2L^2}\,. \tag{1.3.5}$$

Δ turns out to be the scaling dimension of the dual operator. Requiring that Δ be real results in

$$m^2 \geq -\frac{d^2}{4L^2}\,. \tag{1.3.6}$$

This is the famous Breitenlohner-Freedman (BF) bound. Scalar fields in AdS can be a bit tachyonic; below this bound AdS is unstable.

With an understanding of the bulk field in hand, the basic relation which provides a means to construct a phrase book from the gravity side to the field theory side is the Gubser-Klebanov-Polyakow-Witten (GKPW) relation [50], [51]. It relates the partition function of the boundary theory to the partition function of the bulk gravity theory

$$Z_{QG}(\psi_{(0)}) = Z_{QFT}(\psi_{(0)}) = \left\langle \exp\left(i\int_{\partial AdS} d^dx\psi_{(0)}(x)\mathcal{O}(x)\right)\right\rangle_{QFT}, \tag{1.3.7}$$

for some bulk field (not necessarily a scalar) $\psi \to \psi_{(0)}$ near the boundary. The integral on the right hand side is taken over the boundary of AdS, ∂AdS. As it stands, this relation is not particularly useful. It equates the partition function of a strongly coupled field theory to the partition function of quantum gravity in AdS, neither of which we can calculate. The relation becomes useful in the saddle point approximation, $Z_{QG} \approx \exp(iS_{\text{bulk}})$, where the bulk side reduces to classical gravity. Going to Euclidean signature so that $Z_{QG} \approx \exp(-S_{\text{E}})$, where S_{E} is the Euclidean bulk action, and evaluating on-shell gives a relation to the generating function of connected graphs in the boundary theory

$$S(\phi_{(0)}) = W_{QFT}[\psi_{(0)}]\,, \tag{1.3.8}$$

where $S(\psi_{(0)})$ is the on-shell Euclidean bulk action, evaluated on $\psi_{(0)}$. In principle, we can now work out arbitrary correlation functions between field theory operators by taking functional derivatives of (1.3.8). There is a technical caveat here; the results tend to diverge, signalling the need for a renormalization scheme which will be discussed in section 1.3.2. For example, for a bulk scalar ϕ, the expectation value of the dual operator is [71]

$$\langle \mathcal{O} \rangle = \frac{2\Delta - d}{L} \phi_{(2\Delta - d)} \, . \tag{1.3.9}$$

As asserted, the coefficient of the second mode $\phi_{(2\Delta-d)}$ is dual to the expectation value of the boundary operator (up to a constant coefficient). This result is also consistent with the expectation value of a CFT operator with scaling dimension Δ. Another way to see that Δ is the scaling dimension of $\mathcal{O}$ is to perform a scale transformation in the bulk $(r, \vec{x}) \to (\xi r, \xi \vec{x})$. This leaves ϕ unchanged. A near boundary analysis of ϕ then shows that the dual operator transforms as $\mathcal{O}(\vec{x}) \to \xi^{\Delta} \mathcal{O}(\xi \vec{x})$.

For the scalar field example, the identification of $\phi_{(0)}$ and $\phi_{(2\Delta-d)}$ as the dual source and expectation value, respectively, is a choice of boundary conditions. This assumes that the leading order fall-off is $d - \Delta$ (that is, we have chosen the positive sign in (1.3.5)) . This does not necessarily need to be the case, and different choices of boundary conditions will result in a reversed identification. Regardless of the choice, it can be shown [36] that $\Delta \geq (d-2)/2$, which corresponds to the CFT unitarity bound. The lesson is that a different choice of boundary condition leads to a different boundary CFT, even though the bulk action is the same. In this sense, deriving a result from a particular bulk action is deriving the corresponding result for a class of CFTs, all of which display the same behaviour.

So far, the focus has been on scalar fields dual to scalar operators. The dictionary extends beyond this to other quantities, many of which can be fixed purely by symmetry. For example, a massless bulk gauge field A_μ is expanded near the boundary as [36]

$$A_\mu = A_{(0)\mu} + \left(\frac{r}{L}\right)^{d-2} A_{(1)\mu} + \cdots \, . \tag{1.3.10}$$

Here, the two leading order coefficients, dual to the source and expectation value, are shown. There are, of course, other terms in the expansion as well as the possibility of a logarithmic term, depending on the dimension d. Analyzing the Maxwell equations near the boundary shows that the conformal dimension of the dual operator for the gauge field is $d-1$, as expected for a current in the dual CFT. In particular, for the time component A_t, the source term is the chemical potential in the dual theory $A_{(0)} \sim \mu$ and the expectation value is then the charge density $A_{(1)} \sim \rho$. These relations hold up to some constants that we will fix after renormalization in sections 1.3.2 and 1.3.3. Gauge fields play a special role in applications of holography. A global $U(1)$ symmetry of the field theory is dual to a gauged symmetry in the bulk [71]. This way, to describe a boundary theory with a gobal $U(1)$ symmetry, we must include a gauge field in the bulk action.

A similar analysis applies to the bulk metric, $g_{\mu\nu}$. This is dual to the boundary energy-momentum tensor. This had to be the case, since the boundary energy-momentum tensor encodes the response of the field theory to a change in the metric. In pure Einstein gravity, this identification can be shown to lead to the correct Ward identities, namely $\nabla^a \langle T_{ab} \rangle = 0$ and $\langle T_a{}^a \rangle = \mathcal{A}$, where $\mathcal{A}$ is related to the Weyl anomaly [70].

Turning on a finite temperature in the boundary theory corresponds to turning on a temperature in the bulk, which is associated to an event horizon [71]. In other words, the bulk spacetime now has a black hole. Turning on a temperature introduces a scale into the problem, so full conformal symmetry must be broken. Insisting that the geometry approach AdS near the boundary is tantamount to saying that in the deep UV, the conformal symmetry of the dual field theory is restored. This makes sense; at a scale much higher than the deformation introduced (in this case, temperature, but it may also be a relevant operator), the effect should be washed out and conformal invariance recovered. The geometric dual to this situation is the AdS-Schwarzschild spacetime

$$ds^2 = \frac{L^2}{r^2}\left(-f(r)dt^2 + \frac{dr^2}{f(r)} + dx^i dx_i\right), \tag{1.3.11}$$

where $f(r) = 1 - (r/r_h)^d$, r_h being the horizon position. The corresponding temperature is the Hawking temperature of (1.3.11) $T = d/(4\pi r_h)$. The AdS-Schwarzschild geometry is a solution to pure Einstein gravity with a cosmological constant; no matter source is required to support it. Note that, in these coordinates, the boundary is at $r \to 0$. In this limit, the geometry approaches AdS asymptotically, as desired. As written here, the solution is in the Poincaré patch. The corresponding global AdS-Schwarzschild geometry is a bit different. In particular, below a certain critical temperature, the black hole geometry becomes thermodynamically unfavourable compared to radiation in pure (global) AdS. This transition, called the Hawking-Page transition, has been proposed to be dual to a confinement/deconfinement transition in the dual theory [8].

Similarly, turning on finite charge density in the boundary theory implies a bulk gauge field, meaning the bulk theory is, at a minimum, the Einstein-Maxwell model

$$S_{EM} = \int d^{d+1}x\sqrt{-g}\left[\frac{1}{16\pi G_N}\left(R + \frac{d(d-1)}{L^2}\right) - \frac{1}{4e^2}F^2\right], \tag{1.3.12}$$

where e is the electromagnetic coupling. If we assume no other charged matter in the bulk, it may be set to one. Assuming a purely electric charge (so that only A_t is turned on), the bulk solution is the Reissner-Nordström-AdS black hole [71]

$$ds^2 = \frac{L^2}{r^2}\left(-f(r)dt^2 + \frac{dr^2}{f(r)} + dx^i dx_i\right), \tag{1.3.13}$$

where

$$f(r) = 1 - \left(1 + \frac{(d-2)\kappa^2\mu^2 r_h^2}{2(d-1)L^2e^2}\right)\left(\frac{r}{r_h}\right)^d + \frac{(d-2)\kappa^2\mu^2 r_h^2}{2(d-1)L^2e^2}\left(\frac{r}{r_h}\right)^{2(d-1)}, \tag{1.3.14}$$

where $\kappa^2 = 8\pi G_N$. The gauge field solution is

$$A_t = \mu\left(1 - (r/r_h)^{d-2}\right). \tag{1.3.15}$$

The Hawking temperature in this case is

$$T = \frac{1}{4\pi r_h}\left(d - \frac{(d-2)^2\kappa^2 r_h^2\mu^2}{(d-1)e^2L^2}\right). \tag{1.3.16}$$

Notice that it is possible for $T = 0$ while there is still a finite charge density. The generalization to having a magnetic field turned on may be found in [71]. Once again, as $r \to 0$, the RN-AdS geometry approaches pure AdS.

To fully understand how to compute quantities via holography, we need a renormalization scheme, which we will review in the next section 1.3.2.

1.3.2 Holographic renormalization

As pointed out in section 1.3.1, holographic calculations tend to diverge meaning we need a renormalization scheme. The procedure closely parallels field theory renormalization and results in finite answers. For a comprehensive review see [70]. The central quantity is the on-shell Euclidean action of the bulk theory (the real time formalism will be discussed below in section 1.3.4). The first step is to regularize the action. This is done by restricting the range of integration of the radial coordinate $r \geq \epsilon$. Conceptually, this cutoff makes sense; the boundary of the bulk spacetime is reached as $\epsilon \to 0$. According to the holographic dictionary, this region of the bulk corresponds to the UV of the dual field theory. Hence, imposing a radial cutoff is like imposing a UV cutoff in the field theory, exactly as one would expect from a renormalization scheme. We the conclude that gauge/gravity duality "geometrizes" the UV cutoff as $\epsilon \leftrightarrow \Lambda_{UV}$. The idea is then to break up the integral in the on-shell action into terms that diverge as $\epsilon \to 0$ and terms which vanish since the bulk equations of motion are satisfied. The result is a regulated action of the form [70]

$$S_{\text{reg}} = \int_{r=\epsilon} d^{d+1}x\sqrt{g_{(0)}}\left[\epsilon^{-c}a_{(0)} + \epsilon^{-(c+1)}a_{(1)} + \cdots - \ln(\epsilon)a_{(2c)} + \mathcal{O}(\epsilon^{(0)}\right] , \qquad (1.3.17)$$

where c is a positive constant (depending on the bulk field in question) and $g_{(0)}$ is the determinate of the bulk metric evaluated at $r = \epsilon$. Given the general asymptotic expansion for a field (1.3.3), the $a_{(i)}$ are local functions of the leading order F_0 term which plays the role of the source term of the dual field theory operator.

Before continuing, it should be pointed out that the bulk gravitational action needs to be supplemented with a boundary action in order to make the variational principle well defined. This is the familiar Gibbons-Hawking story; for an asymptotically AdS spacetime with curvature radius L, the relevant boundary action is [71]

$$S_{\rm GH} = \frac{1}{8\pi G_N}\int_{\partial M} d^d x\sqrt{\gamma}\left(-\mathcal{K} + \frac{(d-1)}{L}\right), \tag{1.3.18}$$

where γ_{ab} is the induced metric on the boundary of the bulk spacetime, ∂M and $\mathcal{K} = \gamma^{\mu\nu}\nabla_\mu n_\nu$ is the trace of the extrinsic curvature; n^μ being an outward pointing normal vector.

Neglecting the Gibbons-Hawking term can produce incorrect answers, depending on the kind of boundary quantity being computed. For instance, it is absolutely necessary in order to get the right boundary energy-momentum tensor [72].

With the regulated action (1.3.17) in hand, the second step is to identify the counterterm action, S_{ct} needed to remove the divergent pieces. This is conceptually easy; the counterterm action is just the negative of the divergent terms in the regulated action (1.3.17). To actually compute the counterterm action, it is first necessary to invert the asymptotic field expansion (1.3.3). This is required in order to solve for the source term $F_{(0)} = F_{(0)}\left(F(\epsilon, \vec{x})\right)$. The regulated action should then be expressed in terms of the inverted $F_{(0)}$ and the induced metric on the regulated surface $\gamma_{ab} = (L/\epsilon)^2 g_{ab}(\epsilon, \vec{x})$ [70]. The reason why this is necessary is so that the counterterm action may be expressed entirely in terms of local quantities living entirely on the regulated surface at $r = \epsilon$.

The third step in the process is to calculate the subtracted action, that is the action with the divergent pieces removed. Schematically, this is just

$$S_{\rm sub}\left[F(\epsilon, \vec{x}); \epsilon\right] = S_{\rm reg}\left[F_{(0)}; \epsilon\right] + S_{\rm ct}\left[F(\epsilon, \vec{x}); \epsilon\right]. \tag{1.3.19}$$

The subtracted action has a finite limit as $\epsilon \to 0$ by construction. To obtain the renormalized action, just take the $\epsilon \to 0$ limit of the subtracted action (1.3.19). It should be pointed out that the subtracted action is necessary as the variations needed to compute

correlation functions must be done before taking the $\epsilon \to 0$ limit. We can now compute to our heart's content. For example the one point function of the boundary operator $\mathcal{O}$, dual to some bulk field F with an asymptotic expansion (1.3.3) is

$$\langle \mathcal{O} \rangle = \frac{1}{\sqrt{g_{(0)}}} \frac{\delta S_{\text{ren}}}{\delta F_{(0)}} = \lim_{\epsilon \to 0} \left(\frac{L^{d/2-m}}{\epsilon^{d/2-m}} \frac{1}{\sqrt{\gamma}} \frac{\delta S_{\text{sub}}}{\delta F(\epsilon, \vec{x})} \right) , \tag{1.3.20}$$

where in the second equality, the bulk quantity has been re-expressed in terms of quantities entirely on the regulated surface $r = \epsilon$. When applied to the action of a massive scalar (1.3.20) correctly reproduces (1.3.9), as claimed. As another example, we can apply this formalism to the electric $RN - AdS$ solution (1.3.13) and compute the charge density of the dual field theory. This can be done either directly, or by using the following trick [71].

The relevant bulk action is

$$S_{\text{E}} = -\int d^{d+1}x \sqrt{g} \left[\frac{1}{16\pi G_N} \left(R + \frac{d(d-1)}{L^2} \right) + \frac{1}{4e^2} F^2 \right] + S_{\text{GH}} \, , \tag{1.3.21}$$

where S_{GH} is the Gibbons-Hawking term (1.3.18). Note that we are working with the Euclidean action, so the F^2 term comes in with a plus sign. We are working with an electric ansatz, so only A_t is turned on. It turns out that no additional counterterms are necessary for the bulk gauge field as it falls off sufficiently fast near the boundary [71]. Instead of working through the full holographic RG procedure again, define a new scalar field $\psi = (r/L)A_t$. The relevant part of the action (1.3.21) may be re-expressed in terms of ψ to give

$$S_\psi = -\frac{1}{2e^2} \int d^{d+1}x \sqrt{g} \left\{ \frac{r^2}{L^2} \left[(\partial_r \psi)^2 + (\partial_a \psi)^2 \right] + 2V_{\text{eff}}(\psi) \right\} , \tag{1.3.22}$$

where $V_{\text{eff}}(\psi)$ is an effective scalar potential for ψ which depends only on ψ^2 and radial derivatives of ψ. We are explicitly interested in quantities near the asymptotic AdS boundary, so $g_{\mu\nu} \sim (L^2/r^2)$. The expectation value for a scalar operator in this background with action

$$S_\phi = \frac{\eta}{2} \int d^{d+1}x \sqrt{-g} \left[(\partial \phi)^2 + 2V(\phi) \right] , \tag{1.3.23}$$

is (up to a normalization constant η) given by (1.3.9). Now, use the FG expansion (1.3.10) on the solution for A_t in the $RN-AdS$ background (1.3.15) to find that $\psi^{(1)} = (-\mu L^{d-2})/(r_h^{d-2})$ and that ψ has $\Delta = d-1$. The action (1.3.22) can be brought into the form of (1.3.23) by comparing the normalization between the actions and setting $\eta = -1/e^2$. Since $\psi = (r/L)A_t$, the coefficient $\psi_{(1)}$ is actually $A_{t(1)}$, so the expectation value of the operator dual to ψ is actually the dual charge density. Applying the result for the expectation value of a scalar operator (1.3.9) gives

$$\langle J^t \rangle = \frac{\mu(d-2)L^{d-3}}{e^2 r_h^{d-2}}\,, \tag{1.3.24}$$

as the charge density of the dual field theory.

Holographic renormalization has also been approached in terms of a bulk Hamilton-Jacobi formulation, first proposed in [38]. For reviews, see [73] and [74]. The idea is to study the Hamilton-Jacobi equations for the various bulk fields and the metric. The caveat is that instead of following the Hamiltonian evolution through time, like in classical mechanics, the evolution is followed along the radial direction. The bulk radial direction encodes the energy scale in the boundary field theory, so flowing along r is equivalent to flowing in E. It turns out that the divergent terms in the bulk action can be identified by imposing the Hamiltonian constraints on a bulk cut-off surface near the boundary, meaning that the necessary counterterms may be identified. It turns out that by following this procedure, the Callan-Symanzik equation for the dual field theory can be obtained.

1.3.3 Correlation functions

Armed with a holographic renormalization technique, we can now compute quantities as desired. As an example, after a lengthy calculation, the scalar two point function in pure AdS turns out to scale like

$$\langle \mathcal{O}(x)\mathcal{O}(0)\rangle \sim |x|^{-2\Delta}\,, \tag{1.3.25}$$

as would be expected in a CFT where the scaling dimension of $\mathcal{O}$ is Δ. The coefficient needed to make the equality in (1.3.25) exact may be found in [46].

Computing n-point functions goes through the same way as the two point function (1.3.25). As in standard QFT, there is a way to visualize these computations in AdS, analogous to Feynman diagrams, called Witten diagrams. In this context, the external legs of a process connect to the boundary and represent the boundary behaviour of the bulk field and as such, these lines are called "bulk-to-boundary" propagators. There are also "bulk-to-bulk" propagators which connect possible internal lines in the AdS bulk, representing possible bulk interactions. A comprehensive review may be found in [75].

So far, our focus has been on computing dual field theory properties starting from a Euclidean bulk action and applying the technology of holographic renormalization. This procedure may be long and cumbersome and we would also like to be able to say something about real-time physics. To understand strong time dependence in the dual field theory, it is necessary to work in a fully time-dependent gravitational background. This is difficult and there is, as of yet, no well defined process for approaching this kind of situation. In lieu of this, it is possible to consider small time dependent perturbations around equilibrium and study the response of the system. This is just linear response theory à la gauge/gravity duality.

In order to get a handle on real time physics, we need to compute the Green's function associated with the quantity of interest. There are many choices here as they are many different types of Green's functions. The most interesting choice is the retarded Green's function which encodes the causal response of a system to a perturbation. The first proposal for how to calculate retarded Green's functions using holography was presented in [76] and was later shown to arise from a holographic version of the Schwinger-Keldysh formalism in [77], [78] and [79]. Calculating the retarded Green's function will also play a crucial role in the next section 1.3.4 where transport properties will be discussed.

Consider a perturbation to the dual field theory by an operator $\mathcal{O}_\psi$ and source $\delta\psi_{(0)}$.

Going to frequency space, the response of the system is [71], [36]

$$\delta\langle\mathcal{O}_\psi\rangle(\omega, k\vec{k}) = G^R_{\mathcal{O}_\psi\mathcal{O}_\psi}(\omega, \vec{k})\delta\psi_{(0)}(\omega, \vec{k})\,, \tag{1.3.26}$$

where $G^R_{\mathcal{O}_\psi\mathcal{O}_\psi}(\omega, \vec{k})$ is the retarded Green's function. The source, $\psi_{(0)}$ will be related to a bulk field via the holographic dictionary. Since we are looking at a perturbation of the boundary theory, this should correspond to a perturbation in the bulk. In other words, given the dual bulk field ψ, we should look for perturbations around its background value by

$$\psi \to \psi + \delta\psi(r)\, e^{-i\omega t + i\vec{k}\cdot\vec{x}}\,. \tag{1.3.27}$$

The added perturbation must still obey the Fefferman-Graham expansion in an asymptotically AdS geometry. That is, the boundary conditions on the perturbation are fixed to $\delta\psi = (r/L)^m\delta\psi_{(0)} + \cdots$. It is also necessary to impose boundary conditions in the interior of the geometry; this is where the real time requirement comes in. The retarded Green's function must be related to a bulk field that is infalling into the geometry. This is easier to understand in an asymptotically AdS geometry with a black hole in the interior. Bulk matter can fall into the horizon, but it cannot come back out. Borrowing an apt description from [36], the choice of infalling boundary conditions corresponds to an event that can happen, rather than "unhappen". Geometrically, this requires a future horizon in the interior, which is where the boundary condition will be set. The future horizon is a surface in the bulk. Once passed this surface, causal contact with asymptotically AdS boundary is no longer possible. For a black hole geometry the future horizon is just the event horizon. In the Poincaré patch of AdS, there is such a horizon at $r \to \infty$.

With a perturbation satisfying the correct boundary conditions, the retarded Green's function can be essentially read off from (1.3.26)

$$G^R_{\mathcal{O}_\psi\mathcal{O}_\psi} = \frac{\delta\langle\mathcal{O}_\psi\rangle}{\delta\psi_{(0)}}\,. \tag{1.3.28}$$

A value for $\langle\mathcal{O}_\psi\rangle$ is still required to make progress, the result for which was given for a scalar operator (1.3.9). Recall that the calculation relied on the holographic renormaliza-

tion procedure with the Euclidean action. The choice of working in Euclidean signature is a computational crutch designed to get around the issue of imposing a boundary condition on the future horizon, thereby breaking time reversal symmetry. In fact, this is not necessary as long as the correct causal behaviour of the bulk fields is enforced, in particular, the basic relation (1.3.7) is valid in Lorentzian and Euclidean signature. In general, the expectation value can be computed in the classical bulk limit (large N in the dual theory) [36]

$$\langle \mathcal{O}_\psi \rangle = \frac{\delta W[\psi_{(0)}]}{\delta \psi_{(0)}} = \lim_{r\to 0} \left(\frac{r}{L}\right)^m \Pi(r, \vec{x}) \,. \tag{1.3.29}$$

Note, no assumption about the signature of the bulk spacetime has been made. Here, the quantity $W[\psi_{(0)}]$ should be thought of as already containing the required bulk counterterms. Also Π is defined as

$$\Pi(r, \vec{x}) = \frac{\partial \mathcal{L}}{\partial(\partial_r \psi)} \,. \tag{1.3.30}$$

The quantity (1.3.30) is reminiscent of the bulk field momentum, except with the radial coordinate r used in place of time. This is very much in line with the philosophy of holographic renormalization in the Hamilton-Jacobi approach [38]. The momenta of fields are also related to the variation of the action with respect to the initial value of the field [36], hence the second equality in (1.3.29). Note also that near the boundary $\psi \sim (r/L)^m \psi_{(0)}$, so $\partial/\partial\psi_{(0)} \sim r^{-m}(\partial/\partial\psi)|_{r=\epsilon}$. That is, the quantity Π should be computed in the bulk, at a cutoff surface ϵ and then the limit to $\epsilon \to 0$ taken, taking into account the hidden r dependence in the field derivative. Applying this formulation to the case of a scalar field reproduces the result already obtained (1.3.9) [36].

With (1.3.29) and (1.3.30), the retarded Green's function is

$$G^R_{\mathcal{O}_\psi \mathcal{O}_\psi} = \lim_{r\to 0} \frac{\delta \Pi_\psi}{\delta \psi} \,. \tag{1.3.31}$$

This equation is valid for a general bulk mode. When applied to a scalar field, it returns [71]

$$G^R_{\mathcal{O}_\phi \mathcal{O}_\phi} = \frac{2\Delta - d}{L} \frac{\delta \phi_{(2\Delta - d)}}{\delta \phi_{(0)}} \,, \tag{1.3.32}$$

hence the retarded Green's function is described by the ratio of the expectation value and the source, as expressed via the bulk field. This will be true for the other examples which will be described in section 1.3.4. In particular, this means that the retarded Green's function can computed directly from the bulk solution for the field. When applying linear response theory, the bulk field is a perturbation, meaning that the equations of motion should be expanded to linear order and solved. This is not always as tractable as it sounds, and sometimes a numerical solution is required.

1.3.4 Transport properties

With an understanding of how to compute retarded Green's functions, it is now possible to calculate transport properties of the field theory using gauge/gravity duality. In the hydrodynamic limit, transport properties are related to the retarded Green's function by a Kubo formula [46]

$$\chi = -\lim_{\omega\to 0}\lim_{\vec{k}\to 0}\frac{1}{\omega}\mathrm{Im}G^R(\omega,\vec{k})\,, \tag{1.3.33}$$

where χ is the transport coefficient. Note that the order of limits is not arbitrary here, the $\vec{k}\to 0$ limit must be taken first. Notice also that this formula is restricted to the case where the transport coefficient is a constant, so χ could be, for example, the DC conductivity. In general, it is interesting to understand the frequency and spatial dependence of transport properties of the system. This is also possible to access holographically via (1.3.31), which makes no assumption about small ω or $\vec{k}$. An example with frequency dependence will be discussed shortly and an example where spatial dependence can show up will be given in chapter 3.

To get a feel for how this process works, we can compute the conductivity dual to pure AdS_4. Explicitly, the metric is

$$ds^2 = \frac{L^2}{r^2}\left(-dt^2+dr^2+dx^2+dy^2\right)\,, \tag{1.3.34}$$

where the boundary is at $r=0$. The first step is to compute Π_{A_x} from the Lagrangian.

AdS is a vacuum solution to the Einstein equations, so there is no initial bulk matter. To compute the conductivity, we need to turn on a boundary electric field and measure the response of the system. The applied field should be thought of as small, so that it may be treated by the linear response techniques set up in section 1.3.3. The conductivity is then really just a consequence of Ohm's law, $J = \sigma E$.

The metric (1.3.34) is homogeneous and isotropic along the boundary $[x, y]$ directions, so $\sigma_{xx} = \sigma_{yy} \equiv \sigma$, meaning we can turn on an electric field in any direction we chose and get the same result. Turning on a perturbation $\delta A_x(t, r)$ then ensures an electric field along the boundary x direction $E = \partial_t \delta A_{(x)}|_{r\to 0}$. The relevant action for this perturbation is then

$$S_M = -\zeta \int d^4x \sqrt{-g} F^2 \,, \tag{1.3.35}$$

where ζ is a normalization constant. Computing Π_{A_x} as in (1.3.30), gives

$$\Pi_{A_x} = -4\zeta \partial_r \delta A_x \,. \tag{1.3.36}$$

The perturbation must still obey the Fefferman-Graham expansion (1.3.10), so near the boundary $\delta A_x = \delta A_{x(0)}(t) + r\delta A_{x(1)}(t) + \cdots$. The Green's function then follows from (1.3.31)

$$G^R_{J_x J_x} = \lim_{r\to 0} \frac{\Pi_{A_x}}{\delta A_x} \,. \tag{1.3.37}$$

In order to make sure that we are getting the right retarded Green's function, we must ensure that the gauge field perturbation δA_x respects infalling boundary conditions as $r \to \infty$, meaning we need to solve the linearized Maxwell's equations in the AdS background for $\delta A_x(t, r)$. This can be done analytically with the result

$$\delta A_x(t, r) = C_0 \exp(i\omega r) \exp(-i\omega t) \,, \tag{1.3.38}$$

where C_0 is a constant. To prove that this is actually the correct infalling solution, switch to ingoing coordinates in the metric (1.3.34), $v = t - r$ for which the gauge field solution is $\delta A_x = C_0 \exp(-iv\omega)$. The v coordinate is constant along null paths which

are travelling into the geometry towards $r \to \infty$. As t grows, so must r in order to keep v constant along any null line. In this sense, v is the ingoing coordinate, following trajectories of increasing r into the geometry a time evolves. Hence, δA_x in (1.3.38) describes an infalling mode.

Evaluating the limit in (1.3.37) and using the Kubo formula (1.3.33) gives the conductivity. Choosing the usual normalization for the electromagnetic action $\zeta = 1/(4e^2)$ gives

$$\sigma = \lim_{\omega \to 0} \frac{1}{e^2} = \frac{1}{e^2} \,. \tag{1.3.39}$$

The DC conductivity is a constant, set only by the coupling e^2. Moreover, the AC conductivity (i.e. before taking the $\omega \to 0$ limit in (1.3.39)) is also a constant, totally independent of the frequency of the applied field ω.

The same result turns out to be true in the AdS-Schwarzschild background (1.3.11) as well, even though the system is at finite temperature. This counter-intuitive result turns out to be due to electric-magnetic duality in the bulk [80]. Given that the action for the gauge field only contains $F_{\mu\nu}F^{\mu\nu}$, either $F_{\mu\nu}$ itself, or its dual $*F_{\mu\nu} = -(1/2)\epsilon_{\mu\nu\sigma\lambda}F^{\sigma\lambda}$ could be the fundamental field strength. In other words, the action is unchanged by switching the electric and magnetic fields. For a dyonic black hole with electric charge q and magnetic charge h, the duality transformation requires $h \to -q$ and $q \to h$. The original conductivity is constrained to be inversely related to the duality transformed conductivity (up to a constant) [81]. A constraint on the conductivity of the uncharged AdS geometry can then found by setting $q = 0$ and $h = 0$. Since there is no charge, the duality transformation simply maps the conductivity to one over itself (up to a constant) and so the conductivity as a whole must be a constant.

The same kind of calculation can be carried out for the $RN - AdS$ geometry (1.3.13) to find the dual conductivity when a background charge density is turned on. In this case, it is necessary to include a metric perturbation δg_{tx} on top of the gauge field perturbation δA_x. The reason is that the δA_x perturbation of the gauge field can couple

to the original A_t component in the baseline solution and show up at linear order in the energy-momentum tensor. In order for the Einstein equations to remain consistent, a metric perturbation δg_{tx} must be sourced to compensate for this mixing. The linearized Einstein and Maxwell equations may be solved numerically in this case [71]. The AC conductivity approaches a delta function as $\omega \to 0$, meaning that the DC conductivity diverges. This is the result of translational invariance along the boundary directions, which means the momentum is conserved in the boundary theory and the resulting DC conductivity is infinite. To remedy this situation, a mechanism to break translational invariance in holography is needed. This will be discussed in more detail in section 1.5.

Note that the DC conductivity in pure AdS (and AdS-Schwarzschild) is finite even though the boundary directions are translationally invariant. This is because there is no net charge in these backgrounds, so the dual theory has particle-hole symmetry [71]. If a particle collides with a hole head on and they are both at rest afterwards, then the total current will relax to zero, but total momentum is still conserved (it was just zero to start with). If there is a net charge density, then there will, on average, be some amount of momentum left over as there is a surplus of one charge over its opposite. Since charge is conserved, this means there will always be some finite current. When $\omega \to 0$ and the applied electric field approaches a constant, the conductivity will inevitably diverge as there is nothing to prevent the charges from accelerating infinitely.

Another powerful example of the application holographic of techniques is to calculate the shear viscosity of the dual theory [7]. In the context of hydrodynamics, the shear viscosity shows up as a dissipative term in the energy-momentum tensor. The energy-momentum tensor itself is defined by the variation of the matter Lagrangian with respect to the metric tensor. Therefore, to measure shear viscosity with holography, we need to look at a metric perturbation, $\bar{g}_{\mu\nu} = g_{\mu\nu} + h_{\mu\nu}$, where $g_{\mu\nu}$ is the original metric and $h_{\mu\nu}$ is the perturbation. Again, to ensure the validity of linear response theory, the metric perturbation will be taken to be small and only contribute at linear order. We will

work at finite temperature, so the background is the AdS-Schwarzschild metric (1.3.11). Turning on a perturbation along the xy direction $(L^2/r^2)h_{xy}$, the metric, at linear order, takes the form

$$ds^2 = \frac{L^2}{r^2}\left(-f(r)dt^2 + \frac{dr^2}{f(r)} + dx^2 + \frac{L^2}{r^2}\left(dy + h_{xy}dx\right)^2\right). \tag{1.3.40}$$

Plugging this ansatz into the Einstein equations results in the equations of motion for the perturbation h_{xy} which turns out to be [46]

$$S_h = -\frac{1}{32\pi G_N}\int d^{d+1}x\sqrt{-g}\,\bar{g}^{\mu\nu}(\partial_\mu h_{xy})(\partial_\nu h_{xy})\,. \tag{1.3.41}$$

Note that the determinate of the metric here is with respect to the unperturbed metric. The procedure is now the same as for the conductivity case above. Examining the equations of motion resulting from the action (1.3.41) and imposing regularity here the horizon $r \to r_h$ results in a boundary condition for h_{xy}

$$h_{xy} \approx C\exp\left(-\frac{i\omega}{4\pi T}\ln(r-r_h)\right)\exp(-i\omega t)\exp(i\vec{k}\cdot\vec{x})\,. \tag{1.3.42}$$

Again, by changing to ingoing coordinates $v = t - r_*$, where r_* is the usual tortoise coordinate, this boundary condition can be seen to be the correct infalling behaviour. The field momentum in this case is

$$\Pi_{h_{xy}} = -\frac{1}{16\pi G_N}\left(\frac{L}{r}\right)^{d-1} f(r)(\partial_r h_{xy})^2\,, \tag{1.3.43}$$

and so using the Kubo formula, the shear viscosity is

$$\eta = -\lim_{\omega\to 0}\lim_{\vec{k}\to 0}\lim_{r\to 0}\frac{1}{\omega}\mathrm{Im}\left(\frac{\Pi_{h_{xy}}}{h_{xy}}\right). \tag{1.3.44}$$

It turns out [46] that $\Pi_{h_{xy}}/(\omega h_{xy})$ is independent of r and so can be evaluated anywhere in the bulk. In particular, it is convenient to set $r = r_h$, since the horizon encodes the thermodynamic properties of the geometry. The viscosity is then

$$\eta = \frac{1}{4G_N}\left(\frac{L}{r_h}\right)^{d-1}. \tag{1.3.45}$$

The entropy density of the AdS-Schwarzschild geometry follows from the Bekenstein-Hawking formula

$$s = \frac{A_H}{4G_N V} = \frac{1}{4G_N}\left(\frac{L}{r_h}\right)^{d-1}, \tag{1.3.46}$$

where A_H is the horizon area and V is the volume of the boundary region. The second equality is the result for the AdS-Schwarzschild geometry. The ratio of shear viscosity to entropy density for the holographic dual theory is then given by the famous KSS (Kovtun-Son-Starinets) formula [7], [82]

$$\frac{\eta}{s} = \frac{1}{4\pi}. \tag{1.3.47}$$

There is nothing particularly special about the choice of the AdS-Schwarzschild geometry. The result is true in any two derivative theory of gravity along with the modest assumptions that the bulk geometry is translationally invariant along the boundary directions, asymptotically AdS (or any other geometry in which a sensible holographic prescription may be set up) and that there is a an event horizon [36]. In this sense, (1.3.47) is a universal bound valid at strong coupling. For other theories of gravity, the KSS bound may be violated. For example, in Gauss-Bonnet gravity in $D = 4 + 1$ dimensions [83]

$$S = \frac{1}{16\pi G_N}\int d^5x\sqrt{-g}\left[R - 2\Lambda + \eta_{GB}\left(R^2 - 4R_{\mu\nu}R^{\mu\nu} + R_{\mu\nu\lambda\sigma}R^{\mu\nu\lambda\sigma}\right)\right], \tag{1.3.48}$$

where η_2 is a constant coupling to the curvature squared terms. In this case, the KSS bound becomes [84]

$$\frac{\eta}{s} = \frac{1}{4\pi}\left(1 - \frac{8\eta_{GB}}{L^2}\right) \geq \frac{1}{4\pi}\frac{16}{25}, \tag{1.3.49}$$

where L is the AdS radius. The value on the right hand side comes from demanding a well behaved bulk solution. Arbitrary values of η_{GB} may lead to the appearance of ghosts in the gravity theory; they can be avoided in certain backgrounds for a restricted range of η_{GB}. In chapter 2, curvature squared corrections will be studied in a different holographic context where more comments about ghosts will be made.

Beyond transport properties, there is a slew of other quantities in the dual field theory that are interesting to study. One such quantity is entanglement entropy which, over the

course of the last several years, has shown that there is a deep connection between quantum information theory on the boundary and the bulk geometry.

1.3.5 Entanglement Entropy

The holographic dictionary also allows us to access information related to non-local probes of the dual field theory. A particularly pertinent example is a Wilson loop [85].

According to the holographic dictionary, the endpoints of strings on $D3$-branes are to be thought of as quarks in the dual theory [46]. This way, the Wilson loop may be represented by a string worldsheet, Σ, which extends into the bulk and ends on a $D3$-brane. The boundary of the worldsheet, $\partial\Sigma$, which ends on the brane forms a closed curve $\mathcal{C}$, which is interpreted precisely as the closed curve around which the Wilson loop is calculated in the dual theory. Taking the brane to the (Euclidean) AdS boundary means that the closed curve $\mathcal{C}$ lies entirely on the AdS boundary. This limit corresponds to the field theory UV, so the quarks are infinitely heavy. The vacuum expectation value of the Wilson loop is [46]

$$\langle W(\mathcal{C})\rangle = Z(\partial\Sigma = \mathcal{C}) = \exp(-S_{NG}(\mathcal{C}))\,, \tag{1.3.50}$$

where $Z(\partial\Sigma = \mathcal{C})$ is the string partition function subject to the boundary condition that the worldsheet has a boundary $\mathcal{C}$. In the last equality, the large 't Hooft limit has been used to express Z in terms of the on-shell Nambu-Goto action. This formalism has been generalized to finite temperature and used to examine holographic quark-antiquark potentials in strongly coupled $\mathcal{N} = 4$ SYM where confining behaviour is observed. A review of these results may be found in [46].

Another particularly interesting non-local probe of the boundary theory is entanglement entropy, S_{EE}. The entanglement entropy is a measure of how closely entangled a given wave function is. For example, consider a quantum system described by a Hamiltonian $\mathcal{H}_{\text{tot}}$ at a fixed time $t = t_0$. Suppose the system is divided into two regions A and B

such that the total Hamiltonian may be written as a direct product of two Hamiltonians, one for each subsystem A and B, $\mathcal{H}_{\text{tot}} = \mathcal{H}_{\text{A}} \otimes \mathcal{H}_{\text{B}}$. If an observer is restricted to only being able to measure quantities in the subsystem A, then it will appear as if the total system is described by a reduced density matrix

$$\rho_A = \text{tr}_{\text{B}}\, \rho_{\text{tot}}\,, \tag{1.3.51}$$

where the trace is restricted to be taken over only the Hilbert space associated with the subsystem B, $\mathcal{H}_{\text{B}}$. That is, any information about the state of the subsystem B is traced out. An analogous result holds for the reduced density matrix on the subsystem B. The entanglement entropy of the subsystem A is then defined as the von Neumann entropy of the reduced density matrix associated to A [86]

$$S_{\text{A}} = -\text{tr}_{\text{A}}\left[\rho_{\text{A}} \log(\rho_{\text{A}})\right]\,. \tag{1.3.52}$$

The entanglement entropy is a measure of how correlated the subsystems A and B are with each other. In other words, it counts the number of entangled bits between subsystems A and B. In order to define the entanglement entropy for a finite temperature system, it suffices to take the total density matrix to be $\rho_{\text{tot}} = \exp(-\beta H)$, with $\beta = T^{-1}$. In this case, when the subsystems A and B are chosen to overlap completely (i.e. they are the same), the entanglement entropy as defined in (1.3.52) reduces to the thermal entropy [86].

Entanglement entropy is an interesting quantity from the perspective of field theory. A useful feature is that S_{EE} does not vanish at zero temperature and so may be used to probe the ground states of quantum systems. It may also be a useful order parameter for zero temperature quantum phase transitions which will be discussed in more detail in sections 1.4.2 and 1.5.5. Entanglement entropy is also an important quantity in the context of quantum information theory. With regards to holography, it serves as a basis for many modern studies on the emergence of spacetime, progress and future directions on this front will be discussed in chapter 4.

There are a variety of general properties that are satisfied by entanglement entropy. These properties are generally encoded in terms of inequalities that place strong restrictions on quantum systems from the point of view of quantum information theory. For example, on very general grounds, given any three non-intersecting subsystems, A, B and C [87].

$$S(A \cup B \cup C) + S(B) \leq S(A \cup B) + S(B \cup C)\,, \tag{1.3.53}$$

$$S(A) + S(C) \leq S(A \cup B) + S(B \cup C)\,. \tag{1.3.54}$$

By setting C to be empty in (1.3.53) and (1.3.54), a new quantity called the mutual information may be defined with the property [86]

$$I(A, B) = S(A) + S(B) - S(A \cup B) \geq 0\,. \tag{1.3.55}$$

As we will discuss in more detail shortly and in chapter 4, some of these properties may be translated directly into geometric constraints in any potential gravity dual.

Entanglement entropy is generally difficult to calculate in quantum field theories. One technique is called the replica trick where n-copies of the theory are considered and the entanglement entropy for a region A is calculated in the limit as $n = 1$ [86]

$$S_A = -\frac{\partial}{\partial n}\mathrm{tr}_{\mathrm{A}}\rho_{\mathrm{A}}^{\mathrm{n}}|_{\mathrm{n}=1}\,. \tag{1.3.56}$$

In some cases, the entanglement entropy may be exactly computed. For example, in a 2D CFT, the entanglement entropy of a strip of length l is [88]

$$S_A = \frac{c}{3}\log\left(\frac{l}{a}\right)\,, \tag{1.3.57}$$

where c is the central charge of the CFT and a is a UV cutoff which is required to regulate the entanglement entropy [86].

In [22] and [89], a proposal for how to compute entanglement entropy via holography was proposed. The idea is to consider a CFT in d spacetime dimensions with a dual in (static) AdS_{d+1}. The boundary of the AdS geometry is split into two regions A and

B and the entanglement entropy between the two regions is measured. The boundary of the region A (∂A) is associated to a bulk surface which ends on the boundary and is homologous to ∂A. The RT (Ryu, Takayanagi) proposal states that the area of the minimal such bulk surface, γ_A, computes the entanglement entropy in the dual theory. More specifically, the RT formula is

$$S_A = \frac{\text{Area}(\gamma_\text{A})}{4G_N}\,, \tag{1.3.58}$$

where G_N is the Newton constant in $d+1$ dimensions. For a $d+1=3$ dimensional bulk and by selecting an infinite strip region on the boundary, the RT prescription (1.3.58) correctly reproduces the 2D CFT result (1.3.57). In higher dimensions, the holographic entanglement entropy can be difficult to calculate since finding a minimal bulk surface is not an easy task. In AdS_3, the situation is a bit simpler as the bulk minimal surfaces are just one dimensional spacelike geodesics. Recently, a proof of the RT formula has become available via an implementation of the replica trick in the bulk [23].

The RT formula applies for a bulk gravity theory described by Einstein gravity. Extensions to to gravity theories with higher curvature corrections have been considered in [90], [91], [92], [93] and [94], although a well established procedure is only currently known for Gauss-Bonnet gravity.

A prescription to extend the RT formula to time dependent cases was made in [95] called the HRT (Hubeny, Ryu, Takayanagi) proposal and is generally covariant in the bulk. Here, the dual entanglement computes the dual entanglement entropy in the full Lorentzian bulk geometry by finding the area of an extremal codimension 2 spacelike surface. As of yet, there is no proof for the HRT proposal like there is for the RT formula.

The RT formula may be used to show that the holographic entanglement entropy satisfies the basic relations known from quantum information theory, for example strong subadditivity (1.3.53) and (1.3.54) as well as the positivity of mutual information (1.3.55). These relations follows from geometric properties of minimal surfaces in AdS, fullfilling

one of the basic tenets of holography; boundary properties are geometrized in the bulk. For a review of the many properties satisfied by holographic entanglement entropy and their proofs, see [96].

As we will discuss in more detail in chapter 4, the holographic entanglement entropy has motivated the study of many other information theoretic concepts in the context of gauge gravity duality, residual entropy being a particularly popular example [97]. These concepts, along with ideas about bulk locality suggest interesting and unexpected links between the emergence of gravity and quantum information theory.

Holographic entanglement entropy is also an interesting quantity with regards to thermalization. The idea is to model a quench in the boundary theory by studying gravitational collapse in the theory. The collapsing geometry is sourced by a scalar perturbation (sudden injection of energy) near the boundary and results in a Vaydia-AdS spacetime. Ultimately, the geometry collapse into an AdS-Schwarzschild geometry. The behaviour of a variety of probes may be studied before and after the quench and used to establish timescales over which thermalization occurs. In [98], numerical simulations in three, four and five bulk spacetime dimensions show that the entanglement entropy thermalizes the slowest and thereby sets the overall equilibration time scale.

More recently, [99] and [100] studied the evolution of holographic entanglement entropy after a global quench in the dual field theory. It is observed that the growth of entanglement is characterized by an "entanglement tsunami" which carries entanglement from the boundary into the bulk resulting in different regimes of equilibration times. Based on these observations, a bound is conjectured on the maximal rate of the growth of entanglement entropy in a relativistic systems. Understanding how and when a strongly coupled field theory equilibrates is central to studying quantum many-body systems. We will discuss further aspects of progress on holographic models of this phenomenon in chapter 4.

We end this section with a short summary table of some of the important entries in

the holographic dictionary.

Boundary	**Bulk**
scalar operator	scalar field
fermion	fermion
conserved current	gauge field
spin	spin
conformal dimension	mass
global symmetry	local isometry
chemical potential	finite charge density
energy-momentum tensor	metric
finite temperature	black hole horizon
deconfinement transition	Hawking-Page transition
entanglement entropy	minimal surface
multiparticle state	product of operators at distinct points $\mathcal{O}_{\Delta_1}(x_1)\cdots\mathcal{O}_{\Delta_n}(x_n)$
bound state	product of operators at the same point $\mathcal{O}_{\Delta_1}(x)\cdots\mathcal{O}_{\Delta_n}(x)$

1.4 AdS/CMT

A particularly useful feature of gauge/gravity duality is that, in the strong coupling limit, the field theory is dual to classical gravity, providing a powerful tool for accessing strong coupling phenomena that would otherwise be intractable. This feature motivates the application of holographic techniques to problems of condensed matter physics and QCD, to gain some degree of analytical control over strong coupling phenomena where previously there was none. This program has enjoyed numerous successes over the last decade. On the QCD front, gauge/gravity duality (known as AdS/QCD) has provided

a prediction of the shear viscosity of a strongly coupled plasma, in agreement with the value measured at RHIC [7]. For a review see [101].

In context of condensed matter physics, application of gauge/gravity duality (called AdS/CMT) has also revealed surprising results, including descriptions of holographic superconducting phases, fluid mechanics, quantum criticality and even new solutions to general relativity. Some highlights of this research program are described below. For comprehensive reviews of AdS/CMT techniques see [71], [81], [36], as well as the more recent overview [102].

1.4.1 Bottom up phenomenology versus top down

An immediate obstruction to using the AdS/CFT correspondence to study condensed matter physics or QCD is that the dual field theory is $\mathcal{N} = 4$ SYM. For starters, this field theory is conformal, which is not true of almost any "real-world" systems. Secondly, the theory is supersymmetric, which is certainly not a property of conventional condensed matter models.

There is a long history of holographic symmetry reduction with a major focus being the reduction of supersymmetry and the breaking of conformal invariance. For reviews see [103] and [55]. The simplest thing to do is turn on a finite temperature in the gravity background, which breaks conformal symmetry as a scale is introduced [43]. This also breaks supersymmetry as periodic and anti-periodic boundary conditions around the thermal period $1/T$ must be imposed on bosonic and fermonic fields respectively [104]. This leads to different mode expansions for the bosons and the fermions and breaks supersymmetry.

Other studies have focused on modifications of the original $AdS_5 \times S^5$ correspondence by putting the stack of $D3$-branes on a curved background [105], [106]. The net result is that the geometry of the original duality is modified to $AdS_5 \times \mathcal{M}_5$, where $\mathcal{M}_5$ is a manifold which depends on the background chosen. Near a conifold singularity, $\mathcal{M}_5 =$

$(SU(2) \times SU(2))/U(1)$ and the dual field theory has $\mathcal{N} = 1$ supersymmetry. These constructions may be generalized to include both N regular and M fractional $D3$-branes sitting at the conifold singularity [107], [108], [109]. The fractional $D3$-branes can be thought of as $D5$-branes wrapped on S^2. As the conifold singularity is approached, the S^2 shrinks away and two of the worldvolume directions are effectively lost. These branes are stuck at the singularity of the background. The holographic result of this construction is a non-conformal $\mathcal{N} = 1$ supersymmetric dual theory with an $SU(N + M) \times SU(N)$ gauge group. This construction displays chiral symmetry breaking and is confining in the deep IR.

Another approach to reducing supersymmetry is to wrap higher dimensional branes along sub-manifolds of the full ten dimensional geometry [110], [111]. These models are dual to $\mathcal{N} = 1$ SYM in the IR. Confinement and chiral symmetry breaking are also present.

Flavour may be introduced in the AdS/CFT framework by including $N_f \ll N$ $D7$-branes to the $D3$-brane background [112], [113], [114] which lead to holographic models with dynamical quarks. It turns out that these models preserve $\mathcal{N} = 2$ supersymmetry.

Conformal symmetry and supersymmetry breaking has also been approached by building in other kinds of deformations of the original AdS_5/CFT_4 correspondence. In [115], a family of solutions to type IIB supergravity which contains a non-constant S^5 radius and a non-constant dilaton that approaches $AdS_5 \times S^5$ asymptotically are constructed. The resulting dual field theory has $\mathcal{N} = 0$ supersymmetry. The addition of probe $D7$-branes in this setup is studied in [116]. In [117], finite mass perturbations are added to the AdS_5/CFT_4 which break conformal invariance and supersymmetry in the IR, resulting in $\mathcal{N} = 1$. A holographic dual for four-dimensional $SU(N)$ Yang-Mills (i.e. without supersymmetry) was proposed in [8]. The gravity side contains N $D4$-branes compactified on a circle with anti-periodic boundary conditions on the worldvolume fermions. By adding N_f probe $D6$-branes, this model was studied in [118] as

a model of four dimensional QCD with $N_f \ll N$ flavours. This model was modified in [119] to contain N_f $D8$-branes. For a review see [120]. Furthermore, a non-conformal $\mathcal{N} = 2^*$ dual field theory is obtained by including a mass deformation on top of the usual conformal $\mathcal{N} = 4$ SYM [121].

Motivated by these observations, "bottom-up" models that are inspired by the AdS/CFT correspondence but do not descend from any particular full string theory construction have been proposed to capture QCD phenomenology. This program is called AdS/QCD, for a review see [122]. In a similar spirit, the AdS/CMT program is intended to use gauge/gravity duality to point towards universal features of strong coupling behaviour, and give us a window into what to expect for strongly coupled systems where a reliable quasiparticle description is not available.

The approach then is to start from the bottom-up by constructing an effective gravitational model with the kinds of ingredients necessary for capturing the strongly coupled behaviour we are interested in. Only the minimal ingredients necessary for a holographic duality are assumed. We need to know the dimensionality of the system, whether or not the system is at finite temperature and/or charge density, and what kind of symmetries we expect to find (for example, translational invariance). With these basic ingredients, a spacetime which captures these properties and a model which contains the spacetime as a solution is proposed. A variety of bulk models are available, starting with pure Einstein gravity with a negative cosmological constant. Generalizations include adding matter content such as scalars or fermions which are useful for studying condensates of the dual operators, bulk gauge fields which can encode global symmetries of the boundary theory, higher curvature corrections which describe $1/N$ corrections, and so on. These specific models are not full fledged string theory on the bulk side, but rather contain components common to all known holographic theories. The results, then, are expected to apply to a wide class of holographic theories and help us understand a broad range of features of strongly coupled field theories.

With the model in hand, the idea is to use the known holographic dictionary to compute properties of the strongly coupled dual field theory. Usually, the interesting spacetime geometries are meant to be thought of as being asymptotically AdS (that is, they approach an AdS solution near their boundary) so that the holographic dictionary may be applied more reliably. Actually demonstrating that the a geometry has an AdS completion can be tricky and we will discuss mechanisms by which this can occur in chapter 2 for a certain class of holographic spacetimes. The bottom-up approach has proven surprisingly useful for capturing broad classes of potentially interesting phenomenology. Furthermore, it has sparked renewed interest in finding solutions to classical gravity systems in novel settings, revealing a rich landscape of spacetimes with unconventional properties

An obvious drawback to the bottom-up approach is that it does not provide a "top-down" UV embedding of the model in full string theory, or even into a supergravity theory. Actually constructing string embeddings can be a daunting task. While this has been achieved in certain cases (some examples from the literature are provided below in sections 1.5.2, 1.5.3 and 1.5.4), there is no known general procedure. Pursuing purely bottom-up models does not generally point towards a top-down embedding, while starting from the top-down is technically challenging. The idea then is to pursue both approaches in parallel with the aim of meeting somewhere in the middle; using both bottom-up and top-down models to motivate constructing full holographic solutions.

Below we will review a few important applications of holography which exemplify the long reaching power of gauge/gravity duality. In the process, links between seemingly unrelated systems will appear.

1.4.2 Quantum criticality

A quantum phase transition is a continuous (second order) transition that occurs at zero temperature, driven by quantum fluctuations. Such transitions can occur in a variety of

systems, see [123] for a description of some real world examples. Since the transition is occurring at zero temperature, it is controlled by tuning some other external parameters, such as the applied magnetic field or pressure. At a critical value of the coupling to the external parameter, a measurable change to the ground state wavefunction can occur: this is the quantum phase transition. As the phase transition is approached, any energy gap in the system vanishes, and so the coherence length also diverges with a specific scaling law. At the quantum critical point, the system is described by a quantum critical theory [71]. The theory is scale invariant, but it is not necessarily relativistic, meaning that space and time may scale differently. In some circumstances, the critical point may be described by a fully relativistic CFT. The parameter which governs how space and time scale differently is called the dynamical critical exponent, z; it will play a special role when we discuss non-relativistic holography in sections 1.5.1-1.5.5. Within the context of field theory, z sets the upper critical dimension of interactions [71]. It is also known that in $2+1$ dimensions, quantum critical theories are typically strongly coupled; a reliable quasiparticle description is often not available and this is an opportunity for holography [123].

The effects of a quantum critical point are not solely confined to zero temperature; their imprint can be felt even at finite temperature. At the quantum critical point, the system is not gapped and at $T = 0$ critical excitations require no energy to be excited. Turning up the temperature is equivalent to adding a thermal noise with a characteristic energy $k_B T$, so any fluctuation with a smaller energy than this can be thermally excited. As long as the correlation length of an excitation is long enough, it can still display critical behaviour even though it has moved off of the critical point [124]. In fact, as the temperature is increased, the imprint of the quantum critical point grows [123], [71].

Based on the presence of strong coupling, along with the observations about scale invariance and in some case full conformal invariance, it is expected that gauge/gravity duality may play an important role in understanding these systems. As we will see, using

holography to model scale invariant systems without relativistic symmetry will lead to new holographic dualities. An example of a quantum critical phase is the so called "strange metal" phase in which properties of a metallic system, such as resistivity, differ drastically from those predicted by standard Fermi liquid theory. This phase has gained considerable attention in the holographic context and will be discussed more thoroughly in section 1.5.5.

Quantum critical points seem almost tailor made for a holographic analysis, but they are not the only interesting class of systems to explore. At sufficiently long wavelengths, many systems, including quantum systems, can be effectively described by hydrodynamics, even at strong coupling. Perhaps unsurprisingly then, gauge/gravity duality has quite a bit to say about fluid mechanics.

1.4.3 Fluid/gravity

The relationship between gravity at long wavelengths and fluid dynamics, in the context of gauge/gravity duality, goes back almost fifteen years to [125], which was interested in studying the shear viscosity of strongly coupled plasmas. A flurry of active later strengthened the linkage and gave rise of to notion of the fluid gravity correspondence. Detailed reviews and a comprehensive list of references may be found in [82], [126] and [127].

For a gas, collisions between the constituents will occur over a time scale set by the mean free time τ and a length scale equal to the mean free path λ. If L is another length scale which characterizes the scale of variations for temperature and velocity, the the ratio $K \equiv \lambda/L$, called the Kundsen number, characterizes the scale over which thermal equilibrium is achieved. When $K \ll 1$, thermal equilibrium can be achieved locally in a finite time and the gas is in the hydrodynamic regime. The local properties of the system, such as temperature T, velocity u^a and local density (of all conserved charges), vary slowly over spacetime in this regime. It is believed that every non-trivial

quantum field theory, even at strong coupling, equilibrates to such a fluid phase at high temperatures [126].

The dynamics of the fluid are described by the conservation of the energy-momentum tensor $\nabla_a \tilde{T}^{ab} = 0$ and conservation of any other conserved charges. In what follows, we will imagine the indices a and b as being boundary indices, and so they do not include the holographic radial coordinate. Supplementing these conservation conditions is a set of constitutive relations which allow the energy momentum tensor to be expressed in terms of the dynamical variables, $T(x)$, $u^a(x)$, which are functions of the boundary coordinates. If this system is to be described by a simple gravity dual, it should also have a conformal symmetry which further restricts the form of the energy-momentum tensor.

A minimal requirement to having a gravitational dual is to find a spacetime solution that describes the same set of dynamical variables as the fluid. A first guess at a solution would be the static AdS-Schwarzschild solution (1.3.11) in $4+1$ dimensions, boosted along one of the boundary directions. This captures, via the holographic dictionary, the requirement that the boundary fluid have a finite temperature, as well as the dependence on the velocity field since this it is a boosted solution. It does not handle the fact that the dual fluid is, globally, out of equilibrium since T and u^a do not depend on the boundary coordinates. Since the dynamical variables of the fluid are meant to be slowly varying functions of the boundary coordinates, the dependence may be built into the solution to the Einstein equations perturbatively, expanding the bulk equations of motion in a derivative expansion of the dynamical variables and solving them order by order. This was first done in [17]. For a review of the technical details, see [126].

The upshot to this procedure is that, at the fully nonlinear level, the constraint equation coming from the off-diagonal $[r, a]$ components of the Einstein equations (which is now non-trivial since the temperature and velocity field now depend on the boundary directions) turn into the Navier-Stokes equations – generalized to a relativistic conformal fluid. The holographic dictionary can then be applied and the transport properties of

the dual fluid can be read off. Generalizations of this construction to non-conformal and non-relativistic as well as rotating fluids also exist [127].

Starting with the analysis in [19] and later complemented by [18] and [128], the fluid/gravity correspondence was generalized to include a chemical potential in order to study the dual dynamics of a fluid which preserves an additional $U(1)$ charge. This was accomplished within a bulk Einstein-Maxwell-Chern-Simons model which has the charged $RN - AdS$ geometry as a solution. Performing the same derivative expansion as in the original AdS-Schwarzschild case, it was found that a new term appears in the charge current, modifying the classic textbook result for a relativistic charged fluid.

There has also been interest in the fluid gravity correspondence from the gravity side. In [129] and [130], it was shown that for every incompressible solution of the Navier-Stokes equations, there is an associated dual solution of the Einstein equations in one higher dimension. Moreover, the dual gravity solution is uniquely determined . For $2+1$ dimensional incompressible fluids, it was shown that the associated spacetime falls under the Petrov classification which is a class of spacetimes categorized by the symmetries of their respective Weyl tensors. An algorithmic approach to reconstructing the dual spacetime solutions was developed in [131] which also used to the gravity solution to study the transport properties of the dual fluid.

The fluid/gravity correspondence may yet reveal other interesting facts about fluid dynamics. It is still unclear how much can be learned in regards to long standing problems of turbulence. Recently, [21] and [132] constructed numerical black hole solutions which are asymptotically AdS_4 and flat, respectively, which display a turbulent instability. In both cases, an inverse energy cascade, reminiscent of Kolmogorov scaling, is observed. Whether or not turbulence is related to the instability of global AdS, first observed in [133], is still an open question.

The hydrodynamic regime is familiar territory with respect to the behaviour of matter. We would like gauge/gravity duality to be useful for exploring less conventional phases;

a prime example is superconductivity.

1.4.4 Holographic superconductors

The existence of superconducting phase transitions within holography is a spectacular example of how gravitational physics in asymptotically AdS geometries can be substantially different from asymptotically flat spacetime; no-hair theorems are different in AdS. It is this difference that allows a superconducting phase transition in the dual theory to occur. For example, a charged asymptotically AdS black hole can have charged scalar hair [134]. Suppose the charged asymptotically AdS black hole has an initial charge Q and there is a bulk scalar field with charge q living on the horizon, the total charge is then qQ. Near the event horizon, the electric field is strong enough to pair produce charged particle pairs out of the vacuum due to the Schwinger mechanism. The particle with charge opposite that of the black hole gets pulled into the event horizon while the particle with the same sign charge as the black hole escapes. In asymptotically flat spacetime, the particle with the same sign charge would escape off to infinite and the geometry would be the standard Reissner-Nördstrom black hole. Asymptotically AdS space behaves like a confining box due to the negative cosmological constant in which the outgoing charged particles are trapped. Ultimately, they settle somewhere outside the event horizon and make up the charged scalar hair [135].

Historically, early studies of holographic superconductors include [134], [12] and [136]. By now, there is a vast literature on this subject. A comprehensive review is provided in [124]. For a recent review of bottom-up models see [137]. Here, we will review the basics of constructing a holographic s-wave superconductor and discuss generalizations to p and d-wave cases.

In order to have superconductivity, it is necessary to break a $U(1)$ gauge symmetry down to a discrete subgroup [138]. Specifically, consider a system with a gauge field $A_\mu(x)$ and a fermion $\psi(x)$ which is charged under the $U(1)$ gauge group. For simplicity, we work

in Euclidean signature, the coordinate x is meant to collectively define the coordinates in this theory. Accordingly, the theory enjoys a gauge symmetry [124]

$$A_\mu(x) \to A_\mu(x) + \partial_\mu \alpha(x)\,, \tag{1.4.1}$$

$$\psi(x) \to e^{iq\alpha(x)}\psi(x)\,, \tag{1.4.2}$$

where $\alpha(x)$ is the gauge parameter and q is the electric charge of $\psi(x)$. Consider the spontaneous breaking of this gauge symmetry down to a discrete subgroup $U(1) \to \mathbb{Z}_n$ by the formation of a charged condensate. According to Goldstone's theorem, this spontaneous symmetry breaking produces a Goldstone boson $\theta(x)$ which behaves as a phase and transforms as $\theta(x) \to \theta(x) + \alpha(x)$ under the original gauge transformation. An action appropriate for describing the dynamics of the gauge field and the Goldstone boson is

$$S = -\frac{1}{4}\int d^{d+1}x \left\{F^2 + L[A - d\theta]\right\}\,, \tag{1.4.3}$$

where $L[A - d\theta]$ is the Lagrangian for the Goldstone boson, which does not need to be precisely specified for this argument to work. The functional dependence of L on $A - d\theta$ is required by gauge invariance. Given the action (1.4.3), the charge density then follows from

$$J^t = \frac{\delta L}{\delta A^t} = -\frac{\delta L}{\delta(\partial_t \theta)}\,. \tag{1.4.4}$$

Notice that $-J^t$ is then the conjugate variable to θ meaning that, given a Hamiltonian $\mathcal{H}$, we have

$$\partial_t \theta = -\frac{\delta \mathcal{H}}{\delta J^t} = -V(x)\,, \tag{1.4.5}$$

where $V(x)$ is the electric potential. The identification in the second equality follows from noting that $\partial_t\theta$ is proportional to the variation of the energy density (i.e. $\mathcal{H}$) with respect to the charge density. Consider now a stationary state so that there is no time dependence in the system. Assume also that there is a steady current flowing through the system which is given by

$$J^i = \frac{\delta L}{\delta A_i}\,. \tag{1.4.6}$$

This implies that $V(x) = 0$ by (1.4.5), so there is a net current while the electrical potential vanishes. In other words, the DC conductivity (since we are considering a stationary state) must be infinite, i.e. this is a superconducting state.

While this argument does not provide an explicit microscopic model of a superconductor, it does help point towards the minimal ingredients necessary to construct a holographic superconductor. On top of the usual Einstein-Hilbert action, we need a bulk gauge field which, in conjunction with the holographic dictionary entry (1.3.10), will encode a finite chemical potential in the boundary theory, as well as a charged field in the bulk. The role of the additional bulk charged field is to mock up the formation of a non-zero vev for a charged operator in the dual theory due to spontaneous symmetry breaking. There is more than one possible choice for the charged bulk field, depending on whether or not the condensate in the boundary theory carries any angular momentum. If it does not, then the condensate is a scalar and we have an s-wave superconductor. The corresponding bulk field is then itself a scalar. Other choices for the bulk field can lead to p and d-wave superconductors, depending on the symmetries of the vev of the order parameter. A minimal bulk action for an s-wave holographic superconductor in $3+1$ dimensions is then [71]

$$S = \int d^4\sqrt{-g}\left\{\frac{1}{16\pi G_N}\left(R + \frac{6}{L^2}\right) - \frac{1}{4e^2}F^2 - |\nabla\phi - iqA\phi|^2 - m^2|\phi|^2\right\}, \qquad (1.4.7)$$

where ϕ is a complex scalar (i.e. it is charged). If a superconducting transition exists in this model, then there must be both a normal (i.e. non-superconducting) and a superconducting phase that need to be identified. Since the onset of superconductivity is signalled by the formation of a non-zero vev for the operator dual to ϕ, the normal phase must correspond to a solution to the bulk equations to motion with $\phi = 0$. In this case, the bulk action is just the usual Einstein-Maxwell model and the solution is the $RN - AdS$ geometry (1.3.13).

The identification of the normal state as being dual to the $RN - AdS$ geometry is a crucial observation. In order for the superconducting transition to exist, there must be

a critical temperature below which a solution with $\phi \neq 0$ is possible. In other words, the $RN - AdS$ black hole must somehow be unstable to the formation of scalar hair. This is precisely what happens and is an example of how gravitational physics in an asymptotically AdS spacetime can be remarkably different from an asymptotically flat geometry where no hair theorems would suggest that such a solution should not be possible [139].

Ultimately, the mechanism responsible for this instability is the Breitenlohner-Freedman (BF) bound (1.3.6). The scalar field, which vanishes in the normal phase, is treated as a perturbation on top of the $RN - AdS$ background. Since the scalar is meant to be charged under the gauge field A_μ, the equations of motion for the scalar field couple the mass parameter with the background charge via the gauge covariant derivative. Near the horizon, this adds an overall negative contribution to the mass squared of the scalar field. The net effect is that the effective mass squared of the scalar field may be different near the horizon [71].

As the temperature is lowered, an AdS_2 near horizon geometry appears in the $RN - AdS$ spacetime. Ultimately what this means is that even though the scalar field may have a mass which satisfies the BF bound in $3 + 1$ dimensions, the effective mass near the horizon does not necessarily satisfy the analogous criterion for AdS_2. In other words, at low enough temperature, the near horizon geometry may become unstable to a scalar perturbation. The precise combinations of parameter values for T, m and q for which this instability occur are found numerically. For these values, holographic superconductor solutions are possible.

In light of this instability, the spacetime solution must be different when $\phi \neq 0$ and the dual theory will have a non-zero vev for the corresponding scalar operator. The solution may be found numerically and its conductivity calculated (also numerically) using the same technique outlined in section 1.3.4. The end result is a divergent DC conductivity in the superconducting geometry. As the frequency of the conductivity is

increased, the normal state is approached. There is a caveat here that should be pointed out. The normal state is dual to the $RN - AdS$ geometry which itself has a divergent DC conductivity due to momentum conservation along the boundary directions as we discussed in section 1.3.4, so it is not immediately obvious that the superconducting result is due to a different mechanism. In the probe limit for the charge density, the normal state is effectively the AdS-Schwarzschild geometry (1.3.11). As discussed in section 1.3.4, the dual theory does not suffer from a divergent DC conductivity. In [12] it was shown that, even in this probe limit, the scalar instability persists and the resulting geometry describes an infinite DC conductivity in the dual theory, characteristic of a superconducting state.

By now, several top down and supergravity embeddings of the s-wave holographic superconductor exist. In [139], instabilities similar to the bottom-up holographic s-wave superconductor were found within M-theory and $D = 11$ supergravity [140]. The formation of a condensate analogous to the holographic superconductor was found within a dual to type IIB supergravity in [141].

The first extension to a holographic p-wave superconductor was given in [142]. Here, the scalar field of the s-wave model is replaced by an $SU(2)$ Yang-Mills field and the gauge symmetry associated to a $U(1)$ subgroup is spontaneously broken. In this context, the superconducting state is described by a black hole solution with vector hair. Correspondingly, the resulting conductivity is not necessarily isotropic. Generalizations to the p-wave $SU(2)$ model include the addition of curvature squared corrections to the gravity action [143], [144], the addition of a Chern-Simons coupling [145] as well as accounting for the backreaction of the gauge field on the metric [146]. p-wave holographic superconductors with helical order were constructed in [147] and [148]. Top down models have been approached by adding probe $D7$-branes embedded in the AdS black hole background in [149], [150] and [151].

A d-wave holographic superconductor was proposed in [152]. A natural approach

is to introduce a minimal model which contains a massive, symmetric and traceless rank-2 tensor coupled to a $U(1)$ gauge field (i.e. it is complex). Starting from a AdS-Schwarzschild background, a superconducting transition is observed within this model at a critical temperature. Including another rank-2 tensor into the matter sector of the theory can lead to the appearance of ghosts. To this end, a more refined model using the same matter content as [152] was studied in [153] which is ghost free.

Numerous models which display the coexistence of multiple order parameters have been proposed. By including multiple bulk fields which encode different order parameters and including interactions amongst them, competition between s-wave, p-wave and d-wave states can be achieved. Examples include the competition between two s-wave orders [154], [155], [156], s-wave and p-wave orders [157], [158], two p-wave orders [159], as well as s-wave and d-wave orders [160], [161]. A comprehensive list of references as well as detailed descriptions of the models discussed in this section may be found in [137].

Pushing the boundaries of symmetry breaking in holography is the next step required for modelling more realistic condensed matter systems. Impressive progress has been made on this front and we dedicate the next section to describing some aspects of this program.

1.5 Reducing symmetry

The applications of holography discussed in the previous section 1.4, while immensely successful, are not general enough to model realistic condensed matter systems. In order to make progess on this front, it is necessary to reduce the amount of symmetry in holographic models.

Systems which possess too many symmetries display behaviours that are not desirable in condensed matter models. A prime example is the DC conductivity calculated from the $RN-AdS$ black hole, dual to a system with finite charge density. Unlike the case of the

AdS-Schwarzschild black hole, the dual optical conductivity is not a constant and does depend on frequency ω. As $\omega \to 0$, the optical conductivity approaches a delta function, signalling the divergence of the dual DC conductivity [162]. This is not a surprising feature. The underlying $RN - AdS$ geometry possesses translational invariance along the boundary directions. This means that the charge carriers in the dual theory have no means by which to dissipate momentum, resulting in an infinite DC conductivity. Realistic condensed matter systems do not display this behaviour, so if a holographic model is going to be useful for studying these kinds of problem, we need a way to break translational invariance.

Translational invariance is only one example of the types of symmetries we might be interested in breaking within holographic models and in this section we will discuss several proposals for achieving reduced symmetry. Holographic models with reduced symmetry should be expected to exist if we are going to take the AdS/CMT proposal seriously. Low temperature phases of condensed matter systems display phase transitions in which the symmetries of the system are different from those of the high temperature phase. In this sense, a holographic model should, vis-a-vis the UV-IR relations, be able to connect an asymptotically AdS (UV) region with lots of symmetry, to an interior geometry (IR) where some of the symmetry is broken, signalling in the existence of a different low energy phase. The types of accessible interior solutions and their classification is a subject of ongoing study. Recent progress suggests that there may be a veritable zoo of new solutions to be found. Below, we present some known solutions and proposals.

1.5.1 Breaking boost symmetry

As a first example, consider breaking boost symmetry. Generally, the low energy phases of matter that holography may be useful for modelling do not typically possess relativistic symmetry. Therefore, any realistic holographic model will need to take this reduction of symmetry into account. Two major directions have been pursued in this context:

spacetimes with Schrödinger symmetry [163] and spacetimes with Lifshitz symmetry [164]. Extensions to holographic models to include violation of the hyperscaling relation have also been proposed [165],[166]. In this section we will review the salient features of these proposals, the models that give rise to them and their utility with regards to AdS/CMT.

1.5.2 Schrödinger geometries

Historically, the first proposal for breaking relativistic symmetry in a holographic model were geometries with Schrödinger symmetry [163], i.e. the symmetry group of the Schrödinger equation in free space. The symmetry group describes a non-relativistic extension of conformal symmetry and as such has generators corresponding to: temporal translations H, spatial translations P^i, rotations M^{ij}, Galilean boosts K^i, dilatation D, a special conformal transformation C and a mass operator M, which encodes a conserved rest mass or particle number. In order for the conservation of particle number to make sense here, the dual field theory must not have particle production. Note that because the group describes a non-relativistic symmetry, time and space behave differently under the dilatation operator D, namely $t \to \lambda^2 t$, $x_i \to \lambda x_i$ [163]. The list of commutation relations between the various generators may be found in [163] and [167]. Note that the asymmetry between the scaling of time and space indicates that the model has a dynamical critical exponent $z = 2$. Extensions to models with arbitrary z were proposed in [167].

The motivation behind looking for a holographic model which encodes this kind of symmetry rests in recent success with cold atom systems. These systems are experimental realizations of a unitary Fermi gas, which respect Schrödinger symmetry, and provide a window to the physics of strongly coupled fermions. A geometry which obeys Schrödinger

symmetry with arbitrary z is [167]

$$ds^2 = L^2\left(-\mathcal{R}^{2z}dt^2 + \frac{d\mathcal{R}^2}{\mathcal{R}^2} + \mathcal{R}^2(dx^i dx_i + 2d\xi dt)\right), \tag{1.5.1}$$

where $\mathcal{R}$ is the radial coordinate and x_i are the boundary directions. In these coordinates, the boundary is located at $\mathcal{R} \to \infty$. The coordinate ξ encodes the action of the mass operator M in the Schrödinger symmetry group with the identification $M = i\partial_\xi$ [167].

Schrödinger geometries have been found as solutions to Einstein gravity with a negative cosmological constant coupled to a massive vector field [163] as well as an Abelian Higgs model [167]. Flows between Schrödinger geometries and an asymptotically AdS region were constructed in [168]. Finite temperature counterparts to the Schrödinger geometries as well as several supergravity and top-down string embeddings for various values of z have been constructed over the years [169], [170], [171], [172].

There has also been some progress in constructing the holographic dictionary for the Schrödinger geometries. In [173], the dictionary is studied as a perturbation about the relativistic AdS case by an irrelevant operator. This was followed up in [174], [175] and [176]. Later, non-perturbative constructions were given in [177] for $z < 2$ and in [178] and [179] for $z = 2$.

1.5.3 Lifshitz geometries

The other major direction for breaking relativistic symmetry via holography focuses on Lifshitz geometries. First proposed in [164], the metric takes the form

$$ds^2_{d+2} = L^2\left(-\mathcal{R}^{2z}dt^2 + \frac{d\mathcal{R}^2}{\mathcal{R}^2} + \mathcal{R}^2 dx_i^2\right), \tag{1.5.2}$$

where $\mathcal{R}$ is the radial coordinate, which ranges from $\mathcal{R} \to 0$ in the interior to $\mathcal{R} \to \infty$ at asymptopia. The bulk spacetime respects Lifshitz scaling symmetry $t \to \lambda^z t\,, x_i \to \lambda x_i$ with $\mathcal{R} \to \lambda^{-1}\mathcal{R}$. Here, d is the number of transverse dimensions x_i and L sets the length scale in the bulk.

The difference between the Lifshitz geometry (1.5.2) and the Schrödinger geometry (1.5.1) is the lack of the extra coordinate ξ, which is the holographic avatar of conservation of particle number in the dual theory. In this sense, the Lifshitz geometry should be dual to a non-relativistic field theory with no conserved particle number. A classic toy model of a field theory with, $z = 2$, is the Lifshitz field theory with action [164]

$$S = \int d^2x\, dt \left((\partial_t \phi)^2 - \kappa (\nabla^2 \phi)^2 \right) , \tag{1.5.3}$$

where κ is a dimensionless constant. Lifshitz critical behaviour arises at critical points of many known systems, such as high T_c superconductors, liquid crystals and others. Further discussion of systems where Lifshitz scaling arises may be found in [180].

Note that the value of the dynamical critical exponent, z, sets the effective speed of light in the boundary theory. To see this, change the radial coordinate to $\rho = \ln(R)$. In this way, the boundary corresponds to $\rho \to \infty$. The metric now reads

$$ds_s = L^2 \left(-e^{2z\rho} dt^2 + d\rho^2 + e^{2\rho} dx_i^2 \right) . \tag{1.5.4}$$

Consider a radial slice, Σ, at some $\rho = \rho_*$. The induced metric on this surface can be viewed as a flat space with a speed of light dependent on ρ_* [181]. The induced metric is

$$ds_\Sigma^2 = L^2 e^{2\rho_*} \left(-c_\rho^2 dt^2 + dx_i^2 \right) , \tag{1.5.5}$$

where the effective speed of light is $c_\rho = e^{(z-1)\rho_*}$. In the limit that $\rho_* \to \infty$, the effective speed of light then approaches infinity, as would be expected in a non-relativistic theory, provided that $z > 1$. If $z < 1$, then superluminal propagation becomes possible.

The Lifshitz metric and its finite temperature counterpart are exact solutions to Einstein gravity with a nontrivial matter sector. Two popular options for the matter sector are Einstein gravity coupled to a massive gauge field [182],[36],[183] and Einstein-Maxwell-dilaton theory [184],[185],[14],[186]

$$S = \frac{1}{16\pi G_N} \int d^{d+2}x \sqrt{-g} \left(R - \frac{1}{2} (\partial \phi)^2 - V(\phi) - \frac{1}{4} f(\phi) F^2 \right) . \tag{1.5.6}$$

In order to obtain Lifshitz solutions, it suffices to consider $f(\phi) \propto e^{\lambda_1 \phi}$ and $V(\phi) = \Lambda$, where λ_1 is a constant and Λ is the (negative) cosmological constant. Lifshitz solutions have also been found within an Einstein-Maxwell-dilaton model including higher derivative corrections in curvature and the field strength tensor [187].

Aspects of the holographic dictionary and holographic renormalization are better developed for Lifshitz geometries compared to their Schrödinger counterparts starting with [181] which constructed the dual stress tensor for Lifshitz and Schrödinger geometries within an Einstein-Proca model. This was subsequently generalized in [188] which also, along with [189] for $z = 2$, studied aspects of holographic renormalization for Lifshitz geometries in an Einstein-Proca model in $3+1$ dimensions. A Hamilton-Jacobi formulation of holographic renormalization for Lifshitz solutions in $3 + 1$ dimensions in this model was provided in [190]. The holographic dictionary for special values of z has also been derived in a variety of places, including [191] and [192] for z near 1, where the Lifshitz solution is treated as a perturbation about AdS. More recently, [193] and [194] constructed the holographic dictionary within a large class of Einstein-Proca-dilaton models for all values of z and arbitrary dimensions. Here, the dictionary is worked out by recursively solving the radial Hamilton-Jacobi equations in the bulk. The analogue of the Fefferman-Graham expansion for asymptotically Lifshitz spacetimes is also worked out. See [195] for a review.

The Lifshitz geometry (1.5.2) has finite curvature scalars throughout the spacetime and so does not contain any unphysical curvature singularities. Nevertheless, the geometry does display diverging tidal forces in the deep interior as $\mathcal{R} \to \infty$ [164]. Such a divergence is only a problem if an infalling observer can actually reach the interior in finite proper time (or affine parameter in the case of a null geodesic). In fact, this is the case for the Lifshitz geometry. To see this, consider an ingoing null geodesic. The Lifshitz metric has no explicit time dependence, so there is a conserved quantity

$$E = L^2 \mathcal{R}^{2z} \dot{t}\,, \tag{1.5.7}$$

where $\dot{} \equiv d/d\lambda$, λ being the affine parameter. Examining the equations of motion yields an expression for the affine parameter for a null particle moving inward from some finite $\mathcal{R}_*$ to $\mathcal{R} = 0$

$$\mathcal{R}_*^z = -\frac{Ez}{L^2}(\lambda - \lambda_0)\,, \tag{1.5.8}$$

where λ_0 is some initial affine parameter. The take home message is that this value is finite. The same result holds for radial timelike geodesics [196].

The surfaces of constant $\mathcal{R}$ are null as $\mathcal{R} \to 0$ in the interior. To see this, simply consider the contraction of the normal vector to a surface at constant radial slice

$$\nabla_a \mathcal{R} \nabla^a \mathcal{R} = g^{\mathcal{R}\mathcal{R}} = \frac{\mathcal{R}^2}{L^2}\,, \tag{1.5.9}$$

which becomes null as $\mathcal{R} \to 0$. The index a runs over all of the bulk coordinates except for the radial coordinate, $\mathcal{R}$.

To see that there are divergent tidal forces in the interior of the Lifshitz geometry, look at the form of the Riemann tensor in a parallelly propagated orthonormal frame (in this case, a frame which follows a timelike observer) that is radially infalling [196]. The idea is then that if the components of the Riemann tensor diverge in this frame, then initially parallel geodesics develop a diverging relative acceleration. In other words, they experience a diverging tidal force. An appropriate frame is [196]

$$\tilde{e}_{\hat{t}\mu} = -E\partial_\mu t + E\mathcal{R}^{-(z+1)}\sqrt{1 + \frac{L^2\mathcal{R}^{2z}}{E^2}}\partial_\mu \mathcal{R} \tag{1.5.10}$$

$$\tilde{e}_{\hat{\mathcal{R}}\mu} = -E\sqrt{1 - \frac{L^2\mathcal{R}^{2z}}{E^2}}\partial_\mu t + E\mathcal{R}^{-(z+1)}\partial_\mu \mathcal{R} \tag{1.5.11}$$

$$\tilde{e}_{\hat{i}\mu} = L\mathcal{R}\partial_\mu x_i\,, \tag{1.5.12}$$

where indices with a hat indicate flat space directions (i.e. which live in the tangent space). The components of the Riemann tensor with curved indices are related to the components with flat indices by

$$\tilde{R}_{\hat{\alpha}\hat{\beta}\hat{\xi}\hat{\chi}} = R_{\mu\nu\lambda\sigma}\tilde{e}^{\mu}{}_{\hat{\alpha}}\,\tilde{e}^{\nu}{}_{\hat{\beta}}\,\tilde{e}^{\lambda}{}_{\hat{\xi}}\,\tilde{e}^{\sigma}{}_{\hat{\chi}}\,. \tag{1.5.13}$$

The full set of components of the Riemann tensor in this frame may be found in [196]. An example of a diverging component is

$$\tilde{R}_{\hat{t}\hat{i}\hat{t}\hat{i}} = \frac{1}{L^2} + \frac{E^2(z-1)}{L^4\mathcal{R}^{2z}}\,, \tag{1.5.14}$$

which diverges in the interior $\mathcal{R} \to 0$ for $z > 1$. This result, coupled with the fact that surfaces of constant radial coordinate R are null in the interior (1.5.9) tells us that a null tidal force singularity is present at $\mathcal{R} = 0$. Note that for $z = 1$, the divergence is not present. This had to be the case, as $z = 1$ is AdS.

The null singularity is even a problem for string probes as they become infinitely excited as they pass through the interior of the geometry [197]. In order to make sense of these geometries from the point of view of applied holography, it is necessary to resolve this unphysical singularity. Several approaches to solving this problem have been taken which we will discuss more fully in chapter 2.

Several supergravity and string embeddings of Lifshitz geometries for various values of the dynamical critical exponent, z, have been constructed, including: [198], [199], [200], [201], [202], [203], [204], [205], [206], [207], [208], [209], [210], [211], [172] and [192].

Bottom-up holographic models, such as the Einstein-Maxwell-dilaton model (1.5.6) support a wide range of possible gravitational solutions. A notable generalization of the Lifshitz spacetime (1.5.2) which violates the hyperscaling relation is particularly useful for condensed matter models, as we now discuss.

1.5.4 Hyperscaling violation

The Einstein-Maxwell-dilaton theory (1.5.6) supports a broader class of interesting spacetime geometries; the hyperscaling violating (HSV) metric

$$ds^2_{d+2} = L^2\left(-\mathcal{R}^{2(z-\theta/d)}dt^2 + \frac{d\mathcal{R}^2}{\mathcal{R}^{2(1+\theta/d)}} + \mathcal{R}^{2(1-\theta/d)}dx_i^2\right)\,, \tag{1.5.15}$$

where z is the dynamical critical exponent, d is the number of boundary directions and θ is the hyperscaling violation parameter [165],[166],[212]. Metrics of HSV form are not

scale invariant, but rather transform covariantly,

$$ds^2_{d+2} \to \lambda^{2\theta/d} ds^2_{d+2}\,. \tag{1.5.16}$$

From the perspective of the dual theory, hyperscaling is the property that the free energy of the system should scale with its naïve dimension. At finite temperature, theories with hyperscaling have an entropy density which scales with temperature as $S \sim T^{d/z}$. When hyperscaling is violated, there is a modified relationship, $S \sim T^{(d-\theta)/z}$, indicating the system lives in an effective dimension $d_{\text{eff}} = (d-\theta)$ [14],[213].

HSV solutions and their finite temperature counterparts have also been studied in a variety of other models, including Einstein gravity coupled to a massive gauge field [183] and within an Einstein-Dirac-Born-Infeld-dilaton [214].

The HSV geometries, just like their Lifshitz cousins, generally have a null tidal force singularity in the deep interior $\mathcal{R} \to 0$. This can be seen by carrying out exactly the same procedure as in the Lifshitz case; by constructing a parallelly propagated orthonormal frame and examining the form of the Riemann tensor. If there is a divergence in the components of the Riemann tensor as $\mathcal{R} \to 0$, then this indicates that there are diverging tidal forces in the interior. The full set of Riemann tensor components may be found in [215], [216] and [217]. As an example,

$$\tilde{R}_{\hat{t}\hat{i}\hat{t}\hat{i}} = \frac{[d(z-1)-\theta]}{L^4(d-\theta)} \frac{E^2}{R^{2z}} + \frac{d}{L^2(d-\theta)} R^{2\theta/d}\,, \tag{1.5.17}$$

where, again, the components of the Riemann tensor in this frame are related to the usual components with curved space indices by (1.5.13). Notice, when $\theta = 0$, the result is the same as the Lifshitz case (1.5.14). In general, the divergence of the Riemann tensor components will depend on the combination of solution parameters (z, θ). These values are not totally arbitrary. They can be restricted by applying a standard energy condition from general relativity, called the null energy condition (NEC)[14]. The NEC is a restriction on the energy-momentum tensor of the model, namely

$$T_{\mu\nu} N^\mu N^\nu \geq 0\,, \tag{1.5.18}$$

where N^μ is any arbitrary null vector of the spacetime. This condition, when applied to a perfect fluid, simply states that the sum of the energy density and pressure of the fluid should not be negative, $\rho + p_i \geq 0$. This condition is natural from the boundary perspective, since we are interested in geometries which are dual to condensed matter systems, so the energy content of the bulk theory should be reasonably well behaved. The NEC and the other energy conditions are ubiquitous in gravitational physics. When applied to the Raychaudhuri equation, they lead to conditions on geodesic focusing and are important in singularity theorems. For a review see [218]. It has been argued that violation of the NEC will lead to acausal behaviour [219], [220]. Unsurprisingly then, when applied to the Lifshitz geometry (1.5.2), the NEC requires $z \geq 1$.

With regards to holography, the NEC is important in the construction of the holographic c-theorem in AdS [221], [222], [223] and [224] as well as in constructing flows between UV and IR Lifshitz geometries [225]. The averaged null energy condition in a certain class of bulk spacetimes has recently been shown to be a consequence strong subadditivity of entanglement entropy in the boundary theory [226].

The NEC, by virtue of the Einstein equations, is also a restriction on the spacetime geometry itself. When applied to the HSV geometry (1.5.15), the equivalent condition $R_{\mu\nu}N^\mu N^\nu \geq 0$ constrains the possible values of the solution parameters (z, θ) to be [14]

$$(z-1)(z-\theta+d) \geq 0\,, \tag{1.5.19}$$

$$(d-\theta)(d(z-1)-\theta) \geq 0\,. \tag{1.5.20}$$

Physically, the effective dimension of the dual theory should be positive, so we expect that $d > \theta$ for a reasonable boundary theory. It can be shown [216] that when $d = dz - \theta \geq 2(d-\theta)$, all of the components of the Riemann tensor in the radial ingoing parallelly propagated orthonormal frame are finite, so there is no tidal force singularity. Notice, these values of z and θ saturate the second null energy condition (1.5.20). For other generic values of z and θ (except $z = 1$, $\theta = 0$ which is AdS) there is a null tidal

force singularity in the deep interior.

As in the Lifshitz case, this IR singularity must be resolved in order to make the geometry sensible for condensed matter applications. A full discussion of the techniques used to revolve this singular behaviour in different models is delayed until chapter 2, where it will be shown that curvature squared corrections to an Einstein-Maxwell-dilaton can act as a mechanism to induce a crossover to a regular interior geometry.

For positive values of θ, there is a curvature singularity as $\mathcal{R} \to \infty$; the boundary of the HSV geometry (1.5.15). This can be seen by computing the Kretschmann scalar $K \equiv R_{\mu\nu\lambda\sigma}R^{\mu\nu\lambda\sigma}$. Since we generally expect θ to be positive, a curvature singularity at the boundary is extremely problematic vis-à-vis constructing a sensible holographic dictionary. We will show in chapter 2 that for certain values of z and θ, curvature squared corrections to an Einstein-Maxwell-dilaton model can also support a crossover solution to an asymptotic AdS region.

Recently, the holographic dictionary for HSV geometries within a large class of Einstein-Proca-dilaton models for all values of z, θ and d which satisfy the null energy condition (1.5.19) (1.5.20) was worked out in [194]. This is achieved by using the same technique of recursively solving the bulk Hamilton-Jacobi equations as in the case of the Lifshitz holographic dictionary. A review is contained in [195].

As with the Lifshitz geometries discussed in section 1.5.3, a number of supergravity and string embeddings of the HSV geometries have been found for various z and θ [212], [227], [228], [229], [230], [231], [183], [232], [233], [234], [235] and [236].

The purpose of studying Lifshitz type geometries in the context of applied holography is that they represent gravitational duals to non-relativistic field theories. The HSV geometries provide holographic models that capture the behaviour of strange metals.

1.5.5 Application: strange metals

Historically, HSV geometries were first studied in [166], where it was pointed out that these spacetimes possess a holographic entanglement entropy which violates the area law.

The entanglement entropy of a conformal field theory in $d+1$ dimensions on $\mathbb{R}^{d,1}$ satisfies an area law, for $d > 1$. The leading order term in the entanglement entropy between a spatial region, A and its complement is proportional to the area of the region A. As an example, consider a strip of width l. This defines a spatial region $A \equiv \{x_1, x_2, \dots x_d\}$, where $-l/2 \leq x_1 \leq l/2$ and $0 \leq x_1, x_2, \dots x_d \leq L$. The entanglement entropy between this region and its complement, $S_A = -\mathrm{tr}\rho_A \log(\rho_A)$ is given by [166]

$$S_A = a\frac{L^{d-1}}{\epsilon^{d-1}} - b\frac{L^{d-1}}{l^{d-1}}\,, \tag{1.5.21}$$

where ϵ is a UV cutoff which should be taken to zero in the high energy limit, and a and b are constants [166]. Several examples may be found in [237]. Notice that the leading term as $\epsilon \to 0$ is proportional to the area of the entangling region A, this is called the area law for entanglement entropy. For a review, see [238].

The area law may be violated in some situations. QFTs in $d+1$ dimensions with a Fermi surface display logarithmic violations of the area law [239]. The same is true for CFTs in $d+1$ dimensions, where the leading term in (1.5.21) is replaced by a log [240].

Violations of the area law are expected to occur for compressible phases of matter, that is, a translationally invariant quantum system with a globally conserved $U(1)$ charge $\mathcal{Q}$ such that $\langle\mathcal{Q}\rangle$ changes smoothly as a function of chemical potential μ and $d\langle\mathcal{Q}\rangle/d\mu \neq 0$ [213]. A realization of a compressible phase is a system of finite temperature fermions at non-zero density coupled to a gauge field in 2+1 dimensions. This system, which is known to possess a Fermi surface [213], displays non-Fermi liquid behaviour, meaning that its thermodynamic and transport properties do not match those predicted by standard Fermi liquid theory. This phase is called a "strange metal" and is associated with quantum critical behaviour [123] (see section 1.4.2). The Fermi surface in this case is exotic and

is referred to as a hidden Fermi surface as it turns out that it is not a gauge invariant quantity. Regardless, the Fermi surface still obeys the Luttinger relation which requires that the Fermi surfaces encloses a volume proportional to $\mathcal{Q}$ [14]. The entropy density in this case scales with temperature as $S \sim T^{1/z}$. It is also known that $z = 3/2$ to three loop order for this model [213].

For the HSV geometries (1.5.15), the holographic entanglement entropy was first calculated for a strip region and a circular region for a 2+1 dimensional boundary in [166] where in both cases, logarithmic violations of the area law were found. This calculation was later extended in [14] where it was shown that leading term in the holographic entanglement entropy is independent of the specific shape of the boundary entangling region. The result depends on the value of θ. A logarithmic violation of the area law is observed for $\theta = d - 1$, whereas the area law is obeyed for $\theta < d - 1$ and is strongly violated for $\theta > d - 1$ [213].

HSV geometries with finite temperature and charge density capture a number of non-Fermi liquid properties. Firstly, setting $\theta = d - 1$ implies a logarithmic violation of the area law of entanglement entropy, as pointed out above. This violation suggests that the HSV geometry is dual to a system with a Fermi surface. By applying the Luttinger relation, it turns out that the holographic entanglement entropy has the same dependence on k_F as predicted from field theory calculations [14]. Furthermore, for $\theta = d - 1$, the entropy density of the finite temperature solutions scales as $S \sim T^{1/z}$. Setting the number of spatial dimensions to $d = 2$ and applying the NEC in this case (1.5.19) (1.5.20), requires that $z \geq 3/2$, which captures the known value of $z = 3/2$.

The values for z and θ are not uniquely determined by the NEC and selecting $\theta = d - 1 = 1$ and $z = 3/2$ is an arbitrary choice. In this sense, the holographic model is "too good", providing too many possible choices. In chapter 2, we will discuss how the addition of curvature squared corrections to the bulk action modify the form of the NEC and impose further restrictions on the possible choices of z and θ. Generally,

holographic models of non-Fermi liquid behaviour do not reproduce all of the expected properties of the dual phase. An early example constructed in [199] correctly reproduced the linear scaling of resistivity with temperature, but did not get the correct scaling for the Hall conductivity (which goes like T^3). More recently, it was pointed out that the correct scaling may be reproduced at the expense of introducing a new scaling parameter beyond z and θ [241].

Holographic Fermi surfaces and non-Fermi liquid behaviour have also been approached by studying probe fermions in Einstein-Maxwell theory [242], [243], [13]. The background geometry is the finite charge density $RN-AdS$ black hole (1.3.13) and the probe fermions are charged under the $U(1)$ gauge field and are dual to a fermionic operator in the dual field theory. The retarded Green's function for the fermions is computed by solving the bulk Dirac equation. The non-analyticities in the retarded Green's function are used to diagnose the existence of a Fermi surface at a Fermi momentum k_F. The DC conductivity of this model is calculated and it is found that, in some cases, the conductivity scales linearly with temperature. For a review see [244].

Holography is also useful for modelling other phases of matter at strong coupling. In particular, it is interesting to wonder what phases may be accessible vis-a-vis the kinds of symmetries that are available to be broken in a holographic system. While classifying all of these possibilities within a general holographic framework is an ongoing avenue of research, impressive progress has thus far been made. The first step is identifying mechanisms to further reduce the number of symmetries.

1.5.6 Breaking rotational symmetry

Another kind of symmetry we are interesting in breaking is rotational symmetry along the boundary directions. From the gravitational perspective, breaking rotational symmetry turns out be a slightly easier problem than full translational symmetry breaking. There already exists a class of spatially anisotropic, but still homogeneous, solutions to general

relativity; the Bianchi classification. Historically, these geometries have been studied in the context of cosmology. The extension of this classification to holography was first discussed in [245]. Homogeneity of the Bianchi geometries implies that the equations of motion are ODEs as opposed to PDEs, which makes finding analytic solutions more feasible. More direct methods of breaking translational invariance, such as holographic lattices, do not have this simplification, as will be reviewed in section 1.5.7.

For d spatial dimensions, homogeneity requires that there are d Killing vectors ξ_i, where $i = \{1, 2, \cdots, d\}$. The geometries of the Bianchi types are classified by the commutation relations satisfied by the Killing vectors

$$[\xi_i, \xi_j] = C_{ij}^k \xi_k \,, \tag{1.5.22}$$

where the C_{ij}^k are constants. Here $[\xi_i, \xi_j] \equiv \xi_i^\mu \partial_\mu \xi_j^\nu - \xi_j^\mu \partial_\mu \xi_i^\nu$ is the Lie bracket. The relations (1.5.22) define a real Lie algebra. For three spatial dimensions, there are nine inequivalent such algebras, defining nine different geometries in the Bianchi classification [245]. For example, with three spatial dimensions $\{x^1, x^2, x^3\}$, the type VII_0 geometry has constants $C_{23}^1 = -C_{32}^1 = -1$, $C_{13}^2 = -C_{31}^2 = 1$ and all other $C_{ij}^k = 0$. The Killing vectors are

$$[\xi_1^\mu] = [0, 1, 0] \,, \quad [\xi_2^\mu] = [0, 0, 1] \,, \quad [\xi_3^\mu] = [1, -x^3, x^2] \,,$$

with the vector notation $[x^1, x^2, x^3]$; one component for each spatial direction. The spatial metric which encodes this symmetry takes the form

$$ds_3^2 = (dx^1)^2 + \left[\cos^2(x^1) + (1+\lambda)\sin^2(x^1)\right](dx^2)^2 + \left[\sin^2(x^1) + (1+\lambda)\cos^2(x^1)\right](dx^3)^2 \,, \tag{1.5.23}$$

where λ is a real parameter. The metric (1.5.23) has a helical symmetry; the pitch of the helix is set by the parameter λ. Symmetries of this kind, and of the other Bianchi types, can arise in systems with a vector order parameter [245].

In the context of holography, one of the spatial directions is interpreted as the usual holographic radial direction, while the Bianchi symmetries are encoded along the re-

maining three spatial directions defining the boundary. In $4+1$ dimensions, solutions for all nine possible homogeneous symmetry transformations along the boundary directions are found within Einstein gravity with a massive Abelian gauge field and a negative cosmological constant [245].

Bianchi type geometries have found application in holographic models of zero-temperature metal-insulator transitions [246], where the interior geometry has a Bianchi type VII_0 symmetry group. The geometry was found to be a solution to an Einstein-Proca-Chern-Simons model. The solution is asymptotically AdS_5 and the interior geometry is $AdS_2 \times \mathbb{R}^3$, which describes a metallic phase. The interior geometry is found to be unstable to the formation of a helical lattice under perturbation by a relevant operator, signalling a zero-temperature metal-insulator transition. This model was further generalized [247], where it was shown that a superconducting phase with a helical symmetry also exists. Conductor-insulator transitions with a helical interior geometry were also investigated within an Einstein-Maxwell-dilaton model in [248]. Extensions of the Bianchi geometries to include hyperscaling violation and Lifshitz scaling were discussed in [249].

It is unclear if every geometry in the Bianchi classification can be completed to AdS at the boundary. Partial progress to answering this question was provided in [250] where geometries obeying standard energy conditions in general relativity which interpolate between an interior Bianchi geometry and an asymptotically AdS or Lifshitz geometry (see section 1.5.3) were presented. In principle, such geometries were constructed for interior Bianchi types II, III, VI and IX. At present, it is unclear if these interpolating geometries are solutions to a gravitational theory with a simple matter sector.

In contrast with rotational symmetry breaking, an explicit lattice is expected to fully break translational invariance. Constructing such a lattice solution is generally difficult since the simplification of a homogenous geometry, afforded by the Bianchi type models, is no longer valid. Impressive progress has been made on this front in recent years which we will review in the next section.

1.5.7 Holographic lattices

An important feature of many condensed matter systems is a lattice. The presence of a lattice breaks translational symmetry down to a discrete subgroup and so can have a measurable impact on the transport properties of the system. In particular, since translational invariance is now broken by the lattice structure, momentum can be dissipated and unphysical divergences in electrical transport are not present.

In a holographic context, this breaking of translational invariance is exactly the ingredient needed to make progress on more realistic models of condensed matter phenomena. In particular, this explicit breaking of translational invariance is what is required in order to resolve the issue of the divergent DC conductivity in models of holographic transport and finite density, such as the dual to the $RN - AdS$ black hole.

The first class of holographic lattices studied appeared in [251] and a follow up paper [252]. In this construction, a periodic lattice of impurities is set up by placing an array of probe $D5$-branes in the background of N $D3$-branes. The lattice is doped by replacing some of the $D5$-branes with anti-$D5$-branes and thermodynamic properties of the system are worked out. It was found that below a critical temperature the system dimerizes, in sense that the $D5$-branes and anti-$D5$-branes pair up with each other via brane recombination. There is also some evidence that at very low temperatures, the system displays glassy behaviour.

In [162], a more bottom-up approach to holographic lattices was taken. Here, the model is bulk Einstein gravity with a neutral scalar field. The scalar field is imbued with a periodic boundary condition so that the operator dual to the scalar in the boundary theory has a periodic source term. The scalar field is allowed to backreact on the bulk geometry and the resulting spacetime is the holographic lattice. Solving for the backreacted geometry is difficult since the system is no longer homogeneous: translational invariance has been broken explicitly. The equations are solved in [162] numerically for a $3+1$ dimensional bulk and the optical conductivity is studied. It is found that the diver-

gent DC conductivity is smoothed out, being replaced by a Drude peak. An interesting scaling power law regime is also identified at intermediate frequencies, where

$$|\sigma(\omega)| = \frac{B}{\omega^{2/3}} + C\,, \tag{1.5.24}$$

where B and C are constants. Interestingly enough, this power law scaling is observed in some of the cuprate superconductors [253]. These results were extended in [254] to include a study of the thermoelectric conductivity and an analogous power-law scaling with frequency was found. A holographic lattice was also constructed numerically in $4+1$ dimensions, where a similar power-law scaling was observed for the optical conductivity, except with $|\sigma| \sim \omega^{\sqrt{3}/2}$. A numerical ionic lattice in $4+1$ dimensions was constructed by sourcing the lattice with a periodic chemical potential, as opposed to a scalar. The optical conductivity for the ionic lattice displays the same power-law scaling for intermediate frequencies as the scalar lattice (1.5.24). This model of an ionic lattice was extended to a minimal ingredient model of a holographic superconductor in [255]. Here too, in the normal phase, a Drude peak is observed in the low frequency limit. The intermediate frequency range still satisfies the power law (1.5.24). Evidence for the existence of a superconducting gap is shown and a sum rule for the conductivity was found to be satisfied.

In [256], a perturbative approach to a scalar holographic lattice was taken. Here, the lattice is considered as a small perturbation around an initial $RN-AdS$ geometry, parameterize by a "strength", which is taken to be small. The DC conductivity, to leading order in the lattice strength, is found analytically and is seen to match previous field theory results [257]. Interestingly, the authors argue that, under certain constraints, to leading order in the lattice strength, the equations of motion for the perturbative scalar lattice are the same as those for a class of gravitational theories with a massive graviton. This observation suggests a possible link to holographic studies of massive gravity which will be discussed in more detail below in section 1.5.9.

Recently, [258] showed that a wide variety of inhomogeneous IR geometries arise as

solutions to Einstein-Maxwell theory with a single periodic source at the boundary, leaving open the possibility that a large number of possible new solutions may be obtained. The classification of these IR geometries and their holographic interpretation is an open question. The AC conductivity of finite temperature ionic lattices in in $3+1$ dimensions were obtained numerically in [259].

In a somewhat related approach, momentum dissipation can be built into holography by letting translational symmetry be broken spontaneously by an instability, rather than explicitly as in the case of a holographic lattice. The result is a striped phase, first studied in [260], [261], where it was shown that in $4+1$ dimensions, the $RN-AdS$ black brane is unstable in Einstein-Maxwell theory with a Chern-Simons term, when the Chern-Simons coupling becomes large. Various other striped solutions have since been found, including duals to charge density waves where the boundary current dual to the bulk gauge field can acquire a spatially modulated vev [262], holographic insulator/superconductor transitions [263] and hyperscaling violation [264], [265].

Lattices are not the only way to break translational invariance. A common occurrence in condensed matter systems is disorder. In this case, translational invariance is broken by a "dirty" (random noise) source, as opposed to a periodic source. Despite technical challenges, progress has been made on holographic models with disorder.

1.5.8 Disorder

Disorder is a common feature in most real world condensed matter systems and as such holography should be able to say something about it. Disordered systems are difficult to model using traditional field theory approaches and little is known at strong coupling. This is especially true in the context of localization. It is well known that in a non-interacting system, the addition of disorder can completely suppress conductivity [266]. For a comprehensive review, see [267]. Turning on interactions complicates the situation and theoretical and experimental studies of many-body localization are in their infancy.

A recent review may be found in [268].

Single body localization can be observed experimentally, however the many body analogue is difficult to achieve. The problem is that to have a localized state, constructive coherence is required; this leads to long lived states. In the many body situation, this is hard, because the system is immersed in a bath of phonons that interact with the modes that participate in localization, effectively disrupting the process. A holographic approach is well suited to handling this sort of problem, as the gravity theory is strong/weak dual to a field theory, so it is already a many body problem. In this sense, understanding what the gravity dual tells us about localization could provide a definition of many body localization. Exactly what this would look like in a gravitational theory and how the bulk fields would behave is an open and interesting question.

Several approaches to disorder within holography have been proposed. An early study was presented in [269] which was interested in studying transport near a superfluid-insulator transition in $2+1$ dimensions with impurities from weak magnetic and electric perturbations. Holographically, the weak magnetic and electric impurities on the field theory side were translated to a $3+1$ dimensional dyonic black hole solution. The field theory and gravity results for transport coefficients were found to agree in the hydrodynamic limit. Soon after, [270] calculated the momentum relaxation time scale due to weak dilute impurities in a CFT and compared to results obtained in a truncation of M-theory. The replica trick for disordered CFTs was extended to holography in [271] and later in [272]. It was ultimately found that for any CFT with a holographic dual, corrections due to the presence of disorder in the CFT to any connected correlation function vanishes at leading order in large N. This result assumes that replica symmetry is unbroken in the CFT [272]. In [273], disorder was modelled within the usual AdS/CFT setup by adding probe D-branes with random fluctuating closed and open string background fields into the mix.

The above mentioned studies were carried out in fixed spacetime backgrounds, either

pure AdS or asymptotically AdS black hole solutions. To fully see the effect of quenched random disorder, [274] proposed that disorder should be modelled by applying random boundary conditions to a bulk field and allowing the field to backreact on the geometry. The source of disorder in this study is assumed to be self-averaging and characterized by a distribution $P_V[W(x)]$, over random functions $W(x)$. The subscript V is in reference to another function $V(x)$, which is taken to be the boundary value of a gauge field in the bulk. The system is assumed to be self-averaging in the sense that, over length scales much larger than than a typical disorder scale, homogeneity is restored. This construction is somewhat complicated as the entire functional $P_V[W(x)]$ runs as the energy scale changes. To this end, [274] and later [275], worked to construct a holographic functional renormalization scheme so that disorder averaged thermodynamic quantities could be computed.

An interesting approach to disorder in gauge/gravity duality was proposed in [276]. A particular background is considered which is already deformed away from AdS, but still satisfies the null energy condition. The degree to which the geometry is deformed is controlled by a parameter which is meant to represent the amount of disorder in the system. The wave function of a probe scalar in this background is studied by looking at the nearest neighbour spacing distribution of the pole spectra of the two-point correlator. By increasing the amount of disorder, a transition in the distribution is observed between an initial distribution and a Poisson distribution, which is analogous to what happens in a disorder driven metal-insulator transition. It is still unclear how this approach ties into other models of holographic disorder. Studying the interconnection between the methods developed in [276] and backreacted disordered solutions is an interesting and open question.

More recently, [277] applied a spectral approach to modelling disorder in a holographic superconductor. The basic idea is similar to [274] where the disorder is sourced by a random space-dependent chemical potential by setting the boundary condition on a bulk

$U(1)$ gauge field. In this proposal, the chemical potential takes the form of a sum over a spectrum which depends on one of the boundary directions, x

$$\mu(x) = \mu_0 + \bar{V} \sum_{k=k_0}^{k_*} \sqrt{S_k} \cos(kx + \delta_k) \,, \tag{1.5.25}$$

where S_k is a function of the momenta k which controls the correlation function for $\mu(x)$; different choices of S_k lead to a different values of the disorder distribution average and moments. $\bar{V}$ is a tuneable parameter which sets the "strength" of the disorder. k_0 and k_* define an IR and UV length scale cutoff for the disorder. δ_k is a random phase for each value of k. A spectral representation like this is known to simulate a stochastic process when k_* is large [278].

There is a resemblance between this spectral approach to disorder and the construction of a holographic ionic lattice [162] (see also section 1.5.7) where the lattice is set up by a periodic boundary chemical potential. The difference is that for a holographic lattice, there is only a single periodic source of a fixed wavelength. In the spectral approach to disorder, there is a sum over periodic sources of arbitrary wavelength, so the effect of disorder may resonant more strongly throughout the entire bulk geometry, having non-trivial effects deep in the interior.

The "dirty" chemical potential (1.5.25) is incorporated into an Einstein-Maxwell model in [277]. The Maxwell equations are solved numerically in an electric ansatz with the boundary condition that A_t approaches (1.5.25) near the boundary. The analysis is done in a fixed AdS-Schwarzschild background, so no backreaction is considered. Evidence is found for an enhancement of the critical temperature of the superconductor for increasing disorder strength. Numerical evidence that localization occurs in this model was reported in [279]. This model has also been extended to holographic p-wave superconductors in [280] where the same behaviour of the critical temperature with disorder strength was observed.

Recently, [281] applied a spectral approach to modelling disorder sourced by a scalar

field in $2+1$ bulk dimensions. The initial clean geometry in this case is AdS_3 and the scalar field is allowed to backreact on the geometry in the spirit of [274]. By treating the disorder strength as a perturbative handle, a second order analytic solution for the backreacted geometry is obtained. It is observed that the disorder averaged geometry, in the deep interior, takes the form of a Lifshitz metric (see section 1.5.3) with a dynamical critical exponent z set by the disorder strength. Numerical solutions are constructed for strong disorder, where the analytic perturbative approach fails. The numerical solutions also show that the interior geometry develops an emergent Lifshitz scaling. These results have been extended to finite temperature in [282]. A similar implementation to scalar disorder was used in [283] and [284] to study the conductivity of holographic strange metals with weak quenched disorder.

We will return to the problem of disorder in gauge/gravity duality in chapter 3 and show that by adopting the technique proposed in [281] and adapting it to the kind of disorder source considered in [277] and [280], we can construct an analytic solution perturbatively in the disorder strength and study the resulting DC conductivity [285].

Implementing explicit disorder and lattice structures into holography is technically challenging. For one, explicit breaking of translational invariance implies loss of homogeneity. Secondly, taking the backreaction of the disordered sources into account is nontrivial, especially when moving beyond perturbative disorder. To this end, a few simplifying models of gauge/gravity duality without translational invariance have been proposed which retain homogeneity, making analytic treatments more manageable.

1.5.9 Other proposals

Finding lattice solutions (see section 1.5.7), with explicit breaking of translational invariance, is technically challenging. A few proposals have been put forward for finding gravity models which are dual to systems with momentum dissipation yet still preserve bulk homogeneity. The basic idea revolves around conservation of the energy-momentum tensor

of the dual field theory. In general, conservation of the field theory energy-momentum tensor is related to diffeomorphism invariance in the bulk. Consider a bulk gravitational model with a matter sector comprising a scalar field ϕ and a gauge field A_μ. Applying the holographic dictionary (see section 1.3.1), $\phi_{(0)}$ is a source for the dual scalar operator $\langle \mathcal{O} \rangle$ and the pullback to the boundary of $A_{(0)\mu}$ is a source for a boundary current $\langle J_i \rangle$. These bulk fields should correspond to relevant deformations so that an asymptotic AdS solution is available. The boundary energy-momentum tensor satisfies the conservation equation (Ward identity) [286]

$$\nabla_i \langle T^{ij} \rangle = \nabla^j \phi_{(0)} \langle \mathcal{O} \rangle - F^{ij}_{(0)} \langle J_i \rangle \,. \tag{1.5.26}$$

If the bulk fields in (1.5.26) depend on the spatial coordinates along the boundary, then momentum-conservation can be violated. Moreover, if the spatial dependence can be chosen in such a way that the bulk energy-momentum tensor remains homogeneous (i.e. does not depend on the boundary coordinates), then it should be possible to find a corresponding homogeneous bulk geometry. This can be achieved by exploiting a continuous global symmetry in the matter sector of the theory. An example was constructed in [286], where the bulk model is Einstein-Maxwell coupled to set of massless scalar fields with linear dependence on the boundary directions. The bulk energy-momentum tensor is homogeneous in this case due to the shift symmetry of the massless scalars. The resulting, finite temperature, geometry is worked out and the DC conductivity is shown to be finite. Several extensions of this model exist, including the addition of finite chemical potential where a coherent (Drude-like)/incoherent metal transition was identified [287], [288], [289] as well as within the framework of holographic superconductors [290].

Similarly, [291] considered an Einstein-Maxwell model with an additional complex scalar field $\phi = e^{ikx}\varphi(r)$, where x is a boundary direction, r is the bulk radial coordinate and k is a constant. A finite temperature and finite charge black hole solution to this model was found and dubbed a "Q-lattice". The optical conductivity was observed to be finite as $\omega \to 0$, displaying a Drude peak. Holographic metal/insulator transitions

within a Q-lattice model were found in [291] and [292]. The thermoelectric transport properties for $3+1$ dimensional Q-lattices were obtained in [293]. The model has also been embedded within a holographic s-wave superconductor where the presence of the Q-lattice was shown to lower the critical temperature.

Another approach to holographic momentum dissipation is massive gravity [294]. The idea is that since conservation of the boundary energy-momentum tensor is a consequence of bulk diffeomorphism invariance, working in a gravitational theory without diffeomorphism invariance might be dual to a field theory without conservation of momentum. In [294], the gravity theory contains a Maxwell field and explicit mass terms for the graviton. It was proposed that this model may capture the physics of disordered systems. Electric and thermoelectric transport properties have been worked out in [295], [296], [297], [298] and [299]. An extension of this model including magnetic transport was discussed in [300]. At this point, it is unclear if massive gravity has a sensible holographic dual. It is not known to arise from a string model and there is still some debate about its stability. While it is known that the model used in [294] is ghost-free in some circumstances (see [301] for a review), it still has many unusual features including superluminal propagation, loss of unique evolution and acausality [302]. It remains to be seen if these issues can be addressed within the context of applications to holography.

Having reviewed symmetry reduction scenarios in gauge/gravity duality, we return to non-relativistic holography and the HSV type geometries in chapter 2. It was pointed out in section 1.5.4 that the HSV geometries generically possess unphysical singularities that need to be regulated. Chapter 2 describes a mechanism by which this can be accomplished within a certain class of holographic model. In chapter 3, an explicit holographic model of perturbatively charged disorder is presented and its transport properties discussed. Finally, in chapter 4, we will discuss possible avenues for further research and make some speculations about the future of applied holography.

Chapter 2

Electric hyperscaling violating solutions in Einstein-Maxwell-dilaton gravity with R^2 corrections

This chapter studies hyperscaling violating solutions within Einstein-Maxwell-dilaton gravity with curvature squared corrections. The contents of this chapter were first presented in [303], written in collaboration with Amanda W. Peet.

The AdS/CFT correspondence is a remarkable construction which has sparked many new opportunities to study the detailed structure of strongly coupled quantum field theories. Among new avenues of investigation it has spawned are applications to modelling the quark-gluon plasma and condensed matter systems. The goal of modelling strongly coupled field theory systems at quantum critical points will be the context for the work reported here. Our perspective will be bottom-up, in the sense that we will seek particular classes of spacetime solutions in curvature squared gravity with dilaton potential and dilaton-dependent gauge couplings in order to seek out physical constraints on the

theory functions and parameters and on parameters of solutions within it. Finding string theory embeddings for this class of models and analyzing technical stability properties (ghosts, etc) of the solutions that we investigate is beyond the scope of this work.

Condensed matter systems typically do not possess relativistic symmetry. For instance, for field theories at finite charge density Lorentz invariance is broken by the presence of a current [199]. Breaking of relativistic symmetry in the field theory implies that the bulk gravity/string dual should also break relativistic symmetry. Two major directions have been pursued in this context: spacetimes with Schrödinger symmetry [163] and spacetimes with Lifshitz symmetry [164]. Aspects of the dictionary are better developed for Lifshitz, such as holographic renormalization [188], [190], so we choose this as our context.

Lifshitz quantum critical points are invariant under the scaling symmetry

$$t \to \lambda^z t\,, \qquad x_i \to \lambda x_i\,. \tag{2.0.1}$$

where z is the dynamical critical exponent. In [164] a candidate gravity dual for Lifshitz fixed points was proposed, with spacetime metric

$$ds^2_{d+2} = L^2\left(-\mathcal{R}^{2z}dt^2 + \frac{d\mathcal{R}^2}{\mathcal{R}^2} + \mathcal{R}^2 dx_i^2\right)\,, \tag{2.0.2}$$

where $\mathcal{R}$ is the radial coordinate, which ranges from $\mathcal{R} \to 0$ in the interior to $\mathcal{R} \to \infty$ at the boundary. The bulk spacetime respects Lifshitz scaling symmetry with $\mathcal{R} \to \lambda^{-1}\mathcal{R}$. Here, d is the number of transverse dimensions x_i and L sets the length scale in the bulk.

The Lifshitz metric and its finite temperature counterpart are exact solutions to Einstein gravity with a nontrivial matter sector. Two popular options for the matter sector are Einstein gravity coupled to a massive gauge field [182],[36],[183] and Einstein-Maxwell-dilaton theory [184],[185],[14],[186]

$$S = \frac{1}{16\pi G_N}\int d^{d+2}x\sqrt{-g}\left(R - \frac{1}{2}(\partial\phi)^2 - V(\phi) - \frac{1}{4}f(\phi)F^2\right)\,. \tag{2.0.3}$$

In order to obtain Lifshitz solutions, it suffices to consider $f(\phi) \propto e^{\lambda_1 \phi}$ and $V(\phi) = \Lambda$, where λ_1 is a constant and Λ is the (negative) cosmological constant. Lifshitz solutions have also been found within an Einstein-Maxwell-dilaton model including higher derivative corrections in curvature and the field strength tensor [187].

Einstein-Maxwell-dilaton theory also supports a broader class of interesting spacetime geometries, the hyperscaling violating (HSV) metric

$$ds^2_{d+2} = L^2 \left(-\mathcal{R}^{2(z-\theta/d)} dt^2 + \frac{d\mathcal{R}^2}{\mathcal{R}^{2(1+\theta/d)}} + \mathcal{R}^{2(1-\theta/d)} dx_i^2 \right) , \tag{2.0.4}$$

where z is the dynamical critical exponent and θ is the hyperscaling violation parameter [165],[166],[212]. Metrics of HSV form are not scale invariant, but rather transform covariantly,

$$ds^2_{d+2} \to \lambda^{2\theta/d} ds^2_{d+2} \, . \tag{2.0.5}$$

From the perspective of the dual theory, hyperscaling is the property that the free energy of the system should scale with its naïve dimension. At finite temperature, theories with hyperscaling have an entropy density which scales with temperature as $S \sim T^{d/z}$. When hyperscaling is violated, there is a modified relationship, $S \sim T^{(d-\theta)/z}$, indicating the system lives in an effective dimension $d_{\text{eff}} = (d - \theta)$ [14],[213]. Candidate HSV gravity duals for systems of this sort will be the focus of this study.

Compressible phases of matter have strongly coupled quantum critical points in $2+1$ dimensions, making them obvious targets for holographic modelling. The HSV sub-case $\theta = d - 1$ is particularly interesting because it describes the case of strange metals [199], a type of non-Fermi liquid. In $D = d + 2 = 4$ specifically, compressible non-Fermi liquid states are known from field theory analysis to have dynamical critical exponent $z = 3/2$ up to three loop order and $\theta = 1$ [14]. Another motivation for studying candidate HSV gravity dual spacetimes in Einstein gravity is that there are [14],[213] logarithmic violations of the area law for entanglement entropy.

We may ask which types of theory functions $f(\phi), V(\phi)$ can support HSV solutions

and, if so, what physical parameters z, θ might be available. For HSV solutions of Einstein-Maxwell-dilaton gravity, it suffices [14] to take $f(\phi) \propto e^{\lambda_1 \phi}$ and $V(\phi) \propto -e^{\lambda_2 \phi}$, where λ_1 and λ_2 are constants and the dilaton runs logarithmically: $\phi(\mathcal{R}) \propto \ln(\mathcal{R})$+const. HSV solutions have also been found within an Einstein-Dirac-Born-Infeld-dilaton model [214]. From the condensed matter perspective, having HSV solutions in Einstein gravity causes an embarrassment of riches, in the sense that it gives too many allowed values of z, θ. A natural question from a microscopic perspective is whether or not introducing curvature squared corrections might help constrain the parameter space more tightly.

Introducing curvature squared corrections to Einstein gravity alters the structure of the null energy condition (NEC), which we use as a primary tool to discriminate physical solutions from unphysical ones. Accordingly, via the NEC, solution parameters z, θ can be constrained in terms of theory parameters $\{\eta_i\}$, whose magnitude must be small in order that the semiclassical approximation we make in the gravity sector be believable. In addition to the NEC, we will insist on two basic requirements motivated from the field theory side: that the physical effective dimension d_{eff} for the dual field theory be positive [14] and that $z \geq 1$ to ensure causal signal propagation.

Curvature squared corrections are also motivated from study of singularities in Lifshitz-type and HSV-type solutions. First, consider Lifshitz. At first glance, it appears that the Lifshitz gravity dual of [164] is nonsingular, because all curvature invariants remain finite in the interior. However, the Lifshitz-type geometries display divergent tidal forces in the interior [164], [196], [197] which disturb string probes. For Lifshitz solutions with a magnetic ansatz for the gauge field, logarithmic running of the dilaton runs the gauge coupling to infinity as $\mathcal{R} \to 0$. In [304], it was shown for $D = 4$ that quantum corrections to $f(\phi)$ can stabilize the dilaton and replace the deep interior geometry with $AdS_2 \times \mathbb{R}^2$. For electric Lifshitz solutions, the gauge field runs to weak coupling in the interior so quantum corrections to $f(\phi)$ do not provide a mechanism for resolving the tidal force singularity. However, recently it has been found [305] that in $D = 4$ curvature

squared corrections are capable of stabilizing the dilaton of electric Lifshitz, crossing over to $AdS_2 \times \mathbb{R}^2$. We will build on this observation. Another feature of the electric equations of motion is that demanding that the spacetime be asymptotically Lifshitz (i.e. at $\mathcal{R} \to \infty$) makes the gauge coupling function formally diverge there. This was addressed in [305] which displayed a crossover to AdS_4 near the boundary (UV). Lifshitz solutions in Einstein-Weyl were also studied in [306].

For HSV-type spacetimes with Einstein as the gravity sector, the situation is more involved. Tidal forces still generally diverge in the interior, but are avoided for specific ranges of z and θ as pointed out in [215], [217]. Curvature invariants remain finite in the interior for $\theta > 0$ [216], but diverge at the boundary, necessitating a UV completion to AdS there. Magnetic HSV solutions display the same type of logarithmic running as their Lifshitz cousins and become strongly coupled in the interior. Using the same quantum corrections to $f(\phi)$ as [304], [307] constucted flows from HSV in to $AdS_2 \times \mathbb{R}^2$ in the interior and out to AdS_4 at the boundary. Electric HSV solutions, like for Lifshitz, do not run to strong coupling in the interior. Motivated by the observations in [305], we will investigate curvature squared solutions with hyperscaling violation and investigate whether there are IR and UV completions.

The chapter is organized as follows. In section 2.1, we look for HSV-type solutions to Einstein-Maxwell-dilaton theory with curvature squared corrections, and present the theory functions $f(\phi), V(\phi)$ needed to support these solutions. In section 2.2 we discuss how the NEC along with the constraints $0 < d_{\text{eff}} \leq d$ and $z \geq 1$ restricts polynomial combinations of solution parameters z, θ and theory parameters $\{\eta_i\}$. In section 2.3, we discuss the question of crossovers between HSV, (a) AdS_D asymptotically, and (b) $AdS_2 \times \mathbb{R}^d$ in the deep interior, supported by the curvature squared corrections. In section 2.4, we summarize our findings and comment on possible directions for future work.

2.1 A curvature squared model and its HSV solution

We will be interested in classes of models with curvature squared corrections to Einstein gravity, coupled to a $U(1)$ gauge field and a scalar which we will refer to as the dilaton. The action for the class of models we study is of the form

$$S = \frac{1}{16\pi G_N}\int d^{d+2}x\sqrt{-g}\left(R - \frac{1}{2}(\partial\phi)^2 - V(\phi) - \frac{1}{4}f(\phi)F^2 \right.$$
$$\left. +\eta_1 R_{\mu\nu\rho\sigma}R^{\mu\nu\rho\sigma} + \eta_2 R_{\mu\nu}R^{\mu\nu} + \eta_3 R^2 \right). \qquad (2.1.1)$$

Here, the η_i are constant couplings for the higher curvature terms measured in units of the Planck length ℓ_P. Generically, curvature squared corrections lead to ghosts appearing in the theory, depending on the background geometry and values of the coupling constants η_i. For example, in the context of Gauss-Bonnet gravity[1] applied to holography, requring a ghost free AdS solution as well as ensuring causality of the dual boundary theory places nontrivial constraints on the possible values of the coupling constant [308], [309][2]. Our goal in this section is to find HSV-type solutions to the field equations of the model (2.1.1). We will use the metric ansatz

$$ds^2_{d+2} = -L^2 r^{2\alpha}dt^2 + L^2\frac{dr^2}{r^{2\beta}} + L^2 r^2 dx_i^2\,. \qquad (2.1.2)$$

This form of the ansatz is chosen in order that the (fourth order) equations of motion have a good chance of being tractable analytically. Here, d is the number of transverse dimensions, $D = d + 2$ is the bulk spacetime dimension, and L sets the overall length scale. The dynamical exponent z and the hyperscaling violation parameter θ are related to the parameters α and β by

$$\alpha = \frac{dz-\theta}{d-\theta}\,, \qquad \beta = \frac{d}{d-\theta}\,. \qquad (2.1.3)$$

[1] In the action (2.1.1), the curvature squared terms reduce to the Gauss-Bonnet term $\chi_4 = \left(R_{\mu\nu\lambda\sigma}R^{\mu\nu\lambda\sigma} - 4R_{\mu\nu}R^{\mu\nu} + R^2\right)$ for $\eta_2 = -4\eta_1$, and $\eta_3 = \eta_1$.

[2] In the notation of section 2.2 the Gauss-Bonnet coupling in $D = d + 2 \geq 5$ is constrained to be between $-(3d+5)/[4(d+3)^2(d-2)] \leq \eta_{GB}/L^2 \leq (d^2+d+6)/[4(d^2-d+4)^2]$, where L^2 sets the bulk length scale.

This metric (2.1.2) is related to that of the previous section (2.0.4) by a coordinate transformation $\mathcal{R} = r^{d/(d-\theta)}$ which will help make our equations simpler. The Riemann curvature components of (2.1.2) are

$$R^{tr}{}_{tr} = -\alpha(\alpha+\beta-1)r^{2(\beta-1)}/L^2\,, \qquad R^{ri}{}_{ri} = -\beta r^{2(\beta-1)}/L^2\,,$$
$$R^{it}{}_{ti} = \alpha r^{2(\beta-1)}/L^2\,, \qquad R^{ij}{}_{ji} = r^{2(\beta-1)}/L^2\,, \tag{2.1.4}$$

where repeated indices i, j are not summed over. From this it is straightforward to obtain the Ricci tensor and Ricci scalar for the equations of motion.

In order to support a HSV spacetime, it will be necessary to include a nontrivial potential for the the dilaton $V(\phi)$. In the case of pure Lifshitz ($\theta = 0$ or $\beta = 1$), the dilaton potential reduces to a constant and plays the role of a cosmological constant: $V(\phi) \to \Lambda_{\text{Lif}}$ as $\theta \to 0$. Later on when we investigate the possibility of producing AdS completions to the HSV geometries in both the boundary (UV) and interior (IR) regions, we will see that $V(\phi)$ will also set the individual AdS scales. That is, we will look for a mechanism by which the higher curvature corrections to the action stabilize the dilaton at some constant value $\phi = \phi_0$. When evaluated on this solution, $V(\phi_0)$ will set the AdS scale for us.

The lore for the hyperscaling violating metrics of the form (2.1.2) is that the minimum ingredients needed to support such a metric are a gauge coupling $f(\phi)$ and dilaton potential $V(\phi)$ that are exponentials in the dilaton ϕ [304],[212]. This is valid in the limit of matter plus Einstein gravity, but not in the case when higher curvature terms like those in our action (2.1.1) are present, as was pointed out recently in [310]. Indeed, as we will see, the form of the dilaton potential and gauge coupling will need to be modified in order to support the HSV spacetime in our theory with curvature squared corrections. We will see that not all parameters support HSV solutions, and we will explore the admissible ranges of $\{\eta_i\}$ using two tools: (1) the NEC and (2) constraints on parameters from the condensed matter side. The hope is that bottom-up investigations of this sort may help

serve as a partial guide to top-down string embedders. We now turn to the equations of motion and solving them.

The Maxwell field equation takes the form

$$\nabla_\mu \left[f(\phi) F^{\mu\nu} \right] = 0 \,, \tag{2.1.5}$$

while the dilaton equation of motion is

$$\Box\phi - \frac{1}{4}\partial_\phi f(\phi) F_{\mu\nu}F^{\mu\nu} - \partial_\phi V(\phi) = 0 \,. \tag{2.1.6}$$

Via repeated application of the Bianchi identities, the equations of motion for the metric become

$$\begin{aligned} T_{\mu\nu} \equiv \widetilde{G}_{\mu\nu} = R_{\mu\nu} - \frac{1}{2}g_{\mu\nu}R + 2\eta_1 R_{\mu\lambda\rho\sigma}R_\nu{}^{\lambda\rho\sigma} + (4\eta_1 + 2\eta_2)R_{\mu\lambda\nu\sigma}R^{\lambda\sigma} - 4\eta_1 R_{\mu\lambda}R_\nu{}^\lambda \\ - (2\eta_1 + \eta_2 + 2\eta_3)\nabla_\mu\nabla_\nu R + (4\eta_1 + \eta_2)\Box R_{\mu\nu} + 2\eta_3 R R_{\mu\nu} \\ - \frac{1}{2}g_{\mu\nu}\left[\eta_1 R_{\alpha\beta\rho\sigma}R^{\alpha\beta\rho\sigma} + \eta_2 R_{\lambda\sigma}R^{\lambda\sigma} + \eta_3 R^2 - (\eta_2 + 4\eta_3)\Box R\right] \,, \end{aligned} \tag{2.1.7}$$

while the energy-momentum tensor is

$$T_{\mu\nu} = \frac{1}{2}(\partial_\mu\phi)(\partial_\nu\phi) - \frac{1}{2}g_{\mu\nu}V(\phi) - \frac{1}{4}g_{\mu\nu}(\partial\phi)^2 + \frac{1}{2}f(\phi)\left(F_{\mu\sigma}F_\nu{}^\sigma - \frac{1}{4}g_{\mu\nu}F_{\lambda\sigma}F^{\lambda\sigma}\right) \,. \tag{2.1.8}$$

Making use of an electric ansatz for the gauge field yields a solution to the Maxwell field equation (2.1.5)

$$F^{rt} = \frac{Q}{\sqrt{-g}f(\phi)} = \frac{Q}{f(\phi)L^{d+2}r^{\alpha-\beta+d}} \,, \tag{2.1.9}$$

where Q is a constant of integration.

Note that for a magnetic HSV solution in a radial ansatz we would seek $F_{(2)} = \mathcal{B}(r)dx \wedge dy$, where

$$\mathcal{B}(r) = \frac{P}{f(\phi)L^{d-4}r^{\alpha-\beta+d-4}} \,. \tag{2.1.10}$$

We will stick with the electric case.

Now, using the components of the energy-momentum tensor (2.1.8), the equations for the metric may be recast in a more useful form,

$$\begin{aligned} V(\phi(r)) &= -\frac{1}{L^2}\left(r^{-2}\widetilde{G}_{ii} + r^{2\beta}\widetilde{G}_{rr}\right) , \\ (\partial\phi)^2 &= \frac{2}{L^2}\left(r^{-2\alpha}\widetilde{G}_{tt} + r^{2\beta}\widetilde{G}_{rr}\right) , \\ \frac{Q^2}{f(\phi(r))L^{2d}}r^{-2d} &= \frac{1}{2L^2}\left(r^{-2\alpha}\widetilde{G}_{tt} + r^{-2}\widetilde{G}_{ii}\right) , \end{aligned} \tag{2.1.11}$$

where there is no sum on repeated indices i. It is straightforward to obtain the components of $\widetilde{G}_{\mu\nu}$, and they turn out to be a sum of two competing powers of r. This is easiest to see by raising one index:

$$\begin{aligned} \widetilde{G}^t{}_t &= -\frac{C_1}{L^2}r^{2(\beta-1)} - \frac{C_2}{L^2}r^{4(\beta-1)} , \\ \widetilde{G}^r{}_r &= \frac{C_3}{L^2}r^{2(\beta-1)} + \frac{C_4}{L^2}r^{4(\beta-1)} , \\ \widetilde{G}^i{}_i &= \frac{C_5}{L^2}r^{2(\beta-1)} + \frac{C_6}{L^2}r^{4(\beta-1)} . \end{aligned} \tag{2.1.12}$$

Here, the C_i are constants in α, β, d, η_1, η_2, and η_3. The details of the long expressions are relegated to the appendix (A); let us briefly summarize their features. First, the odd numbered constants: $C_1(d,\beta)$ is linear in β and quadratic in d; $C_3(d,\alpha)$ is linear in α and quadratic in d; and $C_5(d,\alpha,\beta)$ is linear in β and quadratic in d and α. Second, the even constants. C_2, C_4 and C_6 are linear in $\{\eta_i\}$, quartic in d (with coefficients depending on $\{\eta_i\}$), quartic in α, and cubic in β (except for C_4 which is quadratic). Only C_2, C_4 and C_6 contain information about the higher curvature terms in the action (2.1.1), so those are the ones to watch.

The final result for the field equations in this ansatz simplifies to

$$V(\phi(r)) = -\frac{1}{L^2}\left[D_1 r^{2(\beta-1)} + D_2 r^{4(\beta-1)}\right] , \tag{2.1.13}$$

$$(\partial\phi)^2 = \frac{2}{L^2}\left[D_3 r^{2(\beta-1)} + D_4 r^{4(\beta-1)}\right] , \tag{2.1.14}$$

$$\frac{Q^2}{f(\phi(r))L^{2d}}r^{-2d} = \frac{1}{2L^2}\left[D_5 r^{2(\beta-1)} + D_6 r^{4(\beta-1)}\right] , \tag{2.1.15}$$

where the constants $\{D_1 \dots D_6\}$ are linear combinations of the $\{C_1 \dots C_6\}$ constants as follows,

$$D_1(d,\alpha,\beta) = C_5 + C_3, \quad D_2(d,\alpha,\beta,\eta_1,\eta_2,\eta_3) = C_4 + C_6\,, \tag{2.1.16}$$

$$D_3(d,\alpha,\beta) = C_1 + C_3, \quad D_4(d,\alpha,\beta,\eta_1,\eta_2,\eta_3) = C_2 + C_4\,, \tag{2.1.17}$$

$$D_5(d,\alpha,\beta) = C_1 + C_5, \quad D_6(d,\alpha,\beta,\eta_1,\eta_2,\eta_3) = C_2 + C_6\,. \tag{2.1.18}$$

Once we integrate (2.1.14), we have both the required form of the theory functions and the form of the solutions, from (2.1.13-2.1.15). Note that we believe the curvature squared HSV solutions presented here to be novel in the context of AdS/condensed matter but unlikely to be so as GR spacetimes.

Before proceeding to analytic solutions, we should ask what kind of restrictions we can impose on the parameter space of the theory. A very natural choice is to insist on satisfying the null energy condition $T_{\mu\nu}N^\mu N^\nu \geq 0$ in order to ensure that we are dealing with a sensible matter source for the model. Here, the inequality must hold for any arbitrary null vector N^μ. Using the field equations (2.1.7) for the metric, this statement may be translated into the condition $\widetilde{G}_{\mu\nu}N^\mu N^\nu \geq 0$. An appropriate null vector is

$$N^t = \left(\sum_{i=1}^{d} s_i^2 + s_r^2\right)^{1/2} \frac{1}{Lr^\alpha}\,, \qquad N^r = s_r \frac{r^\beta}{L}\,, \qquad N^i = s_i \frac{1}{Lr}\,, \tag{2.1.19}$$

where s_r and s_i (d of them) are arbitrary positive constants. Using this N^μ, the NEC translates into the following conditions on the constants D_i:

$$D_3(d,\alpha,\beta) \geq 0\,, \qquad D_4(d,\alpha,\beta,\eta_1,\eta_2,\eta_3) \geq 0\,, \tag{2.1.20}$$

$$D_5(d,\alpha,\beta) \geq 0\,, \qquad D_6(d,\alpha,\beta,\eta_1,\eta_2,\eta_3) \geq 0\,. \tag{2.1.21}$$

(Note that there are no conditions on D_1 or D_2 coming from the NEC.) Two of these conditions, $D_3 \geq 0$ and $D_5 \geq 0$, collapse into the simple relations

$$(z-1)(z-\theta+d) \geq 0\,, \tag{2.1.22}$$

$$(d-\theta)(d(z-1)-\theta) \geq 0\,, \tag{2.1.23}$$

respectively. These are identical to conditions found when applying the NEC to HSV solutions of Einstein-Maxwell-dilaton theory [14], [212]. This had to be the case, as our higher curvature model contains the Einstein gravity terms. Only the conditions $D_4 \geq 0$ and $D_6 \geq 0$ depend on the couplings η_i.

The NEC is expected to hold for any reasonable source of matter and it has been argued that its violation will lead to, for example, acausal behaviour [219], [220]. The NEC is used in Einstein [221], [222], [223] and higher curvature gravity [224] to derive a holographic c-theorem. Recently, the weak energy condition (which implies the NEC) has also been used to constrain geometries which interpolate between asymptotically Lifshitz or AdS spacetimes and IR geometries with Bianchi symmetries [224].

In Einstein gravity, the energy conditions applied to the Raychaudhuri equations leads to geodesic focusing. In higher curvature theories, the structure of the Raychaudhuri equations do not change as they are mathematical identities and only become equations once the Einstein equations are applied; for a review, see [311]. The relation between the energy-momentum tensor and the Ricci tensor does change as a result of the modified equations of motion, hence the conditions on geodesic focusing do change in a higher curvature theory. In the context of holography, we are interested in theories which support geometries dual to condensed matter systems. As such, the matter content supporting the geometry should still satisfy the reasonable condition that $T_{\mu\nu}N^\mu N^\nu \geq 0$ (For a perfect fluid, this translates into a condition on ρ and p_i; $\rho + p_i \geq 0$).

Now let us move to solving these equations analytically. We may start by solving the differential equation for $(\partial\phi(r))^2$, (2.1.14) directly, to get

$$\begin{aligned}\phi(r) = &-\frac{\sqrt{2D_3}}{\beta-1}\left[\sqrt{1+\frac{D_4}{D_3}r^{2(\beta-1)}} - \text{arccsch}\left(\sqrt{\frac{D_4}{D_3}}r^{\beta-1}\right)\right] \\ &+\frac{\sqrt{2D_3}}{\beta-1}\left[\sqrt{1+\frac{D_4}{D_3}} - \text{arccsch}\left(\sqrt{\frac{D_4}{D_3}}\right)\right] + c\,, \end{aligned} \tag{2.1.24}$$

where c is a constant. Note that, at first glance, this solution may seem to be undefined in the limit that $\beta \to 1$ ($\theta \to 0 \Rightarrow \alpha = z$). However, this is just an illusion. The constant

(r-independent) terms in $\phi(r)$ are precisely those needed to cancel the divergence from the first two terms, and the limit is well defined:

$$\phi(r) \to -\sqrt{2D_3 + 2D_4}\,\Big|_{\beta\to 1} \ln(r) + c\,. \tag{2.1.25}$$

This is precisely the kind of logarithmic behaviour of the dilaton we would expect for a purely Lifshitz behaviour [305].

It is instructive to study the asymptotic behaviour of $\phi(r)$. By expanding the solution (2.1.24) as $r \to \infty$ and $r \to 0$, we can see what the dilaton is doing in the UV and IR respectively. The result in the UV is

$$\phi(r)|_{r\to\infty} \to -\frac{\sqrt{2D_4}}{(\beta-1)}\, r^{\beta-1} + c\,, \tag{2.1.26}$$

while in the IR it is

$$\phi(r)|_{r\to 0} \to -\frac{\sqrt{2D_3}}{(\beta-1)} \ln\left(\frac{1}{2}\sqrt{\frac{D_4}{D_3}} r^{\beta-1}\right) + c\,. \tag{2.1.27}$$

In a putative string theory embedding, this would imply that the string coupling involving e^{ϕ} is diverging in the deep interior where we know the null singularity lurks, and dies out to zero out at the boundary.

In order to satisfy the remaining gravity equations, we need a form for $V(\phi)$ and $f(\phi)$ such that

$$V(\phi(r)) = -\frac{1}{L^2}\left[D_1 r^{2(\beta-1)} + D_2 r^{4(\beta-1)}\right]\,, \qquad f(\phi(r)) = \frac{2Q^2}{L^{2(d-1)}} \frac{r^{-2(\beta+d-1)}}{(D_5 + D_6 r^{2(\beta-1)})}\,. \tag{2.1.28}$$

In general, for arbitrary D_i (i.e., arbitrary η_i and arbitrary α, β), it is difficult to invert the solution (2.1.24) for $\phi(r)$. The analytic functions encountered are Lambert W-functions, which do not have visually pleasant representations, so we do not display them here. Instead, we leave $V(\phi(r))$ and $f(\phi(r))$ in implicit form along with (2.1.24) describing $\phi(r)$ or alternately (2.1.14)) describing $d\phi(r)/dr$.

Regardless of the detailed form of $f(\phi)$ and $V(\phi)$, it is straightforward to examine their asymptotic behaviours using the results in (2.1.26) and (2.1.27):

$$V(\phi)|_{r\to\infty} \to -\frac{(\beta-1)^2}{2D_4L^2}\left[D_1+\frac{(\beta-1)^2}{2D_4}D_2(\phi-c)^2\right](\phi-c)^2\,, \tag{2.1.29}$$

$$V(\phi)|_{r\to 0} \to -\frac{4D_3}{D_4L^2}\exp\left(\frac{2(\beta-1)}{\sqrt{2D_3}}(c-\phi)\right)\left[D_1+\frac{4D_3D_2}{D_4}\exp\left(\frac{2(\beta-1)}{\sqrt{2D_3}}(c-\phi)\right)\right].$$

Obviously, these formulæ are not valid for $\eta_i \to 0$; there the form changes back to what we expect from an Einstein gravity sector. Note that the magnitude of the potential is controlled by $1/\eta_i$, and that at large r the potential naturally measures ϕ in units of $\sqrt{\eta_i}$.

Recall that $f(\phi)$ plays the role of the coupling for the Maxwell field: $f(\phi(r)) \sim 1/g_M^2$. Hence $g_M \sim (L^{d-1})/(\sqrt{2}Q)\left(D_5+D_6r^{2(\beta-1)}\right)^{1/2} r^{2(\beta+d-1)}$. In terms of z and θ: $2(\beta-1) = (2\theta)/(d-\theta)$ and $\beta+d-1 = d+\theta/(d-\theta)$. Hence, $g\to 0$ as $r\to 0$ provided that $\theta \geq 0$ and $(d-\theta) > 0$, meaning that we get to weak gauge coupling in the interior of the spacetime for physically sensible parameter ranges, as desired. Furthermore,

$$f(\phi)|_{r\to\infty} \to \frac{2D_4Q^2}{(\beta-1)^2L^{2(d-1)}}\frac{\left[-\frac{(\beta-1)}{\sqrt{2D_4}}(\phi-c)\right]^{(-2d)/(\beta-1)}}{\left[D_5+\frac{D_6(\beta-1)^2}{2D_4}(\phi-c)^2\right](\phi-c)^2}\,. \tag{2.1.30}$$

As $r\to\infty$, the coupling $f(\phi)$ goes to zero. The remaining dilaton equation of motion (2.1.6) then collapses to

$$(\alpha+\beta+d-1)D_3-(\beta+d-1)D_5+(\beta-1)D_1 = 0\,, \tag{2.1.31}$$

$$(\alpha+2\beta+d-2)D_4-(d+2\beta-2)D_6+2(\beta-1)D_2 = 0\,. \tag{2.1.32}$$

It is easy to verify that these two equations are satisfied identically for all d, α, β and η_i by virtue of the ansatz.

Finally, we note that by saturating one of the NEC inequalities, $z = 1+\theta/d$, it is possible to reduce the complexity of $V(\phi), f(\phi)$ to power laws in the dilaton.

The next step is to explore which parameter ranges are physically admissible when we have HSV solutions in our theory with curvature squared corrections. Our main physics tool for investigating this will be the NEC, the details of which we derived earlier in this section. We now turn to visualizing the NEC constraints graphically.

2.2 Exploring parameter ranges using the NEC

In the previous section, we used $\{\eta_1, \eta_2, \eta_3\}$ to parametrize the curvature squared corrections to Einstein gravity in our model. It is convenient at this point to change basis to the more traditional basis $\{\eta_W, \eta_{GB}, \eta_R\}$ for the higher curvature terms where

$$\mathcal{L}_{HC} = \eta_W C_{\mu\nu\lambda\sigma} C^{\mu\nu\lambda\sigma} + \eta_{GB} G + \eta_R R^2 \,, \tag{2.2.1}$$

where $G = R_{\mu\nu\rho\sigma}R^{\mu\nu\rho\sigma} - 4R_{\mu\nu}R^{\mu\nu} + R^2$ is the usual Gauss-Bonnet term and the Weyl tensor is

$$C_{\mu\nu\rho\sigma} = R_{\mu\nu\rho\sigma} - \frac{2}{d}\left(g_{\mu[\rho}R_{\sigma]\nu} - g_{\nu[\rho}R_{\sigma]\mu}\right) + \frac{2}{d(d+1)} R\, g_{\mu[\rho}g_{\sigma]\nu} \,. \tag{2.2.2}$$

Here, anti-symmetrization of the indices is defined as $T_{[\mu\nu]} = \frac{1}{2}\left(T_{\mu\nu} - T_{\nu\mu}\right)$. It is straightforward to work out the relation between the coupling constants above and those in our original basis:

$$\begin{aligned}
\eta_w &= \frac{d(\eta_2 + 4\eta_1)}{4(d-1)} \,, \\
\eta_R &= \frac{4\eta_1 + (d+2)\eta_2 + 4(d+1)\eta_3}{4(d+1)} \,, \\
\eta_{GB} &= -\frac{(4\eta_1 + d\eta_2)}{4(d-1)} \,.
\end{aligned}$$

There are a few sanity checks that we can make in this basis. In particular, the Gauss-Bonnet term should vanish for $d = 1$ and is topological for $d = 2$ ($D = d + 2 = 3$ and $D = d + 2 = 4$), hence the equations of motion should be independent of η_{GB} for $d \leq 2$. This is straightforwardly verified. Furthermore, the Weyl tensor vanishes in AdS, so in the limit that $\alpha = 1$ and $\beta = 1$ ($z = 1$ and $\theta = 0$, respectively), we expect the equations of motion to be independent of η_W. Again, this is straightforwardly verified. In fact, it is true for $\alpha = 1$ even for $\beta \neq 1$ ($z = 1$, $\theta \neq 0$, respectively).

It is difficult to visualize the influence of the three independent couplings $\eta_{GB}, \eta_W, \eta_R$ at once. We will address this complexity in stages by examining the cases in which (i) only one parameter is turned on; (ii) two parameters are turned on; and (iii) three parameters are turned on. Again, our main physics tool will be the NEC.

2.2.1 Gauss-Bonnet gravity

Gauss-Bonnet gravity is the case where $\eta_R = \eta_W = 0$. We begin with this case because it turns out to be the simplest one. Note that in every case we study, the conditions (2.1.22) and (2.1.23) are always taken into account as well.

In terms of z and θ, the NEC for HSV solutions reduces to

$$-\eta_{GB}\, d\,(d-1)(d-2)\,[d(z-1)-\theta] \geq 0\,, \tag{2.2.3}$$

$$-\eta_{GB}\, d\,(d-1)(d-2)(z-1)\,[d^2+dz-d\theta+2\theta] \geq 0\,. \tag{2.2.4}$$

Notice that both conditions (2.2.3) and (2.2.4) are trivial when $d = 1$ or $d = 2$. As we pointed out in the previous subsection (3.1), the Gauss-Bonnet term vanishes for $d = 1$ and is topological for $d = 2$ (i.e. $D = d + 2 = 4$) and so does not contribute to the equations of motion. This is why the NEC reduces to (2.1.22) and (2.1.23) of Einstein gravity.

For $d > 2$ where the Gauss-Bonnet term is nontrivial, combining (2.1.22) and (2.1.23) with (2.2.3) and (2.2.4) produces different outcomes depending on the sign of η_{GB}. For $\eta_{GB} > 0$, there is only one way to support HSV: $z = 1$ and $\theta = 0$, i.e. the AdS_{d+2} limit. For $\eta_{GB} \leq 0$, we end up with the Einstein gravity NEC.

In general terms, we want to understand how the NEC conditions in our R^2 HSV model restrict the theory parameters η_i and the solution parameters z, θ. To see how, it is instructive to plot the inequalities as a function of η_i, z, and θ while fixing the number of transverse dimensions d. For the Gauss-Bonnet case, the permissible parameter regions are shown in Fig (2.1), for two values of d. The plots look so simple here because the constraints are linear. For every other case that we will discuss in this section, the constraints will look more opaque and we use the plots to help shed light on them.

Our conventions for figure features are as follows. (i) Allowed regions are bounded by the metallic grey surface(s) labeled "S", which we will refer to in the following as the constraint surface. (ii) An arrow indicates that the object shown – whose cross section

is depicted as a light grey surface perpendicular to the base of the arrow – continues on infinitely in the direction indicated by that arrow. (iii) Black indicates that either (a) the HSV parameter θ leaves the physically acceptable regime of $0 \leq \theta < d$ or (b) the η_i parameters become inadmissible, i.e. do not support HSV solutions satisfying the NEC.

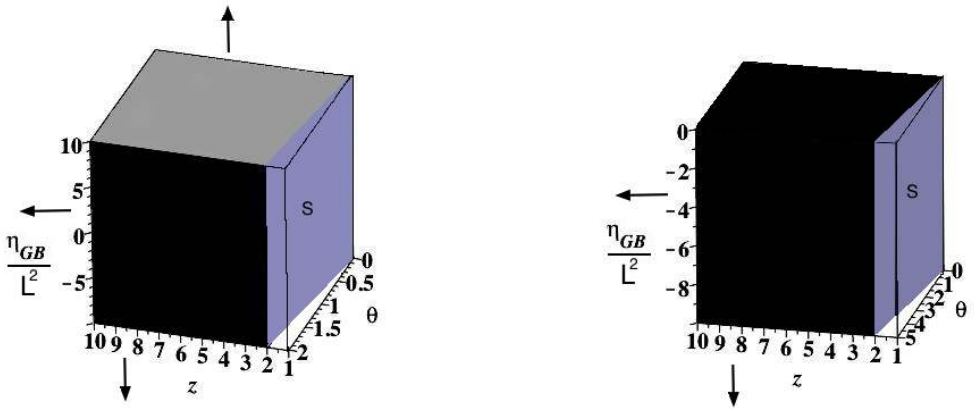

(a) $d = 2$, only $\eta_{GB} \neq 0$.

(b) $d = 5$, only $\eta_{GB} \neq 0$.

Figure 2.1: Restrictions on η_{GB} from the NEC for $d = 2$ and $d = 5$ respectively. Note that there is only one arrow towards decreasing η_{GB} for the $d = 5$ case (2.1b).

2.2.2 Einstein-Weyl gravity

Einstein-Weyl gravity is what we get when we set $\eta_{GB} = \eta_R = 0$. This is of interest in its own right because the Weyl tensor vanishes in AdS.

In this case, we find that

$$-\frac{4\eta_W}{(d+1)L^2}(d-1)(d+2\beta-2)(\alpha-1)(\alpha+\beta-1)(\alpha-3\beta-d+1) \geq 0\,, \tag{2.2.5}$$

$$-\frac{4\eta_W}{(d+1)L^2}(d-1)(\alpha-1)(\alpha+\beta-1)(3\beta+\alpha+d-3)(d\alpha-2d\beta+2-2\beta-d^2) \geq 0\,, \tag{2.2.6}$$

Before we move to the plot, let us verify that our solution recovers the known Lifshitz solution [305] in the limit that $\beta \to 1$ (which implies that $\alpha \to z$). This is indeed precisely what we obtain: $V(\phi(r))$ reduces to the cosmological constant for the Lifshitz case, $\phi(r) \propto \ln(r)$ and $f(\phi(r))$ is an exponential of the dilaton.

A curious sub-case is the one with $\alpha = 1$ (so $z = 1$), but $\beta \neq 1$, that is, the "purely" hyperscaling violating solution. In this case, we find a logarithmic dilaton and an exponential potential

$$\phi(r) = -\sqrt{2d(1-\beta)}\ln(r) + \text{const}\,, \tag{2.2.7}$$

$$V(\phi) = -\frac{\tilde{A}}{L^2}\exp\left(\sqrt{\frac{2(1-\beta)}{d}}\phi\right)\,, \tag{2.2.8}$$

where $\tilde{A}$ is a constant which depends on d and β, and

$$f(\phi) \to \infty\,. \tag{2.2.9}$$

The logarithmic running of the dilaton and a potential that is exponential in ϕ is to be expected here [14], [305]. Recall the solution to Maxwell's equations (2.1.5) is $F^{rt} = Q/[\sqrt{-g}f(\phi)] = Qr^{\beta-\alpha-d}/[f(\phi)L^{d+2}]$. Hence, as $f(\phi) \to \infty$, the field strength vanishes, meaning that the gauge field reduces to a constant. This is to be expected as the role of the gauge field was to break the usual relativistic scaling symmetry to the non-relativistic Lifshitz case. When $z = 1$, this scaling symmetry is restored and the gauge field is no longer necessary.

The NEC conditions in this case are

$$\eta_W(d-1)[d(d-\theta) - d(z-2) + 2\theta] \geq 0\,, \tag{2.2.10}$$

$$\eta_W(d-1)[d^3 - d^2(z+\theta-2) + (d+2)\theta] \geq 0\,, \tag{2.2.11}$$

which we plot along with the other two NEC constraints (2.1.22) and (2.1.23). Several example plots are shown below.

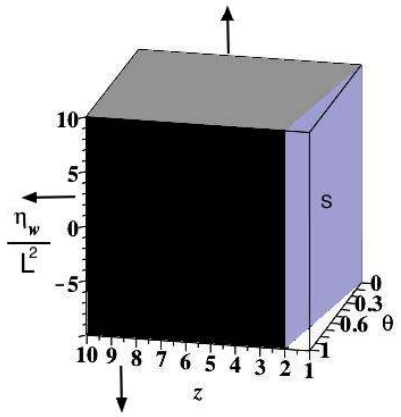

(a) $d = 1$, only $\eta_W \neq 0$

Figure 2.2: NEC restrictions on η_W for $d = 1$.

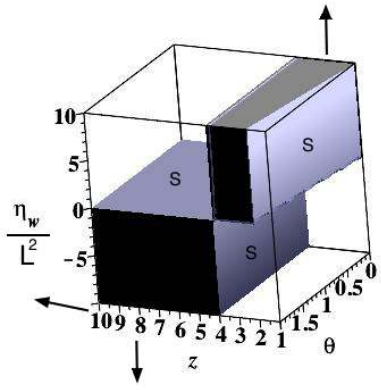

(a) $d = 2$, only $\eta_W \neq 0$.

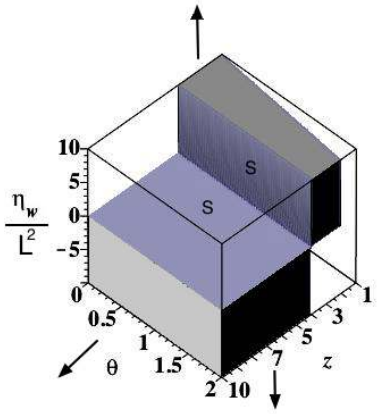

(b) $d = 2$, only $\eta_W \neq 0$, side view.

Figure 2.3: Restrictions on η_W from the NEC for $d = 2$. For $z < 4$, the NEC is satisfied in the hexahedral region in the upper right hand side of both sub-figures. For $z > 4$, the NEC is satisfied in the rectangular region in the lower left hand side of both sub-figures.

Figure (2.2) shows the restrictions imposed by the NEC in $d = 1$. Notice that there are no constraints on η_W. This is not troubling as in $d = 1$, the conditions (2.2.10) and (2.2.11) vanish and what we are plotting then is nothing more than the conditions (2.1.22) and (2.1.23) familiar from Einstein gravity. In $d = 1$, the Weyl tensor vanishes for the HSV metric and so η_W plays no role.

Figure (2.3) shows the allowed regions for $d = 2$. Curiously, there is a transition at $z = 4$; for $z < 4$ the NEC is satisfied in the hexahedral region in the upper right hand side, as seen in figures (2.3b) and (2.3a), which restricts $\eta_W \geq 0$. For $z > 4$, the situation is flipped and the allowed region is the box in the lower left hand side, restricting $\eta_W \leq 0$. When $z = 4$ and $d = 2$, the conditions (2.2.10) and (2.2.11) vanish and the NEC is satisfied for all sensible values of θ and there are no restrictions on η_W. This is indicated in (2.2.10) and (2.2.11) by the plane cutting through the figures at $z = 4$. Curiously enough, for $d = 2$ and $z = 4$, the Weyl tensor does not vanish as it does for $d = 1$ and for $z = 1$, and so is still contributing to the equations of motion. For $d > 2$, a qualitatively similar transition in behaviour occurs, however the crossover now happens for a range of values of z and θ.

From the perspective of condensed matter theory, there is interest in holographic theories with $d = 2$, $\theta = d - 1 = 1$ and $z = 3/2$, which are proposed to capture some of the mysterious physics of strange metal phases [14]. Figures (2.3b) and (2.3a) shows that this range sits comfortably within the hexahedral region in the upper right hand side.

2.2.3 R^2 gravity

Consider the case that $\eta_R \neq 0$, $\eta_{GB} = 0$, and $\eta_W = 0$, so that R^2 is the only higher curvature contribution. In this case, the NEC conditions are

$$-\eta_R[(d+1)\theta^2+d^2(d+1)+2(d+z)(dz-d\theta-\theta)][(d-8)\theta^2-d(d-2)z\theta+d^3(z-1)] \geq 0\,, \tag{2.2.12}$$

$$-\eta_R[(d+1)\theta^2+d^2(d+1)+2(d+z)(dz-d\theta-\theta)][(z-1)(d(z-\theta+d+2\theta)] \geq 0\,, \tag{2.2.13}$$

along with (2.1.22) and (2.1.23). These conditions are shown in Fig (2.4) for two representative values of d.

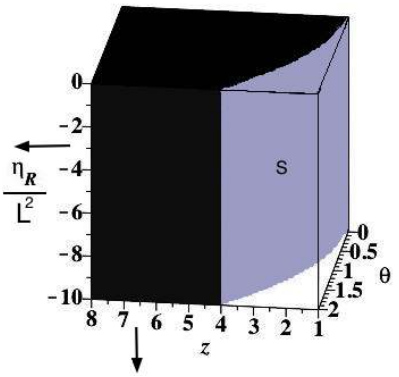

(a) $d = 2$, only $\eta_R \neq 0$.

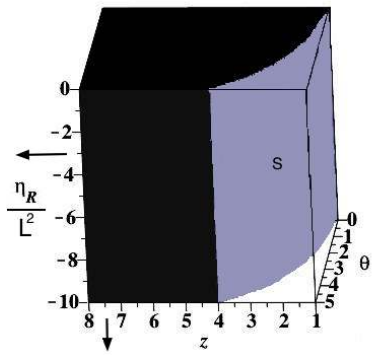

(b) $d = 5$, only $\eta_R \neq 0$.

Figure 2.4: Restrictions on η_R from the NEC for $d = 2$ and $d = 5$. Note that there are two black sides in both plots, unlike earlier cases.

The results for $d > 5$ are all qualitatively similar. In all cases, the allowed region is bounded by the curved surface ("S" in figures (2.4)). This surface is always bounded by lines along the η_R axis at $z = 0$ and $z = 4$. The NEC also restricts $\eta_R \leq 0$ in all d. In fact, the only way to support $\eta_R > 0$ is to set $z = 1$ and $\theta = 0$. In this case, both conditions (2.2.12) and (2.2.13) vanish.

We can also consider turning on more than one coupling at a time. In the next four sections we will investigate the constraints on multiple ηs imposed by d, z and θ.

2.2.4 R^2 and Weyl terms

As a first example, consider the case $\eta_R \neq 0$, $\eta_W \neq 0$, but $\eta_{GB} = 0$. The conditions are

$$-\eta_R \left\{ d(d+1)(\theta^2+d^2) + 2(d+z)(dz-d\theta-\theta)[(d-8)\theta^2 - d(d-2)z\theta + d^3(z-1)] \right\}$$
$$+ \frac{2\eta_W}{(d+1)} d^2(d-1)(z-1)[d^2-(d-2)\theta][d(d-\theta)-d(z-2)+2\theta] \geq 0\,, \qquad (2.2.14)$$

$$- \eta_R \left\{ d^2(z-1)(\theta^2+d^2) + 2(d+z)(dz - d\theta - \theta)(d(z-\theta+d)+2\theta) \right\}$$
$$+ \frac{2\eta_W}{d(d+1)} d^2 z(z-1)(d-1)[d^3 - d^2(z+\theta-2) + (d+2)][dz + 2\theta + d(d-\theta)] \geq 0\,. \tag{2.2.15}$$

Given a value for d, and z, it is instructive to plot these inequalities (along with (2.1.22) and (2.1.23)) for the physically sensible range of θ. This is depicted in Fig (2.5) for several different values. Note that because we now have two theory parameters varying in the plots, we have to fix one of the other parameters per plot to fit the plot into 3D. For clarity, we choose to fix z for any given plot (as well as d, as before) in order to visualize the constraint surfaces for θ.

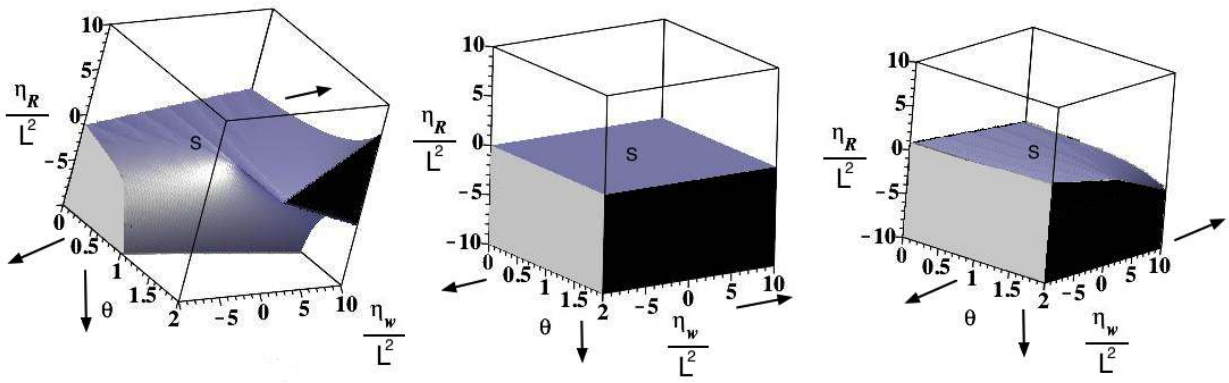

(a) $d = 2$, $z = 2$ (b) $d = 2$, $z = 4$ (c) $d = 2$, $z = 6$

Figure 2.5: Restrictions on η_W and η_R from the NEC for $d = 2$ and several values of z. Notice the sharp change in behaviour in Fig (2.5b) where $d = 2$, $z = 4$.

The figures for $d = 3, 4, 5$ look qualitatively similar, with only minor quantitative differences.

Notice that for $d = 2$, there is an interesting change in behaviour at $z = 4$ in Fig (2.5). At this point, the contribution from the Weyl term vanishes from the NEC and we are left simply with the the conditions of pure R^2 gravity. As we found in section (2.2.3), when only the η_R term is non-zero, then physically sensible ranges of z and θ restrict $\eta_R < 0$. We see precisely this kind of behaviour in the case of having both η_R and η_W

turned on; at $d = 2$ and $z = 4$, the η_W contribution vanishes and we are left with only η_R which is required to be less than or equal to zero, consistent with our previous result.

$d = 2$ and $z = 4$ is special in that it is the unique combination of parameters for which the η_W term does not contribute to the NEC. At the level of the equations of motion (2.1.12), the relevant equations reduce down to those of pure R^2 gravity for this choice of parameters. In dimensions other than $d = 2$, a qualitatively similar transition is observed, but the transition is not as sharp as the contribution from the η_W term never drops out completely.

2.2.5 R^2 and Gauss-Bonnet terms

Consider $\eta_W = 0$, $\eta_{GB} \neq 0$ and $\eta_R \neq 0$. The NEC conditions are

$$-\eta_R[2dz(d+z) + d^2(d+1) - 2(d+1)z\theta - 2d(d+1) + (d+1)\theta^2][(d-8)\theta^2 - d(d-2)z\theta + d^3(z-1)] - \eta_{GB}(d-1)(d-2)(d-\theta)^3[d(z-1)-\theta] \geq 0\,, \quad (2.2.16)$$

$$-\eta_R d(z-1)[d(z-\theta+d)+2\theta)][2dz(d+z) + d^2(d+1) - 2(d+1)z\theta - 2d(d+1) + (d+1)\theta^2] - \eta_{GB}(d-1)(d-2)(z-1)(d-\theta)^2[d(z-\theta+d)+2\theta] \geq 0\,, \quad (2.2.17)$$

which are to be supplemented by (2.1.22) and (2.1.23). Notice that for $d = 1$ and $d = 2$, the Gauss-Bonnet contribution to (2.2.16) and (2.2.17) vanishes and we are left simply with pure R^2 gravity as in section (2.2.3). Fig (2.6) and Fig (2.7) plot the restrictions on η_{GB} and η_R for $d = 3$ and a few values of z.

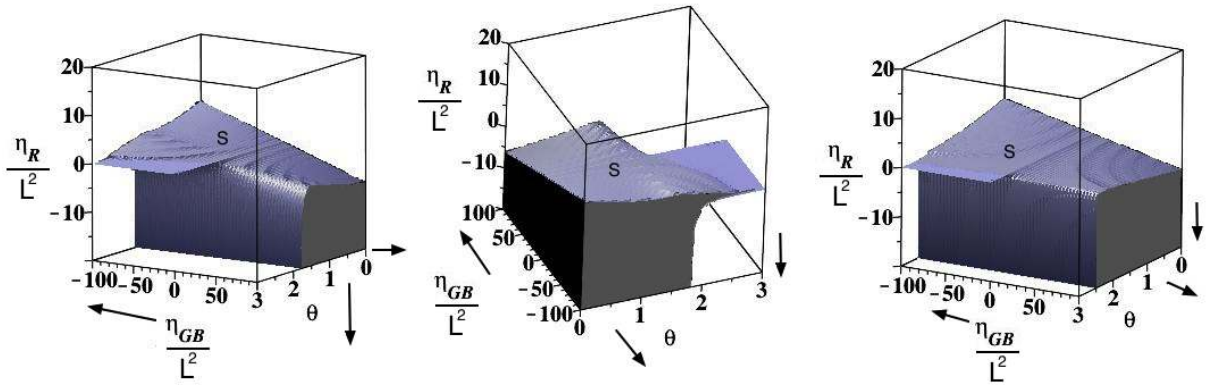

(a) $d = 3$, $z = 2$ (b) $d = 3$, $z = 2$, side view (c) $d = 3$, $z = 3$

Figure 2.6: Restrictions on η_{GB} and η_R from the NEC for $d = 3$ and $z = 2$ and $z = 3$.

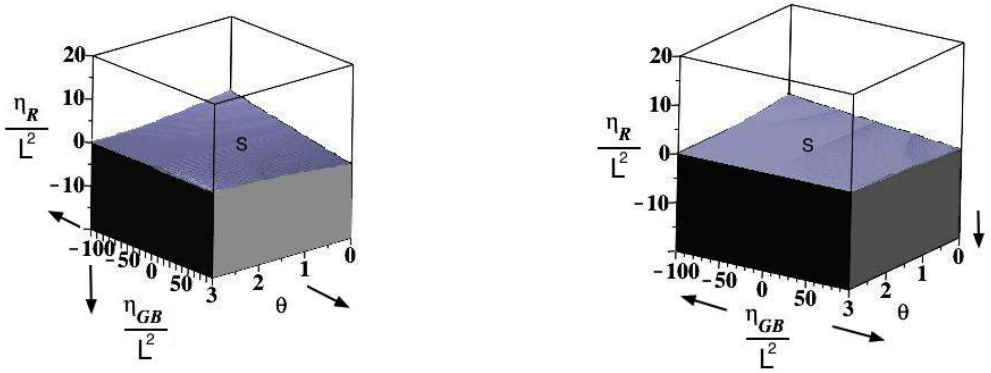

(a) $d = 3$, $z = 4$ (b) $d = 3$, $z = 6$

Figure 2.7: Restrictions on η_{GB} and η_R from the NEC for $d = 3$ and $z = 4$ and $z = 6$. Notice the sharp change in behaviour compared Fig (2.6) where $d = 3$, $z < 4$.

Notice the sharp change in behaviour for $z \geq 4$ in Fig (2.7). Below $z = 4$, both positive and negative values of η_R and η_{GB} are allowed up to a maximum value of θ (for $z = 2$, this value is $\theta = 1.8$, for example). Above this value of only $\eta_{GB} < 0$ is allowed and η_R is also severely restricted, as seen in Fig (2.6b). In fact, this transition in behaviour is independent of d and always occurs at $z = 4$. As in previous sections, $z = 4$ turns out to be special.

For $d > 3$, qualitatively similar behaviour is observed. Fig (2.8) and Fig (2.9) provide a few salient examples.

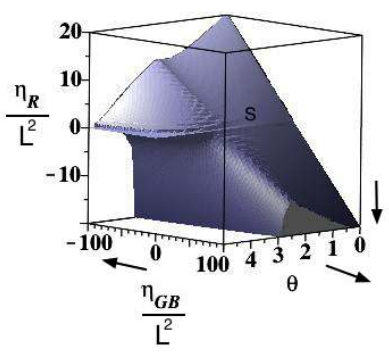

(a) $d = 5$, $z = 2$

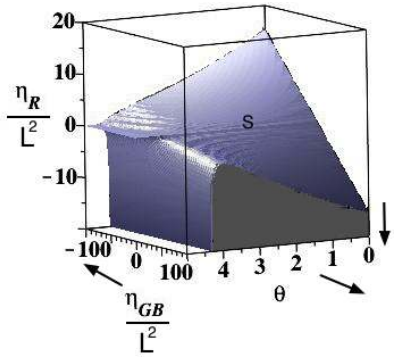

(b) $d = 5$, $z = 3$

Figure 2.8: Restrictions on η_{GB} and η_R from the NEC for $d = 5$ and $z = 2$ and $z = 3$.

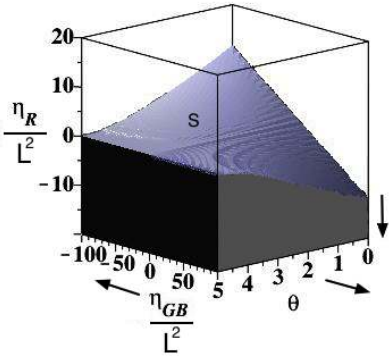

(a) $d = 5$, $z = 4$

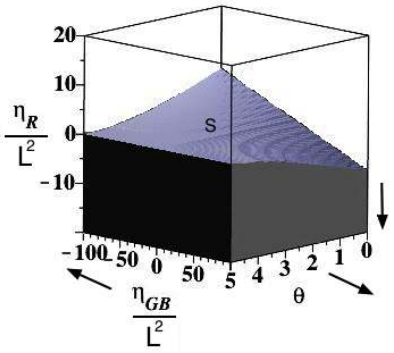

(b) $d = 5$, $z = 6$

Figure 2.9: Restrictions on η_{GB} and η_R from the NEC for $d = 5$ and $z = 4$ and $z = 6$. Notice the sharp change in behaviour compared to Fig (2.8) where $d = 5$, $z < 4$.

2.2.6 Gauss-Bonnet and Weyl

Turning our attention to the case of $\eta_R = 0$ and $\eta_{GB} \neq 0$ and, $\eta_W \neq 0$, the conditions are

$$\begin{aligned} &2dz(z-1)(d-1)(d(d-\theta)+d(z-2)+2\theta)\eta_W \\ &-(d-1)(d-2)(d+1)(d-\theta)^3(d(z-1)-\theta)\eta_{GB} \geq 0\,, \end{aligned} \tag{2.2.18}$$

$$\begin{aligned} &2z(z-1)(d-1)(d(d-\theta)+dz+2\theta)(d^2(d-\theta)-d^2(z-2)+(d+2)\theta)\eta_W \\ &-(z-1)(d-1)(d-2)(d+1)(d-\theta)^2(d(z-\theta+d)+2\theta)\eta_{GB} \geq 0\,, \end{aligned} \tag{2.2.19}$$

which are to be supplemented by (2.1.22) and (2.1.23). As we have seen in previous cases, for $d = 1$ and $d = 2$, the Gauss-Bonnet term does not contribute and we are back to simply the case of $\eta_W \neq 0$ examined in section (2.2.2). Plots of allowed regions of η_{GB} and η_W are shown below for representative values of $d \geq 3$, z and θ.

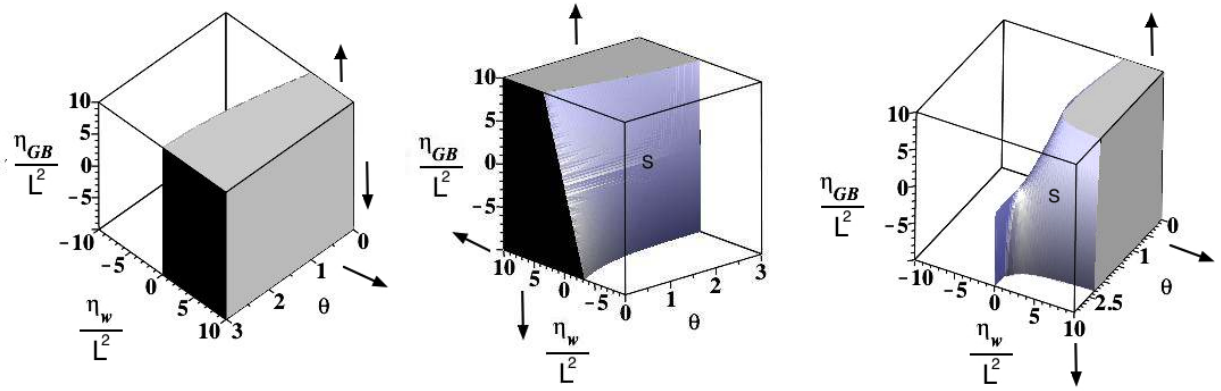

(a) $d = 3$, $z = 2$. (b) $d = 3$, $z = 2$, back view. (c) $d = 3$, $z = 4$.

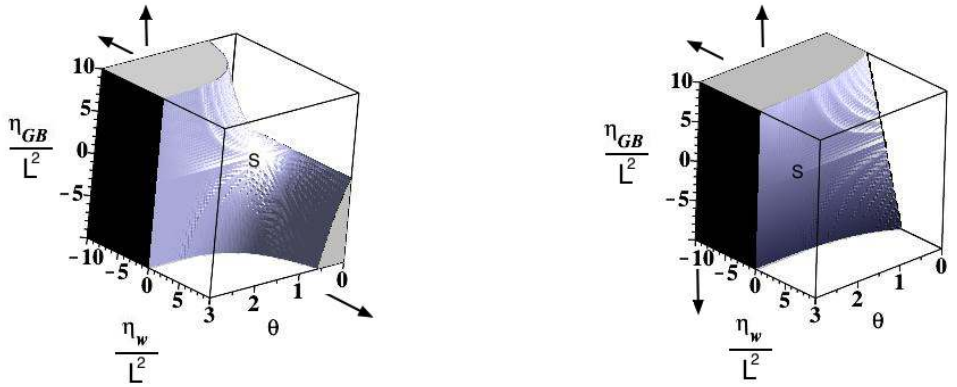

(d) $d = 3$, $z = 5$. (e) $d = 3$, $z = 6$.

Figure 2.10: Restrictions on η_{GB} and η_W from the NEC for $d = 3$ and $z = 2$, $z = 4$, $z = 5$ and $z = 6$.

For $d = 3$ depicted above in Fig (2.10), there are distinct transitions in behaviour that occur at $z = 4$ and $z = 5$. Once we hit $z = 6$, the allowed region is similar to that of $z = 2$, except that the allowed values of η_W are reflected by a minus sign. This effect happens for higher dimensions as well, although the precise value of z depends on d and is not universal. Following the common theme that we have seen in previous sections, values of z around 4 mark a noticeable change in the allowed parameter region. Higher dimensions display analogous behaviour. We provide a few examples in figures (2.11) and (2.12) below for $d = 4$ and $d = 5$, respectively.

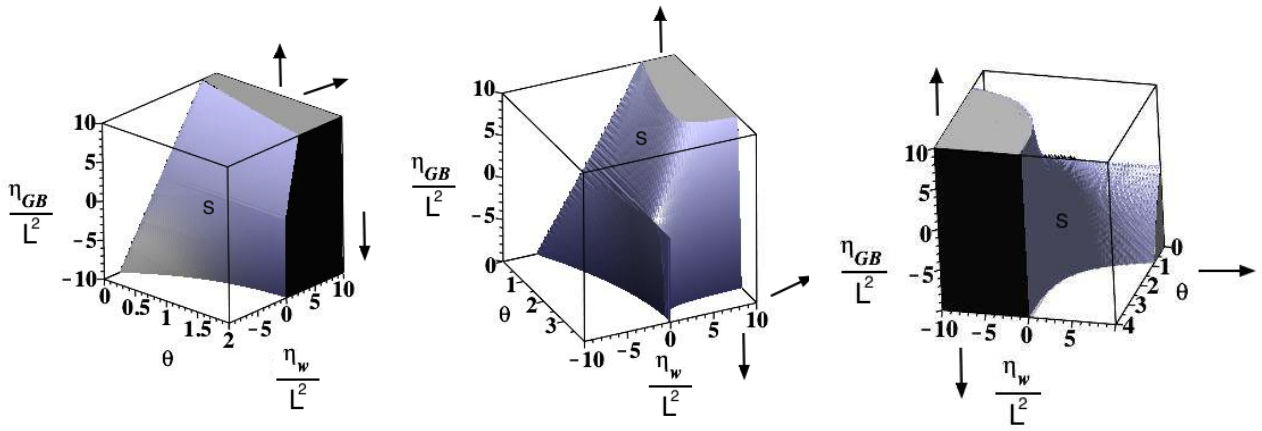

(a) $d = 4$, $z = \frac{3}{2}$. (b) $d = 4$, $z = 4$. (c) $d = 4$, $z = 6$.

Figure 2.11: Restrictions on η_{GB} and η_W from the NEC for $d = 4$ and $z = \frac{3}{2}$, $z = 4$ and $z = 6$.

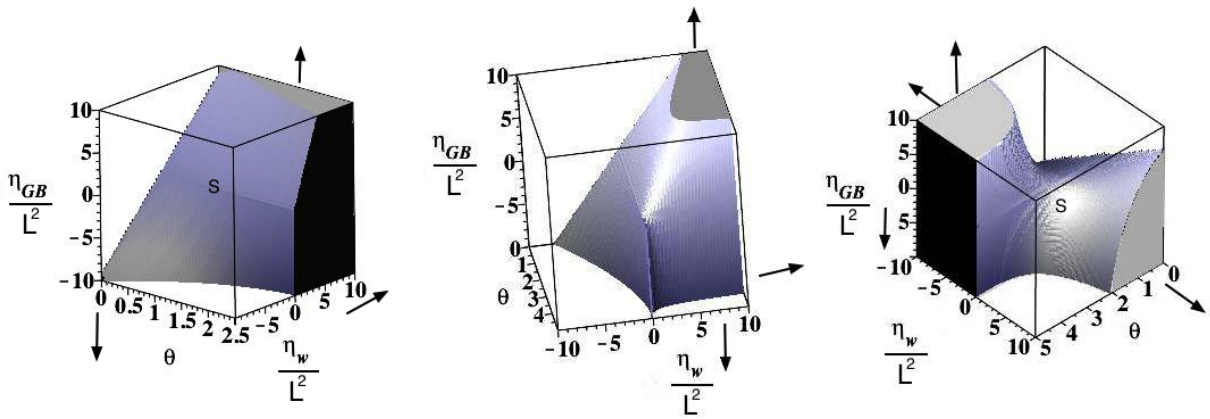

(a) $d = 5$, $z = \frac{3}{2}$. (b) $d = 5$, $z = 4$. (c) $d = 5$, $z = 6$.

Figure 2.12: Restrictions on η_{GB} and η_W from the NEC for $d = 5$ and $z = \frac{3}{2}$, $z = 4$ and $z = 6$.

2.2.7 R^2, Gauss-Bonnet and Weyl

Finally, let us consider the case of having all three η_R, η_{GB} and η_W turned on at once. It is easiest to visualize the impact of different theory parameter choices by having all three vary in our plots. This requires us to show different z, θ with different plots. So in this subsection, we are showing different slicings through the five-dimensional parameter

space $\{\eta_{GB}, \eta_W, \eta_R, z, \theta\}$ than we did in the single-η and pair-of-ηs cases. The plots may look less structured but this is just a slicing artefact.

The conditions we need to satisfy are

$$\begin{aligned}
&-\eta_{GB}(d-1)(d-2)(d+1)(d-\theta)^3(d(z-1)-\theta)\\
&-\eta_R(d+1)\{d^3(z-1)-dz\theta(d-2)+(d-8)\theta^2\}\\
&\times[(d+1)\theta^2-2(d+1)z\theta-2(d+1)d\theta+d^2(d+1)+2d(d+z)z]\\
&+2\eta_W z(z-1)d(d-1)\{d(d-\theta)+2\theta\}[d(d-\theta)-d(z-2)+2\theta)]\geq 0\,,
\end{aligned} \tag{2.2.20}$$

$$\begin{aligned}
&-\eta_{GB}(z-1)(d-1)(d-2)(d+1)(d-\theta)^2[d(z-\theta+d)+2\theta]\\
&-\eta_R d(d+1)(z-1)\left\{d(z-\theta+d)+2\theta\right\}\\
&\times[(d+1)\theta^2-2(d+1)z\theta-2d(d+1)+d^2(d+1)+2d(d+z)z]\\
&+2\eta_W z(z-1)(d-1)\{d(z-\theta+d)+2\theta\}[d^2(d+2)+(d+2)\theta-d^2(z+\theta)]\geq 0\,,
\end{aligned} \tag{2.2.21}$$

which are to be supplemented by (2.1.22) and (2.1.23). Once again, for $d = 1$ and $d = 2$, the Gauss-Bonnet term does not contribute, so we will begin our analysis at $d = 3$. In this case, we have three ηs but only two conditions to satisfy, hence there is a wide range of possible values to choose from. Nevertheless, we can still generate markedly different behaviour by change the value of the hyperscaling violation parameter, θ. Figure (2.13) below provides an example for $d = 3$, $z = 2$ and $\theta = 1$ and $\theta = 2$, respectively. In going from $\theta = 1$ to $\theta = 2$, a wide range of possible combinations of the ηs is lost.

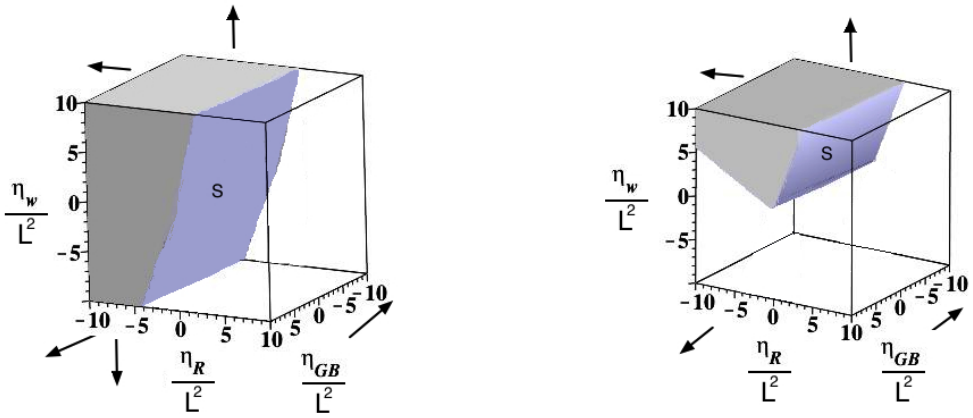

(a) $d = 3$, $z = 2$, $\theta = 1$. (b) $d = 3$, $z = 2$, $\theta = 2$.

Figure 2.13: Restrictions on η_R, η_{GB} and η_W from the NEC for $d = 3$ and $z = 2$, and $\theta = 1$ and $\theta = 2$, respectively. Note the change in the allowed region when going from $\theta = 1$ to $\theta = 2$.

The behaviour changes once again around $z = 4$. This is depicted in Fig (2.14) for $d = 3$. For larger values of z, the allowed region is qualitatively similar to that of $z = 4$, this is also depicted in Fig(2.14).

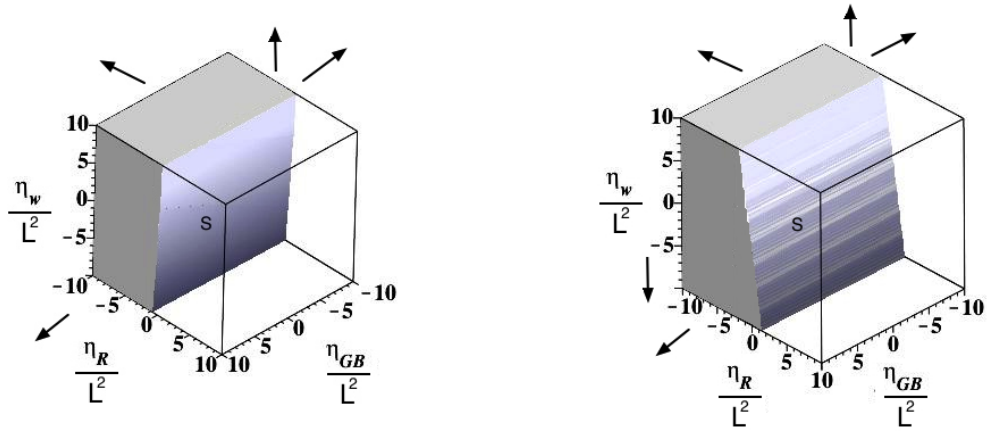

(a) $d = 3$, $z = 4$, $\theta = 1$. (b) $d = 3$, $z = 6$, $\theta = 2$.

Figure 2.14: Restrictions on η_R, η_{GB} and η_W from the NEC for d =3, $z = 4$, $\theta = 1$ and $d = 3$, $z = 6$, $\theta = 2$, respectively.

Again, qualitatively similiar results are obtained for higher dimensions. Below $z = 4$, the allowed region of ηs can be quite different, depending on the value of θ. Above, $z \geq 4$,

the shape of the allowed region is not as sensitive to changes of θ. Figures (2.15) and (2.16) provide examples for $d = 5$.

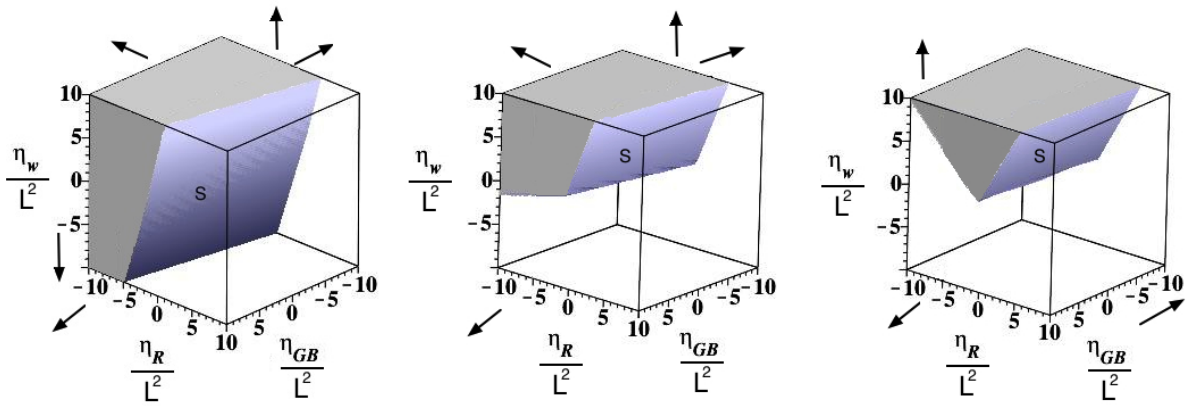

(a) $d = 5$, $z = 2$, $\theta = 1$. (b) $d = 5$, $z = 2$, $\theta = 3$. (c) $d = 5$, $z = 2$, $\theta = 4$.

Figure 2.15: Restrictions on η_R, η_{GB} and η_W from the NEC for $d = 5$ and $z = 2$, and $\theta = 1$, $\theta = 3$, and $\theta = 4$, respectively. Note the change in the allowed region when going from $\theta = 1$ to $\theta = 3$ and $\theta = 4$.

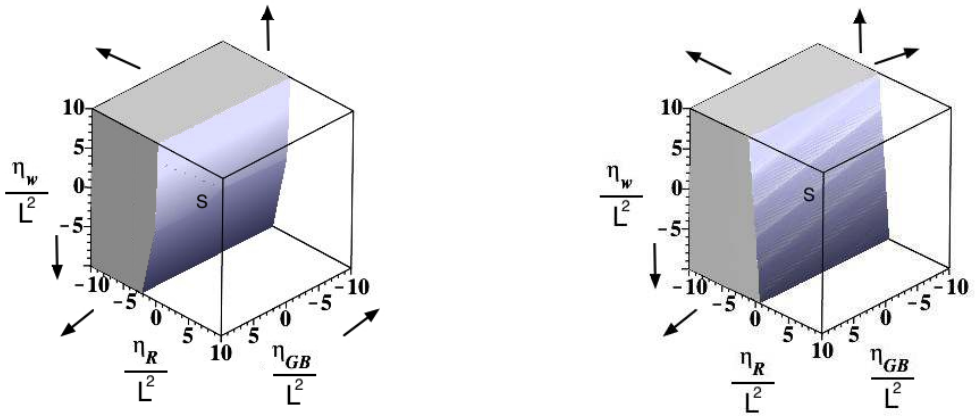

(a) $d = 5$, $z = 4$, $\theta = 4$. (b) $d = 5$, $z = 6$, $\theta = 3$.

Figure 2.16: Restrictions on η_R, η_{GB} and η_W from the NEC for d =5, $z = 4$, $\theta = 4$ and $d = 5$, $z = 6$, $\theta = 3$, respectively.

We will summarize the general features of all these NEC plots and their physical implications in Section 2.4.

2.3 Crossover solutions

In this section we are interested in constructing completions to the $D = d + 2$ HSV geometry in the deep interior (IR) and asymptotic (UV) region. We will specialize to Einstein-Weyl gravity because the Weyl tensor vanishes in AdS, which means that the curvature squared terms will not source the dilaton regardless of the form of its coupling. This ensures that we have a chance at an AdS UV completion to the geometry. We also seek an IR completion to $AdS_2 \times \mathbb{R}^d$ so that any gravitational (tidal force) singularities in the deep interior of the HSV spacetime are resolved by the crossover to the singularity-free $AdS_2 \times \mathbb{R}^d$. We also hope to tame potential curvature invariant blowups in the asymptotic region, in this case by the AdS_D. This type of analysis was performed for the Lifshitz case in [305], which provided one of the motivations for the analysis of this section, but it uses a different set of theory functions than ours.

The HSV solution that was constructed in Section 2.1 contains a running dilaton. If we want to be able to complete the spacetime into an $AdS_2 \times \mathbb{R}^d$ in the IR, we need a mechanism by which the dilaton is stabilized to some constant value, ϕ_0. This is where the curvature squared corrections to the action come into play. An immediate question that arises is whether we need to add any further terms to our effective action in order to support crossovers. After allowing corrections to the Lagrangian of the form $k(\phi)C_{\mu\nu\lambda\sigma}C^{\mu\nu\lambda\sigma}$, we find that it is possible to have HSV as a solution of the equations as well as AdS_D and $AdS_2 \times \mathbb{R}^d$ without needing any more theory functions than $f(\phi)$ and $V(\phi)$.

It is most sensible for us to seek crossovers to HSV starting from the AdS_D and $AdS_2 \times \mathbb{R}^d$ ends, aiming to pick up the HSV solution as we evolve in radius in between. This is because classification of relevant/irrelevant perturbations is much better understood in AdS.

In order to find crossovers, it helps to pick a convenient gauge for the metric (2.0.4). Under a coordinate transformation $\mathcal{R} = \rho^{-1/z}$ and a rescaling of L and the other coordi-

nates, the line element takes the form

$$ds^2 = L^2\rho^{-2(dz-\theta)/dz}\left[-dt^2 + d\rho^2 + \rho^{2(z-1)/z}d\vec{x}_d^2\right] . \tag{2.3.1}$$

In the new ρ coordinate, the deep interior (IR) corresponds to $\rho \to \infty$ and the UV corresponds to $\rho \to 0$. Since we wish to construct solutions which flow from $AdS_2 \times \mathbb{R}^d$ in the IR to an intermediate HSV regime and finally to AdS_D, it is convenient to parametrize the metric as [305]:

$$ds^2 = a_1^2(\rho)\left[-dt^2 + d\rho^2 + a_2^2(\rho)d\vec{x}_d^2\right] . \tag{2.3.2}$$

In this parametrization, $AdS_2 \times \mathbb{R}^d$ corresponds to $a_1(\rho) = L_\flat/\rho$ and $a_2(\rho) = \rho$, whereas AdS_D corresponds to $a_1(\rho) = L_\sharp/\rho$ and $a_2(\rho) = \text{const}$.

In what follows we denote radial coordinate derivatives by $' = \partial_\rho$. We will also abbreviate dilaton field derivatives of theory functions as $\dot{} \equiv \partial_\phi$. This is not a time derivative; instead, it is a *field* derivative. We trust the reader not to get confused by this.

It is easiest to begin our study of the field equations with the gauge field. The Maxwell field equation is

$$\nabla_\mu\left[f(\phi)F^{\mu\nu}\right] = 0\,. \tag{2.3.3}$$

In our metric ansatz, this equation becomes

$$\left[a_1^{d+2}a_2^d f(\phi)\mathcal{E}\right]' = 0\,, \tag{2.3.4}$$

where $\mathcal{E} \equiv F^{\rho t}(\rho)$ is a solution function of ρ. Clearly, this equation has a first integral,

$$\mathcal{E}(\rho) = \frac{Q}{a_1^{d+2}a_2^d f(\phi)}\,, \tag{2.3.5}$$

where Q is an integration constant. Note that there is a theory function involved here: $f(\phi)$. Note also that although Q is a constant, it will be a *different* constant for our three different solutions involved in the crossover: AdS_D, $AdS_2 \times \mathbb{R}^d$, and HSV. This is related to the fact that the electric field must have perturbations if the dilaton and metric do,

in accordance with the terms in the original effective action. It is the total electric field which obeys the Maxwell equation: the background, about which one is expanding, plus the perturbation. (Note that if we had done magnetic perturbations staying in a radial ansatz, the perturbed magnetic field would be unconstrained by the Maxwell equation.) The last ingredient we need is $\partial_\rho f(\phi)$. This is directly available because we are working within an ansatz with only radial coordinate dependence, so

$$[f(\phi(\rho))]' = \frac{df}{d\phi}\frac{d\phi}{d\rho}\,, \tag{2.3.6}$$

or, more succinctly, $f' = \dot{f}\phi'$. This gives the full Maxwell equation as

$$\left[(d+2)\frac{a_1'}{a_1} + d\frac{a_2'}{a_2}\right]\mathcal{E} + \frac{\dot{f}(\phi)}{f(\phi)}\phi'\mathcal{E} + \mathcal{E}' = 0\,. \tag{2.3.7}$$

The dilaton field equation is

$$\Box\phi - \frac{1}{4}\dot{f}(\phi)F_{\mu\nu}F^{\mu\nu} - \dot{V}(\phi) = 0\,. \tag{2.3.8}$$

When evaluated on the metric ansatz (2.3.2), this gives the full dilaton equation as

$$\frac{1}{a_1^2}\phi'' + \frac{d}{a_1^2}\left(\frac{a_1'}{a_1} + \frac{a_2'}{a_2}\right)\phi' - \dot{V}(\phi) + \frac{1}{2}\dot{f}(\phi)a_1^4\mathcal{E}^2 = 0\,. \tag{2.3.9}$$

These coupled equations (2.3.7) and (2.3.9) for $\mathcal{E}$ and ϕ show us that it is impossible to turn on dilaton perturbations without also exciting electric perturbations.

The next step is to write down the energy-momentum tensor for the right hand side of the tilded gravitational equations of motion. The components of $T^\mu_{\ \nu}$ are

$$T^t_{\ t} = -\frac{1}{2}V(\phi) - \frac{1}{4a_1^2}(\phi')^2 - \frac{1}{2}f(\phi)a_1^4\mathcal{E}^2\,, \tag{2.3.10}$$

$$T^\rho_{\ \rho} = -\frac{1}{2}V(\phi) + \frac{1}{4a_1^2}(\phi')^2 - \frac{1}{2}f(\phi)a_1^4\mathcal{E}^2\,, \tag{2.3.11}$$

$$T^x_{\ x} = -\frac{1}{2}V(\phi) - \frac{1}{4a_1^2}(\phi')^2 + \frac{1}{2}f(\phi)a_1^4\mathcal{E}^2\,. \tag{2.3.12}$$

For the $\widetilde{G}_{\mu\nu}$s in the Weyl corrected gravity equations $\widetilde{G}_{\mu\nu} = T_{\mu\nu}$, we write the second and fourth order pieces as

$$\begin{aligned}\widetilde{G}_{tt} \equiv &+ c_1^t \left(\frac{a_1'}{a_1}\right)^2 + c_2^t \left(\frac{a_2'}{a_2}\right)^2 + c_3^t \frac{a_1''}{a_1} + c_4^t \frac{a_2''}{a_2} + c_5^t \frac{a_1'}{a_1}\frac{a_2'}{a_2} \\ &+ \frac{4\eta_W}{3a_1^2}\left\{ + c_6^t \left(\frac{a_2'}{a_2}\right)^4 + c_7^t \frac{a_2''''}{a_2} + c_8^t \frac{a_2''}{a_2}\left(\frac{a_2'}{a_2}\right)^2 + c_9^t \frac{a_2'''}{a_2}\frac{a_2'}{a_2} + c_{10}^t \left(\frac{a_2''}{a_2}\right)^2 \right. \\ &\qquad + c_{11}^t \frac{a_2'''}{a_2}\frac{a_1'}{a_1} + c_{12}^t \frac{a_1''}{a_1}\left(\frac{a_2'}{a_2}\right)^2 + c_{13}^t \frac{a_1'}{a_1}\left(\frac{a_2'}{a_2}\right)^3 + c_{14}^t \frac{a_1''}{a_1}\frac{a_2''}{a_2} \\ &\qquad \left. + c_{15}^t \frac{a_2''}{a_2}\frac{a_1'}{a_1}\frac{a_2'}{a_2} + c_{16}^t \left(\frac{a_1'}{a_1}\right)^2\left(\frac{a_2'}{a_2}\right)^2 + c_{17}^t \left(\frac{a_1'}{a_1}\right)^2 \frac{a_2''}{a_2} \right\}, \end{aligned} \tag{2.3.13}$$

and similarly for the $\widetilde{G}_{\rho\rho}$, and for $a_2^{-2}\,\widetilde{G}_{xx}$ for each coordinate in the $\vec{x}$. Note that at fourth order, in principle there might have been three other types terms of the form (a_1''''/a_1), $(a_1'''/a_1)(a_1'/a_1)$, $(a_1'''/a_1)(a_2'/a_2)$, but these are absent in conformal gauge.

The 17 constants $\{c_I^t\}$ in these expressions are all functions of d, and similarly with the $\{c_I^\rho\}$ and $\{c_I^x\}$. We now list them. The coefficients of the second order terms for $\widetilde{G}_{tt}$ are

$$\begin{aligned} c_1^t &= -\frac{1}{2}d(d-3)\,, & c_2^t &= -\frac{1}{2}d(d-1)\,, & c_3^t &= -d\,, \\ c_4^t &= -d\,, & c_5^t &= -d^2\,; \end{aligned} \tag{2.3.14}$$

while the fourth order terms are

$$\begin{aligned} c_6^t &= +\frac{3(d-1)[2d^2-8d+7]}{2(d+1)}\,, & c_7^t &= -\frac{3(d-1)}{(d+1)}\,, \\ c_8^t &= -\frac{3(d-1)[d^2-7d+8]}{(d+1)}\,, & c_9^t &= -\frac{3(d-1)(2d-3)}{(d+1)}\,, \\ c_{10}^t &= -\frac{3(d-1)(2d-5)}{2(d+1)}\,, & c_{11}^t &= -\frac{6(d-1)(d-2)}{(d+1)}\,, \\ c_{12}^t &= -\frac{1}{2}c_{11}^t\,, & c_{13}^t &= +\frac{3(d-1)(d-2)(2d-3)}{(d+1)}\,, \\ c_{14}^t &= +\frac{1}{2}c_{11}\,, & c_{15}^t &= -\frac{3(d-1)(d-2)(2d-5)}{(d+1)}\,, \\ c_{16}^t &= +\frac{3(d-1)(d-2)(d-3)}{(d+1)}\,, & c_{17}^t &= -c_{16}^t\,. \end{aligned} \tag{2.3.15}$$

The coefficients of the second order terms for $\widetilde{G}_{\rho\rho}$ are

$$c_1^\rho = +\frac{d(d+1)}{2}\,, \qquad c_2^\rho = +\frac{d(d-1)}{2}\,, \qquad c_3^\rho = 0\,,$$
$$c_4^\rho = 0\,, \qquad c_5^\rho = +d^2\,; \tag{2.3.16}$$

while the fourth order terms are

$$c_6^\rho = +\frac{3(d-1)(2d-3)}{2(d+1)}\,, \quad c_7^\rho = 0\,, \quad c_8^\rho = -\frac{3(d-1)(d-2)}{(d+1)}\,, \quad c_9^\rho = -\frac{3(d-1)}{(d+1)}\,,$$
$$c_{10}^\rho = -\frac{1}{2}c_9^\rho\,, \quad c_{11}^\rho = 0\,, \quad c_{12}^\rho = 0\,, \quad c_{13}^\rho = -c_8^\rho\,,$$
$$c_{14}^\rho = 0\,, \quad c_{15}^\rho = -c_8^\rho\,, \quad c_{16}^\rho = 0\,, \quad c_{17}^\rho = 0\,. \tag{2.3.17}$$

The coefficients of the second order terms for each of the $(a_2^{-2})\widetilde{G}_{xx}$ are

$$c_1^x = +\frac{1}{2}d(d-3)\,, \qquad c_2^x = +\frac{1}{2}(d-1)(d-2)\,, \qquad c_3^x = +d\,,$$
$$c_4^x = +(d-1)\,, \qquad c_5^x = +d(d-1)\,; \tag{2.3.18}$$

while the fourth order terms are

$$c_6^x = +\frac{3(d-1)(d-4)(2d-3)}{2d(d+1)}\,, \qquad c_7^x = -\frac{3(d-1)}{d(d+1)}\,,$$
$$c_8^x = -\frac{3(d-1)[d^2-9d+12]}{d(d+1)}\,, \qquad c_9^x = -6\frac{(d-1)(d-2)}{d(d+1)}\,,$$
$$c_{10}^x = +\frac{3}{4}c_9^x\,, \qquad c_{11}^x = +c_9^x\,,$$
$$c_{12}^x = -\frac{1}{2}c_9^x\,, \qquad c_{13}^x = +\frac{6(d-1)(d-2)^2}{d(d+1)}\,,$$
$$c_{14}^x = +\frac{1}{2}c_9^x\,, \qquad c_{15}^x = -2c_{16}^x\,,$$
$$c_{16}^x = +\frac{3(d-1)(d-2)(d-3)}{d(d+1)}\,, \qquad c_{17}^x = -c_{16}^x\,. \tag{2.3.19}$$

Now that we have the full equations of motion, we can set about demanding that the three different spacetimes which we want to participate in the crossover solve the equations of motion: (1) AdS_D, (2) $AdS_2 \times \mathbb{R}^d$, and (3) HSV. We next consider these in turn. Our convention will be that quantities in AdS_D will be labeled with a subscript $\sharp$, while quantities in $AdS_2 \times \mathbb{R}^d$ will be labeled with a subscript $\flat$.

First, we need to verify that AdS_D is a solution of our Einstein-Weyl-Maxwell-dilaton action. AdS_D has $a_2 = 1$ and $a_1 = L_\sharp/\rho$. Let the constant dilaton in the AdS_D region be $\phi_\sharp$, along with $V_\sharp \equiv V(\phi_\sharp)$, $f_\sharp \equiv f(\phi_\sharp)$, and similarly for higher derivatives of theory functions. Then the equations of motion for the metric coefficients evaluated on AdS_D (in D dimensions) yield two conditions,

$$Q_\sharp^2 = 0\,, \qquad V_\sharp = -\frac{d(d+1)}{{L_\sharp}^2}\,. \tag{2.3.20}$$

Next, let us see whether $AdS_2 \times \mathbb{R}^d$ is also a solution. This has $a_1(\rho) = L/\rho$ and $a_2(\rho) = \rho$, and $\phi(\rho) = \phi_\flat = \text{const}$. Adding and subtracting two Einstein equations yields

$$Q_\flat^2 = L_\flat^{2(d-1)} f(\phi_\flat)\left[1 - \frac{4(d-1)}{(d+1)L_\flat^2}\eta_W\right], \qquad V_\flat = -\frac{1}{L_\flat^2}\,. \tag{2.3.21}$$

As expected, $V(\phi_\flat)$ sets the scale for the $AdS_2 \times \mathbb{R}^d$ solution. Notice that the presence of the Weyl squared term changes the effective charge compared to Einstein gravity, reducing or increasing it depending on the sign of η_W.

Lastly, we can ask whether HSV is a solution. This was already ensured by design in Section 2.1.

In linearized perturbation theory, the Maxwell field equation guarantees that the electric field will be perturbed along with the dilaton. We expand

$$\mathcal{E}(\rho) = \bar{\mathcal{E}}(\rho) + E(\rho)\,, \tag{2.3.22}$$

where $\bar{\mathcal{E}}(\rho)$ is the background electric field and $E(\rho)$ the perturbation. We also split the dilaton into a background piece $\bar{\phi}(\rho)$ (which will be just a constant for AdS_D and $AdS_2 \times \mathbb{R}^d$) and a perturbation Φ,

$$\phi(\rho) = \bar{\phi}(\rho) + \Phi(\rho)\,. \tag{2.3.23}$$

Using the form of our metric ansatz, the linearized electric equation becomes

$$\left[(d+2)\frac{\bar{a}_1'}{\bar{a}_1} + d\frac{\bar{a}_2'}{\bar{a}_2}\right]\left\{f_0 E + \dot{f}_0\bar{\mathcal{E}}\Phi\right\} + \dot{f}_0\bar{\mathcal{E}}\Phi' + f_0 E' = 0\,, \tag{2.3.24}$$

where f_0 denotes the theory function $f(\phi)$ evaluated at its background value and $\bar{a}_1$, $\bar{a}_2$ are the background metric coefficients. The linearized dilaton perturbation equation becomes

$$\frac{1}{\bar{a}_1^2}\phi'' + \frac{d}{\bar{a}_1^2}\left[\frac{\bar{a}_1'}{\bar{a}_1} + \frac{\bar{a}_2'}{\bar{a}_2}\right]\phi' - \dot{V}_0 - \ddot{V}_0\Phi + 2\bar{a}_1^4\left[\bar{\mathcal{E}}^2\left(\dot{f}_0 + \ddot{f}_0\Phi\right) + 2\dot{f}_0\bar{\mathcal{E}}E\right] = 0\,. \tag{2.3.25}$$

We can also write the linearized energy-momentum tensor for use in finding crossovers. Since at linear order the $(\Phi')^2$ terms drop out,

$$T^t{}_t\big|_{\rm lin} = -\frac{1}{2}V_0 - \frac{1}{2}\dot{V}_0\Phi - \frac{Q_0}{2\bar{a}_1^{d-2}\bar{a}_2^d}\left\{\frac{Q_0}{\bar{a}_1^{d+2}\bar{a}_2^d f_0}\left(1 + \frac{\dot{f}_0}{f_0}\Phi + \frac{4AL}{\bar{a}_1}\right) + 2E\right\}\,, \tag{2.3.26}$$

and

$$T^t{}_t\big|_{\rm lin} = T^\rho{}_\rho\big|_{\rm lin}\,, \tag{2.3.27}$$

while

$$T^x{}_x|_{\rm lin} = -\frac{1}{2}V_0 - \frac{1}{2}\dot{V}_0\Phi + \frac{Q_0}{2\bar{a}_1^{d-2}\bar{a}_2^d}\left\{\frac{Q_0}{\bar{a}_1^{d+2}\bar{a}_2^d f_0}\left(1 + \frac{\dot{f}_0}{f_0}\Phi + \frac{4AL}{\bar{a}_1}\right) + 2E\right\}\,, \tag{2.3.28}$$

where $A = A(\rho)$ is a metric perturbation: $a_1 = \bar{a}_1 + L\,A(\rho)$. The form of the metric perturbation equations depends on the background around which we expand. In particular, the analysis differs for AdS_D and $AdS_2 \times \mathbb{R}^d$, so we split the discussion at this point.

Before we do, some quick comments about crossover scales are in order. It is the potential $V(\phi)$ which sets the crossover scales. Using the values of the potential $V_\sharp$ (2.3.20) and $V_\flat$ (2.3.21) required for AdS_D and $AdS_2 \times \mathbb{R}^d$ solutions, and the form of $V(\phi)$ (2.1.28), we find the values of the radial coordinates $\rho_\sharp$ and $\rho_\flat$ where the crossovers occur in the bulk. These values depend on d, the solution parameters z and θ, and the theory parameter η_W through the constants D_1 and D_2 (2.1.16). In the physical range of z and θ, D_1 is positive and D_2 can be positive, negative or zero. In the $AdS_2 \times \mathbb{R}^d$ region,

$$\rho_\flat^{-2\theta/dz} = \begin{cases} -\dfrac{1}{2D_2}\left(D_1 - \sqrt{D_1^2 + 4\dfrac{L^2 D_2}{L_\flat^2}}\right), & \text{if } D_2 \neq 0 \\ \dfrac{L^2}{L_\flat^2 D_1}, & \text{if } D_2 = 0\,. \end{cases}$$

For the AdS_D region,

$$\rho_\sharp^{-2\theta/dz} = \begin{cases} -\frac{1}{2D_2}\left(D_1 - \sqrt{D_1^2 + 4d(d+1)\frac{L^2 D_2}{L_\sharp^2}}\right), & \text{if } D_2 \neq 0 \\ d(d+1)\frac{L^2}{L_\sharp^2 D_1}, & \text{if } D_2 = 0\,. \end{cases}$$

The radial coordinate is dual to the field theory energy scale. Different probes will result in different energy-radius relations. For example, a string [312] stretched from the interior to a radial coordinate ρ results in $E = [z\,d\,L^2/2\pi\alpha'(z\,d - 2\theta)]\rho^{-(1-2\theta/z\,d)}$. Note that for physical values of z and θ (obeying the NEC and $d_{\text{eff}} > 0$), $z\,d - 2\theta$ is positive.

2.3.1 UV crossover

The perturbed AdS_D metric is in conformal gauge

$$ds^2_{AdS_D} = \left\{\frac{L_\sharp}{\rho} + L_\sharp A(\rho)\right\}^2 \left[-dt^2 + d\rho^2 + \{1 + B(\rho)\}^2\, d\vec{x}_d^2\right]\,. \tag{2.3.29}$$

We now expand the curvature squared equations of motion at linear order in perturbations $\{A(\rho), B(\rho), \Phi(\rho), E(\rho)\}$. We obtain for the tt gravity field equation

$$\begin{aligned} 0 = &-4(d-1)\frac{\eta_W}{L_\sharp^2}(\rho^4 B'''') + 8(d-1)(d-2)\frac{\eta_W}{L_\sharp^2}(\rho^3 B''') \\ &+ \left[-d(d+1) - 4(d-1)^2(d-2)\frac{\eta_W}{L_\sharp^2}\right](\rho^2 B'') - d(d+1)(\rho^3 A'') \\ &+ d^2(d+1)(\rho B') + d(d+1)(d-3)(\rho^2 A') + 2d^2(d+1)(\rho A)\,, \end{aligned} \tag{2.3.30}$$

while for $\rho\rho$ we obtain

$$0 = d(\rho B') + (d+1)(\rho^2 A') + 2(d+1)(\rho A)\,, \tag{2.3.31}$$

while for (each) xx we get

$$\begin{aligned} 0 = &+\frac{4(d-1)}{d}\frac{\eta_W}{L_\sharp^2}(\rho^4 B'''') - \frac{8(d-1)(d-2)}{d}\frac{\eta_W}{L_\sharp^2}(\rho^3 B''') \\ &\left[-(d-1)(d+1) + \frac{4(d-1)^2(d-2)}{d}\frac{\eta_W}{L_\sharp^2}\right](\rho^2 B'') - d(d+1)(\rho^3 A'') \\ &+ d(d-1)(d+1)(\rho B') + d(d+1)(d-3)(\rho^2 A') + 2d^2(d+1)(\rho A)\,. \end{aligned} \tag{2.3.32}$$

The linearized Maxwell equation is simple by dint of gauge symmetry,

$$E' - \frac{(d+2)}{\rho} E = 0\,. \tag{2.3.33}$$

The linearized dilaton equation of motion (2.3.9) in the perturbed AdS_D background is also quite simple,

$$\Phi'' - \frac{d}{\rho}\Phi' - \frac{L_\sharp^2}{\rho^2}\ddot{V}_\sharp\,\Phi = 0\,. \tag{2.3.34}$$

The form of our perturbation equations (2.3.30-2.3.34) permits power law solutions of the form

$$\Phi = \breve{\Phi}\rho^{\nu_\Phi}\,, \qquad A = \breve{A}\rho^{\nu_A}\,, \qquad B = \breve{B}\rho^{\nu_B}\,, \qquad E = \breve{E}\rho^{\nu_E}\,, \tag{2.3.35}$$

where $\{\breve{A}, \breve{B}, \breve{\Phi}, \breve{E}\}$ are simple constants, as long as two conditions are satisfied relating the metric indices ν_A, ν_B to ν_Φ,

$$\nu_A = \nu_B - 1\,, \tag{2.3.36}$$

$$\nu_\Phi = \nu_B\,. \tag{2.3.37}$$

The electric field index ν_E is determined by the first order Maxwell equation to be

$$\nu_E = d + 2\,. \tag{2.3.38}$$

In other words, there is only one perturbation of the electric field and it is relevant (growing in the IR). This is in accord with our intuition that Q should evolve from $Q_\sharp = 0$ in the asymptotic AdS_D region, increasing in the interior à la HSV, and eventually levelling out to $Q_\flat$ of the interior $AdS_2 \times \mathbb{R}^d$.

The second order dilaton equation of motion determines the two allowed values of the index ν_Φ,

$$\nu_\Phi^\sharp = \frac{(d+1)}{2} \pm \sqrt{\frac{(d+1)^2}{4} + L_\sharp^2 \ddot{V}_\sharp}\,. \tag{2.3.39}$$

Here, we see two perturbations, one relevant and one irrelevant. This simple equation (2.3.39) is the familiar one from AdS, with $\ddot{V}_\sharp$ playing the role of m^2, as we would expect by consistency.

We must inspect the form of our theory function $V(\phi)$ to check that it gives rise to *real* ν_Φ: we certainly do not want oscillatory solutions indicating a (linearized) instability. We require the term under the square bracket to be non-negative,

$$\frac{(d+1)^2}{4} + L_\sharp^2 \ddot{V}_\sharp \geq 0\,. \tag{2.3.40}$$

Let us check what kind of theory parameters can support real dilaton perturbations. We assume for simplicity that $V(\phi)$ and $f(\phi)$ are monotonic; if not, the story becomes more involved. Because we work within a purely radial ansatz and assume monotonicity of $V(\phi), f(\phi)$, we can find $\ddot{V}$ from our implicit expressions in Section 2.1,

$$\ddot{V} = \left(\frac{d\phi}{dr}\right)^{-3} \left\{ \frac{d^2V}{dr^2}\frac{d\phi}{dr} - \frac{dV}{dr}\frac{d^2\phi}{dr^2} \right\}\,. \tag{2.3.41}$$

Previously, we found that our theory could only support HSV solutions for particular classes of functions $f(\phi), V(\phi)$ whose coefficients are specified by six constants $\{D_1, \ldots, D_6\}$. This eventuates because from the structure of the effective action: there cannot be derivatives of theory functions higher than second order, so to specify $f_0, \dot{f}_0, \ddot{f}_0$, $V_0, \dot{V}_0, \ddot{V}_0$ we will need exactly six variables. Let us collect the relevant facts here about the $\{D_i\}$ that follow from the NEC, causality, and physical d_{eff}. The even numbered constants D_2, D_4, D_6 are the only ones that depend on η_W, and they all depend on it linearly. By virtue of the NEC, D_3, D_4, D_5, D_6 are all positive. Also, in the physical ranges of z and θ, D_1 is positive. The most interesting constant is D_2. It can be positive, negative, or zero, and its behaviour depends strongly on whether or not $d = 2$ or $d > 2$. For $d = 2$, $D_2 = 0$ if $z = 4$ for any θ. For $d > 2$, $D_2 = 0$ if $\theta = -d(dz - z - 2d)/(d - \theta)$ so for positive θ (the physical range) we need $z < 2d/(d-1)$. With all that noted, we now have all the ingredients necessary to rule out tachyons.

Examining $L_\sharp^2 \ddot{V}_\sharp$ in the asymptotic region, we can notice something immediately. It is some constants of order one multiplied by one factor of $\eta_W/L_\sharp^2$, a parameter which must be small. Therefore, in our regime of theory parameters, the Φ perturbation is not in danger of becoming tachyonic because $\eta_W/L_\sharp^2$ is tiny. We must also inspect all positive

powers of r in $L_\sharp^2 \ddot{V}_\sharp$ in the AdS_D regime, to ensure that their coefficient(s) go to zero in the UV region. Having a finite $L_\sharp^2 \ddot{V}_\sharp$ requires

$$D_2 = 0\,. \tag{2.3.42}$$

This requires either

$$d = 2: \quad z = 4\,, \text{any } \theta \in [0, d)\,, \tag{2.3.43}$$

or

$$d > 2: \quad z < \frac{2d}{d-1} \quad \text{for} \quad \theta = \frac{d(2d + z - dz)}{d-2} > 0\,. \tag{2.3.44}$$

This provides serious restrictions on the solution parameters in the physically interesting range. Thirdly, inspecting the constant term in $L_\sharp^2 \ddot{V}_\sharp$, which is now the dominant term at $r \to \infty$, we find that its coefficient is $-(\beta-1)^2[D_1 D_4 + 8 D_2 D_3]$, which is proportional to η_W (and terms of order one) and can be positive, negative, or zero depending on solution parameters. In one special case, $d = 2$, this coefficient also turns out to be zero when $z = 4$, making ν_Φ extremely simple.

Let us now outline the numerical shooting problem. The shooting method is a numerical technique used to solve boundary value problems. The idea is to treat the boundary value problem like an initial value problem; starting at one boundary and "shooting" to the other boundary using an initial value solver until the boundary condition at the other end hits the correct value. In the present case, with the equations of motion being fourth order in B, second order in A, Φ, and first order in E, we would need to specify a set of nine items $\{E, \phi, \phi', A, A', B, B', B'', B'''\}$ to solve an initial value problem. For our perturbation problem, we know the initial conditions for the perturbations (they are all zero), but not their derivatives, leaving five to shoot on numerically. Now, notice that the sum of the tt (2.3.30) and xx (2.3.32) linearized gravity field equations produces an expression for $[(\rho^4 B'''') - 2(d-2)(\rho^3 B''')]$ in terms of B'' and B' only – all the terms involving A'', A', A cancel out (and there were no B terms to begin with). Substituting this back into the tt gravity equation (2.3.30) reduces the order of the linearized differ-

ential equation from four to two. Looking back to the $\rho\rho$ linearized constraint equation (2.3.31), we can see that it is first order in A and B, which fits perfectly. The full non-linear equations are still fourth order, but the dimensionality of the shooting problem is reduced by two: we need to shoot on only *three* derivatives A', B', Φ', just like in Einstein gravity. Note that this simplification will not persist for $AdS_2 \times \mathbb{R}^d$; it is specific to the properties of AdS_D. Finally, to recognize the HSV metric while shooting, we would plot the logs of the metric coefficients and pick off z, θ.

2.3.2 IR crossover

This time the perturbed metric that is appropriate to $AdS_2 \times \mathbb{R}^d$ is

$$ds^2_{AdS_2\times\mathbb{R}^d} = \left\{\frac{L_\flat}{\rho} + L_\flat A(\rho)\right\}^2 \left[-dt^2 + d\rho^2 + \{\rho + B(\rho)\}^2\left(dx^2 + dy^2\right)\right] . \tag{2.3.45}$$

Similarly to the AdS_D case, we expand the curvature squared equations of motion at linear order in perturbations $\{A(\rho), B(\rho), \Phi(\rho), E(\rho)\}$. Note that these functions are not the same as for AdS_D and the linearized perturbation equations will obviously differ. We obtain for the tt equation

$$\begin{aligned} 0 = &+\frac{4(d-1)}{(d+1)}\frac{\eta_W}{L_\flat^2}\left\{(\rho^4 B'''') + (\rho^3 B''')\right\} + \left[d - \frac{4d(d-1)}{(d+1)}\frac{\eta_W}{L_\flat^2}\right]\left\{(\rho^2 B'') - (\rho B')\right\} \\ &+ \left[d - \frac{3d(d-1)(d-2)}{d(d+1)}\frac{\eta_W}{L_\flat^2}\right]\left\{(\rho^4 A'') + 3(\rho^3 A')\right\} \\ &+ \left[1 - \frac{4(d-1)}{(d+1)}\frac{\eta_W}{L_\flat^2}\right]\{dB + (d+2)A\} + f_\flat L_\flat^{d-2}\left[1 - \frac{4(d-1)}{(d+1)}\frac{\eta_W}{L_\flat^2}\right]\mathfrak{E} + \frac{3}{4}\dot{V}_\flat\Phi \end{aligned} \tag{2.3.46}$$

where

$$E(\rho) \equiv \frac{Q_\flat}{L_\flat^4}\mathfrak{E}(\rho) . \tag{2.3.47}$$

Apart from dimensional analysis, all this simple redefinition does is to measure $E(\rho)$ perturbations in units of $Q_\flat$. This is a valid operation for this case of $AdS_2 \times \mathbb{R}^d$, but

would clearly make no sense in AdS_D where $Q_\sharp = 0$. For the $\rho\rho$ gravity equation we get

$$\begin{aligned}0 = &-\frac{4(d-1)}{(d+1)}\frac{\eta_W}{L_\flat^2}(\rho^3 B''') - \frac{8(d-2)(d-1)}{(d+1)}\frac{\eta_W}{L_\flat^2}(\rho^2 B'') \\ &+ \left[-d + \frac{4d(d-1)}{(d+1)}\frac{\eta_W}{L_\flat^2}\right]\{(\rho B') - B\} + \left[-d + \frac{4(d-1)(d-2)}{(d+1)}\frac{\eta_W}{L_\flat^2}\right](\rho^3 A') \\ &+ \left[-(d-2) + \frac{4(d-1)(d-6)}{(d+1)}\frac{\eta_W}{L_\flat^2}\right](\rho^2 A) + f_\flat L_\flat^{d-2}\left[1 - \frac{4(d-1)}{(d+1)}\frac{\eta_W}{L_\flat^2}\right]\mathfrak{E} + \frac{3}{4}\dot{V}_\flat\Phi\end{aligned} \tag{2.3.48}$$

and for the xx equation (identical to the other $x_i\, x_i$ equations) we get

$$\begin{aligned}0 = &-\frac{4(d-1)}{d(d+1)}\frac{\eta_W}{L_\flat^2}(\rho^4 B'''') + \left[(d-1) + \frac{8(d-1)^2}{d(d+1)}\frac{\eta_W}{L_\flat^2}\right]\left\{(\rho^2 B'') - 2(\rho B')\right\} \\ &+ \left[d + \frac{4(d-1)(d-2)}{d(d+1)}\frac{\eta_W}{L_\flat^2}\right]\left\{(\rho^4 A'') + 2(\rho^2 A')\right\} + \left[2(d-1) + \frac{16(d-1)^2}{d(d+1)}\frac{\eta_W}{L_\flat^2}\right]B \\ &+ \left[-4 + \frac{16(d-1)}{(d+1)}\frac{\eta_W}{L_\flat^2}\right](\rho^2 A) + f_\flat L_\flat^{d-2}\left[-1 + \frac{4(d-1)}{(d+1)}\frac{\eta_W}{L_\flat^2}\right]\mathfrak{E} + \frac{1}{4}\dot{V}_\flat\Phi\end{aligned} \tag{2.3.49}$$

The dilaton equation is again second order,

$$(\rho^2\Phi'') - \left\{(L_\flat^2\ddot{V}_\flat) + \frac{2\ddot{f}_\flat}{f_\flat}\left[1 - \frac{4(d-1)}{(d+1)}\frac{\eta_W}{L_\flat^2}\right]\right\}\Phi + \frac{2}{\rho^2}(L_\flat^d\dot{V}_\flat)f_\flat\mathfrak{E} = 0\,, \tag{2.3.50}$$

and the electric perturbation equation is

$$\left(1 - \frac{4\eta_W}{3L_\flat^2}\right)f_\flat\left[-\frac{1}{2}\mathfrak{E}' + \frac{1}{\rho}\mathfrak{E}\right] - \frac{1}{4}(L_\flat^2\dot{V}_\flat)\left[\rho^2\Phi' - 2\rho\Phi\right] = 0\,. \tag{2.3.51}$$

In similar spirit to the case of AdS_D in the previous subsection, the form of the perturbation equations about $AdS_2 \times \mathbb{R}^d$ permits power law solutions of the form

$$\Phi = \breve{\Phi}\rho^{\nu_\Phi}\,, \qquad A = \breve{A}\rho^{\nu_A}\,, \qquad B = \breve{B}\rho^{\nu_B}\,, \qquad \mathfrak{E} = \breve{\mathfrak{E}}\rho^{\nu_E}\,, \tag{2.3.52}$$

where $\{\breve{A}, \breve{B}, \breve{\Phi}, \breve{\mathfrak{E}}\}$ are simple constants, as long as the metric indices ν_A, ν_B are tied to the dilaton index ν_Φ and the electric index ν_E by

$$\nu_A = \nu_B - 2\,, \tag{2.3.53}$$

$$\nu_\Phi = \nu_B - 1\,, \tag{2.3.54}$$

$$\nu_E = \nu_B + 1\,. \tag{2.3.55}$$

For the ν_Φ index, we find

$$\nu_\Phi^\flat = \frac{1}{2} \pm \sqrt{\frac{1}{4} + (L_\flat^2 \ddot{V}_\flat) - 2\frac{\ddot{f}_\flat}{f_\flat}\left(1 - \frac{4\eta_W}{3L_\flat^2}\right) - 2(L_\flat^2 \dot{V}_\flat)\frac{\mathfrak{E}_\flat}{\Phi_\flat}}\,. \tag{2.3.56}$$

Note that $\nu_\Phi^\flat$ depends on three theory function derivatives: $(L_\flat^2 \ddot{V}_\flat)$, $(\ddot{f}_\flat/f_\flat)$, and $(L_\flat^2 \dot{V}_\flat)$, as well as one solution parameter $\mathfrak{E}_\flat/\Phi_\flat$ (via the equation of motion) and the Weyl squared correction parameter η_W. In the previous subsection we already found the condition involving $L_\sharp^2 \ddot{V}_\sharp$ required to keep Φ non-tachyonic in AdS_D. We now examine the two new pieces in order to see if our theory functions and theory parameters can support dilaton perturbations about $AdS_2 \times \mathbb{R}^d$ with real values of ν_Φ. Note that such subtleties did not arise in the magnetic Lifshitz crossovers obtained in [304] in a context without Weyl squared corrections to the gravity sector.

We need to know the sign and magnitude of $-2\ddot{f}_\flat/f_\flat$. Calculating it from the implicit form for $f(\phi)$ from Section (2.1) and going into the $AdS_2 \times \mathbb{R}^d$ region, we find a number of order one regardless of β or α,

$$-2\left.\frac{\ddot{f}_\flat}{f_\flat}\right|_{AdS_2\times\mathbb{R}^d} = -\frac{4}{D_3} < 0\,. \tag{2.3.57}$$

Insisting that this term does not overwhelm the $1/4$ under the square root gives a condition on solution parameters,

$$d^2(z-1) + (16-d)\theta > 16d\,. \tag{2.3.58}$$

This condition is compatible with the conditions we found on the existence of UV crossovers to AdS_D: If $d = 2$, we found that we needed $z = 4$ for an AdS_D crossover, in the IR case, then we need $\theta > 20/14$. For $d > 2$, we find a range of $z > 1$ which falls within that required for the existence of UV AdS_D crossovers.

The last terms under the square root in (2.3.56) is more opaque and interesting because it can compete against the other two terms. We would like to ensure that $(L_\flat^2 \dot{V}_\flat)$ has a consistent sign for all ϕ i.e. for all r. This is important because if $(L_\flat^2 \dot{V}_\flat)$ could be

zero at some r (equivalently, at some ϕ), then the $\mathfrak{E}_\flat/\Phi_\flat$ term could drive the ν_Φ imaginary during the crossover evolution, which would not be physical. Calculating $L_\flat^2\dot{V}_\flat$, we find

$$-2(L_\flat^2\dot{V}_\flat) = +\frac{2\sqrt{2}}{\sqrt{D_3}}(\beta-1)D_1 > 0\,, \tag{2.3.59}$$

because $\beta > 1$ in the physical range of parameters. This holds for all parameters, so it is true as a theory function statement.

Einstein-Weyl gravity can also possess ghost-like excitations. It was shown in [313] that ghost-like excitations about an AdS_4 background can be removed provided that $\eta_W < 0$. Looking back at section 2.2.2, we see that $\eta_W < 0$ can support a range of physically acceptable z and θ for $d \geq 2$.

Our analytical results pinpoint the constraints on the theory functions and the solution parameters z and θ in $D = d + 2$ dimensions necessary to find crossover solutions with an asymptotic AdS_D at the boundary, an intermediate HSV region and an $AdS_2 \times \mathbb{R}^d$ in the interior. It is our hope that these results will be useful for pointing out interesting parameter ranges for which to construct such solutions numerically; we leave this to future work.

So far, we have only explored curvature squared corrections of Weyl type, with dilaton-dependent theory function coefficients. It would be interesting to know if it is possible to find crossovers with dilaton-dependent theory function coefficients for Gauss-Bonnet and R^2 terms as well, although we have not investigated this.

2.4 Summary of findings and outlook

In this chapter, we find hyperscaling violating (HSV) solutions to an Einstein-Maxwell-dilaton model with curvature squared corrections (with constant coefficients) and $f(\phi)$ gauge coupling with dilaton potential $V(\phi)$. We make a simple isotropic, static, spherically symmetric ansatz for the HSV metric, and solve the equations for HSV solution parameters z, θ depending on theory parameters $d, \{\eta_i\}$. From a bottom-up perspective,

insisting on having HSV solutions in this curvature squared model puts conditions on the functions $V(\phi), f(\phi)$.

Generally, the expression for ϕ is a competition between a[n asymptotically] logarithmic piece $\text{arccsch}(a\, r^{2\theta/(d-\theta)})$ and a power law piece, $\sqrt{1+a^2\, r^{2\theta/(d-\theta)}}$, where a is linear in $\{\eta_i\}$ and depends on d, z, θ. From this, we can see immediately that turning off the $\{\eta_i\}$ removes the power law piece and leaves only the log, making $V(\phi) \sim -e^{-b\phi}$, where $b = b(z, \theta, d)$, which is the behaviour previously found with Einstein gravity [212]. With the curvature squared terms turned on, obviously the character of the equations of motion changes, and this alters the dependence on ϕ of the dilaton potential $V(\phi)$, in such a way that we do not recover simple exponentials asymptotically far out: $V(\phi) \sim -c_1\phi^4 - c_2\phi^2$, where $c_i = c_i(d, z, \theta, \{\eta_i\})$. This is a nuance of order of limits. Interestingly, deep in the interior it reduces to a sum of exponentials: $V(\phi) \sim -e^{-2c\phi} - e^{-4c\phi}$, where $c = c(z, \theta, d)$. Now let us comment on the gauge coupling function $f(\phi)$. In the limit that $\{\eta_i\} \to 0$, $f(\phi) \sim e^{-f_1\phi}$, where $f_1 = f_1(z, \theta, d)$. Far out in the geometry, $f(\phi) \sim \phi^{-f_2}$, where $f_2 = f_2(\theta, d)$, while deep in the interior $f(\phi) \sim \infty$, which forces F^2 to zero there.

In section 3 we shift gears to constraining allowed ranges of parameters for HSV solutions by using the null energy condition. The NEC restricts polynomial combinations of solution parameters z, θ (or equivalently α, β) and theory parameters $\{\eta_i\}$. These constraints look opaque at first, so we investigate them graphically in stages of complexity. We first visualize the HSV NEC constraints for single η first, then pairs of η_i, then all three at once.

Weyl: For $d = 1$ the C^2 term does not contribute and the NEC reduces to that of Einstein gravity, as studied in e.g. [14]. For $d = 2$, for $\eta_W > 0$, we find $1 \leq z < 4$, while for $\eta_W < 0$ $z > 4$. (Recall that we do not consider $z < 1$ for causality reasons.) At $z = 4$, η_W is unconstrained: the Weyl term simply does not contribute to the equations of motion. For $d > 2$, qualitatively similar behaviour ensues: the range of z is now θ-dependent. When η_W is positive, we find small z, θ. For negative η_W we find $z > 4$;

which θ are admissible depends on d.

Gauss-Bonnet: For $d = 1$ and $d = 2$, the η_{GB} terms vanish from the equations of motion, as expected because the bulk Gauss-Bonnet action is identically zero for $d = 1$ ($D = 3$) and topological for $d = 2$ ($D = 4$). For $d > 2$, for $\eta_{GB} < 0$, the NEC restrictions are the same as for Einstein gravity, whereas for $\eta_{GB} > 0$, only $z = 1, \theta = 0$ is admissible (plain AdS).

R^2 gravity: For $\eta_R > 0$, only $z = 1, \theta = 0$ is admissible. For $\eta_R < 0$, we find two distinct cases. (a) For $z > 4$, any θ is admissible. (b) For $z < 4$, only some θ are allowed; the curved constraint surface is quartic in θ and cubic in z. There are also two other physical constraints illustrated in the plots: the requirements that (i) $d_{\text{eff}} \equiv d - \theta \geq 0$ and (ii) $\theta \geq 0$, which were motivated from the condensed matter side. They are visible in the plots as planar edges to permissible parameter ranges.

R^2 and Weyl: For R^2 and Weyl, ranges of permissible z, θ arise for all four sign choices of the η_W, η_R parameters. The behaviour changes radically at $z = 4$, for any d. (a) For $z = 4$, we need $\eta_R < 0$. For $d = 2$ only, η_W is unconstrained. For $d > 2$, η_W can be positive or negative depending on η_R. (For $d = 1$, the Weyl tensor vanishes so there is no η_W.) (b) For $z > 4$, η_R must still be negative; η_W can be positive or negative depending on η_R. (c) For $z < 4$, η_R can be positive or negative and η_W can be positive or negative, depending on θ. Positive values of η_R only occur for η_W positive. Also, to have θ take every value between 0 and d requires $\eta_W > 0$, whereas for cases (a) and (b) θ can take any value within its physical range.

R^2 and Gauss-Bonnet: In this case, by having η_R turned on, we can now access values of η_{GB} that were previously off limits. The behaviour of the plots again changes qualitatively at $z = 4$ for any $d \geq 3$. (The cases $d = 1, 2$ are not discussed as the Gauss-Bonnet term vanishes, reducing the pair of parameters to a single one covered previously.) (a) For $z < 4$, both positive and negative η_R and η_{GB} are allowed up to a maximum value of θ less than d. (b) For $z \geq 4$, only $\eta_{GB} < 0$ is allowed and η_R sits

within a restricted range that goes from just above zero to the negative region.

Gauss-Bonnet and Weyl: For $d = 1, 2$ the Gauss-Bonnet term vanishes and we reduce back to the Weyl-only case. We therefore take $d \geq 3$. The behaviour in this case depends on z. (a) $z < 4$: All positive values of η_W are allowed; not all negative values are allowed, the boundary of the range depending on θ. η_{GB} can be positive or negative depending on θ (as well as d, z, of course). (b) $z > 4$: Both η_W and η_{GB} can be positive or negative, with the permissible ranges depending on each other and on θ (as well as d, z, of course).

R^2, Gauss-Bonnet, and Weyl: Having all three curvature squared theory parameters turned on is obviously the most complex case. Consider the full NEC conditions (2.2.20) and (2.2.21) on the constants D_4 and D_6. First, we can examine the terms proportional to η_{GB}. These vanish identically in $d = 1, 2$. Since these terms have factors identical to the factors in the Einstein-only NEC, this implies that when there is only η_{GB} it has to be negative; however, when they are turned on, we can access previously prohibited values of η_{GB}. Second, consider the terms in η_R. The D_6 coefficient vanishes when $z = 4$ in $d = 2$, and can also vanish in $d > 2$ but with z now depending on θ in the physical range. Then the plots would just transition back to the two-parameter case studied in Section 2.2.6. (See above for summary.) The cleanest transition is seen in $d = 2$ but it is similar in higher d. The D_4 coefficient, on the other hand, cannot vanish in the physical range of parameters. Finally, consider the terms in η_W. The D_4 coefficient vanishes when $z = 4$ in $d = 2$; for the same values, D_6 is positive, implying that $\eta_W < 0$. For other z, d, the constraints on η_W are less severe: η_W can take on positive or negative values depending on θ, z, d.

Generally, we see 'features' in the plots of Section 2.2 when particular terms in the curvature squared NEC constraints vanish or change sign. This is most notable when the η_R term is turned on, as its change in behaviour is the cleanest. In all the subsections except 2.2.1, we found that $z = 4$ was a special value dividing different types of behaviours. The overall message is that physically acceptable HSV solutions are supported

for a range of $\{\eta_i\}$ parameters, depending on d and solution parameters z, θ.

In section 2.3 we study the question of crossover solutions between AdS_D near the boundary, HSV in the intermediate region, and $AdS_2 \times \mathbb{R}^d$ in the deep interior. The idea is that the AdS_D completion provides a resolution of the large-r curvature singularity of the HSV space, while the $AdS_2 \times \mathbb{R}^d$ completion provides a resolution to its tidal force singularity at small r. The Weyl corrected Einstein-Maxwell-dilaton theory does support both AdS_D and $AdS_2 \times \mathbb{R}^d$ solutions. By linearizing the equations of motion about those backgrounds, we see that perturbations taking us from either background to HSV require conditions on z, θ, d. For AdS_D the condition is

$$d = 2 : \quad z = 4 \,, \text{any } \theta \in [0, d) \,, \tag{2.4.1}$$

or

$$d > 2 : \quad z < \frac{2d}{d-1} \quad \text{for } \; \theta = \frac{d(2d + z - dz)}{d-2} > 0 \,. \tag{2.4.2}$$

For $AdS_2 \times \mathbb{R}^d$, we find an additional conditions on z, θ,

$$d^2(z-1) + (16-d)\theta > 16d \tag{2.4.3}$$

It is possible to satisfy *both* conditions for a range of physically sensible z, θ of order one.

A natural question to ask would be how to generalize our results to other systems with hyperscaling violation. We focused here on the electric ansatz; it would be interesting to know what might change with using instead a magnetic or (in $d = 2$) even a dyonic ansatz. Another interesting direction would be to consider models with more complicated ansatze, such as those with Bianchi type symmetries in the boundary directions as in [249]. It is also important to work out how such bottom-up constructions might mesh with supergravity/string embedding, as in e.g. [314].

Entanglement entropy S_{EE} is interesting because it provides a non-local probe in general AdS/CFT contexts which is different in character from Wilson loops. Calculating S_{EE} from field theory is notoriously difficult, but when the gravity dual is described by

Einstein gravity with matter it can be calculated holographically via the Ryu-Takayanagi (RT) formula [22]. The RT formula calculates the area of the minimal surface which extends into the bulk and is homologous to the entangling region on the boundary. For HSV solutions in Einstein gravity, S_{EE} displays logarithmic violations of the area law, as expected for condensed matter systems with Fermi surfaces [14].

For general $\{\eta_{GB}, \eta_W, \eta_R\}$ curvature squared corrections, the formula for the entanglement entropy is not yet known (see [91], [92], [93] and [94] for recent progress along these lines), except for the sub-case where only η_{GB} is turned on. In [90], a generalization of the Ryu-Takayanagi formula to Lovelock gravity was proposed. The entanglement entropy for our HSV solutions with η_{GB} turned on can in principle be computed from the S_{EE} formula in [90]. In $d = 2$, relevant for condensed matter, because the the η_{GB} term is topological, it does not contribute in the equations of motion, so it should yield the same result as for Einstein gravity. It would be interesting to do the explicit (hard) computation using [90] of the entanglement entropy in this case to check explicitly. Physically, the important question to resolve is whether or not there are log violations in S_{EE} for HSV solutions in gravity theories with curvature squared corrections. Recently, partial progress towards answering this question was provided in [315]. Evidence is found for a new divergent term, on top of the usual logarithmic term from Einstein gravity, for R^2, Gauss-Bonnet and $R_{\mu\nu}R^{\mu\nu}$ curvature squared corrections. The proposals for the gravity functionals whose extremization give the extremal surfaces needed to compute the entanglement entropy in these theories are used. Actually computing the minimal surfaces is difficult, so a near boundary analysis is performed in order to extract the new divergent terms in all cases. The analysis is only reliable when the curvature square corrections die off near the boundary, which occurs for $\theta < 0$. The extension to the case $\theta > 0$ is discussed, but results are incomplete.

Chapter 3

Perturbatively charged holographic disorder

This chapter studies a model of perturbative holographic disorder. The results presented here were first reported in [285], written in collaboration with Amanda W. Peet.

The AdS/CFT correspondence has proven to be a remarkably powerful tool for probing the detailed structure of strongly coupled quantum field theories. Its broad list of successes includes applications to modelling the quark-gluon plasma, condensed matter phenomena such as superconductivity, and even fluid dynamics. Comprehensive reviews of these subjects include, [101], [137] and [127], respectively.

An underlying theme to this progress is the reduction of symmetry in holographic models. Systems which possess too many symmetries display behaviours that are not desirable in condensed matter models, a prime example being the infinite DC conductivity dual to the Reissner-Nordström-AdS ($RN-AdS$) geometry. This is not a surprising feature. The underlying $RN-AdS$ geometry possesses translational invariance along the boundary directions. This means that the charge carriers in the dual theory have no means by which to dissipate momentum, resulting in an infinite DC conductivity. Realistic condensed matter systems do not display this behaviour, so if a holographic

model is going to be useful for studying these kinds of problems, we need a way to break translational invariance.

Several avenues of investigation have been carried out, including explicit holographic lattices: [251], [252], [162], [254], [255], [256], [258], [259], Q-lattices: [291], [292], [293] and breaking diffeomorphism invariance: [286], [287], [316], [317], [318], [288], [289], [290]. Other examples of holographic symmetry breaking include the breaking of rotational symmetry [245], [249], [246], [248], [247], relativistic symmetry [163], [167], [164] and hyperscaling violation [165], [166], [14], [212]. Our focus will be on disorder. Within the context of bottom-up modelling, we will report here on a perturbative construction of holographic disorder. That is, we will seek a particular spacetime solution that is sourced by a disordered, randomly fluctuating field in the dual theory and use it to study the dual DC conductivity.

Disorder is a common feature in real world condensed matter systems, but it is difficult to model using traditional field theory approaches: little is known at strong coupling. This is especially true in the context of localization. It is well known that in a non-interacting system, the addition of disorder can completely suppress conductivity [266]; for a comprehensive review, see [267]. Turning on interactions complicates the situation and many-body localization may occur [319]; a review may be found in [268]. Experimental studies of many-body localization are also in their infancy. Since holography is a strong-weak equivalence, it provides a potential way forward for studying disorder. Understanding what the gravity dual tells us about localization might even provide a definition of many body localization. Exactly what this would look like in a gravitational theory and how the bulk fields would behave is an open and interesting question.

Several approaches to disorder within holography have been proposed and were discussed in section 1.5.8. Early studies were presented in [269], [270] and [273]. The replica trick for disordered CFTs was extended to holography in [271] and later in [272].

To fully see the effect of quenched random disorder, [274] proposed that disorder

should be modelled by applying random boundary conditions to a bulk field and allowing the field to backreact on the geometry. The source of the disorder is characterized by a distribution over random functions and the system is assumed to be self-averaging. In this construction, the entire distribution runs with the energy scale. To this end, [274] and later [275], worked to construct a holographic functional renormalization scheme so that disorder averaged thermodynamic quantities could be computed.

In [276], a particular background which is already deformed away from AdS, but still satisfies the null energy condition, is considered. By studying the level statistics associated with a probe scalar field, a transition is observed between an initial distribution and a Poisson distribution as the amount of disorder is increased in the system. This is analogous to what happens in a disorder driven metal-insulator transition.

More recently, [277] applied a spectral approach to modelling disorder in a holographic superconductor. The basic idea is similar to [274] where the disorder is sourced by a random space-dependent chemical potential by setting the boundary condition on a bulk $U(1)$ gauge field. In this proposal, the chemical potential takes the form (1.5.25), which is repeated here for convenience,

$$\mu(x) = \mu_0 + \overline{V} \sum_{k=k_0}^{k_*} \sqrt{S_k} \cos(kx + \delta_k) \,. \tag{3.0.1}$$

Recall that S_k is a function of the momenta k which controls the correlation function for $\mu(x)$; different choices of S_k lead to a different values of the disorder distribution average. $\overline{V}$ is a parameter which sets the strength of the disorder. k_0 and k_* define an IR and UV length scale cutoff for the disorder, respectively. δ_k is a random phase for each value of k. A spectral representation like this is known to simulate a stochastic process when k_* is large [278].

The dirty chemical potential (3.0.1) is incorporated into an Einstein-Maxwell model. The Maxwell equations are solved numerically in a fixed AdS-Schwarzschild background with an electric ansatz for the gauge field. The boundary condition is set so that A_t

approaches (3.0.1) near the boundary. Evidence is found for an enhancement of the critical temperature of the superconductor for increasing disorder strength. Evidence that localization occurs in this model was found numerically in [279]. This model has also been extended to holographic p-wave superconductors in [280] where the same behaviour of the critical temperature with disorder strength was observed.

There is a resemblance between this spectral approach to disorder and the construction of a holographic ionic lattice in [162] and [320] where the lattice is set up by a periodic boundary chemical potential. The difference is that for a holographic lattice, there is only a single periodic source of a fixed wavelength. In the spectral approach to disorder, there is a sum over periodic sources of arbitrary wavelength, so the effect of disorder may resonate more strongly throughout the entire bulk geometry, having non-trivial effects deep in the interior.

Recently, [281] applied a spectral approach to modelling disorder sourced by a scalar field in $2+1$ bulk dimensions. The initial clean geometry in this case is AdS_3 and the scalar field is allowed to backreact on the geometry in the spirit of [274]. By treating the disorder strength as a perturbative handle, a second order analytic solution for the backreacted geometry is obtained. It is observed that the disorder averaged geometry, in the deep interior, takes the form of a Lifshitz metric with a dynamical critical exponent z set by the disorder strength. Strong disorder is approached numerically and these solutions also display Lifshitz behaviour. This analysis is extended to finite temperature geometries in [282] where it is found that the interior Lifshitz scaling persists. A similar implementation of scalar disorder was used in [283] and [284] to study the conductivity of holographic strange metals with weak quenched disorder.

In [258], it was shown that a wide variety of inhomogeneous IR geometries arise as solutions to Einstein-Maxwell theory with a single periodic source at the boundary. These observations suggest that studying disordered boundary potentials in Einstein-Maxwell theory at both zero and finite net charge density may lead to novel gravitational solutions

and insight into disordered condensed matter systems.

Our goal here is to study charged disorder with backreaction. As we will see, the general problem for a system with baseline charge density is very complicated. Accordingly, we study the story perturbatively. We build in the disorder the same way as [277], [280], with a randomly varying boundary chemical potential, and we also include backreaction. In the bulk, this corresponds to having a fluctuating gauge field and letting it backreact on the initially clean AdS geometry. We then solve the Einstein equations perturbatively in the strength of the disorder and construct an analytic, asymptotically AdS, solution. Similar to the case of scalar disorder studied in [281], the disorder averaged geometry contains unphysical secular terms (terms which grow without bound) which diverge in the deep interior. We explain how these divergences may be tamed and ultimately find a well behaved averaged geometry.

Our primary interest is in investigating the transport properties dual to the disordered geometry. Adapting a technique first developed in [292], we directly calculate the disorder averaged DC conductivity. We find a correction to the conductivity dual to pure AdS starting at second order in the disorder strength which scales inversely with the smallest wavenumber k_0 in the disordered chemical potential. We will also discuss extensions to systems with finite charge density.

Holographic momentum dissipation and disorder has also been approached within the context of massive gravity. See [294], [295], [296], [297], [298], [299], and [300]. While this approach will not be our primary focus here, it will nevertheless be interesting to understand how results within massive gravity mesh with explicit implementations of holographic disorder.

This chapter is organized as follows. In section 3.1 we construct a bottom-up, disordered, holographic spacetime analytically. Using the strength of the disorder as a perturbative handle, we solve the bulk equations of motion up to second order. Using a Gaussian distribution for the disorder source, we explicitly evaluate the disorder average

of the backreacted solution. In section 3.2, we implement a resummation procedure for removing spurious secular terms which develop in the disorder averaged geometry as a result of our perturbative expansion. With the regulated solution in hand, we study the resultant DC conductivity in section 3.3. Section 3.4 points out some features of incorporating disorder in a geometry with an initial charge density. We point out how techniques used to study transport properties of holographic lattices may be used to access the DC conductivity in the finite charge case. Finally, in section 3.5 we summarize our findings and comment on possible directions for future work.

3.1 Perturbatively charged disorder

We are interested in studying the effect of a disordered holographic lattice, with the ultimate goal of understanding transport properties like conductivity in the dual model. To this end, we start with a gauge field in the $D = d + 1$ dimensional bulk and then introduce a random perturbation around the initially clean baseline solution. The model is then Einstein-Maxwell gravity

$$S = \frac{1}{16\pi G_N}\int d^{d+1}x\sqrt{-g}\left(R + \frac{d(d-1)}{L^2} - \frac{1}{4}F^2\right) . \tag{3.1.1}$$

Note that since we want an asymptotically AdS solution, we have set the cosmological constant to $\Lambda = -d(d-1)/2L^2$, where L is the AdS radius. The equations of motion we need to solve are then the Einstein and Maxwell equations. In what follows, it will be convenient to work with the traced Einstein equations. That is we need to solve

$$R_{\mu\nu} + \frac{d}{L^2}g_{\mu\nu} = \frac{1}{2}\left(F^{\sigma}_{\mu}F_{\nu\sigma} - \frac{1}{2(d-1)}g_{\mu\nu}F^2\right) , \tag{3.1.2}$$

$$\nabla_{\mu}F^{\mu\nu} = 0 . \tag{3.1.3}$$

We consider a system where the initial charge density is zero. In this case, the baseline solution is just AdS_{d+1} with $A_t = 0$. That is, the initially clean (no disorder) background

is

$$ds^2 = \frac{L^2}{r^2}\left(-dt^2 + dr^2 + dx_i^2\right) , \tag{3.1.4}$$

where the boundary is at $r = 0$ in these coordinates. To introduce disorder, we will perturb about this background by turning on the gauge field. To get a tractable system, we will introduce disorder along only one of the boundary direction x. According to the holographic dictionary, near the boundary, the time component of the gauge field behaves like

$$A_t(x, r) = \mu(x) + \rho(x) r^{d-2} + \cdots , \tag{3.1.5}$$

where $\mu(x)$ is the chemical potential and $\rho(x)$ is related to the charge density of the dual theory. We source the disorder by taking the chemical potential to be a sum of periodic functions with random phases using a spectral representation

$$\mu(x) = \overline{V} \sum_{n=1}^{N-1} A_n \cos(k_n x + \theta_n) . \tag{3.1.6}$$

Here, $\overline{V}$ is a constant which controls the strength of the disorder which we will use as a perturbative handle. Similar profiles for the gauge field have been studied in the context of disordered holographic superconductors in [277], [279], [280]. A spectral representation for scalar disorder was used in [281]. The wavenumbers $k_n = n\Delta k$ are evenly spaced with $\Delta k = k_0/N$. $1/k_0$ is thought of as a short distance cutoff for the disorder and is held fixed so that in the limit that $N \to \infty$, $\Delta k \to 0$. The θ_n are random angles that are assumed to be uniformly distributed in $[0, 2\pi]$. The amplitudes are

$$A_n = 2\sqrt{S(k_n)\Delta k} , \tag{3.1.7}$$

where $S(k_n)$ controls the correlation functions. Since the θ_n are uniformly distributed, averaging over them (the disorder average) is done simply by taking

$$\langle f \rangle_D = \lim_{N\to+\infty} \int \prod_{i=1}^{N-1} \frac{d\theta_i}{2\pi} f . \tag{3.1.8}$$

If the function $S(k_n)$ is taken to be 1, this leads to $\mu(x)$ describing Gaussian noise. In other words, by explicit calculation, we have that

$$\langle \mu(x) \rangle_D = 0 \,, \quad \langle \mu(x_1)\mu(x_2) \rangle_D = \overline{V}^2 \delta(x_1 - x_2) \,. \tag{3.1.9}$$

The gauge field A_t sources the disorder in the system, which means that it contributes at order $\overline{V}$. This in turn implies that the right hand side of the traced Einstein equations (3.1.2) start contributing at second order in the disorder strength. Only Maxwell's equations receive any corrections at first order in the disorder strength, so we can solve for A_t in the clean AdS background. The solution which obeys the boundary condition (3.1.6) at $r = 0$ is

$$A_t(r,x) = \overline{V} \sum_{n=1}^{N-1} \frac{A_n k_n^{(d-2)/2}}{2^{(d-4)/2}\Gamma(\frac{d-2}{2})} r^{(d-2)/2} K_{(d-2)/2}(k_n r) \cos(k_n x + \theta_n) \,, \tag{3.1.10}$$

where $K_{(d-2)/2}(k_n r)$ is the modified Bessel function of the second kind. Since A_t is now a function of x, the Maxwell equation involves both F_{rt} and F_{xt}. Notice, by turning on disorder, we went from a solution that had zero charge density to one that has a finite charge density. We can compute this in the dual theory: it is $\langle J^t \rangle$, i.e. the expectation value of the current density. The result is

$$\langle J^t \rangle = -\frac{(d-2)\overline{V} L^{d-3}}{8\pi G_N} \sum_{n=1}^{N-1} \frac{A_n k_n^{d-2}}{2^{d-1}} \frac{\Gamma((2-d)/2)}{\Gamma((d-2)/2)} \cos(k_n x + \theta_n) \,. \tag{3.1.11}$$

Note, this formula is valid when $(2-d)/2$ is not a negative integer (which will be the case in what follows). Now, we can plug the solution for A_t back into the traced Einstein equations and work out the metric corrections at second order in $\overline{V}$. This is generally difficult to do in arbitrary dimensions. We will focus on the case with $D = 4$, in this way the dual to the initially clean geometry is a $2+1$ dimensional CFT. We need an ansatz for the backreacted metric. Since we are adding a perturbation in the x direction only, the metric coefficients could generally depend on both the radial direction r and the boundary direction x. Furthermore, we insist that the geometry is asymptotically

AdS and we will work within Fefferman-Graham gauge [321]. At the end of the day, this means that the general form of the backreacted metric is

$$ds^2 = \frac{L^2}{r^2}\left(-\alpha(x,r)dt^2 + dr^2 + \eta(x,r)dx^2 + \delta(x,r)dy^2\right) , \tag{3.1.12}$$

where the functions $\alpha(x,r)$, $\eta(x,r)$ and $\delta(x,r)$ need to be solved for. We solve for them in a perturbative expansion

$$\begin{aligned}\alpha(x,r) &= 1 + \overline{V}^2\alpha_2(x,r) + \cdots \\ \eta(x,r) &= 1 + \overline{V}^2\eta_2(x,r) + \cdots \\ \delta(x,r) &= 1 + \overline{V}^2\delta_2(x,r) + \cdots ,\end{aligned}$$

so to second order we solve for $\alpha_2(x,r)$, $\eta_2(x,r)$ and $\delta_2(x,r)$. The traced Einstein equations (3.1.2) expanded to second order give the following set of equations for the metric coefficient:

$$-2r\partial_r\delta_2 + 2r^2\partial_x^2\alpha_2 - 2r\partial_r\eta_2 + 2r^2\partial_r^2\alpha_2 - 6r\partial_r\alpha_2 = \frac{r^4}{L^2}\left[(\partial_r H)^2 + (\partial_x H)^2\right] , \tag{3.1.13}$$

$$-2r^2\partial_r^2\delta_2 + 2r\partial_r\eta_2 + 2r\partial_r\alpha_2 - 2r^2\partial_r^2\alpha_2 - 2r^2\partial_r^2\eta_2 + 2r\partial_r\delta_2 = -\frac{r^4}{L^2}\left[(\partial_r H)^2 - (\partial_x H)^2\right] , \tag{3.1.14}$$

$$\partial_r\partial_x(\alpha_2 + \delta_2) = \frac{r^2}{L^2}(\partial_r H)(\partial_x H) , \tag{3.1.15}$$

$$6r\partial_2\eta_2 + 2r\partial_r\alpha_2 + 2r\partial_r\delta_2 - 2r^2\partial_x^2\alpha_2 - 2r^2\partial_x^2\delta_2 - 2r^2\partial_r^2\eta_2 = \frac{r^4}{L^2}\left[(\partial_r H)^2 - (\partial_x H)^2\right] , \tag{3.1.16}$$

$$2r\partial_r\eta_2 + 2r\partial_r\alpha_2 + 6r\partial_r\delta_2 - 2r^2\partial_r^2\delta_2 - 2r^2\partial_x^2\delta_2 = \frac{r^4}{L^2}\left[(\partial_r H)^2 + (\partial_x H)^2\right] , \tag{3.1.17}$$

where $H = H(x,r)$ such that $A_t = \overline{V}H(x,r)$ is the solution to the Maxwell equations at first order (3.1.10).

3.1.1 Second order solution

By using combinations of equations (3.1.13)-(3.1.17), we can solve for $\alpha_2(x,r)$, $\eta_2(x,r)$ and $\delta_2(x,r)$. The solutions are:

$$\begin{aligned}
\alpha_2(x,r) &= \frac{1}{2}H_1(x) + \frac{1}{2}c_1 + \frac{1}{2}c_2 r^3 - \frac{1}{16L^2}\sum_{n=1}^{N-1}\frac{A_n^2}{k_n^2} + \frac{1}{32L^2}\sum_{n=1}^{N-1}\frac{A_n^2}{k_n^2}(2k_n^2r^2+2k_nr+1)e^{-2k_nr} \\
&+ \frac{1}{16L^2}\sum_{n=1}^{N-1}\frac{A_n^2}{k_n^2}(2k_n^2r^2+2k_nr+1)\exp(-2k_nr)\cos^2(k_nx+\theta_n) \\
&+ \frac{1}{8L^2}\sum_{n=1}^{N-1}\sum_{m=1}^{n-1}\frac{A_nA_m}{k_nk_m}\left[1+(k_n+k_m)r+2k_nk_mr^2\right]e^{-(k_n+k_m)r}\cos((k_n-k_m)x+\theta_n-\theta_m) \\
&- \frac{1}{8L^2}\sum_{n=1}^{N-1}\sum_{m=1}^{n-1}\frac{A_nA_m}{k_nk_m}\left[1+(k_n-k_m)r\right]e^{-(k_n-k_m)r}\cos((k_n-k_m)x+\theta_n-\theta_m) \\
&+ \frac{1}{2L^2}\sum_{n=1}^{N-1}\sum_{m=1}^{n-1}\frac{A_nA_mk_nk_m}{(k_n+k_m)^4}\left[(k_n+k_m)^2r^2+2(k_n+k_m)r+2\right]e^{-(k_n+k_m)r} \\
&\qquad\times\cos((k_n+k_m)x+\theta_n+\theta_m)\,,
\end{aligned}$$

$$\begin{aligned}
\delta_2(x,r) &= \frac{1}{2}H_1(x) + \frac{1}{2}c_1 + \frac{1}{2}c_2 r^3 + \frac{1}{16L^2}\sum_{n=1}^{N-1}\frac{A_n^2}{k_n^2} - \frac{3}{32L^2}\sum_{n=1}^{N-1}\frac{A_n^2}{k_n^2}(2k_n^2r^2+2k_nr+1)e^{-2k_nr} \\
&+ \frac{1}{16L^2}\sum_{n=1}^{N-1}\frac{A_n^2}{k_n^2}(2k_n^2r^2+2k_nr+1)\exp(-2k_nr)\cos^2(k_nx+\theta_n) \\
&- \frac{1}{8L^2}\sum_{n=1}^{N-1}\sum_{m=1}^{n-1}\frac{A_nA_m}{k_nk_m}\left[1+(k_n+k_m)r+2k_nk_mr^2\right]e^{-(k_n+k_m)r}\cos((k_n-k_m)x+\theta_n-\theta_m) \\
&+ \frac{1}{8L^2}\sum_{n=1}^{N-1}\sum_{m=1}^{n-1}\frac{A_nA_m}{k_nk_m}\left[1-(k_n-k_m)r\right]e^{-(k_n-k_m)r}\cos((k_n-k_m)x+\theta_n-\theta_m) \\
&+ \frac{1}{2L^2}\sum_{n=1}^{N-1}\sum_{m=1}^{n-1}\frac{A_nA_mk_nk_m}{(k_n+k_m)^4}\left[(k_n+k_m)^2r^2+2(k_n+k_m)r+2\right]e^{-(k_n+k_m)r} \\
&\qquad\times\cos((k_n+k_m)x+\theta_n-\theta_m)
\end{aligned}$$

$$\eta_2(x,r) = \frac{1}{4}r^2\partial_x^2 H_1(x) - c_2 r^3 + H_3(x) - \frac{1}{32L^2}\sum_{n=1}^{N-1}\frac{A_n^2}{k_n^2}(2k_n r+1)\exp(-2k_n r)$$
$$+\frac{1}{16L^2}\sum_{n=1}^{N-1}\frac{A_n^2}{k_n^2}(2k_n r+1)\exp(-2k_n r)\cos^2(k_n x+\theta_n)$$
$$+\frac{1}{L^2}\sum_{n=1}^{N-1}\sum_{m=1}^{n-1}\frac{A_n A_m k_n k_m}{(k_n+k_m)^4}\left[(k_n+k_m)r+1\right]\exp(-(k_n+k_m)r)\cos((k_n+k_m)x+\theta_n+\theta_m)\,,$$

where c_1 and c_2 are constants and $H_1(x)$ and $H_3(x)$ are arbitrary functions of x. The solution for the metric coefficient in the x direction, $\eta_2(x,r)$, is the simplest, as the equations of motion (3.1.13)-(3.1.17) can be arranged to give a first order differential equation for $\eta_2(x,r)$.

We want a solution that is asymptotically AdS as $r \to 0$ and is regular in the interior. The former condition is tantamount to insisting that $\alpha_2(x,0) = \eta_2(x,0) = \delta_2(x,0)$ so that the metric takes on the correct asymptotically AdS form in Fefferman-Graham gauge. Imposing these conditions fixes $c_2 = 0$ and $H_1(x) = \text{const}$ and $H_3(x) = \text{const}$. The solutions for $\alpha_2(x,r)$, $\eta_2(x,r)$ and $\delta_2(x,r)$ which are asymptotically AdS are regular in the interior are:

$$\alpha_2(x,r) = \frac{1}{2}c - \frac{1}{16L^2}\sum_{n=1}^{N-1}\frac{A_n^2}{k_n^2} + \frac{1}{32L^2}\sum_{n=1}^{N-1}\frac{A_n^2}{k_n^2}(2k_n^2r^2+2k_n r+1)\exp(-2k_n r)$$
$$+\frac{1}{16L^2}\sum_{n=1}^{N-1}\frac{A_n^2}{k_n^2}(2k_n^2r^2+2k_n r+1)\exp(-2k_n r)\cos^2(k_n x+\theta_n)$$
$$+\frac{1}{8L^2}\sum_{n=1}^{N-1}\sum_{m=1}^{n-1}\frac{A_n A_m}{k_n k_m}\left[1+(k_n+k_m)r+2k_n k_m r^2\right]e^{-(k_n+k_m)r}\cos((k_n-k_m)x+\theta_n-\theta_m)$$
$$-\frac{1}{8L^2}\sum_{n=1}^{N-1}\sum_{m=1}^{n-1}\frac{A_n A_m}{k_n k_m}\left[1+(k_n-k_m)r\right]e^{-(k_n-k_m)r}\cos((k_n-k_m)x+\theta_n-\theta_m)$$
$$+\frac{1}{2L^2}\sum_{n=1}^{N-1}\sum_{m=1}^{n-1}\frac{A_n A_m k_n k_m}{(k_n+k_m)^4}\left[(k_n+k_m)^2r^2+2(k_n+k_m)r+2\right]e^{-(k_n+k_m)r}$$
$$\times\cos((k_n+k_m)x+\theta_n+\theta_m)\,,$$

$$\delta_2(x,r) = \frac{1}{2}c + \frac{1}{16L^2}\sum_{n=1}^{N-1}\frac{A_n^2}{k_n^2} - \frac{3}{32L^2}\sum_{n=1}^{N-1}\frac{A_n^2}{k_n^2}(2k_n^2r^2+2k_nr+1)\exp(-2k_nr)$$
$$+ \frac{1}{16L^2}\sum_{n=1}^{N-1}\frac{A_n^2}{k_n^2}(2k_n^2r^2+2k_nr+1)\exp(-2k_nr)\cos^2(k_nx+\theta_n)$$
$$- \frac{1}{8L^2}\sum_{n=1}^{N-1}\sum_{m=1}^{n-1}\frac{A_nA_m}{k_nk_m}\left[1+(k_n+k_m)r+2k_nk_mr^2\right]e^{-(k_n+k_m)r}\cos((k_n-k_m)x+\theta_n-\theta_m)$$
$$+ \frac{1}{8L^2}\sum_{n=1}^{N-1}\sum_{m=1}^{n-1}\frac{A_nA_m}{k_nk_m}\left[1-(k_n-k_m)r\right]e^{-(k_n-k_m)r}\cos((k_n-k_m)x+\theta_n-\theta_m)$$
$$+ \frac{1}{2L^2}\sum_{n=1}^{N-1}\sum_{m=1}^{n-1}\frac{A_nA_mk_nk_m}{(k_n+k_m)^4}\left[(k_n+k_m)^2r^2+2(k_n+k_m)r+2\right]e^{-(k_n+k_m)r}$$
$$\times\cos((k_n+k_m)x+\theta_n-\theta_m)\,,$$

$$\eta_2(x,r) = c - \frac{1}{32L^2}\sum_{n=1}^{N-1}\frac{A_n^2}{k_n^2}(2k_nr+1)\exp(-2k_nr)$$
$$+ \frac{1}{16L^2}\sum_{n=1}^{N-1}\frac{A_n^2}{k_n^2}(2k_nr+1)\exp(-2k_nr)\cos^2(k_nx+\theta_n)$$
$$+ \frac{1}{L^2}\sum_{n=1}^{N-1}\sum_{m=1}^{n-1}\frac{A_nA_mk_nk_m}{(k_n+k_m)^4}\left[(k_n+k_m)r+1\right]\exp(-(k_n+k_m)r)\cos((k_n+k_m)x+\theta_n+\theta_m)\,,$$

where c is a constant. The fact that an asymptotically AdS solution exists was to be expected as in $d+1=4$ dimensions, the gauge field which encodes the disorder sources a relevant operator in the dual theory. Geometrically, the gauge field falls off sufficiently fast as $r\to 0$ so that it does not disrupt the asymptotic form of the metric.

3.1.2 Disorder average

The solutions we have found for $\alpha_2(x,r)$, $\eta_2(x,r)$ and $\delta_2(x,r)$ simplify considerably under disorder averaging. Using (3.1.8), we average over the random angles θ_n. The resulting

sums may be expressed in terms of special functions

$$\langle \alpha_2 \rangle_D = \lim_{N\to+\infty} \left\{ \frac{1}{2}c - \frac{1}{4k_0L^2}\left[NH^{(2)}_{(N-1)} + 2k_0 r \ln(1-\exp(-2k_0 r/N)) \right.\right. \tag{3.1.18}$$
$$+2k_0 r \exp(-2k_0 r)\Phi(\exp(-2k_0 r/N),1,N) - NLi_2\left[\exp(-2k_0 r/N)\right]\Big]$$
$$\left.\left. + \frac{2k_0^2 r^2}{N}\frac{\exp(-2k_0 r(N-1)/N)-1}{\exp(2k_0 r/N)-1} + N\exp(-2k_0 r)\Phi(\exp(-2k_0 r/N),2,N) \right\},$$

$$\langle \delta_2 \rangle_D = \lim_{N\to+\infty} \left\{ \frac{1}{2}c + \frac{1}{4k_0L^2}NH^{(2)}_{(N-1)} - \frac{1}{4k_0L^2}\left[-2k_0 r \ln(1-\exp(-2k_0 r/N)) \right.\right. \tag{3.1.19}$$
$$-2k_0 r \exp(-2k_0 r)\Phi(\exp(-2k_0 r/N),1,N) + NLi_2\left[\exp(-2k_0 r/N)\right]\Big]$$
$$\left.\left. - \frac{2k_0^2 r^2}{N}\frac{\exp(-2k_0 r(N-1)/N)-1}{\exp(2k_0 r/N)-1} - N\exp(-2k_0 r)\Phi(\exp(-2k_0 r/N),2,N) \right\},$$

$$\langle \eta_2 \rangle_D = c \tag{3.1.20}$$

where $H^{(2)}_{(N-1)} = \sum_{n=1}^{N-1}\frac{1}{n^2}$ is the generalized harmonic number, $Li_2(z) = \sum_{n=1}^{\infty}\frac{z^n}{n^2}$ is the polylogarithm of index 2 and $\Phi(z,a,b) = \sum_{n=0}^{\infty}\frac{z^n}{(b+n)^a}$ is the Lerch Phi function. By taking the large N limit, the above expressions are found to be finite and give

$$\langle \alpha_2 \rangle_D = \frac{1}{2}c + \frac{1}{4k_0L^2}(1-k_0 r) - \frac{1}{4k_0L^2}(1-k_0 r)\exp(-2k_0 r)\,, \tag{3.1.21}$$

$$\langle \delta_2 \rangle_D = \frac{1}{2}c - \frac{1}{4k_0L^2}(1-k_0 r) + \frac{1}{4k_0L^2}(1-k_0 r)\exp(-2k_0 r)\,, \tag{3.1.22}$$

$$\langle \eta_2 \rangle_D = c\,, \tag{3.1.23}$$

The disorder averaged solutions $\langle \alpha_2 \rangle_D$ and $\langle \delta_2 \rangle_D$ are divergent in the interior of the geometry as $r \to \infty$. Since the gauge field which sources the disorder is a relevant perturbation, this is not surprising. In order to have a finite solution in the interior, we should resum the perturbative solution in the spirit of the Poincaré-Lindstedt method for removing secular terms (terms that grow without bound) in perturbative solutions to differential equations. This kind of situation was also encountered in the case of scalar disorder studied in [281].

3.2 Resummation of disordered solution

We have seen that the disorder averaged metric coefficients $\langle\alpha_2\rangle_D$ (3.1.21) and $\langle\delta_2\rangle_D$ (3.1.22) diverge in the deep interior as $r \to \infty$ due to the presence of secular terms. This indicates a breakdown in the perturbative scheme and needs to be corrected. This outcome was not totally unexpected, as a similar sort of divergence in one of the disorder averaged metric components was found [281]. This divergence was corrected by resumming the disordered solution in the spirit of the Poincaré-Lindstedt method. We will adapt this technique to our problem and see that a resummed solution, which has $\langle\alpha_2\rangle_D$ and $\langle\delta_2\rangle_D$ finite in the deep interior, is available.

The procedure is as follows. We look for additional terms that could contribute at the correct order in the disorder strength, $\overline{V}^2$, as they should only correct the unphysical secular terms in the disorder averaged metric. Furthermore, these new terms must not violate the asymptotically AdS condition imposed on the uncorrected disordered geometry. The simplest ansatz then for corrected backreacted metric in Fefferman-Graham coordinates is

$$ds^2 = \frac{L^2}{r^2}\left[-\frac{\alpha(x,r)}{\beta_1(r)^{W(\overline{V})}}dt^2 + dr^2 + \eta(x,r)dx^2 + \frac{\delta(x,r)}{\beta_2(r)^{P(\overline{V})}}dy^2\right]. \tag{3.2.1}$$

The new functions $\beta_1(r)$ and $\beta_2(r)$ may be chosen to remove the secular terms in $\langle\alpha_2\rangle_D$ and $\langle\delta_2\rangle_D$. Hence, they should only contribute starting at second order. Their exponents, then, $W(\overline{V})$ and $P(\overline{V})$ should be expanded in powers of the disorder strength as

$$W(\overline{V}) = W_2\overline{V}^2 + W_4\overline{V}^4 + \cdots, \tag{3.2.2}$$

$$P(\overline{V}) = P_2\overline{V}^2 + P_4\overline{V}^4 + \cdots \tag{3.2.3}$$

where, as in the usual Poincaré-Lindstedt procedure, the W_i and P_i are constant coefficients that we will adjust in order to remove the secular terms in $\langle\alpha_2\rangle_D$ and $\langle\delta_2\rangle_D$. In order to ensure that the spacetime geometry remains asymptotically AdS, we must enforce the boundary condition $\beta_1(r) \to 1$ and $\beta_2(r) \to 1$ as $r \to 0$. Moreover, in order

to ensure that the functions $\beta_1(r)$ and $\beta_2(r)$ have a chance at removing the problematic terms in the disorder averaged metric components, we should have that $\beta_1(r)$ and $\beta_2(r)$ diverge as $r \to \infty$. This is the only way that a new term can compete with (and ultimately regulate) the already divergent secular terms.

The placement of the new functions $\beta_1(r)$ and $\beta_2(r)$ in the metric (3.2.1) is not arbitrary. Expanded to second order in the disorder strength, the right hand side of the traced Einstein equations (3.1.2) is left unchanged. This is sensible since the source of the disorder, namely the gauge field (3.1.10) is not being modified. Notice also that $\beta_1(r)$ and $\beta_2(r)$ are only functions of the radial coordinate r as their sole purpose is to correct the secular terms in the averaged metric components $\langle \alpha_2 \rangle_D$ and $\langle \delta_2 \rangle_D$. There is no new function associated with the x direction as $\langle \eta_2(x,r) \rangle_D$ (3.1.23) is already finite everywhere and does not require a correction.

The off-diagonal $[r,x]$ component of the traced Einstein equations (3.1.15) is also unchanged. This is crucial, as this component allows us to solve for the combination $\alpha_2(x,r) + \delta_2(x,r)$, and so the x dependence in this combination will also not be modified from the original solution. The only difference brought about by including β_1 and β_2 is the possibility of modifying the overall partial integration functions of the radial coordinate in $\alpha_2(x,r)$, $\delta_2(x,r)$ and $\eta_2(x,r)$. It is this modification that will allow us to remove the secular terms from the disorder averaged metric components.

Finding the solution for the metric coefficients in (3.2.1) to second order in the disorder strength goes through in exactly the same way as for the original case. We look for an expansion of the form

$$\begin{aligned} \alpha(x,r) &= 1 + \overline{V}^2 \alpha_2(x,r) + \cdots \\ \eta(x,r) &= 1 + \overline{V}^2 \eta_2(x,r) + \cdots \\ \delta(x,r) &= 1 + \overline{V}^2 \delta_2(x,r) + \cdots . \end{aligned}$$

Plugging this expansion into the traced Einstein equations (3.1.2) yields a set of partial

differential equations

$$-2r\partial_r^2\alpha_2+2\partial_2\delta_2+2\partial_r\eta_2-2r\partial_x^2\alpha_2+6\partial_r\alpha_2-\frac{6W_2}{\beta_1}\partial_r\beta_1-\frac{2P_2}{\beta_2}\partial_r\beta_2$$
$$-\frac{2rW_2}{\beta_1^2}(\partial_r\beta_1)^2+\frac{2rW_2}{\beta_1}\partial_r^2\beta_1=-\frac{r^3}{L^2}\left[(\partial_r H)^2+(\partial_x H)^2\right]\,, \tag{3.2.4}$$

$$2r\partial_r^2\eta_2-2\partial_r\alpha_2-2\partial_r\delta_2+2r\partial_r^2\alpha_2+2r\partial_r^2\delta_2-2\partial_r\eta_2+\frac{2W_2}{\beta_1}\partial_r\beta_1+\frac{2P_2}{\beta_2}\partial_r\beta_2$$
$$+\frac{2rW_2}{\beta_1^2}(\partial_r\beta_1)^2+\frac{2rP_2}{\beta_2^2}(\partial_r\beta_2)^2-\frac{2rP_2}{\beta_2}\partial_r^2\beta_2-\frac{2rW_2}{\beta_1}\partial_r^2\beta_1=\frac{r^3}{L^2}\left[(\partial_r H)^2-(\partial_x H)^2\right]\,, \tag{3.2.5}$$

$$\partial_x\partial_r(\alpha_2+\delta_2)=\frac{r^2}{L^2}(\partial_r H)(\partial_x H)\,, \tag{3.2.6}$$

$$2\partial_r\delta_2-2r\partial_x^2\delta_2-2r\partial_r^2\eta_2+2\partial_r\alpha_2+6\partial_r\eta_2-2r\partial_x^2\alpha_2-\frac{2W_2}{\beta_1}\partial_r\beta_1-\frac{2P_2}{\beta_2}\partial_r\beta_2$$
$$=\frac{r^3}{L^2}\left[(\partial_r H)^2-(\partial_x H)^2\right]\,, \tag{3.2.7}$$

$$2\partial_r\eta_2-2r\partial_x^2\delta_2+2\partial_r\alpha_2-2r\partial_r^2\delta_2+6\partial_r\delta_2-\frac{6P_2}{\beta_2}\partial_r\beta_2-\frac{2W_2}{\beta_1}\partial_r\beta_1$$
$$+\frac{2rP_2}{\beta_2}\partial_r^2\beta_2-\frac{2rP_2}{\beta_2^2}(\partial_r\beta_2)^2=\frac{r^3}{L^2}\left[(\partial_r H)^2+(\partial_x H)^2\right]\,. \tag{3.2.8}$$

Notice, the $[r,x]$ component (3.2.6) is unchanged compared to the original $[r,x]$ component (3.1.15), as promised. In fact, the new traced Einstein equations differ only from the original ones (3.1.13) - (3.1.17) by the addition of terms with derivatives of β_1 and β_2. In particular, this means that the x dependence of the metric coefficient $\alpha_2(x,r)$, $\eta_2(x,r)$ and $\delta_2(x,r)$ will be unchanged. Again, this had to be the case since the source for the disorder, namely the gauge field (3.1.10) has not be modified, nor have the right hand sides of the traced Einstein equations (3.1.2).

The solutions for $\alpha_2(x,r)$, $\eta_2(x,r)$ and $\delta_2(x,r)$ are found to satisfy

$$\alpha_2(x,r)+\delta_2(x,r)=G_1(x)+G_2(r)+\frac{1}{8L^2}\sum_{n=1}^{N-1}\frac{A_n^2}{k_n^2}\left(1+2k_nr+2k_n^2r^2\right)e^{-2k_nr}$$
$$+\frac{1}{L^2}\sum_{n=1}^{N-1}\sum_{m=1}^{n-1}\frac{A_nA_mk_nk_m}{(k_n+k_m)^4}\left[(k_n+k_m)^2r^2+2r(k_n+k_m)+2\right]$$
$$\times\cos((k_n+k_m)x+\theta_n+\theta_m)e^{-(k_n+k_m)r}\,, \qquad (3.2.9)$$

where $G_1(x)$ is an arbitrary function of x and

$$G_2(r)=\tilde{G}_2(r)-\frac{1}{16L^2}\sum_{n=1}^{N-1}\frac{A_n^2}{k_n^2}\left(1+2k_nr+2k_n^2r^2\right)e^{-2k_nr}\,. \qquad (3.2.10)$$

The condition (3.2.9) along with the partial integration function $G_2(r)$ (3.2.10) are also true for the original disordered metric solutions up to a new, potentially different, function $\tilde{G}_2(r)$. It satisfies

$$r\partial_r^2\tilde{G}_2(r)-2\partial_r\tilde{G}_2(r)=\frac{rW_2}{\beta_1}\partial_r^2\beta_1+\frac{rP_2}{\beta_2}\partial_r^2\beta_2-\frac{2P_2}{\beta_2}\partial_r\beta_2$$
$$-\frac{2W_2}{\beta_1}\partial_r\beta_1-\frac{rW_2}{\beta_1^2}(\partial_r\beta_1)^2-\frac{rP_2}{\beta_2^2}(\partial_r\beta_2)^2\,. \qquad (3.2.11)$$

This is the new piece that will allow us to tame the secular terms in the disorder averaged solutions.

The equations of motion (3.2.4) - (3.2.8) may also be combined to get

$$\alpha_2(x,r)-\delta_2(x,r)=\tilde{G}_4(r)-\frac{1}{8L^2}\sum_{n=1}^{N-1}\frac{A_n^2}{k_n^2}+\frac{1}{8L^2}\sum_{n=1}^{N-1}\frac{A_n^2}{k_n^2}\left(1+2k_nr+2k_n^2r^2\right)e^{-2k_nr}$$
$$+\frac{1}{4L^2}\sum_{n=1}^{N-1}\sum_{m=1}^{n-1}\frac{A_nA_m}{k_nk_m}\left[1+(k_n+k_m)r+2k_nk_mr^2\right]\cos((k_n-k_m)x+\theta_n-\theta_m)e^{-(k_n+k_m)r}$$
$$-\frac{1}{4L^2}\sum_{n=1}^{N-1}\sum_{m=1}^{n-1}\frac{A_nA_m}{k_nk_m}\left[1+(k_n+k_m)r\right]\cos((k_n-k_m)x+\theta_n-\theta_m)e^{-(k_n-k_m)r}\,, \qquad (3.2.12)$$

where the function $\tilde{G}_4(r)$ plays an analogous role to $\tilde{G}_2(r)$ in (3.2.9); it satisfies

$$r\partial_r^2\tilde{G}_4(r)-2\partial_r\tilde{G}_4(r)=-\frac{2W_2}{\beta_1}\partial_r\beta_1+\frac{2P_2}{\beta_2}\partial_r\beta_2-\frac{rW_2}{\beta_1^2}(\partial_r\beta_1)^2$$
$$+\frac{rP_2}{\beta_2^2}(\partial_r\beta_2)^2+\frac{rW_2}{\beta_1}\partial_r^2\beta_1-\frac{rP_2}{\beta_2}\partial_r^2\beta_2\,. \qquad (3.2.13)$$

Finally, the solution for $\eta_2(x,r)$ is

$$\begin{aligned}\eta_2(x,r) = &\frac{1}{4}r^2\partial_x^2 G_1(x) + G_3(x) - \tilde{G}_6(r) - \frac{1}{32L^2}\sum_{n=1}^{N-1}\frac{A_n^2}{k_n^2}\left(2k_n r+1\right)e^{-2k_n r} \\ &+ \frac{1}{L^2}\sum_{n=1}^{N-1}\sum_{m=1}^{n-1}\frac{A_n A_m}{(k_n+k_m)^4}\left[(k_n+k_m)r+1\right]\cos((k_n+k_m)x+\theta_n+\theta_m)e^{-(k_n+k_m)r} \\ &+ \frac{1}{16L^2}\sum_{n=1}^{N-1}\frac{A_n^2}{k_n^2}\left(2k_n r+1\right)\cos^2(k_n x+\theta_n)e^{-2k_n r}\,, \end{aligned} \tag{3.2.14}$$

where

$$\tilde{G}_6(r) = \int dr\left[\frac{1}{r}r\partial_r^2\tilde{G}_2 + \frac{rW_2}{2\beta_1^2}(\partial_r\beta_1)^2 + \frac{rP_2}{2\beta_2^2}(\partial_r\beta_2)^2 - \frac{rP_2}{2\beta_2}\partial_r^2\beta_2 - \frac{rW_2}{2\beta_1}\partial_r^2\beta_1\right]. \tag{3.2.15}$$

Using these solutions, we will be able to write down a resummed backreacted metric, devoid of secular terms under disorder averaging.

3.2.1 Resummed disorder average

With the solutions (3.2.9), (3.2.12) and (3.2.14) at hand, we can impose asymptotically *AdS* boundary conditions and require that the secular terms in the disorder average vanish. To do this, we need a choice for $\beta_1(r)$ and $\beta_2(r)$. A natural choice is

$$\beta_1(r) = \beta_2(r) = \exp\left(\frac{r}{4L^2}\right), \tag{3.2.16}$$

with $W_2 = 1 = -P_2$. $\overline{V}$ has units Length$^{1/2}$, so to second order $\beta_1^{W_2\overline{V}^2}$ and $\beta_2^{P_2\overline{V}^2}$ are dimensionless. Different choices of $\beta_1(r)$ and $\beta_2(r)$ which preserve the asymptotically AdS boundary condition and remove the secular divergences in (3.1.21) and (3.1.22) will correspond to different resummations, but will ultimately lead to the same IR geometry in the same way as in the case of scalar disorder [281]. Any choice of $\beta_1(r)$ and $\beta_2(r)$ must behave in a specific way in the interior in order to remove the unphysical divergences, and so result in the same IR geometry. With this choice, the partial integration functions $\tilde{G}_2(r)$ (3.2.10) and $\tilde{G}_4(r)$ (3.2.13) simplify to

$$\tilde{G}_2(r) = d_1 + \frac{1}{3}d_2 r^3\,, \tag{3.2.17}$$

and

$$\tilde{G}_4(r) = d_3 + \frac{1}{3}d_4 r^3 + \frac{1}{2L^2}r\,, \tag{3.2.18}$$

where d_1, d_2, d_3 and d_4 are constants.

Since $\tilde{G}_2(r)$ appears in $\alpha_2+\delta_2$ and $\tilde{G}_4(r)$ appears in $\alpha_2-\delta_2$, the two metric coefficients will be modified from their original values by

$$\frac{1}{2}(\tilde{G}_2+\tilde{G}_4) = \frac{1}{2}(d_1+d_3) + \frac{1}{6}(d_2+d_4)r^3 + \frac{1}{4L^2}r\,, \tag{3.2.19}$$

in $\alpha_2(x,r)$, while

$$\frac{1}{2}(\tilde{G}_2-\tilde{G}_4) = \frac{1}{2}(d_1-d_3) + \frac{1}{6}(d_2-d_4)r^3 - \frac{1}{4L^2}r\,, \tag{3.2.20}$$

appears in $\delta_2(x,r)$. In η_2, $\tilde{G}_6$ (3.2.15) becomes simply

$$\tilde{G}_6(r) = \int dr\left[\frac{1}{2}r\partial_r^2\tilde{G}_2(r)\right] = \frac{1}{3}d_2 r^3\,. \tag{3.2.21}$$

Setting the constant $d_2 = 0$ recovers the original solution for $\eta_2(x,r)$. As such, $\langle\eta_2\rangle_D$ is exactly the same as in (3.1.23). This is precisely as expected, $\langle\eta_2\rangle_D$ was already finite everywhere and requires no correction.

Finally, setting $d_3 = d_4 = 0$ the corrections to $\langle\alpha_2\rangle_D$ and $\langle\delta_2\rangle_D$ are precisely those needed to remove the secular terms. We finally have

$$\langle\alpha_2\rangle_D = \frac{1}{2}c + \frac{1}{4k_0L^2} - \frac{1}{4k_0L^2}(1-k_0r)\exp(-2k_0r)\,, \tag{3.2.22}$$

$$\langle\delta_2\rangle_D = \frac{1}{2}c - \frac{1}{4k_0L^2} + \frac{1}{4k_0L^2}(1-k_0r)\exp(-2k_0r)\,, \tag{3.2.23}$$

and $\langle\eta_2\rangle_D$ is given in (3.1.23). These results constitute the corrected disorder averaged metric coefficients, all of which are now finite everywhere in the bulk.

Note also that the choice for $W_2 = -P_2$ ensures that there are no curvature divergences anywhere in the bulk. Calculating $K \equiv R_{\mu\nu\lambda\sigma}R^{\mu\nu\lambda\sigma}$ through order $\overline{V}^2$ in the disorder averaged metric gives $K = \text{const}$.

With the resummed solution, we can ask about transport properties of the disordered geometry. In particular, we are interested in understanding how the conductivity is modified from the initially clean AdS case. We tackle this question in the next section.

3.3 Conductivity

In order the calculate the conductivity, we need to turn on a perturbation to the gauge field. We will be interested in computing the conductivity along the disordered direction x. In pure AdS, the zero-momentum conductivity can be computed by turning on $A_x(r,t) = a_x(r)e^{-i\omega t}$ and computing the retarded holographic Green's function via the linearized bulk equations of motion. Taking the $\omega \to 0$ limit gives the DC conductivity which turns out to be a constant. This result persists even at finite temperature and is due to bulk electric-magnetic duality [80]. The calculation is simplified in the AdS case, since the gauge field perturbation does not contribute the to linearized energy-momentum tensor and so cannot source any new metric perturbations.

The situation is not so simple when a non-zero background value for another component of the gauge field is turned on, for example in the $RN-AdS$ geometry. This means that, generally speaking, the perturbation of the gauge field needed to measure the conductivity will couple to background gauge field component and contribute at linear order in the equations of motion. As a consequence, new metric perturbations are sourced and can lead to complicated linearized equations.

In the context of holographic lattices, such as those studied in [162], [254] and [255] the problem is magnified. Virtually everything that can be sourced is and the perturbation equations turn into a complicated set of partial differential equations which must be solved using numerical techniques. In [256], a holographic lattice, sourced by a periodic scalar field was studied analytically in a perturbative expansion about the lattice strength. Due to the perturbative nature of the lattice, the linearized equations of motion for the gauge field fluctuation turn out to simplify considerably and only a single metric and scalar perturbation are sourced making the system more amenable to analysis.

For our disordered case, the situation does not simplify quite so drastically, even though the disorder strength is assumed to be weak. The gauge field perturbation A_x will mix with the background A_t, producing terms which are second order in perturba-

tions (i.e. one power of the disorder strength $\overline{V}$ and A_x). These will in turn source metric perturbations of the same order and in principle may source metric perturbations along every direction. We can, nevertheless, still access information about the DC conductivity of the system by employing a technique first proposed in [292]. The idea is to turn on a perturbation that is linear in time. An analysis in linear response theory implies that the DC conductivity may be directly calculated by taking advantage of conserved quantities in the bulk. By using the equations of motion to relate the boundary current to the magnitude of the applied electric field, the DC conductivity follows from Ohm's law. In [259], this technique was adopted to study the DC conductivity of inhomogeneous holographic lattices at finite temperature. In section 3.4, we will discuss how this technique may be applied to holographic disorder with non-vanishing initial charge density.

We consider a perturbation to the gauge field $A_x = a_x(r) - Et$, where E is the constant magnitude of the electric field in the x direction. At the level of the linearized equations of motion, this perturbation may further source metric perturbations $\{\delta g_{tt},\ \delta g_{xx},\ \delta g_{yy},\ \delta g_{xt}\}$. We have already elected to work in Fefferman-Graham gauge when constructing the backreacted spacetime in order to ensure an asymptotically AdS solution. As such, we will impose that the metric perturbations obey the usual Fefferman-Graham expansion near the boundary. In other words, as $r \to 0$, $\delta g_{ab} = (L^2/r^2)\delta g_{ab(0)}(x) + \delta g_{ab(1)}(x) + \mathcal{O}(r^2)$. Note that the metric perturbations will be at most functions of x and r and will be composed of combinations of periodic functions in x. This is because the metric perturbations are being sourced by terms made up of the gauge field perturbation and the original time component of the gauge field that sources the disorder, so there is no possibility to source any other kind of dependence.

From the bulk Maxwell equations $\nabla_\mu F^{\mu\nu} = 0$, we see that the x and r components require that

$$\partial_x \left(\sqrt{-g}F^{xr}\right) = \partial_r \left(\sqrt{-g}F^{xr}\right) = 0\,. \tag{3.3.1}$$

Hence, the current $J^x \equiv \sqrt{-g}F^{xr}$ is a conserved quantity in the bulk. As $r \to 0$, this

defines the boundary current in the x direction.

The conductivity can be read off from Ohm's law, namely $J^x = \sigma E$. Therefore, if we can find an expression for J^x/E and take the disorder average of the result, we will have found the DC conductivity directly (up to an overall normalization constant set by the action (3.1.1)).

Our strategy will be as follows. First, we write down an expression for J^x linearized about the gauge field and metric perturbations. Since this quantity is a constant, we can evaluate it anywhere in the bulk. As we are working at zero temperature, there are no horizons about which to expand. We therefore focus on expanding about the boundary $r = 0$, where, in keeping with our choice of Fefferman-Graham gauge, we enforce asymptotic AdS falloffs for all of the perturbations. We then take advantage of our perturbative handle, the disorder strength $\overline{V}$. The linearized equations of motion generally contain terms at many orders in $\overline{V}$. We start with the leading order Maxwell equations which we solve for $a_x(r)$. This solution is then fed into the next order in perturbations which couples $a_x(r)$ to order $\overline{V}$ terms. These source the metric perturbations, which may be solved for via the Einstein equations and expressed in terms of the magnitude of the applied electric field E. The results solve for σ up to second order, after taking the disorder average. The linearized equations of motion contain higher order terms as well, such as $\overline{V}^2 \delta g_{ab}$. Since the metric fluctuations are already sourced by terms of the form $\overline{V} a_x$, these terms are already fourth order in perturbations and not relevant.

The linearized expression for J^x, expanded near the boundary at $r = 0$ is

$$J^x = \sqrt{\frac{\delta_{(0)}}{\alpha_{(0)}\eta_{(0)}}} \left[\alpha_{(0)} a_{x(1)} + \overline{V} H_{(1)} \delta g_{tx(0)}\right] , \tag{3.3.2}$$

where the gauge field perturbation has been expanded near the boundary $a_x(r) = a_{x(0)} +$

$ra_{x(1)} + \cdots$. Also

$$\alpha(x,r) = \alpha_{(0)}(x) + r\alpha_{(1)}(x) + \cdots$$
$$\eta(x,r) = \eta_{(0)}(x) + r\eta_{(1)}(x) + \cdots$$
$$\delta(x,r) = \delta_{(0)}(x) + r\delta_{(1)}(x) + \cdots ,$$

near $r = 0$. The function $H(x,r)$ is related to the disorder source as $A_t(x,r) = \overline{V}H(x,r)$ and it has also been expanded near $r = 0$ as

$$H(x,r) = H_{(0)}(x) + rH_{(1)}(x) + \cdots . \tag{3.3.3}$$

The next step is to get an expression for the gauge perturbation $a_x(r)$. To do this, we use the linearized Maxwell equations to leading order in perturbations. This is just the Maxwell equation in AdS, so the solution is easy to find

$$a_x(r) = b_1 + b_2 r\,, \tag{3.3.4}$$

where b_1 and b_2 are constants. This solution then couples to the disorder source A_t and the original background metric coefficients to produce the metric fluctuations. In principle, the gauge field fluctuation itself will then receive corrections from the metric perturbations, but this requires going to, at a minimum, third order in perturbation theory. The upshot is that we can use the baseline solution for a_x to extract the DC conductivity to second order in perturbations. The constant b_2 can be fixed in terms of the applied electric field E. To see how, replace the time coordinate t with the ingoing coordinate $v = t - r + \mathcal{O}(\overline{V}^2)$. Then the full gauge field perturbation $A_x = a_x - Et$ is a (finite) ingoing solution provided that $b_2 = E$ up to second order. This is exactly the condition required in pure AdS to recover the correct DC conductivity and it will ensure that our result contains the pure AdS case plus a possible correction, so that the final disorder averaged solution will take the form

$$\langle\sigma\rangle_D = \sigma_{\text{AdS}} + \overline{V}^2\langle\sigma_{\text{Disorder}}\rangle_D\,. \tag{3.3.5}$$

That is, the original constant AdS DC conductivity plus a correction.

With J^x in (3.3.2) we must find an expression for $\delta g_{tx(0)}$ in order to get the conductivity. This can be accomplished via the linearized equations of motion. Despite being linearized, the equations of motion are still quite complex and finding a solution is a difficult task. This difficulty may be circumvented by making use of perturbative expansion in the disorder strength. To get an expression for $\delta g_{tx(0)}$ it suffices to solve the linearized Einstein and Maxwell equations up to second order in perturbations. That is, we keep terms of order a_x, $\overline{V}^2$, $\overline{V}a_x$ and δg.

We have already solved the linearized Maxwell equations through second order in (3.3.4). No further corrections to the Maxwell equations are sourced until at least third order in perturbations. The linearized Einstein equations work out similarly. There are no contributions to the linearized equations at first order in perturbations. This had to be the case as all of the metric coefficients and metric perturbations are at least second order perturbative terms. Every diagonal component of the linearized Einstein equations is just the original equation plus a correction due to a term proportional to $\overline{V}E$ which, in principle could source metric perturbations along these directions. Remarkably, none of the diagonal components of the linearized Einstein equations, nor the $[x, r]$ component contain the metric perturbation δg_{tx} that we need to compute the conductivity. In fact, the relevant metric perturbation decouples completely from the others and only shows up in $[t, r]$ and $[t, x]$ components. The equations are

$$r\partial_x\partial_r\delta g_{tx} + 2r\partial_r\delta g_{tx} + \overline{V}r(\partial_x H)E = 0\,, \tag{3.3.6}$$

$$2\delta g_{tx} - r^2\partial_r^2\delta g_{tx} - 2r\partial_r\delta g_{tx} - \overline{V}r^2(\partial_r H)E = 0\,, \tag{3.3.7}$$

with a solution

$$\delta g_{tx}(x,r) = \frac{\overline{V}E}{r^2}\sum_{n=1}^{N-1}\frac{A_n}{k_n^3}\left(2+2k_nr+k_n^2r^2\right)\cos(k_nx+\theta_n)\exp(-k_nr)+2\frac{\overline{V}E}{r^2}K(x)\,, \tag{3.3.8}$$

where $K(x)$ is a function of x that will be fixed momentarily. As promised, the metric fluctuation is sourced by a term that goes like $\overline{V}$ times a gauge field fluctuation. A

quick comment is in order about boundary conditions. Earlier, above (3.3.5), we argued A_x was ingoing. Nonetheless, the metric perturbation δg_{tx} remains static, because the flux is constant (by design). Therefore, it is not necessary to separately impose ingoing boundary conditions on δg_{tx}; this is already taken care of. With (3.3.8), we can determine $\delta g_{tx(0)}$ and get and expression for J^x in terms of E. We now have all of the ingredients we need to get to the DC conductivity. Inserting the results back into (3.3.2), expanding to second order in the disorder strength

$$\begin{aligned}\frac{J^x}{E} &= 1+\frac{\overline{V}^2}{2}(\alpha_{2(0)}+\delta_{2(0)}-\eta_{2(0)})-\frac{2\overline{V}^2}{L^2}\sum_{n=1}^{N-1}\frac{A_n^2}{k_n^2}\cos^2(k_nx+\theta_n) \\ &\quad -\frac{2\overline{V}^2}{L^2}\sum_{\substack{n,m=1\\ m\neq m}}^{N-1}\frac{A_nA_mk_m}{k_n^3}\cos(k_nx+\theta_n)\cos(k_mx+\theta_m)+2\frac{\overline{V}^2}{L^2}H_{(1)}K(x)\,,\end{aligned} \tag{3.3.9}$$

where, as $r\to 0$

$$\begin{aligned}\alpha(x,r) &= 1+\overline{V}^2\alpha_2(x,r)\to 1+\overline{V}^2\left(\alpha_{2(0)}+r\alpha_{2(1)}+\cdots\right)\,,\\ \eta(x,r) &= 1+\overline{V}^2\eta_2(x,r)\to 1+\overline{V}^2\left(\eta_{2(0)}+r\eta_{2(1)}+\cdots\right)\,,\\ \delta(x,r) &= 1+\overline{V}^2\delta_2(x,r)\to 1+\overline{V}^2\left(\delta_{2(0)}+r\delta_{2(1)}+\cdots\right)\,.\end{aligned}$$

From the metric coefficient α_2, η_2 and δ_2 we get

$$\begin{aligned}\alpha_{2(0)}+\delta_{2(0)}-\eta_{2(0)} &= \frac{1}{16L^2}\sum_{n=1}^{N-1}\frac{A_n^2}{k_n^2}\cos^2(k_nx+\theta_n)-\frac{1}{32L^2}\sum_{n=1}^{N-1}\frac{A_n^2}{k_n^2}\\ &\quad+\frac{1}{L^2}\sum_{n=1}^{N-1}\sum_{m=1}^{n-1}\frac{A_nA_mk_nk_m}{(k_n+k_m)^4}\cos((k_n+k_m)x+\theta_n+\theta_m)\,.\end{aligned}$$

The last step needed to get the DC conductivity is to take the disorder average (3.1.8) of (3.3.9). To do this, we need to know the function $K(x)$ appearing in (3.3.8). This function may be fixed by requiring a finite large N limit for the conductivity as well as a finite value for $\delta g_{tx(0)}$ and a vanishing disorder average for δg_{tx}. The condition on the disorder average of δg_{tx} actually follows from the requirement of a finite large N limit for the conductivity. If $\langle\delta g_{tx}\rangle_D$ was a constant as $r\to 0$, then the $H_{(1)}\delta g_{tx(0)}$ term in J^x (3.3.2) would vanish under disorder averaging and would not be able to regulate the

large N limit. The coefficient of $K(x)$ can then be fixed by dimensional analysis. A good choice is

$$K(x) = \frac{\pi^2}{12\zeta(3)} \sum_{n=1}^{N-1} \frac{A_n^3}{k_n^4} \cos(k_n x + \theta_n) \,, \tag{3.3.10}$$

where $\zeta(n)$ is the Riemann zeta function. There is more than one choice for the coefficient of $K(x)$, however every choice which is dimensionally consistent and satisfies our basic requirements for δg_{tx} returns the same result for the disorder averaged conductivity. Applying (3.1.8) to (3.3.9) and restoring the units (which is due to the overall normalization we have chosen for the action (3.1.1) [1]) we get

$$\langle \sigma \rangle_D = \frac{1}{16\pi G_N} + \frac{\overline{V}^2}{4\pi G_N L^2 k_0} \,. \tag{3.3.11}$$

The disorder averaged conductivity takes the form (3.3.5) as claimed. The overall contribution due to disorder is a constant which comes in a second order in the disorder strength. This is sensible as the disorder induced corrections to the geometry (3.2.1) are at second order. In fact, our result echoes that of the single holographic lattice constructed in [320]. From the point of view of the conductivity, only the metric coefficients $\alpha(x,r)$, $\delta(x,r)$ and $\eta(x,r)$ really matter. Under disorder averaging, these functions approach a constant towards the boundary $r \to 0$ which scales as $\overline{V}^2/(4k_0L^2)$, which is a natural dimensionless constant made up of the three scales in the system. It is therefore not surprising that the correction induced by the disorder source on the DC conductivity involves precisely this combination. Moreover, notice that as $\overline{V} \to 0$, the average DC conductivity (3.3.11) reduces to the expected pure AdS result.

Note that the result (3.3.11) is specific to a disordered source with a Gaussian distribution (3.1.9). It is an interesting question as to whether or not changing the disorder distribution will affect the final result. In particular, the fact that the correction to the conductivity is positive and not negative as might be expected is a result of having

[1] In pure AdS, the dual DC conductivity is $\sigma_{DC} = 1/e^2$, where the bulk gauge field is normalized by $-1/4e^2$. In our conventions, e has been absorbed into the gauge field and we have pulled out an overall factor of $16\pi G_N$.

chosen a Gaussian distribution. It is unclear that this will be the case if the disorder distribution is modified. Moreover, it is also unclear that a positive correction persists to higher orders in the disorder strength. It might be that further corrections come in with the opposite sign, but are only visible at larger disorder strength.

It is tempting to try and address the question of using a different distribution starting from (3.3.9). However, to arrive at this formula, we have explicitly made use of the resummed metric (3.2.1) which implicitly assumes a Gaussian distribution for the disorder source. In particular, the functions $\beta_1(r)$ and $\beta_2(r)$ are specific for this realization of disorder. Understanding how the form of the metric coefficients in the backreacted geometry is dependent on how disorder is implemented in the system and how this affects the dual transport properties are questions we leave for future work.

3.4 Finite charge density

The observations of the previous section all follow from a system with zero initial charge density. Turning on a non-zero background charge density can change the game drastically. The baseline, clean, geometry is now the $RN-AdS$ solution. In the $RN-AdS$ background, the boundary directions preserve translational invariance, and so there is no way to dissipate momentum. Coupled with the fact that the solution no longer possess particle-hole symmetry like the pure AdS case, the net result is a divergent DC conductivity. From the perspective of our previous results in pure AdS, it is a natural question to ask how much we can say about adding disorder to this background.

The action and equations of motion are the same as in (3.1.1), (3.1.2) and (3.1.3). In this case, the initially clean geometry is Reissner-Nordström-AdS and the gauge field is not constant everywhere. The baseline solution is

$$ds^2 = \frac{L^2}{r^2}\left(-f(r)dt^2 + \frac{dr^2}{f(r)} + dx_i^2\right) . \tag{3.4.1}$$

There are $d-1$ boundary directions. The boundary is located at $r=0$ in these coordi-

nates. $f(r)$ is given by

$$f(r) = 1 - \left(1 + \frac{(d-2)\mu_0^2 r_0^2}{2(d-1)L^2}\right)\left(\frac{r}{r_0}\right)^d + \frac{(d-2)\mu_0^2 r_0^2}{2(d-1)L^2}\left(\frac{r}{r_0}\right)^{2(d-1)} , \tag{3.4.2}$$

$$A_t(r) = \mu_0\left(1 - \left(\frac{r}{r_0}\right)^{d-2}\right) , \tag{3.4.3}$$

where r_0 is the location of the outer horizon and μ_0 is a constant associated to the chemical potential of the dual theory [71]. The temperature is

$$T = \frac{1}{4\pi r_0}\left(d - \frac{(d-2)^2\mu_0^2 r_0^2}{2(d-1)L^2}\right) . \tag{3.4.4}$$

We introduce disorder the same way we did before by adding a perturbation to the gauge field and insisting on the boundary condition (3.1.6) and regularity in the interior. As an example, if $d+1 = 5$ and we take the limit where all the horizons coincide at $r = r_0$ (i.e. $T = 0$). The solution to the Maxwell equations at first order is

$$A_t(x,r) = \mu_0\left(1 - \frac{r^2}{r_0^2}\right) + \overline{V}\sum_{n=1}^{N-1}\frac{A_n}{3^{\Delta_n/2}}\frac{\Gamma(1+\frac{\Delta_n}{2})\Gamma(\frac{\Delta_n}{2})}{\Gamma(\Delta_n)}\left(1 + 2\frac{r^2}{r_0^2}\right)\left[\frac{(r_0^2 - r^2)}{r^2}\right]^{\Delta_n/2} \tag{3.4.5}$$

$$\times\, {}_2F_1\left[\frac{\Delta_n}{2}, 1 + \frac{\Delta_n}{2}; \Delta_n; \frac{r^2 - r_0^2}{3r^2}\right]\cos(k_n x + \theta_n) ,$$

where $\Delta_n = 1 + \sqrt{1 + \frac{k_n^2 r_0^2}{3}}$. Note that the solution (3.4.5) vanishes at the horizon $r = r_0$ as required for the gauge field to be well defined.

In $d+1 = 4$, the solution is more complicated.

$$A_t(x,r) = \mu_0\left(1 - \frac{r}{r_0}\right) + \overline{V}\sum_{n=1}^{N-1}\frac{3^{\lambda_n/2}A_n}{r_0}(r_0 - r)^{\lambda_n/2}\left[\frac{i\sqrt{(}2)(r_0 - r) - 2(r_0 + 2r)}{i\sqrt{2} - 2}\right]^{1-\lambda_n/2} \tag{3.4.6}$$

$$\times \frac{{}_2F_1\left[\frac{\lambda_n}{2}, -\frac{1}{2}; \frac{1+\lambda_n}{2}; \frac{2i\sqrt{2}(r-r_0)}{i\sqrt{2}(r_0-r)-2(r_0+2r)}\right]}{{}_2F_1\left[\frac{\lambda_n}{2}, -\frac{1}{2}; \frac{1+\lambda_n}{2}; -\frac{2i\sqrt{2}}{i\sqrt{2}-2}\right]} ,$$

where $\lambda_n = 1 + \sqrt{1 + \frac{r_0^2 k_n^2}{3}}$. The solution (3.4.6) vanishes at the horizon $r = r_0$ and obeys the correct boundary condition (3.1.6) at $r = 0$.

The idea now is to plug this back into the equations of motion and work out the back reacted geometry to next order in $\overline{V}$ perturbations. This is more complicated than the initially uncharged case. Since the initially clean geometry requires a nontrivial gauge field from the get go, there is a baseline term in $A_t(x,r)$ that survives on the right hand side of the equations of motion. In general this will mix perturbative and baseline terms, meaning that the equations of motion must be consistently solved at both first and second order in $\overline{V}$. Also, the solution presented here is not in the Fefferman-Graham coordinates of the previous section. This adds the complication that, in general, the backreacted geometry could have off-diagonal g_{ra} contributions. Since the perturbation is only along the x direction, A_t only mixes the r and x directions. Hence, the only off-diagonal term that can be sourced is g_{rx}. This means that the back-reacted metric should take the form

$$ds^2 = \frac{L^2}{r^2}\left(-\alpha(x,r)dt^2 + \frac{dr^2}{F(r)} + \eta(x,r)dx^2 + \delta(x,r)dy^2 + 2\chi(x,r)dxdr\right) . \tag{3.4.7}$$

The perturbative expansion for the unknown functions this time is then

$$\begin{aligned}
\alpha(x,r) &= f(z) + \overline{V}\alpha_1(x,r) + \overline{V}^2\alpha_2(x,r) + \cdots , \\
F(r) &= f(r) + \overline{V}F_1(r) + \overline{V}^2F_2(r) + \cdots , \\
\delta(x,r) &= 1 + \overline{V}\delta_1(x,r) + \overline{V}^2\delta_2(x,r) + \cdots , \\
\eta(x,r) &= 1 + \overline{V}\eta_1(x,r) + \overline{V}^2\eta_2(x,r) + \cdots , \\
\chi(x,r) &= \overline{V}\chi_1(x,r) + \overline{V}^2\chi_2(x,r) + \cdots ,
\end{aligned}$$

note that the expansion for $\chi(x,r)$ starts at order $\overline{V}$. This off-diagonal component is not present in the initial clean geometry, so in the limit that $\overline{V} \to 0$, this metric coefficient must vanish. Following the same logic as in section 3.1, we should try and solve the traced Einstein equations up to second order in the disorder strength. At zeroth order, the traced Einstein equations are just those of the baseline $RN-AdS$ solution, ensuring that the full solution will be expressed as the $RN-AdS$ geometry plus corrections. This

observation is what constrains the backreacted metric component g_{rr} to be only a function of r. The disorder is turned on along the boundary directions, so we do not expect it to modify the location of the horizon. At higher order, the traced Einstein equations are complicated and it is unclear if a compact analytic solution can be found. While we will not attempt to answer this question here, it would be interesting to understand if the numerical techniques applied to holographic lattices and scalar disorder could be applied here.

In lieu of a full analytic solution, we can nevertheless extract the form of the DC conductivity by applying the technique used for inhomogeneous holographic lattices in [259]. We will briefly review the salient features of this technique as we go along. We will make a modest assumption about the behaviour of the disordered solution near a horizon and see that, given the metric coefficients and gauge field solution, it is possible to extract the form of the disorder averaged DC conductivity directly in terms of horizon data.

We will assume the form of the backreacted metric is (3.4.7) with the event horizon at $r = r_0$ and asymptotes to AdS_4 near the boundary $r = 0$. As $\overline{V} \to 0$, the geometry must reduce to the $RN - AdS$ solution. We will work at finite temperature T and express the gauge field solution as

$$A_t(x, r) = \mu_0 \left(1 - \frac{r}{r_0}\right) + \overline{V} H(x, r)\,, \tag{3.4.8}$$

where near the boundary, $H(x, r)$ respects the disordered boundary condition (3.1.6). In general, it will be a sum over periodic functions in x of arbitrary wavelength k_n. The same must be true of the metric coefficients in (3.4.7). Note that, even though there are many periodicities in the disorder source, and hence the spacetime solution, there is a common periodicity $2\pi N/k_0$. The metric coefficients and gauge field will also be functions of the random angles θ_n in the disorder source (3.1.6). In order for the gauge field to be well defined, it must vanish at the horizon, as in the $RN - AdS$ case. Hence, the solution (3.4.8) should vanish as $r \to r_0$.

We will insist on an asymptotically AdS solution, so the metric coefficients in the backreacted geometry (3.4.7) will need to fall off appropriately near the boundary at $r = 0$. We will also need to insist on regularity of the solution at the event horizon, $r = r_0$. The metric coefficients in (3.4.7) should then be expanded near the horizon as

$$\alpha(x,r) = -4\pi T(r-r_0)\left[\alpha_{(0)}(x) + \mathcal{O}((r-r_0)) + \cdots\right], \tag{3.4.9}$$

$$F(r) = -4\pi T(r-r_0)\left[F_{(0)} + \mathcal{O}((r-r_0)) + \cdots\right] + \cdots, \tag{3.4.10}$$

$$\delta(x,r) = \delta_{(0)}(x) + (r-r_0)\delta_{(1)}(x) + \mathcal{O}((r-r_0)^2) + \cdots, \tag{3.4.11}$$

$$\eta(x,r) = \eta_{(0)}(x) + (r-r_0)\eta_{(1)}(x) + \mathcal{O}((r-r_0)^2) + \cdots, \tag{3.4.12}$$

$$\chi(x,r) = \chi_{(0)}(x) + (r-r_0)\chi_{(1)}(x) + \mathcal{O}((r-r_0)^2)\cdots, \tag{3.4.13}$$

$$H(x,r) = (r-r_0)H_1(x) + \mathcal{O}((r-r_0)^2) + \cdots, \tag{3.4.14}$$

where each of the functions in the near horizon expansion may themselves be expanded in the disorder strength $\overline{V}$. For example $\alpha_{(0)} = \alpha_{0(0)} + \overline{V}\alpha_{1(0)}(x) + \overline{V}^2\alpha_{2(0)}(x) + \cdots$, and similarly for the rest of (3.4.9) - (3.4.14). Note that in the limit that $T \to 0$, there will be terms in $\alpha(x,r)$ and $F(r)$ which are proportional to T^{-1} and stay non-zero. These terms originate from the background charge density in the initial $RN - AdS$ geometry. Our convention will be that the first subscript indicates the power of $\overline{V}$ that multiplies the coefficients while the second subscript in brackets indicates the order in the near horizon expansion. Note also that the function $H(x,r)$ in (3.4.14), which appears in the solution to the gauge field to first order in the disorder strength, only starts at $\mathcal{O}(r-r_0)$. This is to ensure that the gauge field vanishes at the horizon, as required by regularity. To keep the discussion as general as possible, as in [259], we turn on every possible perturbation to both the gauge field and the metric, namely $\{a_t(x,r)\,, a_r(x,r),\, a_x(x,r)\}$ and $\{\delta g_{tt}\,, \delta g_{rr}\,, \delta g_{xx}\,, \delta g_{yy}\,, \delta g_{xr}\,, \delta g_{tr}\,, \delta g_{tx}\}$. Note that we do not need to turn on a y component to the gauge field as we will be interested in measuring the conductivity along the disordered x direction. To this end, we use a linear perturbation

$$A_x(x,r) = a_x(x,r) - Et\,, \tag{3.4.15}$$

where E is the constant magnitude of the applied electric field at the boundary.

The perturbations will need to fall off appropriately near the boundary so as not to destroy the asymptotically AdS region. Moreover, we will insist on regularity at the horizon $r = r_0$. This condition may be enforced on the perturbations by replacing the time coordinate with the ingoing Eddington-Finkelstein like coordinate

$$v = t - (4\pi T)^{-1} \ln(r_0 - r) + \cdots . \tag{3.4.16}$$

In light of the regularity condition, the constraints on the near horizon behaviour of the gauge field are

$$a_t(x, r) = a_{t(0)}(x) + \mathcal{O}(r - r_0) + \cdots , \tag{3.4.17}$$

$$a_r(x, r) = \frac{1}{f(r)} \left(a_{r(0)}(x) + \mathcal{O}(r - r_0) + \cdots \right) , \tag{3.4.18}$$

$$a_x(x, r) = \ln(r_0 - r) \left(a_{x(0)} + \mathcal{O}(r - r_0) + \cdots \right) , \tag{3.4.19}$$

along with the relations

$$a_{r(0)} = -a_{t(0)} , \tag{3.4.20}$$

$$a_{x(0)} = \frac{E}{4\pi T} , \tag{3.4.21}$$

each of which follows as a consequence of regularity after switching to the ingoing coordinate (3.4.16). Whereas for the metric perturbations, regularity requires

$$\delta g_{tt}(x, r) = \frac{L^2}{r_0^2} f(r) \left(\delta g_{tt(0)}(x) + \cdots \right) , \tag{3.4.22}$$

$$\delta g_{rr}(x, r) = \frac{L^2}{r_0^2 f(r)} \left(\delta g_{rr(0)}(x) + \cdots \right) , \tag{3.4.23}$$

$$\delta g_{xx}(x, r) = \delta g_{xx(0)}(x) + \mathcal{O}(r - r_0) + \cdots , \tag{3.4.24}$$

$$\delta g_{yy}(x, r) = \delta g_{yy(0)}(x) + \mathcal{O}(r - r_0) + \cdots , \tag{3.4.25}$$

$$\delta g_{tr}(x, r) = \delta g_{tr(0)}(x) = \mathcal{O}(r - r_0) + \cdots , \tag{3.4.26}$$

$$\delta g_{xr}(x, r) = -\frac{1}{f(r)} \left(\delta g_{xr(0)}(x) + \mathcal{O}(r - r_0) + \cdots \right) , \tag{3.4.27}$$

$$\delta g_{tx}(x, r) = \delta g_{tx(0)}(x) + \mathcal{O}(r - r_0) + \cdots , \tag{3.4.28}$$

along with the conditions

$$\delta g_{tx(0)} = -\delta g_{xr(0)}\,, \tag{3.4.29}$$

$$\delta g_{tt(0)} + g_{rr(0)} - 2g_{tr(0)} = 0\,. \tag{3.4.30}$$

Notice that since the disorder source is a sum over periodic functions in x of arbitrary wavelength, the gauge field and metric perturbations will have to be as well. Again, they will all share the same common periodicity $2\pi N/k_0$. Furthermore, the perturbations will all be functions of the random angles θ_n in the disorder source (3.1.6).

The next step, as in the case of a single holographic lattice, is to identify two useful conserved quantities in our background. The first is the boundary current, $J^x = \sqrt{-g}F^{xr}$ which, just as in section 3.3 is a bulk constant by virtue of the Maxwell equations $\partial_r(\sqrt{-g}F^{rx}) = \partial_x(\sqrt{-g}F^{xr}) = 0$. Again, the gauge field can only be a function of x and r. The boundary current, linearized about the gauge field and metric perturbations, is

$$J^x = \sqrt{\frac{\delta F}{\alpha(\eta - \chi^2 F)}}\left\{\alpha\left(\partial_x a_r - \partial_r a_x\right) + \frac{r^2}{L^2}\left[\overline{V}(\partial_x H)\delta g_{tr} + \left(\frac{\mu_0}{r_0} - \overline{V}\partial_r H\right)\delta g_{tx}\right]\right\}\,. \tag{3.4.31}$$

As we are working at finite temperature, there is another conserved quantity, the heat current Q. This conserved quantity is associated with a tensor [292]

$$G^{\mu\nu} = \nabla^\mu \xi^\nu + \frac{1}{2}\xi^{[\mu}F^{\nu]\sigma}A_\sigma + \frac{1}{4}(\psi - 2\phi)F^{\mu\nu}\,, \tag{3.4.32}$$

where ξ^μ is a Killing vector such that $\mathcal{L}_\xi F = 0$. Also, $\mathcal{L}_\xi A = d\psi$ and $i_\xi F = d\phi$, $i_\xi F$ being the interior product of ξ and F. With these definitions, it can be shown that

$$\nabla_\mu G^{\mu\nu} = 3\xi^\nu\,, \tag{3.4.33}$$

provided that the Maxwell (3.1.3) and traced Einstein (3.1.2) equations are satisfied [292].

An appropriate Killing vector is $\xi^\mu = [\xi^t, \xi^r, \xi^x, \xi^y] = [1, 0, 0, 0]$, which satisfies the requirement $\mathcal{L}_\xi F = 0$. There is a conserved quantity associated with (3.4.32) as can

be seen by observing that $G^{\mu\nu}$ is antisymmetric and that it is only a function x and r. Hence, $\partial_x(\sqrt{-g}G^{rx}) = \partial_r(\sqrt{-g}G^{rx}) = 0$, which follows from (3.4.33). The conserved quantity is $Q = \sqrt{-g}G^{rx}$. As shown in [292], this quantity is the heat current in the boundary theory. Linearized about the perturbations, Q is

$$Q = \frac{1}{2rL^2}\sqrt{\frac{\delta F}{\alpha(\eta - \chi^2 F)}}\left\{rL^2\alpha\left[\mu_0\left(1-\frac{r}{r_0}\right)+\overline{V}H\right](\partial_r a_x - \partial_x a_r)\right. \tag{3.4.34}$$
$$+rL^2\alpha\left(\partial_r\delta g_{tx} - \partial_x\delta g_{tr}\right) + \left(r^3\overline{V}\mu_0\left(1-\frac{r}{r_0}\right)\partial_r H + 2L^2\alpha - \frac{\mu_0^2 r^3}{r_0}\left(1-\frac{r}{r_0}\right) - \frac{\mu_0 r^3\overline{V}}{r_0}H\right.$$
$$\left.\left.-L^2 r\partial_r\alpha + r^3\overline{V}^2 H\partial_r H\right)\delta g_{tx} - \left(L^2 r\partial_x\alpha + \mu_0 r^3\overline{V}\left(1-\frac{r}{r_0}\right)\partial_x H + r^3\overline{V}^2 H\partial_x H\right)\delta g_{tr}\right\}.$$

In what follows, we will make use of the perturbative expansion in the disorder strength and, similarly to the initially uncharged case in section 3.3, we will ignore terms of order $\overline{V}^2\delta g$ and higher. Following [259], the next step is to evaluate the constants J^x (3.4.31) and Q (3.4.34) near the event horizon at a fixed temperature T. Using the expansion for the metric coefficients (3.4.9)-(3.4.14) and the perturbation in (3.4.17)-(3.4.19) and (3.4.22)-(3.4.28), we find

$$J^x = \sqrt{\frac{\delta_{(0)}F_{(0)}}{\alpha_{(0)}\eta_{(0)}}}\left[\alpha_{(0)}\left(E + \partial_x a_{r(0)}\right) + \frac{r_0^2}{L^2}\left(\frac{\mu_0}{r_0} - \overline{V}H\right)\delta g_{tx(0)}\right], \tag{3.4.35}$$

and

$$Q = -2\pi TL\delta g_{tx(0)} = \text{constant}\,, \tag{3.4.36}$$

meaning that $\delta g_{tx(0)} = $ constant. Next, we expand Q (3.4.34) to next order in the near horizon expansion and use the linearized equations of motion to express it entirely in terms of near horizon data. This expression may then be used to find an expression for $\delta g_{tx(0)}$ in terms of E. The next order expansion of Q is messy and contained in appendix B. The result is that

$$\alpha_{(0)}\left(\mu_0 - r_0\overline{V}H_{(1)}\right)\left(E + \partial_x a_{r(0)}\right) - 4\pi T r_0\partial_x\left(\alpha_{(0)}\delta g_{tr(0)}\right) \tag{3.4.37}$$
$$+\left(8\pi T\alpha_{(0)} + 2\frac{r_0^2}{L^2}\overline{V}\mu_0 H_{(1)} - \frac{r_0\mu_0^2}{L^2} + \frac{8\pi^2 T^2 r_0\alpha_{(0)}\chi_{(0)}^2}{\eta_{(0)}} - \Omega_{(0)}(x)\right)\delta g_{tx(0)} = 0\,,$$

where $\Omega_{(0)}(x)$ is a function of metric coefficients near the horizon. It is found in appendix B. To get an expression for J^x in terms of E and $\delta g_{tx(0)}$, we integrate (3.4.36) over the common periodicity $2\pi N/k_0$. Then, doing exactly the same thing with (3.4.37), we can relate E to $\delta g_{tx(0)}$. Substituting this into the expression for J^x gives us the desired relation between J^x and E. The final result is

$$\frac{J^x}{E} = \frac{I_1}{I_2 + I_3}\,, \tag{3.4.38}$$

where

$$I_1 = \frac{k_0}{2\pi N}\int_0^{2\pi N/k_0}\left[\frac{2r_0\mu_0^2}{L^2} - \frac{4r_0^2\mu_0}{L^2}\overline{V}H_{(1)} - 8\pi T\alpha_{(0)} - \frac{8\pi^2T^2r_0}{\eta_{(0)}}\alpha_{(0)}\chi_{(0)}^2 + \Omega_{(0)}(x)\right]dx\,, \tag{3.4.39}$$

$$I_2 = \frac{k_0^2}{4\pi^2N^2}\int_0^{2\pi N/k_0}\sqrt{\frac{\eta_{(0)}}{\alpha_{(0)}\delta_{(0)}F_{(0)}}}dx \tag{3.4.40}$$
$$\times\int_0^{2\pi N/k_0}\left[\frac{2r_0\mu_0^2}{L^2} - \frac{4r_0^2\mu_0}{L^2}\overline{V}H_{(1)} - 8\pi T\alpha_{(0)} - \frac{8\pi^2T^2r_0}{\eta_{(0)}}\alpha_{(0)}\chi_{(0)}^2 + \Omega_{(0)}(x)\right]dx\,,$$

$$I_3 = \frac{k_0^2r_0}{4\pi^2L^2N^2}\int_0^{2\pi N/k_0}\left[\alpha_{(0)}^{-1}\left(\overline{V}r_0H_{(1)} - \mu_0\right)\right]dx \tag{3.4.41}$$
$$\times\int_0^{2\pi N/k_0}\sqrt{\frac{\alpha_{(0)}\eta_{(0)}}{\delta_{(0)}F_{(0)}}}\left(\mu_0 - r_0\overline{V}H_{(1)}\right)dx\,.$$

All of the functions in the integrals (3.4.39)-(3.4.41) may be expanded to second order in the disorder strength $\overline{V}$, provided the solutions are known. The final step after the expansion is to take the disorder average (3.1.8) of (3.4.38). The disorder averaged conductivity is then $16\pi G_N\langle\sigma\rangle_D = \langle J^x/E\rangle_D$.

By taking the $\mu_0 = 0$ limit, it may be possible to find temperature dependent corrections to the disorder averaged DC conductivity in (3.3.11). It may be that a temperature dependence introduces a negative correction to the conductivity. It is possible that the metric coefficients $\alpha(x,r)$, $F(r)$, $\delta(x,r)$, $\eta(x,r)$ and $\chi(x,r)$ in (3.4.7) could contain additional dependence on temperature, so computing the full correction to the conductivity would require knowing these functions. This way, the integrals in (3.4.39), (3.4.40) and (3.4.41) may be evaluated.

While we do not know the solutions to the metric coefficients, any additional temperature dependence must be such that they are not unbounded functions of T since the perturbative corrections should not overwhelm the baseline AdS conductivity. This way, the disorder averaged conductivity would not be at risk of becoming negative. Studying of how temperature dependence alters the disorder averaged DC conductivity in the $\mu_0 = 0$ limit is worth further investigation. This is especially true when thinking beyond a perturbative approach as it may reveal interesting features about the possible suppression of transport in holographic models of disorder.

3.5 Summary and outlook

In section 3.1 we construct a bottom-up holographic model with perturbatively charged disorder. Starting from a bulk Einstein-Maxwell action, we include disorder in the dual theory by using a spectral representation. This technique is known to simulate a stochastic process [278]. This is achieved by including a randomly varying chemical potential (3.1.6) made up of a sum of N periodic functions along one of the boundary directions; an approach reminiscent of the disordered holographic superconductors studied in [277], [279] and [280]. The random chemical potential contains two parameters, a wavenumber k_0 which is held fixed in the large N limit and $\overline{V}$ which controls the strength of the disorder. The parameter $\overline{V}$ is taken to be small and is used as a perturbative handle to construct a bulk solution. A bulk gauge field is turned on which approaches the fluctuating chemical potential (3.1.6) near the spacetime boundary. By letting the gauge field backreact on the initially clean (i.e. zero disorder) AdS_4 geometry, we construct an asymptotically AdS solution to the bulk equations of motion (3.1.2) and (3.1.3) at second order in the disorder strength in section 3.1.1.

We evaluate the disorder average (3.1.8) of the second order metric coefficients (3.1.18), (3.1.19) and (3.1.20), in section 3.1.2 and find that they are compactly expressed in terms

of special functions. By carefully evaluating the large N limit, we find a divergence in the deep interior as $r \to \infty$ in two of the metric coefficients (3.1.21) and (3.1.22), indicating that the solutions must be regulated.

In section 3.2, we resum the disordered solution found in section 3.1 by adapting the standard Poincaré-Lindstedt method for regulating perturbative solutions to differential equations, similarly to the case of scalar sourced disorder in [281]. We find a regulated, second order, solution to the equations of motion with metric functions (3.2.22), (3.2.23) and (3.1.23), where the previously noted divergences are removed. The averaged resummed solution is devoid of curvature singularities through second order in the disorder strength.

With the resummed solution at hand, we study the resulting DC conductivity along the disordered direction in section 3.3. We directly access the DC conductivity of the model by adapting a technique first proposed in [292]. The idea is to turn on a source linear in time and take advantage of the existence of conserved quantities in the bulk to find a relationship between the boundary current and the magnitude of the applied electric field. The DC conductivity may then be extracted from Ohm's law. By virtue of the nature of the disordered spacetime solution in this case, turning on a bulk gauge field perturbation along the disordered direction results in a complicated set of equations of motion. As is the case for single holographic lattices [162], the gauge field perturbation further sources a whole set of possible metric fluctuations. By taking advantage of our perturbative handle, namely the disorder strength, the situation simplifies and the relevant metric fluctuation can be solved via the linearized equations of motion up to second order in perturbations. The disorder averaged DC conductivity is computed in (3.3.11) which is found to be the usual AdS conductivity plus a correction at second order in the disorder strength, a result reminiscent of the single holographic lattices studied in [320].

Section 3.4 makes some observations about adding a disordered chemical potential to an initially clean system with a finite charge density. In this case, the baseline geometry is

the $RN-AdS$ solution. The presence of an initial charge density changes the character of the backreacted equations of motion, as the perturbative contributions originating from the disorder source now mix with the baseline gauge field. The result is that geometry may receive corrections at all orders in the disorder source, unlike the initially uncharged case studied in section 3.1. At second order, the traced Einstein equations are complicated and it is not clear that there is a compact analytic solution. It is still possible to extract some information about the form of the disorder averaged DC conductivity in this case by applying the techniques of [292] and [259]. The procedure is similar to the initially uncharged case in section 3.3, except that now the baseline solution (and hence the disordered solution) has an event horizon. By writing down a broad ansatz for a $3+1$ dimensional disordered geometry at finite charge density and temperature (3.4.7), we show that the disorder averaged DC conductivity may be expressed entirely in terms of near horizon data (3.4.38), as is the case for the holographic lattices studied in [259]. We leave the difficult task of finding a disordered, finite charge density, spacetime solution for future work.

There are many open questions with regard to explicit implementations of holographic disorder, both in terms of studying the properties of the dual field theory as well as understanding the kinds of bulk geometries that arise in the process.

A natural extension to our work here is to disordered holographic superconductors, such as those studied in [277], [279] and [280]. A spectral representation for the disordered chemical potential is also used in these studies and the properties of the superconducting transition are studied numerically. It would be interesting to understand how the inclusion of backreaction of the disorder source onto the spacetime geometry changes the picture here. For example, how is the appearance of the superconducting phase transition affected? Is the critical temperature significantly changed? Is possible to get an analytical handle on a a critical amount of holographic disorder beyond which the conductivity becomes completely suppressed and the superconducting phase transition does

not occur? This previous question is particularly pertinent with regards to many-body localization. If such a transition does occur, what kind of bulk geometry is required and how does it fit into conventional gravitational models? In particular, if a localization transition does occur in the dual theory, would the bulk probe effectively become stuck[2] at some radial position? Would this translate to a well defined mobility edge at the corresponding energy scale in the dual theory? It would also be interesting to understand the behaviour of time dependent probes in such a background.

To fully study this problem, it may be necessary to move beyond the perturbative disorder studied in this paper and an analytical approach may be ill-suited and numerical solutions may be required. In such a case, it would be interesting to understand if the techniques used in [281] for scalar disorder and [258] for holographic lattices would be useful.

In [281], disorder is sourced by a scalar field in $2+1$ dimensions and the disorder averaged metric is found to display an emergent Lifshitz scaling. It would interesting to classify the possible IR geometries that can be produced in this way, hopefully leading to a better understanding of disorder fixed points of condensed matter systems. For example, could an interior geometry with an emergent hyperscaling violation exponent be generated via a back-reacted disordered source? How about IR geometries that break rotations, i.e. in relation to Bianchi models [245], [249]? In other words, what kind of IR disordered fixed points can be constructed via holography?

In [276], an ansatz for a disordered geometry is proposed and the dynamics of a scalar field in this background are studied. Using techniques from random matrix theory, a transition is observed which is reminiscent of a disorder driven metal-insulator transition. Understanding more than one explicit example of a geometry which displays this behaviour as well as the matter content required to support such solutions in a gravitational theory may shed light on the minimal ingredients necessary for accessing

[2]We thank Omid Saremi for raising this issue with us.

disordered phenomena via holography. It would also be worthwhile understanding how the proposed spacetime in [276] fits in with backreacted disordered geometries.

Finally, our results for the initially uncharged case in sections 3.1, 3.2 and 3.3 depend sensitively on the disorder distribution. In this paper we have focused on the effect of Gaussian random disorder. It would be interesting to extend our results to other distributions and understand how the resulting backreacted geometry and transport properties are modified.

Chapter 4

Future Directions

In this chapter we will point out possible future directions with regards to the results presented in chapters 2 and 3 as well as some general future avenues of research in holography. We will focus primarily on future prospects for symmetry breaking in holography with a bent towards potential applications and exploration of their gravitational duals. We will also discuss some aspects of holographic thermalization and what this may tell us about quantum many-body physics. Finally, we will discuss the current program of understanding how quantum information theory constrains potential gravity dual solutions and what this suggests about the emergence of gravity and spacetime emerge from a quantum theory.

4.1 Symmetry breaking in gauge/gravity duality and future applications

Understanding exactly which symmetries are available to be broken in bottom up holographic models and what dual physics they encode is central to mapping out the range of applicability of holography. Many examples have been discussed in this thesis, including boost symmetry, translational symmetry and rotational invariance. In the context of the

latter case, it remains to be shown if in general the Bianchi type geometries discussed in section 1.5.6 can be connected to an asymptotically well behaved region. In [250], it was shown that in principle, there should exist a class of geometries which interpolate between several of the Bianchi type spacetimes and an asymptotically AdS or Lifshitz region. The null energy condition is used as a guiding principle in that the proposed geometries obey this sensible energy condition. It is, as of yet, unclear if these interpolating geometries are solutions to a gravitational theory with a simple matter sector. While the Bianchi type VII geometry has been used to model holographic metal-insulator transitions [246], it still unclear precisely what kind of boundary physics the other geometries in this classification describe. Understanding their dual interpretation would help clarify how these holographic models fit within the larger context of applied holography.

It is also important to address issues of stability when it comes to bottom-up holographic models. The gravity solutions proposed to capture the relevant boundary physics may not also be stable. Ultimately, the bottom-up solutions should somehow descend from a consistent truncation of a higher dimensional theory like supergravity, or optimistically full string theory. As emphasized in [322], it is not sufficient to demonstrate stability in the truncated theory, but rather it is important to study the full theory. In the full theory, it may be that there are additional excitations which violate the Breitenlohner-Freedman bound and render an AdS vacuum unstable. Stability analysis is technically challenging, but would be worth pursuing as it could provide insight into the kinds of top-down embeddings that are available for bottom-up models.

In recent years, it has become clear that a wide variety of interesting interior gravitational solutions are available, even in seemingly simple theories. This has been demonstrated within the context of both Einstein-scalar theory and Einstein-Maxwell [281], [258]. It is interesting to speculate just how far this program of finding and classifying IR geometries may be taken and how they may be applied to modelling real world systems. An example already exists of how to generate an emergent Lifshitz scaling in the deep

IR simply by applying the right kind of perturbation to AdS_3. The idea is to add a disordered scalar field, using a spectral representation as was done in chapter 3 and let it backreact on the geometry. Choosing a Gaussian distribution leads to the emergence of a critical exponent z which is controlled by the strength of the disorder. The effect has now been show to persist in various dimensions even at finite temperature [282]. It is interesting to wonder if any of the other typical interior geometries studied in the context of holographic symmetry breaking (see section 1.5) can be generated in a similar way.

A particularly pertinent example is hyperscaling violation (HSV), introduced in section 1.5.4 and discussed at length in chapter 2. A nontrivial hyperscaling violation exponent may be associated with certain spin-glass phases of the Ising model, where random quenched disorder plays an important role [323]. Given this relationship, it is a natural question as to whether or not such behaviour may be understood holographically.

The critical first step to such an investigation is the identification of the minimal matter content required in a bottom up holographic model. In order to find a HSV solution in Einstein gravity, a scalar field and a gauge field are usually required (although a massive gauge field also works) [212], [183]. By including more than one disordered field in the gravity model, it may be possible to access increasingly exotic IR geometries. Also, selecting different distributions and disorder strengths for the bulk fields may lead to interesting competitions between the disorder sources. Possibilities include disorder driven phase transitions and regimes of coexistence where multiple phases exist simultaneously, similar to the coexistence of several holographic superconducting phases mentioned in section 1.4.4.

There is also evidence that properties of glassy systems can be accessed via holography [324], [325]. The idea is to construct a class of asymptotically AdS metastable black hole bound states at finite temperature and chemical potential. There are an exponentially large number of possible configurations and solutions display logarithmic relaxation times, similar to glassy systems.

As of yet there is no well established complete theory of the glass transition. It is still not exactly known what causes the dynamical slowing down observed in supercooled liquids. Relaxation time scales in the system blow up to huge values. One ubiquitous way to see this is in the dramatic increase of viscosity as the temperature is lowered to the glass transition temperature sufficiently quickly. In particular, this increase in relaxation times happens without any structural changes to the system; there are no changes in spatial order compared to the liquid phase.

Structural glasses are not described by equilibrium thermodynamics; rather they are metastable states that never manage to relax to the true equilibrium configuration of the system in finite time. In particular then, the properties of glasses depend on the details of their history. They are said to display aging, meaning that the properties of the system depend on how long it has been since it fell out of equilibrium (i.e. how long it has been since the glass transition occurred). This phenomenon usually shows up as non-exponential relaxation rates for observables of the system.

One point of view is that glasses have a rugged free energy landscape with exponentially many local minima. For a review see [326]. The system basically gets hopelessly stuck jumping around this landscape trying to find the true global minimum, which it never reaches in finite time. Such systems are inherently non-ergodic as they do not ever manage to explore their entire phase space. An example of such a model is a spin glass, in which there are exponentially many solutions for the local magnetization density below the glass transition temperature.

This landscape perspective does not provide a full picture. While there are no structural changes at the glass transition, there are dynamical changes. Supercooled liquids display localized regions of highly cooperative motion and regions with almost no cooperative motion. That is, regions where the motion of particles are highly correlated with each other and a region where there is virtually no correlation. The size and distribution of these regions changes drastically when approaching the glass transition. The evolution

of these regions may be observed in numerical simulations of supercooled liquids. These phenomena are better explained using a kinetic theory of the glass transition. For a review, see [327].

Crucially, in order to apply holography to this kind of problem, bulk translational invariance must be broken. The reason for this stems from the viscosity bound, $\eta/s = 1/4\pi$ (1.3.47). When the temperature is lowered, the entropy of the black brane decreases and hence the viscosity in the dual theory must also decrease. This is exactly the opposite of what is expected of a glass forming system; as temperature is lowered, viscosity should grow. To get around this problem, translational invariance must be broken in order to circumvent the viscosity bound.

The examples of disordered holographic systems discussed in section 1.5.8 and in chapter 3 concern quenched disorder, meaning that there is no time evolution associated to the source of impurity. While this is the case for spin glasses, it is not true for structural glasses in which disorder is spontaneously generated at the transition temperature. Nevertheless, it would be interesting to probe the backreacted type geometries to see if evidence of glassy behaviour arises, especially in the dual transport properties. Understanding how viscosity is affected by the addition of this kind of disorder would be worthwhile in the sense that it may point towards a class of real world low temperature systems that display similar behaviour. It would also be interesting to understand the behaviour of time dependent probes in such backgrounds. By modifying the disorder strength, interesting transitions in the relaxation time of time dependent probes may result.

Many recents studies of novel IR geometries involve sophisticated numerical techniques. The advantage is that numerical solutions give access to strongly disordered regimes. It is possible that radically different emergent behaviour may occur outside of the range of perturbative disorder. Numerical techniques may be necessary in order to access the regime where a localization transition occurs due to the necessity of having a

strongly disordered system.

Another obvious question is, what happens in more complicated holographic models when disorder is incorporated? In [277], [279] and [280] holographic s-wave and p-wave superconductor models were studied with a disordered chemical potential. The random chemical potential in the boundary theory is introduced using the spectral approach used in chapter 3, and the equations of motion for the bulk fields are solved numerically in a fixed AdS-Schwarzschild geometry, as discussed in section (1.5.8). It is curious to wonder what would happen if gravitational backreaction is taken into account. This is particularly true in light of [282], which showed that taking into account gravitational backreaction due to scalar disorder in an initially clean AdS-Schwarzschild geometry results in an emergent Lifshitz scaling, as in the zero temperature case [281]. Accounting for the effect in a holographic superconductor model may lead to non-trivial modifications of the critical temperature. In particular, for sufficiently strong disorder, it might be expected that the critical temperature becomes highly suppressed, making the transition to a superconductor state increasingly disfavourable. This expectation is grounded in weakly coupled intuition; it is an interesting question as to whether or not this naïve expectation is modified by strong coupling effects.

It would ultimately be interesting to understand how much holography can say about the physics of quantum many-body systems at strong coupling. On way to approach this is by studying equilibration times after a perturbation to a system. A naïve expectation is that a mild perturbation to an asymptotically AdS geometry would eventually settle down and that the spacetime is stable. Remarkably, this turns out not to be the case. In [133] it was shown that the evolution of a real, massless and spherically symmetric scalar field in global AdS will generally result in gravitational collapse for almost any, even arbitrarily small, initial field amplitude. This study describes the onset of the instability as being the result of (nonlinear) resonant interactions between the normal modes that characterize the system at the linear level. It is argued that this leads to a direct turbulent

cascade of energy to high mode numbers and that this makes the gravitational collapse inevitable. The energy transfer seems to be going backwards to what would be expected from usual fluid turbulence. Subsequent analysis showed that if the initial data consisted of only one mode, the resonant self-interaction is avoided and just results in a constant shift of the frequency of the mode.

Following up on this observation, [328] studied this problem from the context of thermalization in a potential dual field theory. If gravitational collapse does occur and a black hole is formed, the dual state is thermal, meaning that the system has reached equilibrium. It is observed that if the system starts off with all of the modes initially populated and the mode amplitudes fall off sufficiently fast for the high mode numbers, the resonant self-interaction has the same effect as in the case of single-mode initial data and behaves like a frequency shift. In this case, gravitational collapse can be avoided. There are two effects coming into play here to determine if gravitational collapse will occur or not: gravitational focusing and nonlinear dispersion of the propagating scalar field. If gravitational focusing dominates, then collapse to a black hole results. On the other hand, if the initial scalar profile is distributed broadly enough, the system evolves without ever approaching a static or stationary solution. In this picture, the boundary CFT never thermalizes at late times. Thermalization times in holographic models in global AdS_5 dual to theories with non-equal central charges $c \neq a$ were studied in [329].

This raises an interesting possible connection to the physics of closed many-body systems. A closed many-body system is one in which the system is not in any contact with an external reservoir. In other words, it is an isolated system. A recent review may be found in [268]. After long time unitary evolution, the system will either thermalize or become localized (in real space). In the former case, the system can act as its own reservoir and thermal equilibrium is achieved with the final state being parameterized by a small number of observables, such as temperature, pressure, etc. In the latter case, the system does not act as its own reservoir and so does not thermalize. Instead, the system

is able to remember some details of its initial state, even after an arbitrarily long time. The states which fail to thermalize are highly-excited and have a non-zero energy density even in the thermodynamic limit. Many-body localized states violate the eigenstate thermalization hypothesis (ETH) [268] which states that all many body eigenstates of a Hamiltonian are thermal. An example of a system which violates the ETH is a system of interacting spins on a lattice with a disordered onsite magnetic field. Once a critical amount of disorder is present in the system, many-body localization occurs in the sense that DC spin and energy transport are suppressed and thermalization can never occur. This is true for both the strongly and weakly interacting cases [268].

The many-body localization transition marks the breakdown of the applicability of equilibrium quantum statistical mechanics to the long-time properties of the system. There is a phase transition at a critical disorder strength between a thermal phase and a many-body localized phase in which the ETH is violated and some memory of the local initial conditions of observables remains even for arbitrarily long times. The transition is not visible to equilibrium thermodynamics, but rather shows up as an eigenstate transition, in which there is a sharp transition in the properties of the many body eigenstates and hence the dynamics of the system.

It is interesting to compare this picture to that of the instability of global AdS, especially in the case pointed out in [328] where a class of scalar perturbations never thermalizes. Specifically, in [328] two modes are initially excited and the rest are set to zero. It is initially found that all the energy is contained in the two modes that are turned on. Energy flows out to the other modes for some time at which point an inverse energy cascade occurs and all of the energy flows back to the initial modes. The state returns to its original configuration and this recurrence behaviour repeats itself. The energy does not just keep cascading to higher and higher modes, instead it sloshes around between the modes and the system settles into a sort of metastable state. Energy equipartition never occurs and the system does not thermalize. This has a striking similarity to the

closed many-body systems with states that localize. There, a memory of the initial state is always preserved. In the gravity case, the active modes eventually return to their original configuration and continue to do so repeatedly. It is tempting to associate this behaviour with a many-body localized state in the dual theory, however care should be taken here. In the field theory example described above, the addition of sufficiently strong disorder is necessary for the many-body localization to occur. In the gravity problem, the system is spherically symmetric and translationally invariant. Could it be that this is describing a kind of translationally invariant many-body localization? How does this reflect the non-ergodicity of a localized system, if at all? It would be interesting to study this problem from the perspective of the eigenvalue distribution of a time dependent bulk probe; how does it differ with respect to the scalar perturbations that do thermalize? Is there any evidence for the suppression of DC transport?

In [271] and later in [272], an implementation of the replica trick was studied in a holographic context. The idea was to translate this standard tool for studying disorder systems in a field theory into a gravity theory and to apply it to learn about disorder at strong coupling. This is achieved by, as in the field theory implementation, replicating every bulk field including the metric n times. By studying the behaviour of correlation functions at leading order in large N, it is argued that n replicated copies of a CFT with a holographic dual may be understood as a CFT with a multi-trace deformation. Using this perspective, [272] showed that to leading order in the large N expansion, the connected correlation functions in the presence of random disorder vanish in the strongly coupled dual field theory. Crucial to this observation was the assumption that replica symmetry is unbroken.

Replica symmetry means that each copy of the theory used in the replica trick is indistinguishable from the other. That is it leaves the permutation symmetry between the replicas unbroken. In such a solution, the degree of correlation between each of the replicas is assumed to be the same. As this symmetry is not present in the initial system,

it should be thought of as auxiliary. This is sensible from the point of view of a model of quenched disorder in that such systems are generally thought to be self-averaging. In other words, the macroscopic properties of the system should be independent of the specific microscopic realization of the disorder. Hence, physical properties can be measured by taking disorder averages.

On the other hand, assuming that each of the replicas is indistinguishable from the others can lead to unphysical solutions in some models. An example is the famous Sherrington-Kirkpatrick (SK) model of a spin glass. The model describes a set of interacting spins where each spin interacts with all of the others in the system, not just nearest neighbours. Each interaction is taken to be described by an independent Gaussian random variable. A review may be found in [330]. A replica symmetric solution is available for the SK model which breaks down at low temperatures, predicting things like a negative entropy density.

Breaking the replica symmetry turns out to be crucial for obtaining the correct low temperature solution. In this situation, it is imagined that the degree of correlation between each of the replicas is not the same. Some replicas could clump together and have a greater overlap with each other than with the other replicas. This process can repeat itself over and over again resulting in increasingly finer regions of overlap between the various replicas. By measuring the distance between the correlated clusters of replicas at each step an ultrametric structure emerges. An ultrametric space is one in which the usual triangle inequality between three points is replaced by a more restrictive inequality of the form [330]

$$d(a,b) \leq \max\{d(b,c), d(c,a)\}\,. \tag{4.1.1}$$

The physical picture in the spin glass case is that as temperature is lowered below the glass transition, the phase space of the system is broken up into increasingly small regions, separated by large free energy barriers. The different separated regions correspond to possible ground states of the macroscopic system which are increasingly dissimilar as a

function of their distance apart in the ultrametric space. This process continues on to zero absolute temperature. The final picture is of a landscape separated by large free energy barriers arranged in a fractal tree branch pattern characteristic of ultrametricity . It is clear that the breaking of replica symmetry and the emergence of an ultrametric pattern is related to the breaking of ergodicity in the sense that not every microscopic state can be accessed by the system.

The physical implications for a holographic gravity model are unclear. It is an interesting question to wonder about how the formation of an ultrametric structure due to replica symmetry breaking in the boundary theory will appear in the gravity theory. This is especially true at finite temperature, as the gravity dual possesses a black hole. As the temperature is lowered, what kind of phase transition occurs with regards to the horizon structure of the black hole? Will it develop a similar ultrametric structure? This might be the case as the breaking of replica symmetry alters the low temperature free energy in the field theory. In the case of KS model, the negative entropy density is also removed. These quantities are geometric in the bulk, being controlled by the black hole horizon, so there should be some corresponding modification of the near horizon physics. It is also unclear how the dimensionality of the bulk plays into such a picture. Higher dimensional black holes display a richer solution space than their lower dimensional counterparts. Is there some critical dimension below which such a phenomenon cannot occur? What would this imply about the boundary dual?

On top of the open applications of holography, there are many remaining questions about the full holographic dictionary. In particular, there is considerable recent evidence that every bulk surface, both minimal and non-minimal, has an interpretation in the boundary theory and are remarkably connected to quantum information theory.

4.2 Gravity and entanglement entropy: the emergence of spacetime

The Ryu-Takayanagi (RT) formula discussed in section 1.3.5 demonstrates that information theoretic concepts have a natural geometric interpretation in a dual gravitational theory. Many generalizations have since been proposed that place this connection on a more solid footing. In [331] and [24], the entanglement entropy of a hole in spacetime was calculated. The hole is constructed by concentrating on a family of observers who are all causally disconnected from a spherical region at the origin of an asymptotically global AdS_3 geometry. It is argued that these observers can only gain access to some of the information about the boundary theory. The bulk observers measure a quantity called residual entropy (also sometimes called differential entropy), which characterizes their uncertainty about the state of the boundary theory based on the information they have access to. This residual entropy is directly reproduced in the bulk by the areas of circular holes. This construction was extended to bulk surfaces which vary in time for a class of planar symmetric geometries in [332]. Furthermore, in [97], it was shown that using the concept of residual entropy in the boundary theory, it is actually possible to reconstruct a wide class of bulk surfaces in more than $2+1$ dimensions. These observations lead to the interesting question of just how much of the bulk geometry can a boundary observer reconstruct? Studying this question has led to interesting extensions of the holographic dictionary. For example, in [333] the residual entropy is shown to encode the entanglement cost of transmitting the state of a subregion on the boundary to another subregion using a merging protocol. This gives a direction information theoretic interpretation of the bulk curves used to calculate the residual entropy.

Another key observation is that, in some cases, there are geometries in which no minimal surface can probe every region. A spacetime with an event horizon is a canonical example [334]. This leads to the notion of an entanglement shadow, or a region of

spacetime not directly accessible by a minimal surface, which nevertheless contributes to the entanglement entropy of the boundary theory. In boundary theory language, there are contributions to the entanglement entropy arising from internal degrees of freedom that are not spatially organized. In [335], a concept termed entwinement was introduced which is associated with the area of non-minimal geodesics which wrap many times around a singularity in the examples considered. It is argued that these surfaces are necessary in order to account for the entanglement entropy due to the shadow region and may be important for reconstructing the inside of a black hole horizon via holography.

An interesting observation in this context stems from locality in the bulk. In [336], [337], [338] it was argued that in the low energy limit localized bulk operators may actually be dual to smeared out, non-local boundary operators. Following up, [339] showed that a semiclassical representation of bulk fields as operators in the dual CFT leads to problematic behaviour near the horizon of a black hole in the bulk. Specifically, there is a break down in locality in that the bulk fields fail to commute at spacelike separations. This failure to commute is characterized by an amount of the order $\exp(-S/2)$, where S is the Bekenstein-Hawking entropy of the black hole. This result stresses that further corrections beyond the semiclassical limit may be necessary to properly reconstruct the bulk geometry.

In [340], it was shown that by taking the RT formula as input and applying it to a CFT at leading order in large N, the equations of motion for a potential gravitational dual theory are the Einstein equations linearized about AdS. Moreover, by using a more general Wald functional instead of the RT formula as input, the bulk must satisfy the linearized equations of motion with higher curvature corrections. This result was extended in the case of the RT formula in [341] and [342] to include $1/N$ corrections and found that the linearized vacuum Einstein equations are supplemented by source term, encoding the bulk energy momentum tensor. These results provide strong evidence that quantum information theory in the boundary and the emergence of spacetime in a

potential dual gravity theory are deeply interconnected. The ultimate fantasy goal here is to completely reconstruct a bulk geometry from nothing more than field theory inputs.

In fact, using the standard inequalities of quantum information theory as input, such as strong subadditivity, [226] pointed out that natural geometric restrictions arise in the dual gravity theory. In particular, enforcing strong subadditivity translates to satisfying the averaged null energy condition in the bulk. This seems like a physically sensible result and it is interesting to wonder about how other information theoretic restrictions on the boundary translate into conditions on the bulk geometry. Ultimately, such studies may help uncover exactly which kinds of geometric theories are accessible via holography given a sensible boundary theory. It is also an interesting question as to whether this construction can be extended to other types of boundary theories. In particular does starting from a non-relativistic boundary theory, working out the information theoretic inequalities and applying the holographic dictionary for the Lifshitz case [195] return a geometry with a non-trivial dynamical critical exponent? It should be expected that the null energy condition would apply here as well and restrict z to values greater than or equal to one. Does the same construction work for the HSV geometries?

Another interesting open problem concerns the available spacetime solutions of Vasiliev higher spin theory in four dimensions, discussed in section 1.2.3. As this class of higher spin gauge theories always contains spin two, there should be a wide variety of possible spacetime solutions available to study within this context. AdS and dS solutions appear as natural vacuum solutions to the Vasiliev equations and may be found by inspection. The Vasiliev equations themselves generally contain many more fields which are set to vanish for the basic AdS and dS type solutions. By including these additional fields, it is natural to suspect that more solutions become available. Exactly what these solutions are and what kind of geometric properties they encode are an open question. Considerable progress has been made on this front in three dimensions where black hole solutions are known [68] as well as asymptotically Lifshitz solutions [343]. The three dimensional case

is comparatively simpler than the four dimensional case owing to the restrictive nature of three dimensional gravity. In particular, the Chern-Simons formulation of three dimensional gravity provides the necessary holonomy condition for diagnosing the existence of a black hole horizon in a higher spin model. There is, as of yet, no analogue for higher dimensional higher spin theory. It would be worth investigating the possible solution space in this context, particularly with regards to holographic applications.

In short, there any many open and interesting avenues of investigation in the context of pure and applied holography. While this program may end up teaching us valuable lessons about strongly coupled quantum field theories and point towards some universal behaviours we might expect to see in condensed matter physics, there are plenty of opportunities to learn about the nature of gravity as well. The connections between quantum information theory and the emergence of spacetime lead to the tantalizing possibility that holography may provide some clues about exactly what it means to have a theory of quantum gravity. The applications that we have pointed to in this thesis suggest that perhaps the worlds of strongly coupled quantum field theory, quantum many-body systems and quantum information theory are not so widely separated from the ultimate question of understanding the nature of quantum gravity.

Appendix A

Constants Appearing in the NEC

In this appendix we provide the constants C_i that arise in the equations of motion and in the null energy condition in chapter 2. Readers who are not interested in the technical details should skip ahead to chapter 3 They are

$$C_1(d,\beta) = -\frac{d}{2}(d+2\beta-1)\,, \tag{A.0.1}$$

$$\begin{aligned} C_2(d,\alpha,\beta,\eta_i) = &-\frac{1}{2L^2}\Big\{\big[4\alpha^4 - 8(1-\beta)\alpha^3 + (-44+88\beta-40d\beta-44\beta^2-8d^2+44d)\alpha^2 \\ &+(-144\beta+16d^2-64d+104d\beta+48-8d^2\beta+144\beta^2-40d\beta^2-48\beta^3)\alpha \\ &+2d-4d\beta^2-2d^2\big]\eta_1 + \big[2\alpha^4+(2d+4\beta-4)\alpha^3 \\ &+(13d-d^2+44\beta-22-22\beta^2-12d\beta)\alpha^2 \\ &+(8d^2-6d^2\beta+72\beta^2+24-72\beta-32d-24\beta^3-26d\beta^2+58d\beta)\alpha \\ &+5d-12\beta^3 d-11d^2\beta^2+16d^2\beta+29d\beta^2-6d^2-22d\beta+d^3-2d^2\beta\big]\eta_2 \\ &+\big[(2\alpha\beta+2d\beta-2\alpha+2\alpha^2-d+2d\alpha+d^2)\times(-24\beta^2+48\beta-24 \\ &+2\alpha\beta-2\alpha+2\alpha^2-10d\beta+9d+2d\alpha-d^2)\big]\eta_3\Big\}\,, \end{aligned} \tag{A.0.2}$$

$$C_3(d,\alpha) = \frac{d}{2}(d+2\alpha-1)\,, \tag{A.0.3}$$

$$
\begin{aligned}
C_4(d,\alpha,\beta,\eta_i) = \frac{1}{2L^2}\Big\{\big[& -12d\beta^2 - 8\alpha^3\beta + 20\alpha^2 d - 8d\alpha\beta + 24\alpha^2\beta - 12\alpha^2\beta^2 \\
& +8\alpha^3 - 12\alpha^2 + 6d^2 + 4\alpha^4 - 8d\alpha^3 - 8d^2\beta + 24d\beta - 6d\big]\eta_1 \\
& +\big[13\alpha^2 d - 3d + 4\alpha^3 - 6\alpha^2 + 2d^2 + 2\alpha^4 + 4d^2\beta - 4\alpha^3\beta - \alpha^2 d^2 \\
& +d^3 - 6\alpha\beta d^2 + 10d\alpha\beta + 6d\beta - 6\alpha^2\beta^2 + 4d^2\alpha - 4d\alpha - 2d\alpha^3 \\
& +12\alpha^2\beta - 3d\beta^2 - 8d\alpha^2\beta - 6d\beta^2\alpha - 2d^3\beta - 3d^2\beta^2\big]\eta_2 \\
& \big[2\alpha^2 + 2\alpha\beta - 2\alpha + 2d\alpha + 2d\beta + d^2 - d) \\
& \times(-6d\beta - 6\alpha\beta + 6\alpha + 2\alpha^2 + 9d - 2d\alpha - d^2\big]\eta_3 \Big\}, \qquad \text{(A.0.4)}
\end{aligned}
$$

$$
C_5(d,\alpha,\beta) = \alpha^2 + (d+\beta-2)\alpha + \frac{1}{2}d(d-3) + (d-1)\beta + 1\,, \qquad \text{(A.0.5)}
$$

$$
\begin{aligned}
C_6(d,\alpha,\beta,\eta_i) = -\frac{1}{2L^2}\Big\{\big[& 28\alpha^2 - 16\alpha^3 - 24\alpha^2\beta + 4\alpha^4 + 8\alpha^3\beta + 8\alpha \\
& -4d\alpha^2 + 48\beta^3 + 30d - 24 + 44d\beta^2 - 6d^2 + 4\alpha^2\beta^2 + 120\beta + 16d\alpha\beta \\
& -144\beta^2 + 40\alpha\beta^2 - 56\alpha\beta + 8d^2\beta - 80d\beta - 8d\alpha\big]\eta_1 \\
& +\big[-12 + 11d + 8\alpha^3\beta - 48\alpha^2\beta + 18\alpha^2\beta^2 - 25d\beta^2 + 28\alpha\beta \\
& +12d\alpha + 2d\beta + 12\beta^3\alpha + 12d\beta^3 - 8\alpha + 36\beta + 2\alpha^4 - 12\alpha^3 + 30\alpha^2 \\
& -36\beta^2 + 12\beta^3 + 2d^2 - 32\alpha\beta^2 - 13d\alpha^2 - 4d^2\alpha - 16d^2\beta + 2d\alpha^3 \\
& +d^2\alpha^2 + 11d^2\beta^2 + 2d^3\beta - 38d\alpha\beta + 12d\alpha^2\beta + 22d\beta^2 \\
& +6d^2\alpha\beta - d^3\big]\eta_2 + \big[(2\alpha^2 + 2\alpha\beta - 2\alpha + 2d\alpha + 2d\beta + d^2 - d) \times (24\beta^2 \\
& -60\beta + 36 + 10\alpha\beta - 14\alpha + 2\alpha^2 + 10d\beta - 13d + 2d\alpha + d^2)\big]\eta_3 \Big\}\,. \qquad \text{(A.0.6)}
\end{aligned}
$$

Appendix B

Next order near horizon expansion

As mentioned in section 3.4, one of the ingredients needed to compute the DC conductivity is the expansion of the heat current Q to order $r - r_0$ near the horizon r_0. This results in the following condition

$$\begin{aligned} &\alpha_{(0)}\left(\mu_0 - r_0\overline{V}H_{(1)}\right)\left(E + \partial_x a_{r(0)}\right) - 4\pi T r_0 \partial_x\left(\alpha_{(0)}\delta g_{tr(0)}\right) \\ &+ \left[8\pi T\alpha_{(0)} + \frac{2r_0^2\mu_0\overline{V}}{L^2}H_{(1)} - \frac{\mu_0^2 r_0}{L^2} + \frac{8\pi^2T^2r_0}{\eta_{(0)}}\alpha_{(0)}\chi^2_{(0)}\right]\delta g_{tx(0)} \\ &- \left[24r_0\pi^2T^2\alpha_{(1)} + 8\pi^2T^2r_0\alpha_{(0)}\frac{F_{(1)}}{F_{(0)}} + 2\pi T r_0\alpha_{(0)}\frac{\delta_{(1)}}{\delta_{(0)}}2\pi T r_0\alpha_{(0)}\frac{\eta_{(1)}}{\eta_{(0)}}\right]\delta g_{tx(0)} = 0\,. \end{aligned} \tag{B.0.1}$$

Using the linearized equations of motion, it is possible to solve for the last term in brackets containing $\alpha_{(1)}$, $F_{(1)}$, $\delta_{(1)}$, $\eta_{(1)}$ and express it entirely in terms of horizon data with the result (3.4.37) mentioned in the main text. To the relevant order in perturbations, we

get

$$\Omega_{(0)}(x) = \frac{1}{2L^2F_{(0)}\eta_{(0)}^2\delta_{(0)}^2(16\pi^2T^2F_{(0)}\alpha_{(0)}\delta_{(0)}-1)}\Big\{2F_{(0)}\eta_{(0)}\delta_{(0)}^2\big[128\pi^3T^3L^2F_{(0)}\alpha_{(0)}^2\eta_{(0)}\delta_{(0)}$$
$$-8\pi TL^2\alpha_{(0)}\eta_{(0)}-2\mu_0\overline{V}r_0^2\eta_{(0)}H_{(1)}+32\pi^2T^2\mu_0r_0^2\overline{V}\alpha_{(0)}F_{(0)}\eta_{(0)}\delta_{(0)}H_{(1)}$$
$$-16\pi^2T62\mu_0^2r_0\alpha_{(0)}F_{(0)}\eta_{(0)}\delta_{(0)}+128\pi^4T^4r_0F_{(0)}^2\alpha_{(0)}^2\delta_{(0)}\chi_{(0)}^2-8\pi^2T^2L^2r_0F_{(0)}\alpha_{(0)}\chi_{(0)}^2\big]$$
$$+4\pi Tr_0L^2F_{(0)}\delta_{(0)}\big[16\pi^2T^2F_{(0)}\alpha_{(0)}^2\delta_{(0)}^2\chi_{(0)}\partial_x\eta_{(0)}+16\pi^2T^2F_{(0)}\alpha_{(0)}\eta_{(0)}\delta_{(0)}\chi_{(0)}\partial_x\alpha_{(0)}$$
$$-32\pi^2T^2F_{(0)}\alpha_{(0)}^2\eta_{(0)}\delta_{(0)}^2\partial_x\chi_{(0)}+16\pi^2T^2\alpha_{(0)}^2F_{(0)}\eta_{(0)}\delta_{(0)}\partial_x\delta_{(0)}+2\alpha_{(0)}\eta_{(0)}\delta_{(0)}\partial_x\chi_{(0)}$$
$$-\alpha_{(0)}\delta_{(0)}\chi_{(0)}\partial_x\eta_{(0)}-3\eta_{(0)}\delta_{(0)}\chi_{(0)}\partial_x\alpha_{(0)}-\alpha_{(0)}\eta_{(0)}\chi_{(0)}\partial_x\delta_{(0)}\big]$$
$$+16\pi^2T^2L^2r_0\big[F_{(0)}\eta_{(0)}\delta_{(0)}^3(\partial_x\alpha_{(0)})^2+F_{(0)}\alpha_{(0)}^2\eta_{(0)}\delta_{(0)}(\partial_x\delta_{(0)})^2+\alpha_{(0)}^2\delta_{(0)}^2(\partial_x\eta_{(0)})(\partial_x\delta_{(0)})$$
$$+F_{(0)}\alpha_{(0)}\delta_{(0)}^3(\partial_x\alpha_{(0)})(\partial_x\eta_{(0)})\big]-L^2r_0\big[\eta_{(0)}\delta_{(0)}(\partial_x\alpha_{(0)})(\partial_x\delta_{(0)})+\alpha_{(0)}\delta_{(0)}(\partial_x\eta_{(0)})(\partial_x\delta_{(0)})$$
$$+\alpha_{(0)}\eta_{(0)}(\partial_x\delta_{(0)})^2\big]-2L^2r_0\alpha_{(0)}\eta_{(0)}\delta_{(0)}\big[16\pi^2T^2F_{(0)}\delta_{(0)}^2\partial_x^2\alpha_{(0)}+16\pi^2T^2F_{(0)}\alpha_{(0)}\delta_{(0)}\partial_x^2\delta_{(0)}$$
$$-\partial_x^2\delta_{(0)}\big]\Big\}$$

Bibliography

[1] J. M. Maldacena, "The Large N limit of superconformal field theories and supergravity," *Int.J.Theor.Phys.* **38** (1999) 1113–1133, arXiv:hep-th/9711200 [hep-th].

[2] M. B. K. Becker and J. H. Schwarz, *String theory and M-theory: A modern introduction*. Cambridge, UK: Cambridge Univ. Pr., 2007.

[3] A. Strominger and C. Vafa, "Microscopic origin of the Bekenstein-Hawking entropy," *Phys.Lett.* **B379** (1996) 99–104, arXiv:hep-th/9601029 [hep-th].

[4] A. Dabholkar and S. Nampuri, "Quantum black holes," *Lect.Notes Phys.* **851** (2012) 165–232, arXiv:1208.4814 [hep-th].

[5] O. Lunin and S. D. Mathur, "AdS / CFT duality and the black hole information paradox," *Nucl.Phys.* **B623** (2002) 342–394, arXiv:hep-th/0109154 [hep-th].

[6] O. Lunin and S. D. Mathur, "Statistical interpretation of Bekenstein entropy for systems with a stretched horizon," *Phys.Rev.Lett.* **88** (2002) 211303, arXiv:hep-th/0202072 [hep-th].

[7] P. Kovtun, D. T. Son, and A. O. Starinets, "Viscosity in strongly interacting quantum field theories from black hole physics," *Phys.Rev.Lett.* **94** (2005) 111601, arXiv:hep-th/0405231 [hep-th].

[8] E. Witten, "Anti-de Sitter space, thermal phase transition, and confinement in gauge theories," *Adv.Theor.Math.Phys.* **2** (1998) 505–532, arXiv:hep-th/9803131 [hep-th].

[9] C. Herzog, A. Karch, P. Kovtun, C. Kozcaz, and L. Yaffe, "Energy loss of a heavy quark moving through N=4 supersymmetric Yang-Mills plasma," *JHEP* **0607** (2006) 013, arXiv:hep-th/0605158 [hep-th].

[10] J. Casalderrey-Solana and D. Teaney, "Heavy quark diffusion in strongly coupled N=4 Yang-Mills," *Phys.Rev.* **D74** (2006) 085012, arXiv:hep-ph/0605199 [hep-ph].

[11] S. S. Gubser, "Drag force in AdS/CFT," *Phys.Rev.* **D74** (2006) 126005, arXiv:hep-th/0605182 [hep-th].

[12] S. A. Hartnoll, C. P. Herzog, and G. T. Horowitz, "Building a Holographic Superconductor," *Phys.Rev.Lett.* **101** (2008) 031601, arXiv:0803.3295 [hep-th].

[13] T. Faulkner, N. Iqbal, H. Liu, J. McGreevy, and D. Vegh, "From Black Holes to Strange Metals," arXiv:1003.1728 [hep-th].

[14] L. Huijse, S. Sachdev, and B. Swingle, "Hidden Fermi surfaces in compressible states of gauge-gravity duality," *Phys.Rev.* **B85** (2012) 035121, arXiv:1112.0573 [cond-mat.str-el].

[15] S. Kachru, R. Kallosh, A. D. Linde, and S. P. Trivedi, "De Sitter vacua in string theory," *Phys.Rev.* **D68** (2003) 046005, arXiv:hep-th/0301240 [hep-th].

[16] A. Strominger, "The dS / CFT correspondence," *JHEP* **0110** (2001) 034, arXiv:hep-th/0106113 [hep-th].

[17] S. Bhattacharyya, V. E. Hubeny, S. Minwalla, and M. Rangamani, "Nonlinear Fluid Dynamics from Gravity," *JHEP* **0802** (2008) 045, arXiv:0712.2456 [hep-th].

[18] J. Erdmenger, M. Haack, M. Kaminski, and A. Yarom, "Fluid dynamics of R-charged black holes," *JHEP* **0901** (2009) 055, arXiv:0809.2488 [hep-th].

[19] N. Banerjee, J. Bhattacharya, S. Bhattacharyya, S. Dutta, R. Loganayagam, *et al.*, "Hydrodynamics from charged black branes," *JHEP* **1101** (2011) 094, arXiv:0809.2596 [hep-th].

[20] L. D. Landau and E. M. Lifshitz, *Fluid Mechanics (Course of Theoretical Physics, Vol. 6)*. Butterworth-Heinemann, 1965.

[21] A. Adams, P. M. Chesler, and H. Liu, "Holographic turbulence," *Phys.Rev.Lett.* **112** no. 15, (2014) 151602, arXiv:1307.7267 [hep-th].

[22] S. Ryu and T. Takayanagi, "Holographic derivation of entanglement entropy from AdS/CFT," *Phys.Rev.Lett.* **96** (2006) 181602, arXiv:hep-th/0603001 [hep-th].

[23] A. Lewkowycz and J. Maldacena, "Generalized gravitational entropy," *JHEP* **1308** (2013) 090, arXiv:1304.4926 [hep-th].

[24] V. Balasubramanian, B. D. Chowdhury, B. Czech, J. de Boer, and M. P. Heller, "Bulk curves from boundary data in holography," *Phys.Rev.* **D89** no. 8, (2014) 086004, arXiv:1310.4204 [hep-th].

[25] M. Rangamani and M. Rota, "Comments on Entanglement Negativity in Holographic Field Theories," *JHEP* **1410** (2014) 60, arXiv:1406.6989 [hep-th].

[26] S. Hawking, "Particle Creation by Black Holes," *Commun.Math.Phys.* **43** (1975) 199–220.

[27] S. Hawking, "Breakdown of Predictability in Gravitational Collapse," *Phys.Rev.* **D14** (1976) 2460–2473.

[28] S. D. Mathur, "What the information paradox is not," `arXiv:1108.0302 [hep-th]`.

[29] A. Almheiri, D. Marolf, J. Polchinski, and J. Sully, "Black Holes: Complementarity or Firewalls?," *JHEP* **1302** (2013) 062, `arXiv:1207.3123 [hep-th]`.

[30] D. Harlow and P. Hayden, "Quantum Computation vs. Firewalls," *JHEP* **1306** (2013) 085, `arXiv:1301.4504 [hep-th]`.

[31] C. R. Stephens, G. 't Hooft, and B. F. Whiting, "Black hole evaporation without information loss," *Class.Quant.Grav.* **11** (1994) 621–648, `arXiv:gr-qc/9310006 [gr-qc]`.

[32] L. Susskind, "The World as a hologram," *J.Math.Phys.* **36** (1995) 6377–6396, `arXiv:hep-th/9409089 [hep-th]`.

[33] J. Polchinski, *String theory. Vol. 1: An introduction to the bosonic string,*. Cambridge, UK: Univ. Pr., (1998).

[34] I. Klebanov and A. Polyakov, "AdS dual of the critical O(N) vector model," *Phys.Lett.* **B550** (2002) 213–219, `arXiv:hep-th/0210114 [hep-th]`.

[35] M. R. Gaberdiel and R. Gopakumar, "Minimal Model Holography," *J.Phys.* **A46** (2013) 214002, `arXiv:1207.6697 [hep-th]`.

[36] J. McGreevy, "Holographic duality with a view toward many-body physics," *Adv.High Energy Phys.* **2010** (2010) 723105, `arXiv:0909.0518 [hep-th]`.

[37] J. D. Brown and M. Henneaux, "Central Charges in the Canonical Realization of Asymptotic Symmetries: An Example from Three-Dimensional Gravity," *Commun.Math.Phys.* **104** (1986) 207–226.

[38] J. de Boer, E. P. Verlinde, and H. L. Verlinde, "On the holographic renormalization group," *JHEP* **0008** (2000) 003, arXiv:hep-th/9912012 [hep-th].

[39] M. Guica, T. Hartman, W. Song, and A. Strominger, "The Kerr/CFT Correspondence," *Phys.Rev.* **D80** (2009) 124008, arXiv:0809.4266 [hep-th].

[40] I. Bredberg, C. Keeler, V. Lysov, and A. Strominger, "Cargese Lectures on the Kerr/CFT Correspondence," *Nucl.Phys.Proc.Suppl.* **216** (2011) 194–210, arXiv:1103.2355 [hep-th].

[41] G. Compere, "The Kerr/CFT correspondence and its extensions: a comprehensive review," *Living Rev.Rel.* **15** (2012) 11, arXiv:1203.3561 [hep-th].

[42] A. W. Peet, "TASI lectures on black holes in string theory," arXiv:hep-th/0008241 [hep-th].

[43] O. Aharony, S. S. Gubser, J. M. Maldacena, H. Ooguri, and Y. Oz, "Large N field theories, string theory and gravity," *Phys.Rept.* **323** (2000) 183–386, arXiv:hep-th/9905111 [hep-th].

[44] E. D'Hoker and D. Z. Freedman, "Supersymmetric gauge theories and the AdS / CFT correspondence," arXiv:hep-th/0201253 [hep-th].

[45] J. Polchinski, "Introduction to Gauge/Gravity Duality," arXiv:1010.6134 [hep-th].

[46] A. V. Ramallo, "Introduction to the AdS/CFT correspondence," *Springer Proc.Phys.* **161** (2015) 411–474, arXiv:1310.4319 [hep-th].

[47] R. C. Myers, "Dielectric branes," *JHEP* **9912** (1999) 022, arXiv:hep-th/9910053 [hep-th].

[48] L. Susskind and E. Witten, "The Holographic bound in anti-de Sitter space," arXiv:hep-th/9805114 [hep-th].

[49] A. W. Peet and J. Polchinski, "UV / IR relations in AdS dynamics," *Phys.Rev.* **D59** (1999) 065011, arXiv:hep-th/9809022 [hep-th].

[50] S. Gubser, I. R. Klebanov, and A. M. Polyakov, "Gauge theory correlators from noncritical string theory," *Phys.Lett.* **B428** (1998) 105–114, arXiv:hep-th/9802109 [hep-th].

[51] E. Witten, "Anti-de Sitter space and holography," *Adv.Theor.Math.Phys.* **2** (1998) 253–291, arXiv:hep-th/9802150 [hep-th].

[52] J. R. David, G. Mandal, and S. R. Wadia, "Microscopic formulation of black holes in string theory," *Phys.Rept.* **369** (2002) 549–686, arXiv:hep-th/0203048 [hep-th].

[53] I. R. Klebanov and G. Torri, "M2-branes and AdS/CFT," *Int.J.Mod.Phys.* **A25** (2010) 332–350, arXiv:0909.1580 [hep-th].

[54] S. Giombi and X. Yin, "The Higher Spin/Vector Model Duality," *J.Phys.* **A46** (2013) 214003, arXiv:1208.4036 [hep-th].

[55] J. D. Edelstein and R. Portugues, "Gauge/string duality in confining theories," *Fortsch.Phys.* **54** (2006) 525–579, arXiv:hep-th/0602021 [hep-th].

[56] N. Beisert, C. Ahn, L. F. Alday, Z. Bajnok, J. M. Drummond, *et al.*, "Review of AdS/CFT Integrability: An Overview," *Lett.Math.Phys.* **99** (2012) 3–32, arXiv:1012.3982 [hep-th].

[57] J. Bagger and N. Lambert, "Modeling Multiple M2's," *Phys.Rev.* **D75** (2007) 045020, arXiv:hep-th/0611108 [hep-th].

[58] O. Aharony, O. Bergman, D. L. Jafferis, and J. Maldacena, "N=6 superconformal Chern-Simons-matter theories, M2-branes and their gravity duals," *JHEP* **0810** (2008) 091, arXiv:0806.1218 [hep-th].

[59] N. B. Copland, "Introductory Lectures on Multiple Membranes," arXiv:1012.0459 [hep-th].

[60] M. Marino, "Lectures on localization and matrix models in supersymmetric Chern-Simons-matter theories," *J.Phys.* **A44** (2011) 463001, arXiv:1104.0783 [hep-th].

[61] N. Drukker, M. Marino, and P. Putrov, "From weak to strong coupling in ABJM theory," *Commun.Math.Phys.* **306** (2011) 511–563, arXiv:1007.3837 [hep-th].

[62] M. Vasiliev, "Higher-Spin Theory and Space-Time Metamorphoses," *Lect.Notes Phys.* **892** (2015) 227–264, arXiv:1404.1948 [hep-th].

[63] X. Bekaert, N. Boulanger, and P. Sundell, "How higher-spin gravity surpasses the spin two barrier: no-go theorems versus yes-go examples," *Rev.Mod.Phys.* **84** (2012) 987–1009, arXiv:1007.0435 [hep-th].

[64] S. Giombi and X. Yin, "On Higher Spin Gauge Theory and the Critical O(N) Model," *Phys.Rev.* **D85** (2012) 086005, arXiv:1105.4011 [hep-th].

[65] D. Anninos, T. Hartman, and A. Strominger, "Higher Spin Realization of the dS/CFT Correspondence," arXiv:1108.5735 [hep-th].

[66] J. Maldacena and A. Zhiboedov, "Constraining Conformal Field Theories with A Higher Spin Symmetry," *J.Phys.* **A46** (2013) 214011, arXiv:1112.1016 [hep-th].

[67] M. R. Gaberdiel and R. Gopakumar, "Higher Spins & Strings," *JHEP* **1411** (2014) 044, arXiv:1406.6103 [hep-th].

[68] M. Ammon, M. Gutperle, P. Kraus, and E. Perlmutter, "Black holes in three dimensional higher spin gravity: A review," *J.Phys.* **A46** (2013) 214001, arXiv:1208.5182 [hep-th].

[69] J. de Boer and J. I. Jottar, "Thermodynamics of higher spin black holes in AdS_3," *JHEP* **1401** (2014) 023, arXiv:1302.0816 [hep-th].

[70] K. Skenderis, "Lecture notes on holographic renormalization," *Class.Quant.Grav.* **19** (2002) 5849–5876, arXiv:hep-th/0209067 [hep-th].

[71] S. A. Hartnoll, "Lectures on holographic methods for condensed matter physics," *Class.Quant.Grav.* **26** (2009) 224002, arXiv:0903.3246 [hep-th].

[72] V. Balasubramanian and P. Kraus, "A Stress tensor for Anti-de Sitter gravity," *Commun.Math.Phys.* **208** (1999) 413–428, arXiv:hep-th/9902121 [hep-th].

[73] J. de Boer, "The Holographic renormalization group," *Fortsch.Phys.* **49** (2001) 339–358, arXiv:hep-th/0101026 [hep-th].

[74] M. Fukuma, S. Matsuura, and T. Sakai, "Holographic renormalization group," *Prog.Theor.Phys.* **109** (2003) 489–562, arXiv:hep-th/0212314 [hep-th].

[75] H. Nastase, "Introduction to AdS-CFT," arXiv:0712.0689 [hep-th].

[76] D. T. Son and A. O. Starinets, "Minkowski space correlators in AdS / CFT correspondence: Recipe and applications," *JHEP* **0209** (2002) 042, arXiv:hep-th/0205051 [hep-th].

[77] C. Herzog and D. Son, "Schwinger-Keldysh propagators from AdS/CFT correspondence," *JHEP* **0303** (2003) 046, arXiv:hep-th/0212072 [hep-th].

[78] K. Skenderis and B. C. van Rees, "Real-time gauge/gravity duality," *Phys.Rev.Lett.* **101** (2008) 081601, arXiv:0805.0150 [hep-th].

[79] B. C. van Rees, "Real-time gauge/gravity duality and ingoing boundary conditions," *Nucl.Phys.Proc.Suppl.* **192-193** (2009) 193–196, arXiv:0902.4010 [hep-th].

[80] C. P. Herzog, P. Kovtun, S. Sachdev, and D. T. Son, "Quantum critical transport, duality, and M-theory," *Phys.Rev.* **D75** (2007) 085020, arXiv:hep-th/0701036 [hep-th].

[81] C. P. Herzog, "Lectures on Holographic Superfluidity and Superconductivity," *J.Phys.* **A42** (2009) 343001, arXiv:0904.1975 [hep-th].

[82] D. T. Son and A. O. Starinets, "Viscosity, Black Holes, and Quantum Field Theory," *Ann.Rev.Nucl.Part.Sci.* **57** (2007) 95–118, arXiv:0704.0240 [hep-th].

[83] M. Brigante, H. Liu, R. C. Myers, S. Shenker, and S. Yaida, "Viscosity Bound Violation in Higher Derivative Gravity," *Phys.Rev.* **D77** (2008) 126006, arXiv:0712.0805 [hep-th].

[84] M. Brigante, H. Liu, R. C. Myers, S. Shenker, and S. Yaida, "The Viscosity Bound and Causality Violation," *Phys.Rev.Lett.* **100** (2008) 191601, arXiv:0802.3318 [hep-th].

[85] J. M. Maldacena, "Wilson loops in large N field theories," *Phys.Rev.Lett.* **80** (1998) 4859–4862, arXiv:hep-th/9803002 [hep-th].

[86] T. Nishioka, S. Ryu, and T. Takayanagi, "Holographic Entanglement Entropy: An Overview," *J.Phys.* **A42** (2009) 504008, arXiv:0905.0932 [hep-th].

[87] M. A. Nielsen and D. Petz, "A simple proof of the strong subadditivity inequality," *Quantum Info. Comput.* **5** no. 6, (Sept., 2005) 507–513, quant-ph/0408130. http://dl.acm.org/citation.cfm?id=2011670.2011678.

[88] P. Calabrese and J. L. Cardy, "Entanglement entropy and quantum field theory," *J.Stat.Mech.* **0406** (2004) P06002, arXiv:hep-th/0405152 [hep-th].

[89] S. Ryu and T. Takayanagi, "Aspects of Holographic Entanglement Entropy," *JHEP* **0608** (2006) 045, arXiv:hep-th/0605073 [hep-th].

[90] L.-Y. Hung, R. C. Myers, and M. Smolkin, "On Holographic Entanglement Entropy and Higher Curvature Gravity," *JHEP* **1104** (2011) 025, arXiv:1101.5813 [hep-th].

[91] A. Bhattacharyya, A. Kaviraj, and A. Sinha, "Entanglement entropy in higher derivative holography," *JHEP* **1308** (2013) 012, arXiv:1305.6694 [hep-th].

[92] A. Bhattacharyya, M. Sharma, and A. Sinha, "On generalized gravitational entropy, squashed cones and holography," *JHEP* **1401** (2014) 021, arXiv:1308.5748 [hep-th].

[93] X. Dong, "Holographic Entanglement Entropy for General Higher Derivative Gravity," *JHEP* **1401** (2014) 044, arXiv:1310.5713 [hep-th].

[94] J. Camps, "Generalized entropy and higher derivative Gravity," *JHEP* **1403** (2014) 070, arXiv:1310.6659 [hep-th].

[95] V. E. Hubeny, M. Rangamani, and T. Takayanagi, "A Covariant holographic entanglement entropy proposal," *JHEP* **0707** (2007) 062, arXiv:0705.0016 [hep-th].

[96] M. Headrick, "General properties of holographic entanglement entropy," *JHEP* **03** (Dec., 2013) 085, 1312.6717.

[97] B. Czech, X. Dong, and J. Sully, "Holographic Reconstruction of General Bulk Surfaces," *JHEP* **1411** (2014) 015, arXiv:1406.4889 [hep-th].

[98] V. Balasubramanian, A. Bernamonti, J. de Boer, N. Copland, B. Craps, *et al.*, "Thermalization of Strongly Coupled Field Theories," *Phys.Rev.Lett.* **106** (2011) 191601, arXiv:1012.4753 [hep-th].

[99] H. Liu and S. J. Suh, "Entanglement Tsunami: Universal Scaling in Holographic Thermalization," *Phys.Rev.Lett.* **112** (2014) 011601, arXiv:1305.7244 [hep-th].

[100] H. Liu and S. J. Suh, "Entanglement growth during thermalization in holographic systems," *Phys.Rev.* **D89** no. 6, (2014) 066012, arXiv:1311.1200 [hep-th].

[101] J. Casalderrey-Solana, H. Liu, D. Mateos, K. Rajagopal, and U. A. Wiedemann, "Gauge/String Duality, Hot QCD and Heavy Ion Collisions," arXiv:1101.0618 [hep-th].

[102] V. E. Hubeny, "The AdS/CFT Correspondence," arXiv:1501.00007 [gr-qc].

[103] O. Aharony, "The NonAdS / nonCFT correspondence, or three different paths to QCD," arXiv:hep-th/0212193 [hep-th].

[104] D. Boyanovsky, "Supersymmetry Breaking at Finite Temperature: The Goldstone Fermion," *Phys.Rev.* **D29** (1984) 743.

[105] I. R. Klebanov and E. Witten, "Superconformal field theory on three-branes at a Calabi-Yau singularity," *Nucl.Phys.* **B536** (1998) 199–218, arXiv:hep-th/9807080 [hep-th].

[106] S. S. Gubser, "Einstein manifolds and conformal field theories," *Phys.Rev.* **D59** (1999) 025006, arXiv:hep-th/9807164 [hep-th].

[107] I. R. Klebanov and N. A. Nekrasov, "Gravity duals of fractional branes and logarithmic RG flow," *Nucl.Phys.* **B574** (2000) 263–274, arXiv:hep-th/9911096 [hep-th].

[108] I. R. Klebanov and A. A. Tseytlin, "Gravity duals of supersymmetric SU(N) x SU(N+M) gauge theories," *Nucl.Phys.* **B578** (2000) 123–138, arXiv:hep-th/0002159 [hep-th].

[109] I. R. Klebanov and M. J. Strassler, "Supergravity and a confining gauge theory: Duality cascades and chi SB resolution of naked singularities," *JHEP* **0008** (2000) 052, arXiv:hep-th/0007191 [hep-th].

[110] J. M. Maldacena and C. Nunez, "Towards the large N limit of pure N=1 superYang-Mills," *Phys.Rev.Lett.* **86** (2001) 588–591, arXiv:hep-th/0008001 [hep-th].

[111] J. D. Edelstein and C. Nunez, "D6-branes and M theory geometrical transitions from gauged supergravity," *JHEP* **0104** (2001) 028, arXiv:hep-th/0103167 [hep-th].

[112] A. Karch and E. Katz, "Adding flavor to AdS / CFT," *JHEP* **0206** (2002) 043, arXiv:hep-th/0205236 [hep-th].

[113] M. Kruczenski, D. Mateos, R. C. Myers, and D. J. Winters, "Meson spectroscopy in AdS / CFT with flavor," *JHEP* **0307** (2003) 049, arXiv:hep-th/0304032 [hep-th].

[114] R. Casero, C. Nunez, and A. Paredes, "Towards the string dual of N=1 SQCD-like theories," *Phys.Rev.* **D73** (2006) 086005, arXiv:hep-th/0602027 [hep-th].

[115] N. R. Constable and R. C. Myers, "Exotic scalar states in the AdS / CFT correspondence," *JHEP* **9911** (1999) 020, arXiv:hep-th/9905081 [hep-th].

[116] J. Babington, J. Erdmenger, N. J. Evans, Z. Guralnik, and I. Kirsch, "Chiral symmetry breaking and pions in nonsupersymmetric gauge / gravity duals," *Phys.Rev.* **D69** (2004) 066007, arXiv:hep-th/0306018 [hep-th].

[117] J. Polchinski and M. J. Strassler, "The String dual of a confining four-dimensional gauge theory," arXiv:hep-th/0003136 [hep-th].

[118] M. Kruczenski, D. Mateos, R. C. Myers, and D. J. Winters, "Towards a holographic dual of large N(c) QCD," *JHEP* **0405** (2004) 041, arXiv:hep-th/0311270 [hep-th].

[119] T. Sakai and S. Sugimoto, "Low energy hadron physics in holographic QCD," *Prog.Theor.Phys.* **113** (2005) 843–882, arXiv:hep-th/0412141 [hep-th].

[120] Y. Kim, I. J. Shin, and T. Tsukioka, "Holographic QCD: Past, Present, and Future," *Prog.Part.Nucl.Phys.* **68** (2013) 55–112, arXiv:1205.4852 [hep-ph].

[121] A. Buchel, S. Deakin, P. Kerner, and J. T. Liu, "Thermodynamics of the N=2* strongly coupled plasma," *Nucl.Phys.* **B784** (2007) 72–102, arXiv:hep-th/0701142 [hep-th].

[122] O. DeWolfe, S. S. Gubser, C. Rosen, and D. Teaney, "Heavy ions and string theory," *Prog.Part.Nucl.Phys.* **75** (2014) 86–132, arXiv:1304.7794 [hep-th].

[123] S. Sachdev and B. Keimer, "Quantum Criticality," *Phys.Today* **64N2** (2011) 29, arXiv:1102.4628 [cond-mat.str-el].

[124] D. Musso, "Introductory notes on holographic superconductors," arXiv:1401.1504 [hep-th].

[125] G. Policastro, D. T. Son, and A. O. Starinets, "The Shear viscosity of strongly coupled N=4 supersymmetric Yang-Mills plasma," *Phys.Rev.Lett.* **87** (2001) 081601, arXiv:hep-th/0104066 [hep-th].

[126] M. Rangamani, "Gravity and Hydrodynamics: Lectures on the fluid-gravity correspondence," *Class.Quant.Grav.* **26** (2009) 224003, arXiv:0905.4352 [hep-th].

[127] V. E. Hubeny, S. Minwalla, and M. Rangamani, "The fluid/gravity correspondence," arXiv:1107.5780 [hep-th].

[128] D. T. Son and P. Surowka, "Hydrodynamics with Triangle Anomalies," *Phys.Rev.Lett.* **103** (2009) 191601, arXiv:0906.5044 [hep-th].

[129] I. Bredberg, C. Keeler, V. Lysov, and A. Strominger, "From Navier-Stokes To Einstein," *JHEP* **1207** (2012) 146, arXiv:1101.2451 [hep-th].

[130] V. Lysov and A. Strominger, "From Petrov-Einstein to Navier-Stokes," arXiv:1104.5502 [hep-th].

[131] G. Compere, P. McFadden, K. Skenderis, and M. Taylor, "The Holographic fluid dual to vacuum Einstein gravity," *JHEP* **1107** (2011) 050, arXiv:1103.3022 [hep-th].

[132] H. Yang, A. Zimmerman, and L. Lehner, "Turbulent Black Holes," *Phys.Rev.Lett.* **114** (2015) 081101, arXiv:1402.4859 [gr-qc].

[133] P. Bizon and A. Rostworowski, "On weakly turbulent instability of anti-de Sitter space," *Phys.Rev.Lett.* **107** (2011) 031102, arXiv:1104.3702 [gr-qc].

[134] S. S. Gubser, "Breaking an Abelian gauge symmetry near a black hole horizon," *Phys.Rev.* **D78** (2008) 065034, arXiv:0801.2977 [hep-th].

[135] G. T. Horowitz, "Introduction to Holographic Superconductors," *Lect.Notes Phys.* **828** (2011) 313–347, arXiv:1002.1722 [hep-th].

[136] S. A. Hartnoll, C. P. Herzog, and G. T. Horowitz, "Holographic Superconductors," *JHEP* **0812** (2008) 015, arXiv:0810.1563 [hep-th].

[137] R.-G. Cai, L. Li, L.-F. Li, and R.-Q. Yang, "Introduction to Holographic Superconductor Models," arXiv:1502.00437 [hep-th].

[138] S. Weinberg, "Superconductivity for Particular Theorists," *Prog.Theor.Phys.Suppl.* **86** (1986) 43.

[139] F. Denef and S. A. Hartnoll, "Landscape of superconducting membranes," *Phys.Rev.* **D79** (2009) 126008, arXiv:0901.1160 [hep-th].

[140] J. P. Gauntlett, J. Sonner, and T. Wiseman, "Holographic superconductivity in M-Theory," *Phys.Rev.Lett.* **103** (2009) 151601, arXiv:0907.3796 [hep-th].

[141] S. S. Gubser, C. P. Herzog, S. S. Pufu, and T. Tesileanu, "Superconductors from Superstrings," *Phys.Rev.Lett.* **103** (2009) 141601, arXiv:0907.3510 [hep-th].

[142] S. S. Gubser and S. S. Pufu, "The Gravity dual of a p-wave superconductor," *JHEP* **0811** (2008) 033, arXiv:0805.2960 [hep-th].

[143] R.-G. Cai, Z.-Y. Nie, and H.-Q. Zhang, "Holographic Phase Transitions of P-wave Superconductors in Gauss-Bonnet Gravity with Back-reaction," *Phys.Rev.* **D83** (2011) 066013, arXiv:1012.5559 [hep-th].

[144] R.-G. Cai, Z.-Y. Nie, and H.-Q. Zhang, "Holographic p-wave superconductors from Gauss-Bonnet gravity," *Phys.Rev.* **D82** (2010) 066007, arXiv:1007.3321 [hep-th].

[145] L. A. Pando Zayas and D. Reichmann, "A Holographic Chiral $p_x + ip_y$ Superconductor," *Phys.Rev.* **D85** (2012) 106012, arXiv:1108.4022 [hep-th].

[146] M. Ammon, J. Erdmenger, V. Grass, P. Kerner, and A. O'Bannon, "On Holographic p-wave Superfluids with Back-reaction," *Phys.Lett.* **B686** (2010) 192–198, arXiv:0912.3515 [hep-th].

[147] A. Donos and J. P. Gauntlett, "Holographic helical superconductors," *JHEP* **1112** (2011) 091, arXiv:1109.3866 [hep-th].

[148] A. Donos and J. P. Gauntlett, "Helical superconducting black holes," *Phys.Rev.Lett.* **108** (2012) 211601, arXiv:1203.0533 [hep-th].

[149] M. Ammon, J. Erdmenger, M. Kaminski, and P. Kerner, "Superconductivity from gauge/gravity duality with flavor," *Phys.Lett.* **B680** (2009) 516–520, arXiv:0810.2316 [hep-th].

[150] P. Basu, J. He, A. Mukherjee, and H.-H. Shieh, "Superconductivity from D3/D7: Holographic Pion Superfluid," *JHEP* **0911** (2009) 070, arXiv:0810.3970 [hep-th].

[151] M. Ammon, J. Erdmenger, M. Kaminski, and P. Kerner, "Flavor Superconductivity from Gauge/Gravity Duality," *JHEP* **0910** (2009) 067, arXiv:0903.1864 [hep-th].

[152] J.-W. Chen, Y.-J. Kao, D. Maity, W.-Y. Wen, and C.-P. Yeh, "Towards A Holographic Model of D-Wave Superconductors," *Phys.Rev.* **D81** (2010) 106008, arXiv:1003.2991 [hep-th].

[153] F. Benini, C. P. Herzog, R. Rahman, and A. Yarom, "Gauge gravity duality for d-wave superconductors: prospects and challenges," *JHEP* **1011** (2010) 137, arXiv:1007.1981 [hep-th].

[154] P. Basu, J. He, A. Mukherjee, M. Rozali, and H.-H. Shieh, "Competing Holographic Orders," *JHEP* **1010** (2010) 092, arXiv:1007.3480 [hep-th].

[155] D. Musso, "Competition/Enhancement of Two Probe Order Parameters in the Unbalanced Holographic Superconductor," *JHEP* **1306** (2013) 083, arXiv:1302.7205 [hep-th].

[156] R.-G. Cai, L. Li, L.-F. Li, and Y.-Q. Wang, "Competition and Coexistence of Order Parameters in Holographic Multi-Band Superconductors," *JHEP* **1309** (2013) 074, arXiv:1307.2768 [hep-th].

[157] Z.-Y. Nie, R.-G. Cai, X. Gao, and H. Zeng, "Competition between the s-wave and p-wave superconductivity phases in a holographic model," *JHEP* **1311** (2013) 087, arXiv:1309.2204 [hep-th].

[158] I. Amado, D. Arean, A. Jimenez-Alba, L. Melgar, and I. Salazar Landea, "Holographic s+p Superconductors," *Phys.Rev.* **D89** no. 2, (2014) 026009, arXiv:1309.5086 [hep-th].

[159] A. Amoretti, A. Braggio, N. Maggiore, N. Magnoli, and D. Musso, "Coexistence of two vector order parameters: a holographic model for ferromagnetic superconductivity," *JHEP* **1401** (2014) 054, arXiv:1309.5093 [hep-th].

[160] L.-F. Li, R.-G. Cai, L. Li, and Y.-Q. Wang, "Competition between s-wave order and d-wave order in holographic superconductors," *JHEP* **1408** (2014) 164, arXiv:1405.0382 [hep-th].

[161] M. Nishida, "Phase Diagram of a Holographic Superconductor Model with s-wave and d-wave," *JHEP* **1409** (2014) 154, arXiv:1403.6070 [hep-th].

[162] G. T. Horowitz, J. E. Santos, and D. Tong, "Optical Conductivity with Holographic Lattices," *JHEP* **1207** (2012) 168, arXiv:1204.0519 [hep-th].

[163] D. Son, "Toward an AdS/cold atoms correspondence: A Geometric realization of the Schrodinger symmetry," *Phys.Rev.* **D78** (2008) 046003, arXiv:0804.3972 [hep-th].

[164] S. Kachru, X. Liu, and M. Mulligan, "Gravity duals of Lifshitz-like fixed points," *Phys.Rev.* **D78** (2008) 106005, arXiv:0808.1725 [hep-th].

[165] B. Gouteraux and E. Kiritsis, "Generalized Holographic Quantum Criticality at Finite Density," *JHEP* **1112** (2011) 036, arXiv:1107.2116 [hep-th].

[166] N. Ogawa, T. Takayanagi, and T. Ugajin, "Holographic Fermi Surfaces and Entanglement Entropy," *JHEP* **1201** (2012) 125, arXiv:1111.1023 [hep-th].

[167] K. Balasubramanian and J. McGreevy, "Gravity duals for non-relativistic CFTs," *Phys.Rev.Lett.* **101** (2008) 061601, arXiv:0804.4053 [hep-th].

[168] T. Ishii and T. Nishioka, "Flows to Schrodinger Geometries," *Phys.Rev.* **D84** (2011) 125007, arXiv:1109.6318 [hep-th].

[169] J. Maldacena, D. Martelli, and Y. Tachikawa, "Comments on string theory backgrounds with non-relativistic conformal symmetry," *JHEP* **0810** (2008) 072, arXiv:0807.1100 [hep-th].

[170] C. P. Herzog, M. Rangamani, and S. F. Ross, "Heating up Galilean holography," *JHEP* **0811** (2008) 080, arXiv:0807.1099 [hep-th].

[171] A. Adams, K. Balasubramanian, and J. McGreevy, "Hot Spacetimes for Cold Atoms," *JHEP* **0811** (2008) 059, arXiv:0807.1111 [hep-th].

[172] P. Dey and S. Roy, "From AdS to Schrödinger/Lifshitz dual space-times without or with hyperscaling violation," *JHEP* **1311** (2013) 113, arXiv:1306.1071 [hep-th].

[173] M. Guica, K. Skenderis, M. Taylor, and B. C. van Rees, "Holography for Schrodinger backgrounds," *JHEP* **1102** (2011) 056, arXiv:1008.1991 [hep-th].

[174] R. Caldeira Costa and M. Taylor, "Holography for chiral scale-invariant models," *JHEP* **1102** (2011) 082, arXiv:1010.4800 [hep-th].

[175] M. Guica, "A Fefferman-Graham-Like Expansion for Null Warped AdS(3)," *JHEP* **1212** (2012) 084, arXiv:1111.6978 [hep-th].

[176] B. C. van Rees, "Correlation functions for Schrodinger backgrounds," arXiv:1206.6507 [hep-th].

[177] T. Andrade, C. Keeler, A. Peach, and S. F. Ross, "Schrodinger Holography for z<2," arXiv:1408.7103 [hep-th].

[178] J. Hartong and B. Rollier, "Particle Number and 3D Schrödinger Holography," *JHEP* **1409** (2014) 111, arXiv:1305.3653 [hep-th].

[179] T. Andrade, C. Keeler, A. Peach, and S. F. Ross, "Schrödinger Holography with $z = 2$," arXiv:1412.0031 [hep-th].

[180] K. Essafi, J. Kownacki, and D. Mouhanna, "Nonperturbative renormalization group approach to Lifshitz critical behaviour," *Europhys.Lett.* **98** (2012) 51002, arXiv:1202.5946 [cond-mat.stat-mech].

[181] S. F. Ross and O. Saremi, "Holographic stress tensor for non-relativistic theories," *JHEP* **0909** (2009) 009, arXiv:0907.1846 [hep-th].

[182] M. Taylor, "Non-relativistic holography," arXiv:0812.0530 [hep-th].

[183] J. Gath, J. Hartong, R. Monteiro, and N. A. Obers, "Holographic Models for Theories with Hyperscaling Violation," *JHEP* **1304** (2013) 159, arXiv:1212.3263 [hep-th].

[184] J. Tarrio and S. Vandoren, "Black holes and black branes in Lifshitz spacetimes," *JHEP* **1109** (2011) 017, arXiv:1105.6335 [hep-th].

[185] J. Tarrio, "Asymptotically Lifshitz Black Holes in Einstein-Maxwell-Dilaton Theories," *Fortsch.Phys.* **60** (2012) 1098–1104, arXiv:1201.5480 [hep-th].

[186] C. Charmousis, B. Goutéraux, B. S. Kim, E. Kiritsis, and R. Meyer, "Effective Holographic Theories for low-temperature condensed matter systems," *JHEP* **1011** (2010) 151, arXiv:1005.4690 [hep-th].

[187] S. Cremonini and P. Szepietowski, "Generating Temperature Flow for eta/s with Higher Derivatives: From Lifshitz to AdS," *JHEP* **1202** (2012) 038, arXiv:1111.5623 [hep-th].

[188] S. F. Ross, "Holography for asymptotically locally Lifshitz spacetimes," *Class.Quant.Grav.* **28** (2011) 215019, arXiv:1107.4451 [hep-th].

[189] R. B. Mann and R. McNees, "Holographic Renormalization for Asymptotically Lifshitz Spacetimes," *JHEP* **1110** (2011) 129, arXiv:1107.5792 [hep-th].

[190] M. Baggio, J. de Boer, and K. Holsheimer, "Hamilton-Jacobi Renormalization for Lifshitz Spacetime," *JHEP* **1201** (2012) 058, arXiv:1107.5562 [hep-th].

[191] Y. Korovin, K. Skenderis, and M. Taylor, "Lifshitz as a deformation of Anti-de Sitter," *JHEP* **1308** (2013) 026, arXiv:1304.7776 [hep-th].

[192] Y. Korovin, K. Skenderis, and M. Taylor, "Lifshitz from AdS at finite temperature and top down models," *JHEP* **1311** (2013) 127, arXiv:1306.3344 [hep-th].

[193] W. Chemissany and I. Papadimitriou, "Generalized dilatation operator method for non-relativistic holography," *Phys.Lett.* **B737** (2014) 272–276, arXiv:1405.3965 [hep-th].

[194] W. Chemissany and I. Papadimitriou, "Lifshitz holography: The whole shebang," *JHEP* **1501** (2015) 052, arXiv:1408.0795 [hep-th].

[195] I. Papadimitriou, "Hyperscaling violating Lifshitz holography," arXiv:1411.0312 [hep-th].

[196] K. Copsey and R. Mann, "Pathologies in Asymptotically Lifshitz Spacetimes," *JHEP* **1103** (2011) 039, arXiv:1011.3502 [hep-th].

[197] G. T. Horowitz and B. Way, "Lifshitz Singularities," *Phys.Rev.* **D85** (2012) 046008, arXiv:1111.1243 [hep-th].

[198] T. Azeyanagi, W. Li, and T. Takayanagi, "On String Theory Duals of Lifshitz-like Fixed Points," *JHEP* **0906** (2009) 084, arXiv:0905.0688 [hep-th].

[199] S. A. Hartnoll, J. Polchinski, E. Silverstein, and D. Tong, "Towards strange metallic holography," *JHEP* **1004** (2010) 120, arXiv:0912.1061 [hep-th].

[200] K. Balasubramanian and K. Narayan, "Lifshitz spacetimes from AdS null and cosmological solutions," *JHEP* **1008** (2010) 014, arXiv:1005.3291 [hep-th].

[201] A. Donos and J. P. Gauntlett, "Lifshitz Solutions of D=10 and D=11 supergravity," *JHEP* **1012** (2010) 002, arXiv:1008.2062 [hep-th].

[202] R. Gregory, S. L. Parameswaran, G. Tasinato, and I. Zavala, "Lifshitz solutions in supergravity and string theory," *JHEP* **1012** (2010) 047, arXiv:1009.3445 [hep-th].

[203] A. Donos, J. P. Gauntlett, N. Kim, and O. Varela, "Wrapped M5-branes, consistent truncations and AdS/CMT," *JHEP* **1012** (2010) 003, arXiv:1009.3805 [hep-th].

[204] D. Cassani and A. F. Faedo, "Constructing Lifshitz solutions from AdS," *JHEP* **1105** (2011) 013, arXiv:1102.5344 [hep-th].

[205] N. Halmagyi, M. Petrini, and A. Zaffaroni, "Non-Relativistic Solutions of N=2 Gauged Supergravity," *JHEP* **1108** (2011) 041, arXiv:1102.5740 [hep-th].

[206] K. Narayan, "Lifshitz-like systems and AdS null deformations," *Phys.Rev.* **D84** (2011) 086001, arXiv:1103.1279 [hep-th].

[207] W. Chemissany and J. Hartong, "From D3-Branes to Lifshitz Space-Times," *Class.Quant.Grav.* **28** (2011) 195011, arXiv:1105.0612 [hep-th].

[208] H. Braviner, R. Gregory, and S. F. Ross, "Flows involving Lifshitz solutions," *Class.Quant.Grav.* **28** (2011) 225028, arXiv:1108.3067 [hep-th].

[209] L. Barclay, R. Gregory, S. Parameswaran, G. Tasinato, and I. Zavala, "Lifshitz black holes in IIA supergravity," *JHEP* **1205** (2012) 122, arXiv:1203.0576 [hep-th].

[210] J. Jeong, O. Kelekci, and E. O Colgain, "An alternative IIB embedding of F(4) gauged supergravity," *JHEP* **1305** (2013) 079, arXiv:1302.2105 [hep-th].

[211] H. Singh, "Lifshitz to AdS flow with interpolating p-brane solutions," *JHEP* **1308** (2013) 097, arXiv:1305.3784 [hep-th].

[212] X. Dong, S. Harrison, S. Kachru, G. Torroba, and H. Wang, "Aspects of holography for theories with hyperscaling violation," *JHEP* **1206** (2012) 041, arXiv:1201.1905 [hep-th].

[213] S. Sachdev, "The Quantum phases of matter," arXiv:1203.4565 [hep-th].

[214] S. S. Pal, "Fermi-like Liquid From Einstein-DBI-Dilaton System," *JHEP* **1304** (2013) 007, arXiv:1209.3559 [hep-th].

[215] E. Shaghoulian, "Holographic Entanglement Entropy and Fermi Surfaces," *JHEP* **1205** (2012) 065, arXiv:1112.2702 [hep-th].

[216] K. Copsey and R. Mann, "Singularities in Hyperscaling Violating Spacetimes," *JHEP* **1304** (2013) 079, arXiv:1210.1231 [hep-th].

[217] Y. Lei and S. F. Ross, "Extending the non-singular hyperscaling violating spacetimes," *Class.Quant.Grav.* **31** (2014) 035007, arXiv:1310.5878 [hep-th].

[218] S. Hawking, "Nature of space and time," arXiv:hep-th/9409195 [hep-th].

[219] S. Dubovsky, T. Gregoire, A. Nicolis, and R. Rattazzi, "Null energy condition and superluminal propagation," *JHEP* **0603** (2006) 025, arXiv:hep-th/0512260 [hep-th].

[220] R. V. Buniy, S. D. Hsu, and B. M. Murray, "The Null energy condition and instability," *Phys.Rev.* **D74** (2006) 063518, arXiv:hep-th/0606091 [hep-th].

[221] D. Freedman, S. Gubser, K. Pilch, and N. Warner, "Renormalization group flows from holography supersymmetry and a c theorem," *Adv.Theor.Math.Phys.* **3** (1999) 363–417, arXiv:hep-th/9904017 [hep-th].

[222] L. Girardello, M. Petrini, M. Porrati, and A. Zaffaroni, "Novel local CFT and exact results on perturbations of N=4 superYang Mills from AdS dynamics," *JHEP* **9812** (1998) 022, arXiv:hep-th/9810126 [hep-th].

[223] L. Girardello, M. Petrini, M. Porrati, and A. Zaffaroni, "The Supergravity dual of N=1 superYang-Mills theory," *Nucl.Phys.* **B569** (2000) 451–469, arXiv:hep-th/9909047 [hep-th].

[224] R. C. Myers and A. Sinha, "Holographic c-theorems in arbitrary dimensions," *JHEP* **1101** (2011) 125, arXiv:1011.5819 [hep-th].

[225] J. T. Liu and Z. Zhao, "Holographic Lifshitz flows and the null energy condition," arXiv:1206.1047 [hep-th].

[226] N. Lashkari, C. Rabideau, P. Sabella-Garnier, and M. Van Raamsdonk, "Inviolable energy conditions from entanglement inequalities," arXiv:1412.3514 [hep-th].

[227] K. Narayan, "On Lifshitz scaling and hyperscaling violation in string theory," *Phys.Rev.* **D85** (2012) 106006, arXiv:1202.5935 [hep-th].

[228] P. Dey and S. Roy, "Lifshitz-like space-time from intersecting branes in string/M theory," *JHEP* **1206** (2012) 129, arXiv:1203.5381 [hep-th].

[229] P. Dey and S. Roy, "Intersecting D-branes and Lifshitz-like space-time," *Phys.Rev.* **D86** (2012) 066009, arXiv:1204.4858 [hep-th].

[230] E. Perlmutter, "Hyperscaling violation from supergravity," *JHEP* **1206** (2012) 165, arXiv:1205.0242 [hep-th].

[231] M. Ammon, M. Kaminski, and A. Karch, "Hyperscaling-Violation on Probe D-Branes," *JHEP* **1211** (2012) 028, arXiv:1207.1726 [hep-th].

[232] P. Dey and S. Roy, "Lifshitz metric with hyperscaling violation from NS5-Dp states in string theory," *Phys.Lett.* **B720** (2013) 419–423, arXiv:1209.1049 [hep-th].

[233] P. Bueno, W. Chemissany, P. Meessen, T. Ortin, and C. Shahbazi, "Lifshitz-like Solutions with Hyperscaling Violation in Ungauged Supergravity," *JHEP* **1301** (2013) 189, arXiv:1209.4047 [hep-th].

[234] A. Donos, J. P. Gauntlett, J. Sonner, and B. Withers, "Competing orders in M-theory: superfluids, stripes and metamagnetism," *JHEP* **1303** (2013) 108, arXiv:1212.0871 [hep-th].

[235] P. Bueno, W. Chemissany, and C. Shahbazi, "On $hvLif$-like solutions in gauged Supergravity," *Eur.Phys.J.* **C74** no. 1, (2014) 2684, arXiv:1212.4826 [hep-th].

[236] P. Dey and S. Roy, "Interpolating solution from AdS_5 to hyperscaling violating Lifshitz space-time," *Phys.Rev.* **D91** no. 2, (2015) 026005, arXiv:1406.5992 [hep-th].

[237] H. Casini and M. Huerta, "Entanglement entropy in free quantum field theory," *J.Phys.* **A42** (2009) 504007, arXiv:0905.2562 [hep-th].

[238] J. Eisert, M. Cramer, and M. Plenio, "Area laws for the entanglement entropy - a review," *Rev.Mod.Phys.* **82** (2010) 277–306, arXiv:0808.3773 [quant-ph].

[239] M. M. Wolf, "Violation of the entropic area law for Fermions," *Phys.Rev.Lett.* **96** (2006) 010404, arXiv:quant-ph/0503219 [quant-ph].

[240] J. L. Cardy and I. Peschel, "Finite Size Dependence of the Free Energy in Two-dimensional Critical Systems," *Nucl.Phys.* **B300** (1988) 377.

[241] A. Karch, "Conductivities for Hyperscaling Violating Geometries," *JHEP* **1406** (2014) 140, arXiv:1405.2926 [hep-th].

[242] S.-S. Lee, "A Non-Fermi Liquid from a Charged Black Hole: A Critical Fermi Ball," *Phys.Rev.* **D79** (2009) 086006, arXiv:0809.3402 [hep-th].

[243] H. Liu, J. McGreevy, and D. Vegh, "Non-Fermi liquids from holography," *Phys.Rev.* **D83** (2011) 065029, arXiv:0903.2477 [hep-th].

[244] N. Iqbal, H. Liu, and M. Mezei, "Lectures on holographic non-Fermi liquids and quantum phase transitions," arXiv:1110.3814 [hep-th].

[245] N. Iizuka, S. Kachru, N. Kundu, P. Narayan, N. Sircar, *et al.*, "Bianchi Attractors: A Classification of Extremal Black Brane Geometries," *JHEP* **1207** (2012) 193, arXiv:1201.4861 [hep-th].

[246] A. Donos and S. A. Hartnoll, "Interaction-driven localization in holography," *Nature Phys.* **9** (2013) 649–655, arXiv:1212.2998.

[247] J. Erdmenger, B. Herwerth, S. Klug, R. Meyer, and K. Schalm, "S-Wave Superconductivity in Anisotropic Holographic Insulators," arXiv:1501.07615 [hep-th].

[248] A. Donos, B. Goutéraux, and E. Kiritsis, "Holographic Metals and Insulators with Helical Symmetry," *JHEP* **1409** (2014) 038, arXiv:1406.6351 [hep-th].

[249] N. Iizuka, S. Kachru, N. Kundu, P. Narayan, N. Sircar, *et al.*, "Extremal Horizons with Reduced Symmetry: Hyperscaling Violation, Stripes, and a Classification for the Homogeneous Case," *JHEP* **1303** (2013) 126, arXiv:1212.1948.

[250] S. Kachru, N. Kundu, A. Saha, R. Samanta, and S. P. Trivedi, "Interpolating from Bianchi Attractors to Lifshitz and AdS Spacetimes," *JHEP* **1403** (2014) 074, arXiv:1310.5740 [hep-th].

[251] S. Kachru, A. Karch, and S. Yaida, "Holographic Lattices, Dimers, and Glasses," *Phys.Rev.* **D81** (2010) 026007, arXiv:0909.2639 [hep-th].

[252] S. Kachru, A. Karch, and S. Yaida, "Adventures in Holographic Dimer Models," *New J.Phys.* **13** (2011) 035004, arXiv:1009.3268 [hep-th].

[253] D. van der Marel, H. J. A. Molegraaf, J. Zaanen, Z. Nussinov, F. Carbone, A. Damascelli, H. Eisaki, M. Greven, P. H. Kes, and M. Li, "Powerlaw optical conductivity with a constant phase angle in high tc superconductors," *Nature* **425,** (2003) 271–274, cond-mat/0309172.

[254] G. T. Horowitz, J. E. Santos, and D. Tong, "Further Evidence for Lattice-Induced Scaling," *JHEP* **1211** (2012) 102, arXiv:1209.1098 [hep-th].

[255] G. T. Horowitz and J. E. Santos, "General Relativity and the Cuprates," *JHEP* **06** (2013) 087, arXiv:1302.6586 [hep-th].

[256] M. Blake, D. Tong, and D. Vegh, "Holographic Lattices Give the Graviton an Effective Mass," *Phys.Rev.Lett.* **112** no. 7, (2014) 071602, arXiv:1310.3832 [hep-th].

[257] S. A. Hartnoll and D. M. Hofman, "Locally Critical Resistivities from Umklapp Scattering," *Phys.Rev.Lett.* **108** (2012) 241601, arXiv:1201.3917 [hep-th].

[258] S. A. Hartnoll and J. E. Santos, "Cold planar horizons are floppy," *Phys.Rev.* **D89** (2014) 126002, arXiv:1403.4612 [hep-th].

[259] A. Donos and J. P. Gauntlett, "The thermoelectric properties of inhomogeneous holographic lattices," *JHEP* **1501** (2015) 035, arXiv:1409.6875 [hep-th].

[260] S. Nakamura, H. Ooguri, and C.-S. Park, "Gravity Dual of Spatially Modulated Phase," *Phys.Rev.* **D81** (2010) 044018, arXiv:0911.0679 [hep-th].

[261] H. Ooguri and C.-S. Park, "Holographic End-Point of Spatially Modulated Phase Transition," *Phys.Rev.* **D82** (2010) 126001, arXiv:1007.3737 [hep-th].

[262] A. Donos and J. P. Gauntlett, "Holographic striped phases," *JHEP* **1108** (2011) 140, arXiv:1106.2004 [hep-th].

[263] J. Erdmenger, X.-H. Ge, and D.-W. Pang, "Striped phases in the holographic insulator/superconductor transition," *JHEP* **1311** (2013) 027, arXiv:1307.4609 [hep-th].

[264] S. Cremonini and A. Sinkovics, "Spatially Modulated Instabilities of Geometries with Hyperscaling Violation," *JHEP* **1401** (2014) 099, arXiv:1212.4172 [hep-th].

[265] N. Iizuka and K. Maeda, "Stripe Instabilities of Geometries with Hyperscaling Violation," *Phys.Rev.* **D87** no. 12, (2013) 126006, arXiv:1301.5677 [hep-th].

[266] P. Anderson, "Absence of Diffusion in Certain Random Lattices," *Phys.Rev.* **109** (1958) 1492–1505.

[267] P. A. Lee and T. Ramakrishnan, "Disordered electronic systems," *Rev.Mod.Phys.* **57** (1985) 287–337.

[268] R. Nandkishore and D. A. Huse, "Many body localization and thermalization in quantum statistical mechanics," arXiv:1404.0686 [cond-mat.stat-mech].

[269] S. A. Hartnoll, P. K. Kovtun, M. Muller, and S. Sachdev, "Theory of the Nernst effect near quantum phase transitions in condensed matter, and in dyonic black holes," *Phys.Rev.* **B76** (2007) 144502, arXiv:0706.3215 [cond-mat.str-el].

[270] S. A. Hartnoll and C. P. Herzog, "Impure AdS/CFT correspondence," *Phys.Rev.* **D77** (2008) 106009, arXiv:0801.1693 [hep-th].

[271] M. Fujita, Y. Hikida, S. Ryu, and T. Takayanagi, "Disordered Systems and the Replica Method in AdS/CFT," *JHEP* **0812** (2008) 065, arXiv:0810.5394 [hep-th].

[272] Y. Shang, "Correlation functions in the holographic replica method," *JHEP* **1212** (2012) 120, arXiv:1210.2404 [hep-th].

[273] S. Ryu, T. Takayanagi, and T. Ugajin, "Holographic Conductivity in Disordered Systems," *JHEP* **1104** (2011) 115, arXiv:1103.6068 [hep-th].

[274] A. Adams and S. Yaida, "Disordered Holographic Systems I: Functional Renormalization," arXiv:1102.2892 [hep-th].

[275] A. Adams and S. Yaida, "Disordered holographic systems: Marginal relevance of imperfection," *Phys.Rev.* **D90** (2014) 046007, arXiv:1201.6366 [hep-th].

[276] O. Saremi, "Disorder in Gauge/Gravity Duality, Pole Spectrum Statistics and Random Matrix Theory," *Class.Quant.Grav.* **31** (2014) 095014, arXiv:1206.1856 [hep-th].

[277] D. Arean, A. Farahi, L. A. Pando Zayas, I. S. Landea, and A. Scardicchio, "A Dirty Holographic Superconductor," *Phys.Rev.* **D89** (2014) 106003, arXiv:1308.1920 [hep-th].

[278] M. Shinozuka and G. Deodatis, "Simulation of stochastic processes by spectral representation," *Applied Mechanics Reviews* **44** (1991) 191–204. http://dx.doi.org/10.1115/1.3119501.

[279] H. B. Zeng, "Possible Anderson localization in a holographic superconductor," *Phys.Rev.* **D88** no. 12, (2013) 126004, arXiv:1310.5753 [hep-th].

[280] D. Arean, A. Farahi, L. A. Pando Zayas, I. S. Landea, and A. Scardicchio, "Holographic p-wave Superconductor with Disorder," arXiv:1407.7526 [hep-th].

[281] S. A. Hartnoll and J. E. Santos, "Disordered horizons: Holography of randomly disordered fixed points," *Phys.Rev.Lett.* **112** (2014) 231601, arXiv:1402.0872 [hep-th].

[282] S. A. Hartnoll, D. M. Ramirez, and J. E. Santos, "Emergent scale invariance of disordered horizons," arXiv:1504.03324 [hep-th].

[283] A. Lucas, S. Sachdev, and K. Schalm, "Scale-invariant hyperscaling-violating holographic theories and the resistivity of strange metals with random-field disorder," *Phys.Rev.* **D89** (2014) 066018, arXiv:1401.7993 [hep-th].

[284] A. Lucas and S. Sachdev, "Conductivity of weakly disordered strange metals: from conformal to hyperscaling-violating regimes," *Nucl.Phys.* **B892** (2015) 239–268, arXiv:1411.3331 [hep-th].

[285] D. K. O'Keeffe and A. W. Peet, "Perturbatively charged holographic disorder," arXiv:1504.03288 [hep-th].

[286] T. Andrade and B. Withers, "A simple holographic model of momentum relaxation," *JHEP* **1405** (2014) 101, arXiv:1311.5157 [hep-th].

[287] B. Goutéraux, "Charge transport in holography with momentum dissipation," *JHEP* **1404** (2014) 181, arXiv:1401.5436 [hep-th].

[288] K.-Y. Kim, K. K. Kim, Y. Seo, and S.-J. Sin, "Coherent/incoherent metal transition in a holographic model," *JHEP* **1412** (2014) 170, arXiv:1409.8346 [hep-th].

[289] R. A. Davison and B. Goutéraux, "Momentum dissipation and effective theories of coherent and incoherent transport," *JHEP* **1501** (2015) 039, arXiv:1411.1062 [hep-th].

[290] T. Andrade and S. A. Gentle, "Relaxed superconductors," arXiv:1412.6521 [hep-th].

[291] A. Donos and J. P. Gauntlett, "Holographic Q-lattices," *JHEP* **1404** (2014) 040, arXiv:1311.3292 [hep-th].

[292] A. Donos and J. P. Gauntlett, "Novel metals and insulators from holography," *JHEP* **1406** (2014) 007, arXiv:1401.5077 [hep-th].

[293] Y. Ling, P. Liu, C. Niu, J.-P. Wu, and Z.-Y. Xian, "Holographic Superconductor on Q-lattice," *JHEP* **1502** (2015) 059, arXiv:1410.6761 [hep-th].

[294] D. Vegh, "Holography without translational symmetry," arXiv:1301.0537 [hep-th].

[295] R. A. Davison, "Momentum relaxation in holographic massive gravity," *Phys.Rev.* **D88** (2013) 086003, arXiv:1306.5792 [hep-th].

[296] M. Blake and D. Tong, "Universal Resistivity from Holographic Massive Gravity," *Phys.Rev.* **D88** no. 10, (2013) 106004, arXiv:1308.4970 [hep-th].

[297] A. Amoretti, A. Braggio, N. Maggiore, N. Magnoli, and D. Musso, "Thermo-electric transport in gauge/gravity models with momentum dissipation," *JHEP* **1409** (2014) 160, arXiv:1406.4134 [hep-th].

[298] A. Amoretti, A. Braggio, N. Maggiore, N. Magnoli, and D. Musso, "Analytic dc thermoelectric conductivities in holography with massive gravitons," *Phys.Rev.* **D91** no. 2, (2015) 025002, arXiv:1407.0306 [hep-th].

[299] M. Baggioli and O. Pujolas, "Holographic Polarons, the Metal-Insulator Transition and Massive Gravity," arXiv:1411.1003 [hep-th].

[300] A. Amoretti and D. Musso, "Universal formulae for thermoelectric transport with magnetic field and disorder," arXiv:1502.02631 [hep-th].

[301] C. de Rham, "Massive Gravity," *Living Rev.Rel.* **17** (2014) 7, arXiv:1401.4173 [hep-th].

[302] S. Deser, K. Izumi, Y. Ong, and A. Waldron, "Problems of Massive Gravities," arXiv:1410.2289 [hep-th].

[303] D. K. O'Keeffe and A. W. Peet, "Electric hyperscaling violating solutions in Einstein-Maxwell-dilaton gravity with R^2 corrections," *Phys.Rev.* **D90** no. 2, (2014) 026004, arXiv:1312.2261 [hep-th].

[304] S. Harrison, S. Kachru, and H. Wang, "Resolving Lifshitz Horizons," *JHEP* **1402** (2014) 085, arXiv:1202.6635 [hep-th].

[305] G. Knodel and J. T. Liu, "Higher derivative corrections to Lifshitz backgrounds," *JHEP* **1310** (2013) 002, arXiv:1305.3279 [hep-th].

[306] H. Lu, Y. Pang, C. Pope, and J. F. Vazquez-Poritz, "AdS and Lifshitz Black Holes in Conformal and Einstein-Weyl Gravities," *Phys.Rev.* **D86** (2012) 044011, arXiv:1204.1062 [hep-th].

[307] J. Bhattacharya, S. Cremonini, and A. Sinkovics, "On the IR completion of geometries with hyperscaling violation," *JHEP* **1302** (2013) 147, arXiv:1208.1752 [hep-th].

[308] A. Buchel, J. Escobedo, R. C. Myers, M. F. Paulos, A. Sinha, *et al.*, "Holographic GB gravity in arbitrary dimensions," *JHEP* **1003** (2010) 111, arXiv:0911.4257 [hep-th].

[309] X. O. Camanho and J. D. Edelstein, "Causality constraints in AdS/CFT from conformal collider physics and Gauss-Bonnet gravity," *JHEP* **1004** (2010) 007, arXiv:0911.3160 [hep-th].

[310] E. Shaghoulian, "FRW cosmologies and hyperscaling-violating geometries: higher curvature corrections, ultrametricity, Q-space/QFT duality, and a little string theory," *JHEP* **1403** (2014) 011, arXiv:1308.1095 [hep-th].

[311] S. Kar and S. SenGupta, "The Raychaudhuri equations: A Brief review," *Pramana* **69** (2007) 49, arXiv:gr-qc/0611123 [gr-qc].

[312] M. Edalati, J. F. Pedraza, and W. Tangarife Garcia, "Quantum Fluctuations in Holographic Theories with Hyperscaling Violation," *Phys.Rev.* **D87** no. 4, (2013) 046001, arXiv:1210.6993 [hep-th].

[313] H. Lu and C. Pope, "Critical Gravity in Four Dimensions," *Phys.Rev.Lett.* **106** (2011) 181302, arXiv:1101.1971 [hep-th].

[314] S. Barisch-Dick, G. L. Cardoso, M. Haack, and A. Véliz-Osorio, "Quantum corrections to extremal black brane solutions," *JHEP* **1402** (2014) 105, arXiv:1311.3136 [hep-th].

[315] P. Bueno and P. F. Ramirez, "Higher-curvature corrections to holographic entanglement entropy in geometries with hyperscaling violation," *JHEP* **1412** (2014) 078, arXiv:1408.6380 [hep-th].

[316] E. Mefford and G. T. Horowitz, "Simple holographic insulator," *Phys.Rev.* **D90** no. 8, (2014) 084042, arXiv:1406.4188 [hep-th].

[317] M. Taylor and W. Woodhead, "Inhomogeneity simplified," 1406.4870.

[318] B. Withers, "Holographic checkerboards," 1407.1085.

[319] D. M. Basko, I. L. Aleiner, and B. L. Altshuler, "Metal-insulator transition in a weakly interacting many-electron system with localized single-particle states," *Annals of Physics* **321,** (2006) 1126, cond-mat/0506617.

[320] P. Chesler, A. Lucas, and S. Sachdev, "Conformal field theories in a periodic potential: results from holography and field theory," *Phys.Rev.* **D89** no. 2, (2014) 026005, arXiv:1308.0329 [hep-th].

[321] C. Fefferman and C. R. Graham, "Conformal invariants," *in The Mathematical Heritage of Élie Cartan (Lyon, 1984)* **Astérisque** no. Numéro Hors Série, (1985) 95–116.

[322] N. Bobev, N. Halmagyi, K. Pilch, and N. P. Warner, "Supergravity Instabilities of Non-Supersymmetric Quantum Critical Points," *Class.Quant.Grav.* **27** (2010) 235013, arXiv:1006.2546 [hep-th].

[323] D. S. Fisher and D. A. Huse, "Ordered Phase of Short-Range Ising Spin-Glasses," *Phys.Rev.Lett.* **56** (1986) 1601–1604.

[324] D. Anninos, T. Anous, J. Barandes, F. Denef, and B. Gaasbeek, "Hot Halos and Galactic Glasses," *JHEP* **1201** (2012) 003, arXiv:1108.5821 [hep-th].

[325] D. Anninos, T. Anous, F. Denef, and L. Peeters, "Holographic Vitrification," *JHEP* **1504** (2015) 027, arXiv:1309.0146 [hep-th].

[326] V. Lubchenko and P. G. Wolynes, "Theory of structural glasses and supercooled liquids," *Annual Review of Physical Chemistry* **58** (May, 2007) 235–266, cond-mat/0607349.

[327] D. Chandler and J. P. Garrahan, "Dynamics on the way to forming glass: Bubbles in space-time," *Annu. Rev. Phys. Chem.* **61,** (Aug., 2009) 191, 0908.0418.

[328] V. Balasubramanian, A. Buchel, S. R. Green, L. Lehner, and S. L. Liebling, "Holographic Thermalization, Stability of Anti de Sitter Space, and the Fermi-Pasta-Ulam Paradox," *Phys.Rev.Lett.* **113** no. 7, (2014) 071601, arXiv:1403.6471 [hep-th].

[329] A. Buchel, S. R. Green, L. Lehner, and S. L. Liebling, "Universality of non-equilibrium dynamics of cfts from holography," 1410.5381.

[330] F. Denef, "TASI lectures on complex structures," arXiv:1104.0254 [hep-th].

[331] V. Balasubramanian, B. Czech, B. D. Chowdhury, and J. de Boer, "The entropy of a hole in spacetime," *JHEP* **1310** (2013) 220, arXiv:1305.0856 [hep-th].

[332] M. Headrick, R. C. Myers, and J. Wien, "Holographic Holes and Differential Entropy," *JHEP* **1410** (2014) 149, arXiv:1408.4770 [hep-th].

[333] B. Czech, P. Hayden, N. Lashkari, and B. Swingle, "The information theoretic interpretation of the length of a curve," 1410.1540.

[334] V. E. Hubeny, H. Maxfield, M. Rangamani, and E. Tonni, "Holographic entanglement plateaux," *JHEP* **1308** (2013) 092, arXiv:1306.4004.

[335] V. Balasubramanian, B. D. Chowdhury, B. Czech, and J. de Boer, "Entwinement and the emergence of spacetime," *JHEP* **1501** (2015) 048, arXiv:1406.5859 [hep-th].

[336] A. Hamilton, D. N. Kabat, G. Lifschytz, and D. A. Lowe, "Local bulk operators in AdS/CFT: A Boundary view of horizons and locality," *Phys.Rev.* **D73** (2006) 086003, arXiv:hep-th/0506118 [hep-th].

[337] A. Hamilton, D. N. Kabat, G. Lifschytz, and D. A. Lowe, "Holographic representation of local bulk operators," *Phys.Rev.* **D74** (2006) 066009, arXiv:hep-th/0606141 [hep-th].

[338] D. Kabat, G. Lifschytz, and D. A. Lowe, "Constructing local bulk observables in interacting AdS/CFT," *Phys.Rev.* **D83** (2011) 106009, arXiv:1102.2910 [hep-th].

[339] D. Kabat and G. Lifschytz, "Finite N and the failure of bulk locality: Black holes in AdS/CFT," *JHEP* **1409** (2014) 077, arXiv:1405.6394 [hep-th].

[340] T. Faulkner, M. Guica, T. Hartman, R. C. Myers, and M. Van Raamsdonk, "Gravitation from Entanglement in Holographic CFTs," *JHEP* **1403** (2014) 051, arXiv:1312.7856 [hep-th].

[341] B. Swingle and M. Van Raamsdonk, "Universality of Gravity from Entanglement," arXiv:1405.2933 [hep-th].

[342] S. Banerjee, A. Kaviraj, and A. Sinha, "Nonlinear constraints on gravity from entanglement," *Class.Quant.Grav.* **32** no. 6, (2015) 065006, arXiv:1405.3743 [hep-th].

[343] M. Gutperle, E. Hijano, and J. Samani, "Lifshitz black holes in higher spin gravity," 1310.0837.